



THE UNIVERSITY *of* EDINBURGH

## Edinburgh Research Explorer

# Late Palaeozoic-Neogene sedimentary and tectonic development of the Tauride continent and adjacent Tethyan ocean basins in eastern Turkey: New data and integrated interpretation

### Citation for published version:

Robertson, AHF, Parlak, O, Ustaömer, T, Taslı, K & Dumitrica, P 2021, 'Late Palaeozoic-Neogene sedimentary and tectonic development of the Tauride continent and adjacent Tethyan ocean basins in eastern Turkey: New data and integrated interpretation', *Journal of Asian Earth Sciences*, vol. 220, 104859. <https://doi.org/10.1016/j.jseaes.2021.104859>

### Digital Object Identifier (DOI):

[10.1016/j.jseaes.2021.104859](https://doi.org/10.1016/j.jseaes.2021.104859)

### Link:

[Link to publication record in Edinburgh Research Explorer](#)

### Document Version:

Peer reviewed version

### Published In:

Journal of Asian Earth Sciences

### General rights

Copyright for the publications made accessible via the Edinburgh Research Explorer is retained by the author(s) and / or other copyright owners and it is a condition of accessing these publications that users recognise and abide by the legal requirements associated with these rights.

### Take down policy

The University of Edinburgh has made every reasonable effort to ensure that Edinburgh Research Explorer content complies with UK legislation. If you believe that the public display of this file breaches copyright please contact [openaccess@ed.ac.uk](mailto:openaccess@ed.ac.uk) providing details, and we will remove access to the work immediately and investigate your claim.



# Journal of Asian Earth Sciences

## Late Palaeozoic-Neogene sedimentary and tectonic development of the Tauride continent and adjacent Tethyan ocean basins in eastern Turkey: new data and integrated interpretation --Manuscript Draft--

<b>Manuscript Number:</b>	JAESS-D-21-00127R2
<b>Article Type:</b>	Research Paper
<b>Keywords:</b>	E Anatolia; Tethys; palaeogeography; tectonics; ophiolites; melange
<b>Corresponding Author:</b>	Alastair H.F. Robertson, Bsc, PhD University of Edinburgh Edinburgh, UNITED KINGDOM
<b>First Author:</b>	Alastair H.F. Robertson, Bsc, PhD
<b>Order of Authors:</b>	Alastair H.F. Robertson, Bsc, PhD Osman Parlak Timur Ustaömer Kemal Taslı Paulian Dumitrica
<b>Abstract:</b>	<p>The eastern Taurus exemplifies continental rifting, passive margin development, Late Cretaceous melange genesis and ophiolite emplacement. Following Triassic rifting, a carbonate platform developed near sea level in the south (Munzur unit), whereas its northern extension (Neritic-pelagic unit) subsided into deep water during Late Jurassic-Late Cretaceous. Triassic-Cretaceous deep-water sediments and volcanics restore as distal deep-water slope/base of slope units. Jurassic-Cretaceous basic volcanics, interbedded with pelagic sediments, represent emplaced oceanic seamounts. Supra-subduction zone ophiolites formed to the north (c. 93 Ma), probably within an Inner Tauride ocean, and were emplaced southwards by trench-margin collision during latest Cretaceous (c. 75-66 Ma). The margin underwent flexural uplift/erosion and then subsidence/foredeep-infill. Part of the Tauride continent in the south (Malatya Metamorphics) deeply underthrust/subducted northwards, then exhumed rapidly by the late Maastrichtian (c. 65 Ma). To the south, oceanic lithosphere (e.g. Göksun ophiolite) was thrust northward beneath Tauride (Malatya) crust from a more southerly oceanic basin (Berit ocean), and intruded by Late Cretaceous subduction-related granitic rocks (88-82 Ma). Allochthonous units were assembled during the latest Cretaceous, followed by thick-skinned folding/thrusting, generally southwards, related to regional collision tectonics during Mid-Late Eocene. Part of the unmetamorphosed Tauride platform and its over-riding Late Cretaceous allochthon were apparently displaced &gt;60 km northeastwards. Mid-Late Miocene regional collision drove variable folding and re-thrusting, in places northwards during the Eocene. Regional comparisons suggest that the Tauride carbonate platform (Geyik Dağ) narrowed eastwards, and that the palaeogeography of the E Taurides differed from farther west and this, in turn, influenced late Mesozoic-Cenozoic structural development.</p>
<b>Suggested Reviewers:</b>	<p>Istvan Dunkl Göttingen Academy of Sciences and Humanities: Akademie der Wissenschaften zu Göttingen istvan.dunkl@geo.uni-goettingen.de Current, experienced international researcher in Taurides geology</p> <p>Tim Kusky Wuhan University of Science and Technology tkusky@gmail.com Experienced current researcher on Tauride geology</p> <p>Yener Eyeboğlu Karadeniz Teknik Üniversitesi yenereyuboglu@gmail.com</p>

	<p>Current Turkish expert on Tauride geology</p> <p>Tamer Duman  Fujiro Consulting, Ankara  duman.tamer@gmail.com  Long-term expert on Tauride geology and tectonics with MTA (geological survey) who recently moved to a consulting company</p> <p>Dov Avigad  Hebrew University of Jerusalem Faculty of Science  dov.avigad@mail.huji.ac.il</p> <p>Demir Altiner  Middle East Technical University, Ankara  demir@metu.edu.tr  Longstanding Turkish expert on the stratigraphy and tectonics of Turkey including the Taurides.</p>
<b>Opposed Reviewers:</b>	

Dear Ibrahim,

Thanks for your assistance. We have now uploaded a further revised version of our paper. We carried out the following minor revisions:

- 1- Please revise the highlights. Each highlight should be full-sentence and indicate the novel conclusion of your study (max 85 characters including spaces). Now provided.
- 2- Please write in full the author names and surnames. Now done
- 3- Please homogenize the font type of the text (I realized that somewhere in the text you used different font type). Now done (globally).
- 4- Would you please check the lines 849-851? I was not able to understand the statement very well (this would be due to my poor English). You were correct. It is now in two sentences.
- 5- I would recommend adding coordinates to your maps; this may help a lot to researchers who will do a further research on the locations you studied.  
We have done this (thanks to the skill of Timur Ustaömer).
- 6- It would be nice if you ask your co-authors to read the final version of the paper to avoid any misspelling errors etc. Although the revised paper is very well-written, there might be some errors in the text/figures/tables (for example on Fig. 24; please correct "lisvanites" to "listvaenites").

We corrected the spelling as suggested (I two figures). Myself, Osman Parlak and Timur Ustaömer rechecked the figures and we made some minor corrections and improvements. The text was also rechecked and some minor re-editing was carried out (but no scientific changes or additions).

We hope that you will now find our paper acceptable.

Many thanks for your help and advice,

Best regards,

Alastair Robertson and co-authors

## Author agreement

All of the authors have participated in this research, and are aware of and have agreed to the submission of this paper.

## Research Highlights

Multidisciplinary data allow a new interpretation of a key Tethyan region in E Turkey. Late Palaeozoic-Mesozoic rifting and passive margin development is exemplified. Ophiolite, melange and continental margin emplacement are explained. Stratigraphical evidence is given for latest Cretaceous metamorphic rock exhumation. Tectonic models are tested related to the Inner Tauride ocean.

## **Detailed Response to reviewers**

Reviewer #1:

1. Several of the Figures have 12 photos or microphotos, which makes individual photos largely unreadable (e.g., Figs. 4, 6, 20). It will be better to have nine or even less well-chosen photos per individual Figure. Please reduce the number of photos per Figure.

Reply. We have carefully considered this request. We think the problem is that the converted PDF for review is low-resolution and indeed does not show all the details of the images. However, on the high-resolution published version there should be no problem to see all the details. The images have been carefully chosen from a large available set, cropped and image processed so that key features are highlighted. Recent previous papers by largely the same authors in JAES and Sedimentary Geology have used exactly same grouped format without adverse comment from the reviewers of the editors (indeed we have been encouraged to group images to save space). Each one illustrates a feature mentioned in the text (one photograph was deleted when two figures were combined). We therefore propose to retain the present format as the photographs are central to the text (as laid out they are economical in space; readers can easily enlarge the PDFs if they wish to see more details).

2. In the geological map in Fig. 2, please indicate the Figure numbers of the subareas. We considered this but adding these numbers would confuse with the Areas labelled and other information (now increased). Instead in the text we refer many times to the sub-areas which are labelled on Fig. 2. The reader can thus easily see the location.

3. The type of faults in Fig. 2 should all be marked (strike-slip, thrust or normal).

This is now done.

4. It will be useful to include a regional cross-section for the map in Fig. 2.

Yes, One is now added below the map on Fig. 2.

5. On line 158 it is stated:

"Precambrian sediments (Emirgazi Formation), Cambrian shelf siliciclastics (Feke Quartzites), carbonates and some volcanics (Çal Tepe Formation),..."

As far as I know, there are no volcanic rocks in the Çal Tepe Formation, please check.

True, this was corrected.

6. İzmir-Ankara-Erzincan suture is not correctly drawn in central Anatolia in Fig. 1. The region marked as "Ankara Melange" includes mostly Pontide sequences.

True, now revised.

7. The microphotos in Fig. 6 need labeling, and the scale bar is most likely incorrect - it is unlikely that all these rocks are so coarse grained.

OK, now corrected. Thanks. Scale bar is correct; coarse-grained sandstones were selected to show lithoclasts.

8. Please correct - . 101 - scale of Gohen et al. (2020).

Corrected

### **Reviewer #2:**

Except that it is quite long, the paper reads well, and I noted only some small minor formal changes (see attached ms). In addition, numerous stratigraphic and sedimentological (including palaeontological) data are provided, which adds significantly on previous knowledge. The discussion and reasoning are generally well written.

Reply: Thanks, the 'minor formal changes' listed on the attached MS have all been made (see below).

The major problems lie in the structural sketches, geological maps and cross-sections (problems of topography, basic structural relationships, see on attached file), that should be enhanced for the comprehension of the structural relationships and tectonic history.

Reply: The specific comments refer to three of the maps. Changes and corrections have been made (see also explanation below).

Especially the general interpretation figure (Fig 28), which I failed totally to understand, should be enhanced. It is a shame because in my opinion the paper will miss to convince and help clarify the tectonic evolution of that sector. The authors should re-draft it taking into account a more realistic geometry of tectonic blocks, shape of oceans, etc...

Reply: This diagram shows alternatives published before. It is not essential and so was deleted to save space (the reader can refer to the published works if interested).

For the integration of previous works, some things are missing (see attached doc). Notably, Age data when they are available.



Reply: We have noted these points and e.g. the additional age data are now added with supporting references (and the references to the Rolland et al. group).

Considering the discussion section, here are several problems that should be addressed (or clarified), which could enhance the insights on a wider regional scale:

-1. The ophiolite obduction occurred on a long distance. Apart from the Kirshehir Block there is no evidence of any suture zone within the whole E Anatolia until the Izmir Ankara Suture. The age of metamorphic sole below ophiolites is very similar in all the region, so there should be one obduction coming from the north (the Kirshehir block is only in the W part). I do not quite understand the arguments used to disqualify the 'northern ophiolite origin' and of one main obduction. The arguments based on ophiolite transport direction that is from N-> S do not disagree with a main northern origin. The fact that no suture-zone rocks like HP rocks etc is observed in between is a major problem for defining a suture. The fact that ophiolites have different ages (C vs. J) can be explained by the size of the obducted sequence. Part of the explanation on the age could also be that amphibole from the gabbro close to the base of the ophiolite recrystallized during obduction ... (so some 'Cretaceous' ophiolites could be Jurassic). The observation of a passive margin deepening towards the north is also in agreement with a N origin, etc... you should also take into account that the TIME of emplacement is the same for all E Anatolia ophiolites (except for the southern Maden etc ophiolites), and that is quite hard to make these two obductions occurred at the same time...

Reply. We agree that there is no suture zone between S and N ophiolites in E Anatolia and that they were all emplaced generally from N to S. Therefore, taking the evidence from this region alone a northerly origin as one oceanic system can't be ruled out. However, we do not think that the radiometrically dated ophiolites in E Taurides are wrongly dated Jurassic ones (we include references to the age data). The E Anatolian ophiolites (e.g. Pinarbaşı and Divriği ophiolites) correlate laterally to the west with e.g. the Aladağ, Alihoca (Pozantı-Karsantı ophiolites, which structurally overlie blueschist facies rock of the Bolkar nappe (Afyon zone) and lie to the south of the Niğde-Kırşehir massif which has not undergone such HP-LP metamorphism. Many authors (e.g. Okay et al., Pourteau et al.) have inferred that the Anatolide HP-LT metamorphic rocks represent a suture zone, related to closure of the Inner Tauride ocean. It is true that the metamorphic soles of the N vs. S ophiolites give similar ages. However, this could be explained by rapid on-going subduction-related contraction affecting a wide area. The information we give in this paper cannot fully distinguish between the alternative models of ophiolite genesis and emplacement (nor was it intended to do so). However, we have revised our discussion and summary of the tectonic alternatives taking into account the points made by reviewer 2, supported by additional references (please see also below).

-2. One major problem is the ophiolite thickness that you show to be very thin in many places, as is generally observed, so there is a need for a thinning process of the obducted lithosphere section (A <1-km thick ophiolite does not travel for long on continental crust... our group published several papers on that topic that should not be avoided (cf Hassig et al., 2016, *terra nova*, *J. of Geody...*)), which matches very well with the extensional core complex phase that we described in NE Anatolia (see also Rolland et al., 2020, *Geosc Frontiers*). There, HT metamorphism at 80±3 Ma was followed by rapid exhumation below a top-to-the-North detachment sealed by the Early Maastrichtian unconformity (ca. 70.6 Ma), which is ascribed to extension and thinning of the ophiolite. You also seem to describe a similar post-obduction extension here (on top of the Goskun ophiolite and on Malatya. However, its significance still lies unclear, so I think you should at least discuss the model proposed in this paper.

Reply. This is indeed an interesting interpretation and a potentially valid way to explain why some of the ophiolites (e.g. Divriği) are relatively thin. Unfortunately, so far there have been no detailed structural studies on any of the E Anatolian ophiolites which could test this hypothesis. Also, we are at the southern end of the inferred extensional collapse and so the evidence could be unclear there. However, published estimates suggest the Pınarbaşı and Divriği ophiolites in particular could be quite thick (c. 5 km). We now mention (and cite) this collapse hypothesis, which could be tested by future work. However, this is still not our preferred interpretation.

On figure 30 I see the melange reworking ophiolite fragments, but where is the ophiolite?

Reply; the related maps show that ophiolites are exposed to the north and as such are a suitable source area. However, there is no field evidence that the ophiolite reached far to the south; only melange emplaced into a Late Cretaceous flexural foredeep is seen there.

Fig. 33. You propose several phases of thrusting on the same structure. It is OK when a deeper rock thrust over a more superficial one, however, it seems the final deformation phase could be accommodated on other structures, it is probably related to the hard collision phase (see Cowgill et al. *tectonics* 2016). How does that Eocene compressional deformation not produce any folding in the upper unit? Note also that Rolland et al., 2012 described collisional deformation also in the Eocene at the base of Puturge unit (dated by Ar/Ar on amphibole at 48 ± 0.8 Ma). further, this figure looks somehow strange because the same surface is first an unconformity, becomes a thrust, then a detachment and ends up again to be an unconformity before being reactivated again by a thrust... Is this realistic? Any alternatives?

Reply: the arrows should indicate the Eocene convergence was thick skinned not focussed on the former detachment. Eocene folding is seen in places. We cannot be sure how exactly the Eocene thrusting was accommodated because there is little overlying Eocene sedimentary cover

in this area. We know the Malatya/Keban metamorphics were exhumed (extension) and later overthrust by allochthonous Mesozoic, presumably related to Eocene convergence. The Cowgill et al. 2016 paper has been checked and the wording here has been slightly revised to emphasise that the Eocene and Miocene convergence events are collision-related. However, we decided to delete this paper to save space as it is not essential.

Check: There is a problem in the order of figure numbers and captions (they do not match). Thanks for noting this; figures were checked for number and order (now revised).

### **Reviewer 2 Comments in stickie notes on PDF**

I. 56 Reference added as requested:

Rolland, Y., Hässig, M., Bosch, D., Bruguier, O., Melis, R., Galoyan, G., ... & Sosson, M. (2020). The East Anatolia–Lesser Caucasus ophiolite: An exceptional case of large-scale obduction, synthesis of data and numerical modelling. *Geoscience Frontiers*, 11(1), 83-108.

I. 60 Reference added as requested:

Hässig, M. Y. M. M., Rolland, Y., Sosson, M., 2017. From seafloor spreading to obduction: Jurassic–Cretaceous evolution of the northern branch of the Neotethys in the Northeastern Anatolian and Lesser Caucasus regions. *Geological society, London, special publications*, 428(1), 41-60.

I. 68 Reference added as requested:

Hässig, M., Rolland, Y., Duretz, T., & Sosson, M. (2016b). Obduction triggered by regional heating during plate reorganization. *Terra Nova*, 28(1), 76-82.

*I. 84 a ' unique combination of palaeogeographic and tectonic features.'*

*Reviewer 2* 'Qualitative. Explain the specificity of the region.'

We now hint at this here by adding: 'The palaeogeography differs significantly from that of the central and western Taurides. Also, the structural development, while showing many common features with areas further west, has some specific features especially the contrasting Eocene deformation.' We also emphasise the specificity in the Discussion and Conclusions.

*l. 92* 'sedimentary petrographic' Deleted as suggested.

*l. 101* 'In this paper, we use the time scale of Gohen et al. (2020).' Comment 'A little bit out of place'

Reply: Now relocated.

*l. 111* provide informations on datings of Malatya Rolland et al. (2012) : 78.7 +/- 1 Ma and 81.8 +/- 0.6 Ma Ar-Ar on Hbd

Reply-now added and cited.

*l. 125* suggested rewording 'by two main and temporally distinct sedimentary basin successions'... is now edited in with minor addition.

*l. 139* 'relatively allochthonous' is now changed to simply, 'allochthonous.'

*l. 200* 'the Malatya Metamorphics (the type area; S of Elbistan)'

provide informations on datings of Malatya Rolland et al. (2012) : 73.8 +/- 0.3 Ma

Reply-now added and cited.

*l. 1259* add 'to lower amphibolite facies...

(cite also Rolland et al., 2012 here'

-Reply Now done

I. 1377 'However, these units are separated, structurally by the Göksun and related ophiolites, which might be explained by strike-slip displacement after the Late Cretaceous but evidence for this is lacking.'

Reply-This option is removed (no evidence either way).

Reply-or alternatively a back-arc basin related to slab roll-back (Rolland et al., 2012)

This option is now cited.

I. 1377 add Rolland et al., 2012; done

-Reply Now done

I 1381 please also provide time constrains for HP metamorphism  $70.7 \pm 0.3$  Ma (Ar-Ar phengite), Rolland et al., 2012.

-Reply Now done

Figures

Fig. 5 cross-sections are misplaced/ do not cross the same units? Topography could be more realistic.

Reply: The lines of sections have been slightly corrected and made bolder to show the correct units. These are intended to show sedimentary and structural relationships; in fact they are rock-relations diagrams rather than true-scale sections. The captions have been

changed to say rock-relations diagrams rather than sections. A true-scale section is now included in Fig. 2.

Fig. 8 section c 'put in conformity the shape of blocks and the stripped lines

OK: revised

Fig. 9 this rectilinear vertical fault geometry is not suggested by the map.

Reply: It is OK; the map contact is linear like a steep fault.

Are you sure it cross-cuts the bedding like that? It should be a late fault (later than thrusts), but the map shows it as ante- and post- regarding the N- and S- thrusts of the map.

Reply: The high-angle fault fits OK with the cross-cutting map relations. Limits of access and outcrop make it difficult to know the angle of dip of this fault at the surface.

However, it was mapped by MTA as a cross-cutting feature, likely as a post-thrust strike-slip fault.

Fig. 9' The fold structure is dissected by the thrust? This structure looks weird'

Reply: On checking photographs this bedding orientation is uncertain so this was changed to a more expected fabric. However, the fold in B is indeed truncated as shown.

Fig. 28 what is here in the north? Ocean? why suture zone then?

Reply: This whole figure is now deleted as not essential.

Fig. 30 I do not understand here, if this were a thrust, there would be older rocks on top of younger ones. Here you just have a ,normal succession.... Essentially lacking is the obduction that is thrust on a large distance and, hence the ophiolite on top of the mélangé. Afterwards, the obducted sheet has been significantly thinned out by the extension?

Reply: This whole figure is now deleted as not essential.

### **Main deletions (to shorten the text)**

Section 2 deleted because it is covered before and after adds little (Reference to Cohen et al., was moved);

I. 196-202. ' Below, we work upwards through the regional tectono-stratigraphy, beginning with the Gürün autochthon, followed by the Malatya Metamorphics, and then by the allochthonous Tauride units including melanges and ophiolites. For each major tectono-stratigraphic unit, existing evidence is summarised, followed by presentation of new data (where available), and a local interpretation. The mutual relationships of the major tectono-stratigraphic units is considered in the wider regional context, including the central and western Taurides in the discussion section of the paper.'

I. 202-205 'Our observations and interpretations are supported by geological maps and local cross-sections of each of the above five sub-areas, together with sedimentary logs, field photographs and photomicrographs. Additional illustrations are included in the Supplementary material.'

I. 780-790 'Using the same name for this deep-sea succession as the Gülbahar Nappe in the western Taurides is potentially misleading for several reasons: (1) Unlike the western Taurides, there is no intact, regionally extensive, nappe in the Eastern Taurides, but instead, there are isolated outcrops of small thrust slices, broken formation and/or blocks. (2) The restored succession is not identical to the Gülbahar Nappe in the western Taurides, which, for example, includes long, intact Triassic volcanic successions (e.g. Turunç unit) (Şenel et al.,

1989; Collins and Robertson, 1998; Sayit et al., 2015) that are not known in the eastern Taurides (although some Triassic volcanics exists; see below); (3) Identical palaeogeographic settings cannot be assumed give the widely separated occurrences (c. 1000 km apart).'

l. 1046-51 In places, the uppermost exposed Malatya (Keban) Metamorphics are associated with calc-mylonites, suggesting intense shearing prior to formation of the Kemaliye Formation unconformably above. The unmetamorphosed Kemaliye Formation contrasts with the Karaböğürtlen Formation, which is part of the intact succession of the Malatya Metamorphics.'

l. 1130 -1140. 'in the following respects: (1) The sediments overlies unmetamorphosed carbonate platform units, whereas the type Kemaliye Formation overlies the Malatya Metamorphics (see above); (2) The sediments are dominated by talus derived from the unmetamorphosed carbonate platform beneath (see below), whereas much of the siliciclastic material in the type Kemaliye area is metamorphic, derived from the Malatya (Keban) Metamorphics; (3) The type area Kemaliye Formation is composite, with several different tectono-stratigraphic elements (e.g. debris-flow deposits; Triassic basalts; serpentinite). However, a more coherent, although variably deformed, sedimentary succession is exposed within the Munzur and Köseyahya thrust sheets. The upper levels of the Kemaliye Formation succession are intercalated with tectonic slices and blocks of other units (e.g. neritic shelf limestone).'

Also Fig. 23 (photos combined with another figure or deleted).

l. '1348 ahead of advancing Tauride allochthons, including carbonate platform, slope, basin and ophiolitic rocks.... Some of neritic blocks and slices can be correlated with the limestone successions of the over-riding Munzur and/or Köseyahya thrust sheets.'

l. 1695-1698 'The more northerly-formed platform slope lithologies (Pelagic (Gülbahar) unit) were detached and bulldozed southwards, in places, putting the ophiolite directly above the neritic carbonate platform.'

'1706-1712 Farther south, the Munzur and Köseyahya platforms subsided and were covered by the Kemaliye Formation, probably contemporaneously. The scattering of blocks and dismembered thrust sheets of the Pelagic (Gülbahar) unit, and also of ophiolitic rocks, suggests that these lithologies were emplaced by gravity sliding into the distal (southerly) part of the foredeep. Munzur and Köseyahya-derived thrust sheets, broken formation and limestone blocks were then emplaced above.'



I. 1918 'Below, we discuss and interpret the mutual relationships of the main tectonic units in the region studied (Fig. 2).'

I. 1964 'The two units are separated by debris-flow units, correlated with the Kemaliye Formation, that include ophiolitic rocks and radiolarian chert.'

I. 2003 'This unit could be a fragment of the Gürün autochthon that was detached, probably during the regional Mid-Late Eocene emplacement event'

I. deleted 2118 'However, the right-lateral displacement appears to pre-date some, or all, of the dominantly left-lateral displacements related to the regional Sürgü–Misis Fault system.'

I. 2268-2274 'Although the western margin of the Darende Basin is, in places, folded and displaced eastwards related to Mid-Late Eocene deformation there is no evidence of deformation within the basin related to regional-scale southward thrusting, together with the underlying Tauride allochthonous units (Booth et al., 2013). Indeed the Eocene sediments are everywhere mapped as being transgressive on the emplaced Mesozoic allochthons (MTA, 2011; Bedi and Yusufoglu, 2018).'

I. 2295-2299 'The Northern and Southern allochthons may therefore represent two different continental margin segments, both with similar allochthonous units in the south (i.e. Munzur and Neritic-pelagic (Köseyahya) thrust sheets, and also ophiolites and related melanges in the north.'

Deleted Fig. 28 as the text is adequate to state the alternatives; two of the three options are illustrated by Robertson et al. 2013c.

I. 2423 'The inferred latest Cretaceous extensional detachment, the Kemaliye Formation and the basal thrust of the over-riding Mesozoic platform/slope units were re-activated by compressional deformation during the Mid-Late Eocene, as seen in the south (Area 3B, Nurhak Dağı) (Fig. 30c)'

I. 2427 These crustal units are restored as the northern part of the Tauride continent and its northward-facing, rifted passive margin (> 150 km wide)

I. 3532 'The Neritic-pelagic succession is, therefore, restored to the north of the Neritic (Munzur) succession in both the Southern and Northern allochthons'

I. 2565 'This also explains the intense internal deformation within the Neritic-pelagic (Köseyahya) thrust sheet compared to the main Munzur thrust sheet'.

I. 2927 'During latest Cretaceous emplacement, the upper stratigraphic levels of the distal, northerly part of the neritic platform were detached and bulldozed towards the foredeep. As

as result, the platform is directly over-riden by or over-riden, such that the proximal foredeep was directly juxtaposed with the over-riding ophiolite (Divriği melange) in places’.

I. 2457 ‘The platform potentially stepped northwards along transcurrent faults that were re-activated as major c. N-S neotectonic strike-slip faults’

I. 2458 ‘The distinctive Gürün curl structure is attributed, mainly to the combined effects of a changed palaeogeography eastwards and late Miocene post-suture oblique contraction.

-While the neotectonic deformation of the region was dominated by left-lateral strike-slip related to the westward tectonic escape of Anatolia, a localised c. NE-SW to ENE-WSW lineament (Göksu fault zone) of dominantly right-lateral displacement appears to predated this westward displacement.....The distinctive Gürün curl structure is attributed, mainly to the combined effects of a changed palaeogeography eastwards and late Miocene post-suture oblique contraction.

On the other hand, some small sections have been added to answer queries and the Discussion is partly re-written in response to comments by Reviewer 2 (please see MS with red lettering).





Dear Ibrahim,

Thanks for your assistance. We have now uploaded a further revised version of our paper. We carried out the following minor revisions:

- 1- Please revise the highlights. Each highlight should be full-sentence and indicate the novel conclusion of your study (max 85 characters including spaces). Now provided.
- 2- Please write in full the author names and surnames. Now done
- 3- Please homogenize the font type of the text (I realized that somewhere in the text you used different font type). Now done (globally).
- 4- Would you please check the lines 849-851? I was not able to understand the statement very well (this would be due to my poor English). You were correct. It is now in two sentences.
- 5- I would recommend adding coordinates to your maps; this may help a lot to researchers who will do a further research on the locations you studied.  
We have done this (thanks to the skill of Timur Ustaömer).
- 6- It would be nice if you ask your co-authors to read the final version of the paper to avoid any misspelling errors etc. Although the revised paper is very well-written, there might be some errors in the text/figures/tables (for example on Fig. 24; please correct "lisvanites" to "listvaenites").

We corrected the spelling as suggested (I two figures). Myself, Osman Parlak and Timur Ustaömer rechecked the figures and we made some minor corrections and improvements.

The text was also rechecked and spelling and punctuation errors were corrected. A paragraph (marked in red) in the Discussion was relocated to improve the flow; also the Conclusions were streamlined (also marked in red), but no scientific changes or additions were made.

We hope that you will now find our paper acceptable.

Many thanks for your help and advice,

Best regards,

Alastair Robertson and co-authors

[Click here to view linked References](#)

1

2 **Late Palaeozoic-Neogene sedimentary and tectonic development of the Tauride continent**  
3 **and adjacent Tethyan ocean basins in eastern Turkey: new data and integrated**  
4 **interpretation**

5

6

7

8

9 Alastair Harry Forbes Robertson<sup>1</sup>, Osman Parlak<sup>2</sup>, Timur Ustaömer<sup>3</sup>, Kemal Taslı<sup>4</sup>, Paulian  
10 Dumitrica<sup>5</sup>

11

12

13 <sup>1</sup>School of GeoSciences, University of Edinburgh, Grant Institute, West Mains Rd.,  
14 Edinburgh, EH9 3JW, UK ([Alastair.Robertson@ed.ac.uk](mailto:Alastair.Robertson@ed.ac.uk); corresponding author)

15 <sup>2</sup>Çukurova Üniversitesi, Jeoloji Mühendisliği Bölümü, 01330 Balcalı, Adana, Turkey

16 <sup>3</sup>İstanbul Üniversitesi-Cerrahpaşa, Jeoloji Mühendisliği Bölümü, Büyükçekmece, İstanbul,  
17 Turkey

18 <sup>4</sup>Mersin Üniversitesi, Jeoloji Mühendisliği Bölümü, Mersin, Turkey

19 <sup>5</sup>Dennigkofenweg 33, CH-3037 Guemligen, Switzerland

20

21

22 **Abstract**

23 The eastern Taurus exemplifies continental rifting, passive margin development, Late  
24 Cretaceous melange genesis and ophiolite emplacement. Following Triassic rifting, a  
25 carbonate platform developed near sea level in the south (Munzur unit), whereas its  
26 northern extension (Neritic-pelagic unit) subsided into deep water during Late Jurassic-Late  
27 Cretaceous. Triassic-Cretaceous deep-water sediments and volcanics restore as distal deep-  
28 water slope/base of slope units. Jurassic-Cretaceous basic volcanics, interbedded with  
29 pelagic sediments, represent emplaced oceanic seamounts. Supra-subduction zone  
30 ophiolites formed to the north (c. 93 Ma), probably within an Inner Tauride ocean, and were  
31 emplaced southwards by trench-margin collision during latest Cretaceous (c. 75-66 Ma). The  
32 margin underwent flexural uplift/erosion and then subsidence/foredeep-infill. Part of the  
33 Tauride continent in the south (Malatya Metamorphics) deeply underthrust/subducted  
34 northwards, then exhumed rapidly by the late Maastrichtian (c. 65 Ma). To the south,  
35 oceanic lithosphere (e.g. Göksun ophiolite) was thrust northward beneath Tauride (Malatya)  
36 crust from a more southerly oceanic basin (Berit ocean), and intruded by Late Cretaceous  
37 subduction-related granitic rocks (88-82 Ma). Allochthonous units were assembled during  
38 the latest Cretaceous, followed by thick-skinned folding/thrusting, generally southwards,  
39 related to regional collision tectonics during Mid-Late Eocene. Part of the  
40 unmetamorphosed Tauride platform and its over-riding Late Cretaceous allochthon were  
41 apparently displaced >60 km northeastwards. Mid-Late Miocene regional collision drove  
42 variable folding and re-thrusting, in places northwards. Regional comparisons suggest that  
43 the Tauride carbonate platform (Geyik Dağ) narrowed eastwards, such that the  
44 palaeogeography of the E Taurides differed from farther west, influencing the late  
45 Mesozoic-Cenozoic structural development.

46

47

48 Key words: E Anatolia, Tethys, palaeogeography, tectonics, ophiolites, melange, deep-sea  
49 sediments

50

51

## 52 1. Introduction

53

54 The geological development of Tethys within and around Anatolia remains of current  
55 interest, with several alternative tectonic models being recently proposed (Moix et al.,  
56 2008; Robertson et al., 2012, 2013a; Rolland et al., 2012, 2020; Maffione et al., 2017; Parlak  
57 et al., 2019; Hinsbergen et al., 2020). In addition to ophiolites, continental margin units and  
58 melanges need to be taken into account. The Taurides represent a key part of Anatolia (Fig.  
59 1), where ophiolites were emplaced onto a regional-scale carbonate platform during latest  
60 Cretaceous time (Juteau, 1980; Şengör and Yılmaz, 1981; Robertson and Dixon, 1984; Ricou  
61 et al., 1984; Dilek and Moores, 1990; Robertson, 2002; Parlak, 2016; Barrier et al., 2018).  
62 There have been several attempts to explain the emplacement of the ophiolites and related  
63 continental margin units as a whole in the western Taurides (Hayward and Robertson, 1982;  
64 Woodcock and Robertson, 1982; Yılmaz and Maxwell, 1984; Şenel, 1984; Marcoux et al.,  
65 1989; Collins and Robertson, 1998), in the central Taurides (Demirtaşlı et al., 1984; Özgül,  
66 1997; Dilek and Whitney, 1997; Andrew and Robertson, 2002; Parlak and Robertson, 2004;  
67 McPhee et al., 2018a), and also in the eastern Taurides (Yılmaz, 1993; Yılmaz et al., 1993,  
68 Robertson et al., 2006, 2007, Robertson et al., 2013a b; Rolland et al., 2012, 2020).

69 The ophiolites, melanges and related continental units of the İzmir-Ankara-Erzincan  
70 (northern Neotethyan) suture zone in the Eastern Turkey have also received a considerable  
71 amount of attention in recent years (e.g., Yılmaz et al., 1997; Okay and Şahintürk, 1997; Rice  
72 et al., 2009; Ustaömer and Robertson, 2010, 2013; Robertson et al., 2013c; Topuz et al.,  
73 2013a, b; Rolland et al., 2012, 2020; Hässig et al., 2013, 2017). However, there have been  
74 few integrated studies that focus on the carbonate platforms, slope/basin facies and the  
75 related melange units in the Eastern Taurides (Fig. 2). These units are located in a critical  
76 position between the Arabian Platform (African plate) to the south and the Pontides  
77 (Eurasian plate) to the north. The eastern Tauride region has some distinctive features,  
78 notably an extraordinary NE-verging fold-like structure, up to 200 km long x 250 km wide  
79 (MTA, 2011), termed the Gürün curl after a town in the core of this structure (Lefebvre et  
80 al., 2013a) (Fig. 2; Supplementary Fig. 1). Is this a primary palaeogeographic feature, or  
81 related to tectonic emplacement, or to some combination of both?

82 A synthesis of the Tethyan geology of the Eastern Taurides is given here, utilising a  
83 combination of new data and also the available literature on this region (Perinçek and Kozlu,



84 1984; Robertson et al., 2013b; Bedi et al., 2004, 2005; Bedi and Yusufoglu, 2018). The region  
85 studied includes a Late Palaeozoic-Mesozoic metamorphosed carbonate platform, an  
86 unmetamorphosed carbonate platform and deeper-water marginal units, several types of  
87 melange, and also Late Cretaceous ophiolites with their metamorphic soles. Latest  
88 Cretaceous-Miocene cover successions help to constrain the distribution and timing of  
89 tectonic events, especially the exhumation of the metamorphic rocks. The assembled  
90 information will be used to test alternative tectonic models for the wider region (Kozlu et  
91 al., 1990; Robertson et al., 2013a, b; Barrier et al., 2018; van Hinsbergen et al., 2020; Rolland  
92 et al., 2012, 2020). We will demonstrate that the geology of eastern Anatolia represents a  
93 unique combination of palaeogeographic and tectonic features. The palaeogeography  
94 differs significantly from that of the central and western Taurides. Also, the Late Cretaceous  
95 ophiolites and related melange units differ significantly from Jurassic counterparts farther  
96 north in the E Pontide-Lesser Caucasus region.

97 In this paper, we use the time scale of Cohen et al. (2020).

98

## 99 **2. Regional tectono-stratigraphy**

100 We utilise a modified version of the tectono-stratigraphy based on mapping by the Turkish  
101 Petroleum Company (TPAO) (Perinçek and Kozlu, 1984), including changes and additions  
102 based on mapping by the Maden Tektik ve Arama (MTA) (Bedi et al., 2009; Bedi and  
103 Yusufoglu, 2018), related studies (Robertson et al., 2013b) and this work.

104 Moving northwards, the Arabian platform is tectonically overlain by a Miocene  
105 imbricate thrust belt, with, to the north of this, the Bitlis and Pütürge allochthonous  
106 continental units (Yılmaz, 1993; Yılmaz et al., 1993; Yazgan, 1984) (Fig. 1). These units are  
107 tectonically overlain by Late Cretaceous ophiolitic rocks, variously known as the Göksun  
108 (Berit), Kömürhan, İspendere or Yüksekova ophiolites. Our study effectively begins in the  
109 south with the Late Palaeozoic-Mesozoic Malatya Metamorphics (including the Keban and  
110 Binboğa metamorphic rocks; see below). To the north, these metamorphic rocks are over-  
111 ridden by allochthonous, unmetamorphosed Tauride carbonate platform, melanges and  
112 ophiolitic units. The allochthonous outcrop in the west of the region is split into two parts,  
113 termed the Northern and the Southern allochthon (Robertson et al., 2013b). Both the  
114 Northern and the Southern allochthon include emplaced thrust sheets of Mesozoic  
115 carbonate platform, slope and deeper-water facies, melanges and ophiolitic rocks. The

116 relationships between the two allochthonous assemblages is debatable as they are  
117 separated by a relatively autochthonous Tauride platform succession, termed the Gürün  
118 autochthon (Kozlu et al., 1990; Atabey, 1993; Atabey et al., 1994, 1997; Robertson et al.,  
119 2013b) (Fig. 2).

120 The Mesozoic-Paleogene units within our study area are unconformably overlain by  
121 two geographically and temporarily distinct types of sedimentary basin. The first is  
122 represented by latest Cretaceous-latest Eocene basins, including the Darende, Hekimhan  
123 and Malatya basins; the second comprises Neogene-Recent sediments (Salyan Formation)  
124 and volcanics (Kepezdağ volcanics), notably within the Afşin-Elbistan basin, the Pınarbaşı-  
125 Kangal basin and the upper part of the large Malatya basin (Fig. 2). The area is dissected by  
126 through-going neotectonic faults, principally the westward-curving Sürgü-Misis Fault  
127 (Duman and Emre, 2013), and also three main NNE-SSW-trending faults, the Sarız, Gürün  
128 and Malatya-Ovacık faults. Of the latter, by far the largest is the Malatya-Ovacık fault, which  
129 is estimated to have accommodated 29 km of left-lateral movement (Fig. 2) (Westaway and  
130 Arger, 2001; Kaymakçı et al., 2006; Sancar et al., 2019). In addition, part of the area is  
131 transected by lesser known, c. SSW-NNE to SW-NE trending faults (Göksu faults of Kozlu et  
132 al., 1990) that are important because they straddle the contact between the Gürün  
133 autochthon and the Southern allochthon (Robertson et al., 2013b)

134 To facilitate description and interpretation, we subdivide our study region into 5 sub-  
135 areas (Fig. 2). *Area 1*, NW of Elbistan (Afşin); *Area 2*, Dağlıca; *Area 3*, E of Elbistan  
136 (subdivided into *Area 3A* in the west and *Area 3B* (Nurhak Dağı) in the east; *Area 4*, S of  
137 Elbistan, and finally, Divriği-Kemaliye in the north-east (subdivided into *Area 5A*, Kemaliye  
138 and *Area 5B*, Divriği farther north).

139

### 140 **3. Tauride carbonate platform**

141

142 To the SW of our study area (Tufanbeyli-Saimbeyli-Sarız) (Fig. 2), the autochthonous Tauride  
143 platform succession encompasses Precambrian sediments (Emirgazi Formation), Cambrian  
144 shelf siliciclastics (Feke Quartzites) and mixed carbonate-siliciclastic sediments (Çal Tepe  
145 Formation), which are overlain by Ordovician mainly argillaceous and silty shelf sediments  
146 (Seydişehir, Bedivan and Halit Yaylası formations) including some glacial deposits. Fine-  
147 grained siliciclastic sediments with calcareous intervals (e.g. Nautiloid limestones) dominate

148 the Silurian (Puşçu Tepe Shale and Yukarı Yayla formations). The Devonian is mainly shelf  
149 carbonates, with minor basaltic volcanics, including a reef-bearing horizon (Şafak Tepe  
150 Formation). The lower interval (Alitepesi Formation) and the upper interval (Gümüşali and  
151 Naltaş formations) are relatively quartz rich. Above a quartz-rich base, the Permian is  
152 dominated by algal carbonates (Yığılı Tepe Formation) (Özgül et al., 1973; Metin et al., 1986;  
153 Kozlu and Göncüoğlu, 1997; Özgül and Kozlu, 2002; Göncüoğlu et al., 2004; Bedi and Usta,  
154 2006; Bedi et al., 2017).

155 The Palaeozoic succession accumulated on a continental platform, punctuated by  
156 unconformities that were probably tectonically influenced; i.e. at the Precambrian-  
157 Cambrian boundary (?), the Early-Late Ordovician boundary, the Silurian-Devonian  
158 boundary, the Early-Middle Devonian boundary and the Carboniferous-Permian boundary.  
159 There was an increased sedimentation rate during the late Carboniferous (Göncüoğlu et al.,  
160 2004). This represents a period of enhanced tectonic subsidence that may relate to Variscan  
161 collisional orogeny farther west, in the Aegean-Balkan region.

162 The Mesozoic succession is dominated by shelf carbonates, with stratigraphic breaks  
163 that are likely to have been tectonically controlled; i.e. during the Middle Triassic, the Early-  
164 Mid Jurassic, the Late Cretaceous ( Turonian-Santonian(?)), and the Early Eocene (Kozlu et  
165 al., 1990). Devonian to Permian, and locally also Triassic, siliciclastic and carbonate rocks  
166 crop out in the northwest of the Gürün autochthon, where they are unconformably overlain  
167 by Early Jurassic to Late Cretaceous shelf carbonates. The Cretaceous carbonates pass  
168 upwards into Cenozoic facies without a structural break (Özgül et al., 1973). The succession  
169 continues with deeper-water (but still shelf-depth) hemipelagic carbonates, siltstones,  
170 mudrocks and sparse sandstones, dated as Maastrichtian-Middle Eocene (Lutetian) (Aziz et  
171 al., 1982; Perinçek and Kozlu, 1984; Yılmaz et al., 1991, 1994; Atabey, 1995; Robertson et al.,  
172 2013b). Locally, Eocene or older sediments in the Gürün autochthon are unconformably  
173 overlain by Miocene sediments (e.g. non-marine conglomerates), and also by Plio-  
174 Quaternary volcanics and sediments (Perinçek and Kozlu, 1984; MTA, 2011). There is no  
175 evidence of any major structural break or suture zone within, or between, the outcrops that  
176 extend northeastwards from the Saimbeyli-Tufanbeyli-Sarız region to the Gürün autochthon  
177 (MTA, 2011). This whole crustal unit can, therefore, be correlated with the relatively  
178 autochthonous Tauride carbonate platform in the central Taurides (Geyik Dağ).

179 The Jurassic-Cretaceous carbonates accumulated on a gently subsiding shelf,  
180 followed by accelerated subsidence that was probably tectonically controlled during the  
181 latest Cretaceous and Palaeocene-Early Eocene. There is no evidence of emplacement of  
182 any allochthonous units over the Gürün autochthon, at least until the Mid-Late Eocene  
183 (Perinçek and Kozlu, 1984; Kozlu et al., 1990; Robertson et al., 2013b); this observation is  
184 critical to any tectonic reconstruction.

185

#### 186 **4. Malatya metamorphics**

187 The regionally extensive Late Palaeozoic (Devonian?) to Late Cretaceous Malatya  
188 Metamorphics (Figs. 2, 3) are widely exposed in the south of the study area (Karaman et al.,  
189 1993; Yılmaz et al., 1991, 1994; MTA, 2011; Bedi and Yusufoglu, 2018). The outcrops are  
190 variously referred to as the Malatya Metamorphics in the type area (S of Elbistan), the  
191 Binboğa Metamorphics (NW of the Sürgü-Misis Fault; i.e. west of Afşin) and the Keban  
192 Metamorphics (east of the Malatya-Ovacık Fault) (Perinçek and Kozlu, 1984; Bedi et al.,  
193 2005, Bedi and Usta, 2006; Kaya, 2016). The Keban Metamorphics have been locally dated  
194 (south of Keban Lake) as  $73.8 \pm 0.3$  Ma (Campanian) based on  $^{40}\text{Ar}/^{39}\text{Ar}$  dating of muscovite  
195 within fluorite-bearing marble (Rolland et al., 2012). However, it is unclear whether this age  
196 is representative of the Malatya Metamorphics as a whole (see below).

197 The outcrop to the east of the Malatya-Ovacık Fault was recently remapped as three  
198 different units, separated by thrusts (Bedi and Yusufoglu 2018). The first unit, termed the  
199 Bodrum nappe (named after a type area in the western Taurides) is a metamorphosed  
200 Middle Devonian to Late Cretaceous succession (Fig. 3). The mineral assemblages in this unit  
201 (Bodrum nappe) are mainly suggestive of greenschist facies metamorphism (Perinçek and  
202 Kozlu, 1984). Local intercalations of basic metavolcanics rock (west of Afşin) are indicative of  
203 amphibolite facies conditions (Robertson et al., in press b). However, reported occurrences  
204 of glaucophane (Bedi et al., 2009) hint at high pressure-low temperature (HP-LT)  
205 metamorphism. The second, structurally overlying, unit is a metamorphosed Carboniferous  
206 to Late Cretaceous succession that is exposed SW of Malatya. This is correlated with the  
207 Yahyalı nappe, which has its type area further west, near Yahyalı. The Yahyalı nappe in its  
208 type area has undergone HP-LT metamorphism, based on the occurrence of carpholite

209 (Pourteau et al., 2010). Structurally above comes as third unit with a Late Devonian to Late  
210 Cretaceous succession, which is correlated with the Aladağ (Hadim) nappe in the central  
211 Taurides (Bedi and Yusufoglu 2018).

212 The thrust sheets, as summarised above, are intruded by Late Cretaceous arc-type  
213 granitoid rocks (Baskil Granitoids). These are mainly I-type, calc-alkaline hornblende-biotite  
214 granodiorites and 'normal' granites, with both mantle and crustal-derived chemical  
215 features. The granitoid rocks are dated, radiometrically, as 88-82 Ma (Santonian-  
216 Campanian) (Parlak, 2006; Yazgan and Chessex, 1991; Rızaoğlu et al., 2009; Karaoğlu et al.,  
217 2016). The Malatya Metamorphics are structurally underlain, directly, by the relatively  
218 intact Göksun ophiolite (Parlak, 2006; Parlak et al., 2004, 2020), also known in this area as  
219 the Berit meta-ophiolite (Genç et al., 1993; Yılmaz et al., 1987; Yılmaz, 1993), the North Berit  
220 ophiolite (Robertson et al., 2006), and the Kömürhan ophiolite (Bedi et al., 2005, 2009).

221 The Malatya Metamorphics (Bodrum nappe) are unconformably overlain by Middle  
222 Palaeocene to Middle Eocene shallow-water calcareous sediments (Seske Formation), as  
223 exposed near, and to the west of Afşin (Perinçek and Kozlu, 1984; Yılmaz et al., 1991, 1994;  
224 Robertson et al., 2006) (Fig. 4a). The succession begins with conglomerate, with clasts  
225 including schist and marble and then passes upwards into shallow-water limestones,  
226 commonly rich in large foraminifera (e.g. *Alveolina* sp.) and ooids (see below).

227 The protoliths of the Malatya Metamorphics (Bodrum nappe) within our main study  
228 area, namely the Binboğa Mountains west of Afşin (Area 1) and the Doğanşehir and  
229 Kemaliye areas farther east (Areas 3B, 5A) (Fig. 2), are dated with variable precision, mainly  
230 using benthic foraminifera and some small gastropods (Bedi et al., 2005, 2009). The overall  
231 succession (Fig. 3) begins with mixed meta-clastic and meta-carbonate rocks (Yoncayolu  
232 Formation) that are dated as Middle Devonian-mid Carboniferous. Meta-volcanic rocks (Fig.  
233 4b) and meta-rudites (Fig. 4c) are intercalated in places (Fig. 5 logs 1, 2). Within the Keban  
234 metamorphics farther east, basic meta-dykes cut the Late Palaeozoic succession; also,  
235 foliated meta-dyabase occurs within the upper part of the early Carboniferous (?) succession  
236 (Kaya, 2016). Overlying meta-limestones and meta-dolomitic carbonates (Çayderesi  
237 Formation) (Fig. 4d) contain a relatively rich, well-dated Late Permian fauna and flora.  
238 Above a meta-bauxite, representing a hiatus, calc-schist and meta-carbonate alternations

239 (Alıçlı Formation) are dated as Early-Mid(?) Triassic (Özgül et al., 1981). Meta-carbonates,  
240 commonly dolomitic, of Mid-Triassic to Early Jurassic age, follow above this (Kayaköy  
241 Formation) (Figs. 5 log 2, 4e). The succession passes upwards into shelf carbonates, with  
242 common nodular chert of diagenetic replacement origin (Ulu Formation), dated as Mid-  
243 Jurassic and Early Cretaceous. There is then a prominent unconformity, followed by meta-  
244 siliceous limestone, meta-mudrock and meta-conglomerate, termed the Karaböğürtlen  
245 Formation (Bedi et al., 2005, 2009). This unit is named after a Late Cretaceous chaotic  
246 'blocky flysch' in the western Taurides (Denizli-Burdur area) (Özgül et al., 1981; Şenel et al.,  
247 1989).

248

#### 249 4.1. Late Cretaceous syn-tectonic sediments

250

251 The succession in the Malatya Metamorphics (Bodrum nappe) extends through the  
252 Cretaceous in the form of mainly siliceous meta-limestones, meta-mudrocks and  
253 subordinate meta-conglomerates (Bedi and Yusufoglu, 2018). Within Area 1 (east of Afşin),  
254 the meta-carbonates are mapped as locally ending in the Triassic (e.g. at Ballık Tepe), or in  
255 the Late Permian (e.g. at Abaz Tepe) (Fig. 5 section b) (Bedi et al., 2009). In several sections,  
256 the platform carbonate succession ends with an unconformity, marked by fissuring with red  
257 iron-oxide infills (Fig. 4f) and an iron-rich layer (up to several cm thick). An intact succession  
258 of mixed meta-carbonate and meta-siliciclastic rocks follows above this, with subordinate  
259 metadeposit-flow deposits (Figs. 4g-i; 5 log 3), representing the Karaböğürtlen Formation.  
260 Clasts and blocks of Jurassic-Cretaceous meta-neritic limestone are present, and also, rarely,  
261 clasts of metabasalt. The matrix includes abundant monocrystalline and polycrystalline  
262 quartz, muscovite, carbonate and, locally, basaltic detritus (Fig. 6a-c). A Late Cretaceous  
263 (Cenomanian age) is inferred, at least for the lower part of this formation, based on local  
264 occurrences of rudist bivalves (Fig. 4k). Similar metamorphosed rudists occur in the  
265 Menderes Massif (Özer, 1998).

266 Thick-bedded meta-debris-flow deposits (calcirudites) are well exposed in a key  
267 section, c. 16 km north of Afşin (3 km S of Tanır) (Fig. 2; also Supplementary Fig. 2), where  
268 they include abundant deformed and fragmented recrystallised rudist bivalves. The meta-  
269 limestones pass into a thin (1m) interval of green meta-chert, formed by diagenetic  
270 replacement of carbonate, followed by reddish-brown meta-conglomerate (several m thick),

271 with abundant rounded pebbles (<10 cm in size) of red radiolarian meta-chert and also  
272 meta-limestone (recrystallised), set in a sandy matrix. After further meta-limestone  
273 conglomerate, with rounded clasts (<10 cm in size), there is a return to thick-bedded detrital  
274 meta-carbonates before the section ends. This section is important as it indicates that  
275 relatively deep-water facies (radiolarian cherts) were redeposited onto the Malatya  
276 carbonate platform during the Late Cretaceous (see below).

277 In another key section, c. 20 km to the NW (near İncirli), where the Malatya  
278 Metamorphics (Bodrum nappe) are thrust northwards over the Southern allochthon (see  
279 below), the Karaböğürtlen Formation (up to 300 m thick) comprises lenses (up to >100 m  
280 long by 20 m thick) of medium-thick bedded meta-limestone (marble), alternating with  
281 sheared and folded meta-mudrock (phyllite.) Both the blocks and the matrix have  
282 undergone similar metamorphism. Near the thrust contact there are marble blocks (tens of  
283 cm-to m-sized) within sheared matrix-supported conglomerates (Fig. 4j). This section  
284 confirms that the Karaböğürtlen Formation includes meta-debris-flow ('olistostromes')  
285 related to Late Cretaceous tectonic instability.

286

#### 287 4.2. Interpretation of the Malatya Metamorphics

288

289 During Middle Devonian to Carboniferous, the Malatya Metamorphics (Bodrum nappe)  
290 accumulated on a mixed carbonate-clastic-depositing shelf, punctuated by tectonic  
291 instability, basaltic volcanism and localised mass-flow deposition. Marine transgression  
292 characterised the Late Permian, followed by rift-related tectonic instability and subsidence  
293 during the Early-Mid Triassic. A relatively stable, gently subsiding carbonate platform  
294 developed during the Late Triassic-Cretaceous, deepening during the Early Cretaceous, as  
295 suggested by increased chert content. The rudist reefs signify shallowing during the  
296 Cenomanian. The carbonate platform was uplifted and variably eroded, in places down to  
297 the Late Permian, resulting in a regional unconformity that was capped by metalliferous  
298 oxides during a hiatus in deposition. The unconformity was then covered by a Late  
299 Cretaceous (but poorly dated), mixed carbonate-siliciclastic succession, including local  
300 debris flow-deposits. The siliciclastic detritus, largely derived from metamorphic and  
301 plutonic igneous rocks, was probably recycled from the underlying Malatya succession. The  
302 well-rounded nature of many of the pebbles, especially meta-chert (Fig. 6a, b) is indicative

303 or reworking in a high-energy shallow-marine or fluvial setting prior to redeposition as  
304 debris flows. The pebbly conglomerates with red chert (near Tanır) show that deep-sea  
305 material, typical of the Southern allochthon to the north, was redeposited into the subsided  
306 Malatya platform.

307         The Late Cretaceous Karaböğürtlen Formation is interpreted as the proximal  
308 (southerly) part of a regional-scale, flexurally-controlled foredeep related to Late Cretaceous  
309 emplacement of continental margin and ophiolitic rocks. However, ophiolitic material is  
310 absent from the Karaböğürtlen Formation, in contrast to structurally higher units (see  
311 Discussion).

312         The timing of metamorphism of the Malatya Metamorphics is stratigraphically  
313 constrained as postdating the youngest deposition (Late Cretaceous (?) Karaböğürtlen  
314 Formation) but predating the Eocene sedimentary cover (Seske Formation) (Özgül et al.,  
315 1981; Perinçek and Kozlu, 1984; Kozlu et al., 1990; Robertson et al., 2006; Bedi et al., 2009).  
316 East of the Malatya-Ovacık Fault, the Keban metamorphics are locally dated radiometrically  
317 as  $73.8 \pm 0.3$  Ma (Campanian) (Rolland et al., 2012). In this area the metamorphics are  
318 unconformably overlain by latest Cretaceous sediments, known as the Gündüzbey  
319 Formation, which correlates with the regional Harami Formation (Erdoğan, 1975). The  
320 Gündüzbey Formation begins with polymictic conglomerates, followed by sandstone-shale-  
321 conglomerate alternations (generally Santonian-Campanian in age) and then shelf  
322 carbonates (Campanian-Maastrichtian) (Bedi and Yusufoglu, 2018). Along the eastern  
323 margin of the Malatya basin, the late Cretaceous sediments are unconformably overlain,  
324 directly, by Eocene conglomerates, limestones and turbidites (Yeşilyurt Formation) (Bedi et  
325 al., 2017; Bedi and Yusufoglu, 2018). The 88-82 Ma (Santonian-Campanian) Baskil Granitoids  
326 that cut the Malatya Metamorphics are inferred to have taken 6–10 Ma to cool below 300  
327 °C, based on  $^{39}\text{Ar}$ – $^{40}\text{Ar}$  dating of amphibole, biotite and K-feldspar (Karaoglan et al., 2016).

328         The Malatya metamorphics as a whole are intruded by the Baskil granites  
329 (unmetamorphosed). The long period of time (6-10 Ma) taken to cool below 300° suggests  
330 that the granites were intruded into crust with a high heat flow, presumably related to arc  
331 magmatism. The U-Pb age (88-83 Ma) of the granitoid intrusions is significantly older than  
332 the reported age of metamorphism ( $73.8 \pm 0.3$  Ma) (Rolland et al., 2012). However, the  
333 fluorite-bearing marble that was dated by these authors could represent a late-stage  
334 metasomatic event. The Malatya Metamorphics including the granite-bearing units were



335 tectonically imbricated after intrusion (e.g. E of Doğanşehir) (Bedi and Yusufoglu, 2018),  
336 probably during the Eocene.

337

## 338 **5. Late Triassic-Late Cretaceous unmetamorphosed platform carbonates**

339

### 340 5.1. Neritic thrust sheets

341

342 The mainly neritic Munzur thrust sheet (Fig. 2) is equivalent to the Munzur nappe of Özgül  
343 et al. (1981) and Bedi et al. (2004, 2009), to the Andırın Limestone of Perinçek and Kozlu  
344 (1984) and to the Neritic nappe of Robertson et al. (2013b). Similar successions are exposed  
345 in both the Northern allochthon and the Southern allochthon, respectively, to the north and  
346 the south of the Gürün autochthon (Fig. 2). South of the Gürün autochthon, in Area 2  
347 (Dağlıca), the Munzur thrust sheet comprises two main units; first, an extensive, relatively  
348 intact, lower Munzur thrust sheet, and secondly a thinner, internally disrupted upper  
349 Munzur thrust sheet (transitional to broken formation). The succession in the lower Munzur  
350 thrust sheet is widely exposed in Area 2 (Dağlıca) (Fig. 7 sections a-f), in Area 3A (E of  
351 Elbistan) (Fig. 8 sections a-e) and in Area 4 (S of Elbistan (Fig. 9). The Munzur thrust sheets  
352 are entirely Mesozoic, with no preserved Late Palaeozoic substratum, in contrast to the  
353 Malatya Metamorphics (Bodrum nappe). The complete Late Triassic to Late Cretaceous  
354 succession is exposed in the lower Munzur thrust sheet (Bedi et al., 2004, 2009; Bedi and  
355 Yusufoglu, 2018), whereas Cretaceous facies are commonly exposed in the more localised  
356 upper Munzur thrust sheet, mainly in Area 2 (Fig. 7) and Area 3A (Fig. 8). During this study,  
357 bioclastic limestones in the upper Munzur thrust sheet were dated as late Barremian-early  
358 Aptian (near Küçük Tatlar) (see Supplementary table 1). Higher stratigraphic levels are rich  
359 in Cenomanian rudist bivalves.

360 Taking the Munzur thrust sheets together, the succession begins with Norian thick-  
361 bedded neritic limestone, rich in calcareous algae (Fig. 10a) and Megalodonts, with local  
362 evidence of intraformational reworking and tectonic instability (Fig. 10b, c). Above an  
363 unconformity, the Early Jurassic begins with a conglomerate, overlain by pinkish nodular  
364 micritic limestone, up to 40 m thick, rich in crinoids, algae, ammonites and gastropods. The  
365 Middle Jurassic to Early Cretaceous interval is neritic, commonly oolitic and/or rich in  
366 benthic foraminifera. The neritic succession typically culminates in a Cenomanian interval

367 rich in rudist bivalves (Fig. 10d), as well-exposed in the upper Munzur thrust sheet in Area 2  
368 (Dağlıca) (Fig. 10e).

369 The neritic limestones are covered by Albian-Santonian pinkish pelagic carbonates,  
370 with sparse thin-bedded bioclastic calcarenites, known as the Kızılkandil Formation  
371 (equivalent to the Kırmızı Kandil Formation of Perinçek and Kozlu 1984) (Fig. 10 f). In places  
372 (e.g. Küçük tepe-Gerdekes yayla), rudist-bearing neritic limestones are reported to grade  
373 laterally and vertically into *Globotruncana*-bearing pelagic limestones (Bedi et al., 2009).  
374 The pelagic carbonates include thin (several cm) interbeds of fine to medium-grained,  
375 neritic-derived calciturbidites; locally (e.g. near Erikli) these include redeposited Late  
376 Jurassic-Early Cretaceous benthic foraminifera (see Supplementary Table 1). The succession  
377 ends with an unconformity, which is covered by a ferruginous oxide crust in some sections  
378 (Fig. 10g); this is overlain by latest Cretaceous syn-emplacement facies (Kemaliye Formation;  
379 see below).

380 In one area (e.g. E of Tavla), a small thrust sheet is dominated by limestone breccia-  
381 conglomerate (mass-flow accumulations) and calciturbidites (c. 150 m thick) (Fig. 10h). This  
382 unit is tentatively interpreted as proximal platform-slope facies.

383 For the Late Triassic, there is widespread evidence of tectonic instability related to  
384 regional rifting. The Jurassic-Cenomanian succession accumulated on the inner part of a  
385 gently subsiding carbonate platform (Yılmaz, 1994), mainly influenced by global sea-level  
386 change. The Albian-Santonian pelagic carbonates (Kızılkandil Formation) accumulated  
387 during a time of overall relatively high global sea level (Miller et al., 2005). However, the  
388 presence of interbedded bioclastic calciturbidites points to sub-aqueous erosion that was  
389 probably triggered by contemporaneous tectonic instability. There was then a hiatus (up to  
390 c. 8 Ma), allowing local precipitation of ferruginous oxide from seawater, before syn-  
391 emplacement facies (Kemaliye Formation) began to accumulate. The hiatus is likely to be  
392 coeval with the break in deposition that affected the adjacent Malatya Metamorphics, and  
393 is interpreted to represent the southward passage of an emplacement-related flexural bulge  
394 (see below).

395

396 5.2. Late Triassic-Late Cretaceous Neritic-pelagic (Köseyahya) thrust sheet

397

398 The traditional Munzur nappe (Perinçek and Kozlu, 1984) is made up of two separate  
399 regional-scale thrust units. The first comprises the Munzur thrust sheets, which are neritic  
400 throughout Late Triassic-Cenomanian, as summarised above. The second is the Köseyahya  
401 thrust sheet, as defined near Köseyahya, to the south of the Gürün autochthon (Bedi et al.,  
402 2005, 2009) (Fig. 8). A similar succession, termed the Neritic-pelagic nappe is exposed to  
403 the north of the Gürün autochthon (Robertson et al., 2013b). The successions in both areas  
404 can be correlated and are here referred to as the Neritic-pelagic (Köseyahya) thrust sheet.

405 The most complete succession (Fig. 3) through the Neritic-pelagic (Köseyahya) thrust  
406 sheet is exposed in the type area, near Köseyahya (Area 3A, near log III) (Fig. 8 sections a, e,  
407 f) (Bedi et al., 2009), with an additional outcrop in Area 4, south of Elbistan (Fig. 9 sections a,  
408 b) and Area 4B, Nurhak Dağı). The type section is located 750 m south of Köseyahya (near  
409 Burmakaya Tepe) (Tekin and Bedi, 2007a, b; Dumitrica et al., 2013). There, the succession  
410 begins in the Middle Carnian, as dated by radiolarians, with alternations of fine-grained  
411 sandstone, calcareous siltstone, marl, mudstone and micritic limestones. Volcaniclastic  
412 interbeds and chert of diagenetic replacement origin are also present, mainly in the higher  
413 levels. The succession continues with Late Carnian pink to red calcilutites (4.6 m thick), rich  
414 in ammonoids, crinoids, conodonts and pelagic bivalves (*Halobia* sp.) ('Hallstatt limestone')  
415 (Fig. 10i, j) (Bedi et al., 2016). Medium to thick-bedded Norian white limestones above  
416 ('Dachstein limestones') (Fig. 10k) include abundant Megalodonts and benthic foraminifera  
417 (Tekin and Bedi, 2007a, b). Above a discontinuity, the Early Jurassic is made up of relatively  
418 thin, stratigraphically condensed (c. 20 m), nodular, ammonite-rich micritic limestone  
419 ('Ammonitico Rosso'). The Mid-Late Jurassic is dominated by redeposited limestones  
420 (calciturbidites), with pelagic carbonate interbeds that are commonly silicified. The  
421 redeposited limestones are rich in neritic grains, especially ooids and are extensively  
422 silicified. Radiolarian chert increases in abundance during the Tithonian-Cenomanian  
423 interval. The Early Cretaceous (Tithonian-Berriasian) is dated using calpionellids within  
424 pelagic interbeds (Area 3A, E of Elbistan) (Fig. 10l) (see Supplementary table 1).

425 The upper part of the succession (Özbey Formation), where exposed, is  
426 positionally overlain by pinkish pelagic carbonates with radiolarian chert intercalations.  
427 The pinkish pelagic carbonates are similar to those of the Munzur thrust sheets (see above)  
428 and have been given the same name (Kızılkandil Formation), although only those in the  
429 Neritic-pelagic (Köseyahya) thrust sheet are siliceous. The type section (near Kızılkandil

430 mezası), c. 40-50 m thick, depositionally overlies a layer of redeposited oolitic limestone  
431 (Özbey Formation). In a nearby succession, the Kızılkandil Formation unconformably overlies  
432 older neritic facies (Demirlitepe Formation), and includes both planktic foraminifera of  
433 Turonian-Santonian age and also radiolarians of Turonian-Santonian age. Another section,  
434 which is faulted against Late Triassic neritic facies (Ortakandil Tepe), contains Turonian  
435 planktic foraminifera and radiolarians; a further section (Han tepe-Toklu tepe) contains  
436 Turonian-Santonian radiolarians (Bedi et al., 2009).

437         The Kızılkandil Formation has been variously dated as Turonian-early Campanian  
438 (Perinçek and Kozlu, 1984), Coniacian-Campanian (Pehlivan et al., 1991), or Albian-  
439 Santonian, using a combination of nannofossils, radiolarians and planktic foraminifera (Bedi  
440 et al., 2009). The shortest-ranging planktic foraminifera, determined by Dr. A. Hakyemez,  
441 are *Rotalipora ticinensis*, *Rotalipora apenninica* (upper Albian), *Helvetoglobotruncana*  
442 *helvetica* (lower-middle Turonian) and *Dicarinella asymetrica* (Santonian) (Robaszynski and  
443 Caron, 1995). Radiolaria range from Albian-Santonian (Bedi et al., 2009). The pelagic  
444 limestones are unconformably overlain by the syn-emplacement Kemaliye Formation (see  
445 below).

446         The succession in the Neritic-pelagic (Köseyahya) thrust sheet began to accumulate  
447 during the Carnian on a submerged shelf, in the form of stratigraphically condensed,  
448 hemipelagic limestones and siliceous sediments, which are variably rich in ammonites,  
449 crinoids, foraminifera, calcareous algae and radiolarians. Condensed ammonite-rich, red  
450 pelagic carbonate deposition persisted during the Early Jurassic. During the Late Jurassic,  
451 the carbonate platform developed into a gently sloping carbonate ramp on which  
452 redeposited ooid-rich facies accumulated. The probable source was the adjacent shallow-  
453 water Munzur carbonate platform. The greatly increased abundance of chert in the  
454 Tithonian-Albian interval points to further deepening. This probably resulted from tectonic  
455 subsidence because global sea-level rise is not inferred during this time interval (Haq, 2014).  
456 Where the pelagic limestones (Kızılkandil Formation) overlie older parts of the succession  
457 (Demirlitepe Formation), tectonically induced uplift and submarine erosion are inferred. The  
458 pelagic carbonates accumulated during the mid-Late Cretaceous (Albian-Santonian), as in  
459 the Munzur thrust-sheet succession. The sea floor was already deep, favouring continuing  
460 radiolarian deposition. The appearance of pelagic carbonate probably represents increased  
461 planktic productivity (Bosellini and Winterer, 1975).

462 The Late Cretaceous pelagic carbonates in both the Munzur and Köseyahya  
463 successions are similar to those overlying the Tauride carbonate platform elsewhere,  
464 including the Bey Dağları (Poisson, 1977, 1984) and the Geyik Dağ (Sarı and Özer, 2002; Sarı  
465 et al., 2004). In the Geyik Dağ (central Taurides), Cenomanian rudist-rich facies are overlain  
466 by pelagic carbonates that accumulated until the Eocene (Solak et al., 2017, 2019), similar to  
467 the Gürün autochthon (Fig. 2).

468

## 469 **6. Late Permian-Late Cretaceous Pelagic (Gülbahar) unit**

470

471 Widely distributed, dismembered Late Permian to Late Cretaceous deep-water successions,  
472 including both pelagic and coarser-grained redeposited facies, and also basaltic rocks were  
473 previously included within the Dağlıca Complex ('flysch with blocks'), together with  
474 dismembered ophiolitic rocks (Kozlu et al., 1990; Perinçek and Kozlu, 1984). However, more  
475 recent mapping and stratigraphical studies indicate the presence of an originally intact  
476 Triassic to Late Cretaceous deep-water platform-margin succession. This has been named  
477 the Gülbahar Nappe (Bedi et al., 2009, 2018), based on a proposed correlation with  
478 comparable deep-sea successions including basaltic volcanics in the western Taurides (Şenel  
479 et al., 1989; Collins and Robertson, 1998; Sayit et al., 2015). The deep-sea platform-margin  
480 succession in the Eastern Taurides has also been termed, informally, as the Pelagic nappe, in  
481 contrast to the traditional Munzur thrust-sheet neritic succession (Robertson et al., 2013b).

482 No complete succession of the Pelagic (Gülbahar) unit is known in any one section,  
483 although an overall stratigraphy can be pieced together (Fig. 3). Local sections show  
484 considerable facies variation and may represent combinations of lateral variation and/or  
485 proximal-distal changes. The most intact sequences are mainly located to the south of the  
486 Gürün autochthon in Area 2 (e.g. Büyük Tatlı), whereas, within the Northern allochthon, the  
487 Pelagic unit is mainly represented by blocks of Mesozoic deep-water facies within melange  
488 (Robertson et al., 2013b).

489 During the present study, local sequences of the Pelagic (Gülbahar) unit were  
490 studied in Areas 2-4 (Figs. 7-9). Relatively intact and continuous sequences (up to c. 80 m  
491 thick) are exposed between the lower and the upper Munzur thrust sheets in Area 2  
492 (Dağlıca) (Fig. 7; e.g. near Tatlar, specifically Büyük Tatlı), although these are too small and  
493 localised to show effectively on regional-scale maps. Up to tens of m-thick sequences are

494 widely exposed beneath the Köseyahya thrust sheets in Area 3A (E of Elbistan) (Fig. 8), and  
495 also occur beneath both the Munzur and Köseyahya thrust sheets in Area 4 (south of  
496 Elbistan) (Fig. 9). In addition, variable-sized, isolated blocks of similar lithologies are strewn  
497 through the late Cretaceous syn-tectonic Kemaliye Formation, as exposed in each of the  
498 above areas (see below).

499         The oldest known lithologies in the Pelagic (Gülbahar) unit are Late Permian  
500 siltstones, marls, siliceous limestones and thin-bedded limestones, including fusulinids and  
501 benthic foraminifera (Bedi et al., 2009) (Fig. 11, logs II, III; see Fig. 8 for locations). There are  
502 also short, highly deformed intervals of Triassic sandstone and shale (Fig. 12a, b). Jurassic-  
503 Cretaceous facies are mainly non-calcareous radiolarites and radiolarian mudstones,  
504 interbedded with pelagic carbonates (Fig. 12c), variably silicified calciturbidites (Fig. 12 d, e)  
505 and carbonate debris flow-deposits, variably rich in chert clasts (Fig. 12 f-i). The redeposited  
506 limestones are rich in redeposited ooids, oolitic limestone, pisoliths, benthic foraminifera  
507 (with oolitic coatings) and calcareous algae. Reworked pelagic limestone, radiolarian chert,  
508 monocrystalline quartz and muscovite are also present.

509         Variably preserved radiolarians, identified during this study (see Table 1), yielded the  
510 following Late Triassic to Late Cretaceous ages for local sections or blocks: Late Norian  
511 (block in serpentinite, near Yoksullu mezra (Area 4; Fig. 11, log I); Middle Jurassic (Bajocian),  
512 near Büyük Tatlı (Area 2) and near Yoksullu mezra; Late Oxfordian near Yoksullu mezra; Late  
513 Oxfordian-Tithonian near Kayseri (Area 2, log VII) and near Topaktaş (Area 2, log VIII);  
514 Kimmeridgian-early Tithonian near Büyük Tatlı and near Yoksullu mezra; Late Tithonian-  
515 Berriasian near Büyük Tatlı); Late Valanginian-Hauterivian (block in debris-flow deposit) near  
516 Kabaktepe; Early Albian at Kırandere (near İncelik köy; Area 2); Aptian at Kırandere; and Late  
517 Albian-Cenomanian also at Kırandere. In addition, redeposited benthic foraminifera are  
518 dated more generally as Late Jurassic-Early Cretaceous (at Kaşanlı, Küçük Tatlı and Büyük  
519 Tatlı, all in Area 2 (see Supplementary Table 1).

520         An overall deep-marine, lower slope to base of-slope setting is inferred for the  
521 Pelagic (Gülbahar) unit. Late Permian pelagic carbonates with relatively fine-grained  
522 siliciclastic turbidites were followed by Early to Middle Triassic hemipelagic mudrocks, fine-  
523 grained sandstone turbidites and thin-bedded hemipelagic carbonates. Middle to Late  
524 Triassic hemipelagic limestones (Halobia limestones), radiolarian sediments, calciturbidites,  
525 quartzose sandstone/siltstone turbidites and, locally redeposited conglomerates, followed

526 above this. The Jurassic-Early Cretaceous encompassed non-calcareous radiolarian muds,  
527 variably silicified calciturbidites and also debris-flow deposits with reworked neritic clasts  
528 (e.g. oolitic limestone) and/or pelagic clasts (radiolarite; pelagic limestone). Deposition  
529 locally culminated in large-scale gravity collapse of slope facies, leading to redeposition,  
530 with clasts of neritic/pelagic limestone and radiolarite in a matrix of lithoclastic debris-flow  
531 deposits, sandstone turbidites, ophiolite-derived debris-flow deposits, calciturbidites and  
532 muds. The ophiolite-bearing mass-flow units represent a depositional-tectonic link between  
533 the passive margin slope lithologies and the emplacement-related mass-flow units which  
534 are located higher in the tectono-stratigraphy (see below).

535 In places (e.g. Dağlıca, Area 2), short, highly deformed sequences of basalt,  
536 volcanoclastic sandstone and/or hyaloclastite are interbedded with Middle-Late Triassic  
537 deep-water calcareous and siliceous facies (Kozlu et al., 1990; Bedi et al., 2009; Robertson et  
538 al., 2013b). Chemically, the basalts are of enriched, alkaline, within-plate type (Robertson et  
539 al., 2013b). A sample of radiolarian chert from Area 2 (Bakış) gave a Norian (Late Triassic)  
540 age (Fig. 11 log II; see Table 1). In addition, in Area 5A (Kemaliye) (Fig. 2) basaltic lavas of the  
541 Pelagic (Gülbahar) unit are interbedded with Late Triassic pelagic limestones (dated) and  
542 radiolarian cherts (see Supplementary Table 1).

543 The Pelagic (Gülbahar) unit accumulated adjacent to the Munzur and Köseyahya  
544 thrust sheet successions, taken together. The Permian siliciclastic material is likely to have  
545 been derived from an original, but now tectonically detached, substratum of the carbonate  
546 platform units. The Triassic records subsidence, localised alkaline basaltic volcanism (rift-  
547 related), terrigenous sand/silt gravity input, hemipelagic carbonate deposition (periplatform  
548 ooze) and radiolarian accumulation in a fertile sea. The Jurassic-Cretaceous was  
549 characterised by 'background' radiolarian and siliceous pelagic carbonate deposition  
550 (diagenetically altered to chert), beneath (or near) the carbonate compensation depth  
551 (CCD). The calciturbidites and carbonate debris-flow deposits accumulated on an unstable  
552 slope, derived from the adjacent carbonate platform. The Late Cretaceous is characterised  
553 by pelagic limestone, marl and chert that accumulated above the CCD, with *Globotrunca* sp.,  
554 as in the adjacent carbonate platform units (equivalent to the Kızılkandil Formation). The  
555 presence of ophiolite-derived debris-flows within a sequence affected by slumping and soft-  
556 sediment deposition suggests that the distal platform slope over-steepened and collapsed  
557 related to ophiolite emplacement.

558

## 559 **7. Late Cretaceous emplacement-related Kemaliye Formation**

560

561 In different areas, the Malatya Metamorphics and both the Munzur and Köseyahya platform  
562 units are positionally overlain by Late Cretaceous syn-tectonic lithologies that provide key  
563 information concerning the nature and timing of both tectonic emplacement and  
564 exhumation in the region. In general, the lithologies form coherent to highly disrupted  
565 successions, which are characterised by matrix-supported conglomerates, blocks, or  
566 dismembered thrust sheets, all set within an argillaceous and/or sandy matrix. The syn-  
567 tectonic units occur at two different structural levels in the regional thrust stack. The  
568 higher-level unit overlies the Munzur/Köseyahya platform units, whereas the lower-level  
569 unit overlies the Malatya (Keban) metamorphics.

570 In the northeast of the region studied, near Kemaliye (Figs. 13, 14 Area 5A), meta-  
571 carbonate rocks (Kaletepesi limestone) that are correlated with the lower part of the Keban  
572 metamorphics (Bilgiç, 2008b, c) are mapped as being unconformably overlain by  
573 'olistostromes', named the Kemaliye Formation, after the town in this area (Figs. 13, 14)  
574 (Özgül et al., 1981; Özgül and Turşucu, 1984; Perinçek and Kozlu, 1984; Bilgiç, 2008b, c). The  
575 formation has been inferred to be Late Senonian (Özgül et al., 1981), or more specifically  
576 Late Campanian-Early Maastrichtian (Bilgiç, 2008b, c), based on the youngest datable  
577 fossiliferous material (i.e. *Globotruncana*-bearing pelagic limestone). In general, the  
578 succession has been described as beginning with localised conglomerates, with clasts of  
579 dark grey limestone, chert and diabase, passing into sandstone, with common basic igneous  
580 rock and limestone grains, and also interbeds of sandstone and marl (Perinçek and Kozlu,  
581 1984). In its type area, the Kemaliye Formation is locally overlain, unconformably, by Early  
582 Eocene lithologies (Subaşı formation) (Bilgiç, 2008b, c). The Kemaliye Formation appears to  
583 correlate with the latest Cretaceous Gündüzbey Formation, to the south of Malatya.

584 The term, Kemaliye Formation was later adopted for all of the Late Cretaceous  
585 unmetamorphosed syn-tectonic facies in the region, including those associated with the  
586 allochthonous Munzur and Köseyahya successions (Bedi and Yusufoglu, 2018). However,  
587 this is problematic for several reasons: (1) The underlying units differ strongly in different  
588 areas (i.e. Malatya (Keban) Metamorphics in the type area, versus Munzur-Köseyahya  
589 unmetamorphosed carbonate platform elsewhere); (2) The Kemaliye Formation in its type



590 area includes lithologies (e.g. basalt-pelagic limestone-radiolarite) that are assigned to the  
591 Pelagic (Gülbahar) unit elsewhere (i.e. it is a composite unit); (3) The Kemaliye Formation, as  
592 previously mapped, is, in part, tectonically assembled rather than an intact sedimentary  
593 succession.

594         Although we retain the general name, Kemaliye Formation here for consistency with  
595 previous work, the occurrences in three different tectono-stratigraphic settings are  
596 discussed separately below. These are: (1) Unconformably overlying the Malatya (Keban)  
597 Metamorphics in Area 5A (Kemaliye) (Figs. 15a, 16a); (2) Unconformably overlying the  
598 Munzur and/or the Köseyahya thrust sheets, and also underlying the Munzur and Köseyahya  
599 thrust sheets where no basement is exposed. Consideration of these two main contrasting  
600 settings allows a more refined interpretation in terms of syn- versus post-emplacement  
601 tectonics.

602

#### 603 7.1. Late Cretaceous Kemaliye Formation overlying the Malatya (Keban) Metamorphics

604

605 An unconformity is mapped between the Kemaliye Formation and the Malatya (Keban)  
606 Metamorphics west of Keban Lake (Bilgiç, 2008b, c) (Fig. 14). The meta-carbonate rocks  
607 near the contact are in places converted to calc-mylonite, indicating high-strain conditions  
608 (Fig. 16b). In some areas, the lower part of the formation is dominated by crudely bedded  
609 debris-flow conglomerates (Fig. 15a; 16c), as logged locally (Fig. 17). These contain  
610 abundant clasts of metamorphic rocks (Fig. 16d), together with radiolarian chert (Fig. 16e),  
611 deformed limestone (Fig. 16f), granite (locally), coral and large bivalves (rudists). Above this,  
612 much of the outcrop is dominated by blocks and dismembered thrust sheets (Fig. 16a).  
613 Many of the blocks are well-bedded, commonly dark, organic-rich limestones (typically 10s  
614 of m in size). Short, intact sequences of well-bedded limestones are intercalated with  
615 limestone conglomerates (calcirudites) that locally include well-rounded clasts and rudist  
616 debris of probable Cenomanian age. Neritic limestones of Triassic-Cretaceous age, chert  
617 (undated) and Late Cretaceous pelagic limestones are also present. A neritic limestone block  
618 (near Yuva; Fig. 14) is dated as Triassic based on benthic foraminifera (Fig. 18a, b; see also  
619 Supplementary Table 1). In one area, slices and/or large blocks of basaltic lava are exposed  
620 above the contact with the metamorphics (Fig. 15b). The lavas are interbedded with pelagic  
621 limestones that contain a typical Triassic fauna, including *Halobia* sp. and radiolarians (see

622 Supplementary Table 1). Although mapped as Kemaliye Formation (Bilgiç, 2008b, c) this  
623 volcanogenic unit belongs to the Pelagic (Gülbahar) unit (see above).

624 The matrix of the Kemaliye Formation in the type area is extremely heterogeneous,  
625 including variable abundances of monocrystalline quartz, polycrystalline quartz, plagioclase  
626 (altered), muscovite, biotite, epidote, clinopyroxene, hornblende, chlorite (including blue  
627 chlorite), zircon, apatite and opaque grains, in generally decreasing order of abundance.  
628 Lithoclasts are mainly micaschist, quartzite, chert, neritic limestone, basalt (with orientated  
629 microphenocrysts), altered basic volcanic glass (palagonite), felsic volcanics (recrystallised),  
630 dacite (with plagioclase phenocrysts), granite, bioclastic carbonate, marble, dolomite,  
631 sandstone (with parallel-orientated muscovite laths), siltstone (locally iron-rich), shale  
632 (partly recrystallised), serpentinite, gabbro, diabase, phyllite, phyllonite and mylonite (Fig.  
633 6d-g). Bioclasts include micritic grains with shell fragments, pellets, benthic foraminifera,  
634 algal grains (pisoliths) and/or oolitic limestone (with clear, plutonic quartz cores). The matrix  
635 is either calcareous (partly recrystallised), or siliciclastic (with fine quartz and muscovite).  
636 Most grains are angular although a few are well-rounded. Some samples have a calcite spar  
637 cement.

638 In the northeast, where the Kemaliye Formation is mainly covered by younger  
639 volcanics (Fig. 14; NE of Yaka), small exposures of debris-flow deposits include clasts and  
640 blocks of altered lava, serpentinite and platy grey-pink Triassic pelagic limestone (see  
641 Supplementary Table 1). Farther northeast again, towards Ovacık (Fig. 13), the formation  
642 includes a large (c. 5 km-long) tabular body of Permian limestone that is tectonically  
643 overlain by serpentinised ultramafic rocks (Bilgiç, 2008b, c; MTA, 2011).

644

## 645 7.2. Kemaliye Formation associated with the Munzur and Köseyahya thrust sheets

646

647 Previous authors reported that the Munzur limestones, including the Late Cretaceous  
648 pelagic limestones (Kızılkandil Formation), pass unconformably upwards into syn-tectonic  
649 calcareous siltstones and sandstones, followed by an incoming of limestone blocks. This unit  
650 was termed the Binboğa Formation by Perincek and Kozlu (1984), named after the Binboğa  
651 Mountains 20 km west of Afşin. However, the term Binboğa Formation was later applied to  
652 the entire Early Triassic-Early Cretaceous succession of the Munzur thrust sheet (Kozlu et al.,  
653 1990), complicating the use of this name. The latest Cretaceous syn-tectonic interval was

654 later correlated with the Kemaliye Formation (Bedi et al., 2009; Robertson et al., 2013b;  
655 Bedi and Yusufoglu, 2018), although, as noted above, this unit differs strongly from the type  
656 Kemaliye area.

657 Planktic foraminifera from the Kemaliye Formation above the Munzur limestones  
658 (Bedi et al., 2009) are long-ranging throughout Campanian-Maastrichtian. The shortest-  
659 ranged taxon is *Globotruncana dupeublei*, whose first occurrence (base) is within the  
660 *Gansserina gansseri* Zone (71.75-72.97 Ma; late Campanian-early Maastrichtian), whereas  
661 the last occurrence (top) is within the *Abatomphalus mayaroensis* Zone (67.30-69.18Ma; top  
662 of Maastrichtian stage) ([microtax.org/pforams/index.php](http://microtax.org/pforams/index.php)). In addition, nannoplankton data  
663 support a late Campanian-late Maastrichtian age for the Kemaliye Formation within the  
664 Munzur and Köseyahya thrust sheets (Bedi et al., 2009).

665 During this study, six sections of the Kemaliye Formation within the main Munzur  
666 thrust sheet were logged in Area 2 (Dağlıca), where they show considerable facies variation  
667 (Fig. 19 logs 1-6). The formation is typically dominated by alternations of calcareous  
668 mudstone-siltstone-sandstone (Fig. 19 logs 1, 2, 4). In places, sandstone, limestone  
669 conglomerates (calcirudites) and limestone breccias appear near the base of the succession  
670 (Fig. 19; logs 3, 5, 6; Fig. 20a, b). During this study, intervals of pinkish pelagic limestone  
671 were dated as Campanian-Maastrichtian (near Kapaklı; see Supplementary Table 1). Benthic  
672 foraminifera within a limestone block, near Kaşanlı, yielded an Early Cretaceous age  
673 (Supplementary Table 1). Other blocks are rich in rudist bivalves (Fig. 20c, d).

674 The upper levels of the succession are commonly tectonically disrupted and include  
675 neritic and pelagic limestone blocks (Fig. 19 log 6; Fig. 20d, e). Clasts of bioclastic calcarenite  
676 yielded reworked Middle-Late Jurassic benthic foraminifera (see Supplementary Table 1). In  
677 places, the outcrop is chaotic with limestone blocks strewn through a sheared mudstone-  
678 sandstone matrix.

679 The sandstone interbeds are heterogeneous and include both monocrystalline and  
680 polycrystalline quartz, muscovite, neritic carbonate, chert, quartzose siltstone and basalt  
681 (Fig. 6h-i). The calcarenites comprise variable mixtures of platform-derived material (e.g.  
682 pisoliths, shells, echinoderm debris, ooids), chert (microcrystalline quartz), altered basalt,  
683 vesicular volcanic glass (with plagioclase microphenocrysts), serpentinite, microgabbro and  
684 dolerite, together with rare monocrystalline quartz, siltstone (terrigenous), phyllite,

685 plagiogranite, amphibolite, muscovite, altered plagioclase and pyroxene. Many grains are  
686 well-rounded. Planktic foraminifera (e.g. *Globotrunca* sp.) occur rarely.

687         Comparable sequences of the Kemaliye Formation are also exposed unconformably  
688 overlying the Late Cretaceous pelagic carbonates of the Köseyahya platform/proximal slope  
689 succession (Kızılkandil Fm.), as well exposed in Area 3A (E of Elbistan) and Area 4 (S of  
690 Elbistan). The succession in Area 3A encompasses interbedded mudstones, siltstones,  
691 sandstones and clasts of limestone (Triassic-Cretaceous), chert and serpentinite (Fig. 6j).  
692 Overlying debris-flow deposits ('blocky flysch') include clasts and blocks that can be  
693 correlated with the platform succession beneath, including micritic, oolitic and pisolitic  
694 limestone, and also pelagic limestones (Kızılkandil Formation). Other lithologies can be  
695 correlated with the over-riding Pelagic (Gülbahar) unit (e.g. radiolarite and volcanic  
696 material). Blocks of pink, chert-bearing pelagic limestone in Area 3A, east of Elbistan (near  
697 Odunluk Tepe and Yumru Tepe) are dated as Campanian-Maastrichtian based on planktic  
698 foraminifera (see Supplementary Table 1). A chalky debris flow-deposit farther northeast  
699 (near Dağdam) includes Late Cretaceous planktic foraminifera (see Supplementary Table 1).  
700 Facies equivalents of the Kemaliye Formation are also well exposed south of Elbistan (Area  
701 4), beneath the Köseyahya thrust sheet and/or the Munzur thrust sheet, with no exposed  
702 stratigraphic base (Fig. 8). In the southern part of Area 4, pelagic limestone blocks contain  
703 Campanian-Maastrichtian planktic foraminifera, as in the Kemaliye Formation generally (Fig.  
704 21a-d). However, a sample from the same local outcrop contains Globigerinidae (Fig. 21e, f),  
705 and also Rotaliidae, indicating a post-Cretaceous (Cenozoic) age, and thus that the Kemaliye  
706 Formation underwent post-depositional reworking in this area (see below).

707         The Kemaliye Formation is also exposed farther east, as a narrow c. NE-SW-trending  
708 strip in Area 3B, Nurhak Dağı which exhibits some critical additional field relationships (Figs.  
709 2, 16g, 22a, b). The uppermost exposed levels of the Malatya Metamorphics there are  
710 represented by well-bedded calc-schists, in places transformed to calc-mylonite (Fig. 16h),  
711 or are isoclinally folded (Fig. 16i). Above a low-angle tectonic contact, meta-carbonate rocks  
712 are overlain by meta-serpentinite (Fig. 22a, b). Both the calc-schist and the meta-  
713 serpentinite are cut by small granitic intrusions (Figs. 22a). The Malatya Metamorphics were  
714 isoclinally folded prior to intrusion (Fig. 16j). The contact between the meta-serpentinite  
715 and the granitic intrusion is brecciated indicating subsequent brittle deformation (Fig. 16k).  
716 Although not dated specifically, these intrusions are likely to form part of the Eocene

717 Doğanşehir granitoids (MTA, 2011; Kuşcu et al., 2013; Karaoğlu et al., 2012, 2016; Bedi and  
718 Yusufoglu, 2018). The serpentinite is overlain, with a low-angle thrust contact, by a thin  
719 facies equivalent of the Kemaliye Formation that includes blocks of Triassic red crinoidal  
720 limestone, similar to the Köseyahya platform/slope succession (see above), and also blocks  
721 of limestone and limestone breccia set in a sandy matrix (Fig. 22b). Further south (near  
722 Beğre), the serpentinite is overthrust by a thin slice of neritic limestone and limestone  
723 debris-flow deposits with rudist debris, of probable Cenomanian age, capped by Fe-oxide  
724 (Figs. 16l; 22a; see also Supplementary Fig. 3). This unit is interpreted as a small thrust slice  
725 of the contact between the Köseyahya platform/slope succession and the overlying  
726 Kemaliye Formation.

727 In thin section, some of the matrix sandstones of the Kemaliye Formation in Area 3B  
728 (Nurhak Dağı) have a well-developed shear fabric, in which large quartz grains are fractured  
729 and veined, with a calcite spar infill at right angles to the shear fabric. Foliated muscovite is  
730 present along shear bands indicating partial recrystallisation. Two phases of deformation  
731 are indicated by the presence of extensional calcite veins orientated at right angles to each  
732 other. *En echelon* cracks are interpreted as riedel shears.

733

### 734 7.3. Interpretation of the syn-tectonic Kemaliye Formation

735

736 The type area of the Kemaliye Formation (near Kemaliye; Area 5A) is a composite unit,  
737 dominated by gravity-controlled deposition, mainly by mass-flow processes. The rudist  
738 bivalves and *Globotruncana*-bearing limestones within slices and blocks indicate a Late  
739 Cretaceous age, although the matrix remains poorly dated. The lower part of the succession  
740 includes debris-flow conglomerates ('olistostromes'), sandstones, shales and exotic blocks  
741 that covered the Malatya metamorphic rocks. The metamorphic and local granitic detritus  
742 were derived from the subjacent Malatya (or Keban) Metamorphics, confirming that they  
743 were exhumed prior to deposition (see Discussion). However, the dominant sources of the  
744 exotic material were the over-riding Munzur thrust sheet, the Pelagic (Gülbahar) unit, and  
745 ophiolitic rocks (e.g. serpentinite). The limestone conglomerates with well-rounded clasts  
746 and rudist debris were sourced from the Munzur platform. The Triassic basalts with Halobia-  
747 limestone and radiolarite are correlated with the Pelagic (Gülbahar) lower slope/basinal

748 unit, as noted above. Ophiolitic rocks are exposed to the northeast of the Kemaliye  
749 Formation type area.

750 The Late Cretaceous pelagic carbonate deposition (Kızılkandil Formation) of both the  
751 Munzur and Köseyahya thrust sheets ended with a hiatus (early Campanian (?); c. 83-78  
752 Ma), commonly marked by iron-oxide accumulation. The likely cause of the hiatus, similar to  
753 that in the Malatya metamorphic succession, was flexural uplift related to the regional  
754 ophiolite emplacement. The hiatus was followed by mixed siliciclastic-carbonate  
755 redeposition during late Campanian-Maastrichtian, forming the Kemaliye Formation. Talus,  
756 ranging from sand-sized, to blocks (up to many-metre-sized), were shed into the basin,  
757 largely derived from the upper levels of the adjacent Mesozoic carbonate platform and/or  
758 slope units (e.g. Cenomanian rudist limestone). The likely cause of basin formation was  
759 regional-scale downflexure ahead of the advancing thrust load, which was dominantly  
760 ophiolitic. The presence of Triassic-Cretaceous clasts suggests that, in places, all levels of the  
761 stratigraphy were exposed and eroded. This, in turn, suggests that platform and slope units  
762 were imbricated and uplifted, eroded, and then collapsed as debris into the flexural  
763 foredeep. Permian limestone is inferred to have existed beneath the Mesozoic platform  
764 and/or slope units, as supported by the presence of the large (km-sized) body of Permian  
765 limestone, as associated with the Kemaliye Formation in the northeast of the type area  
766 (Area 5A; Fig. 13). In addition, the pelagic lithologies (e.g. radiolarian chert, siliceous pelagic  
767 limestone) and also alkaline within plate-type basalt were derived from the Pelagic  
768 (Gülbahar) unit. Ophiolitic material is also variably present in the form of basalt, diabase,  
769 gabbro and/or serpentinite, sourced from the over-riding ophiolitic units. The succession  
770 accumulated in relatively deep water (100s m), as suggested by intercalations of pelagic  
771 carbonate containing Campanian-Maastrichtian planktic foraminifera.

772 Slices of the Munzur limestone were emplaced over the Kemaliye Formation in places,  
773 complicating the local tectono-stratigraphy. For example, in Area 3B (Nurhak Dağı), a slice of  
774 the highest levels of the neritic Munzur platform, complete with its iron-oxide coating (see  
775 above), was imbricated beneath the over-riding Köseyahya thrust sheet. Since the Mesozoic  
776 limestones (Munzur and Köseyahya) now structurally overlie the Kemaliye Formation it can  
777 be inferred that the Malatya-Keban metamorphics were exhumed, eroded to form clastic  
778 material (Kemaliye Formation), and later over-riden by the regional limestone thrust sheet  
779 in this area.

780 The Kemaliye Formation above the Munzur and Köseyahya platform/slope  
781 successions is comparable with the widespread late Cretaceous syn-tectonic Yavça  
782 Formation (and facies equivalents) that intervene between platform carbonates, below and  
783 ophiolitic rock, above throughout the Taurides, for example in the Aladağ Unit  
784 (Maastrichtian Zekeriya Formation) and in the Bolkar Dağ Unit (late Campanian-  
785 Maastrichtian Söğüt Formation). These units unconformably overlie units of different age  
786 and facies in different areas and are generally interpreted as olistostromes or sedimentary  
787 melanges related to regional ophiolite emplacement (Özgül, 1997; Andrew and Robertson,  
788 2002; Parlak and Robertson, 2004; Mackintosh and Robertson, 2012; Bedi and Yusufoglu,  
789 2018). In summary, the Kemaliye Formation in its type area (Area 5A) is a composite unit  
790 which formed above the Malatya (Keban) metamorphics during or after their exhumation.  
791 In contrast, the Kemaliye Formation as mapped regionally above the Tauride platform units  
792 is an intact succession, interpreted as a foredeep related to ophiolite obduction.

793

794

## 795 **8. Volcanic-sedimentary melange**

796

797 Definitions: Melanges comprise disorganised blocks of single, or multiple lithologies, with or  
798 without a matrix, and may be either sedimentary or tectonic origin, or both (see Raymond,  
799 1984). Volcanic-sedimentary melange is a variety of melange in which the blocks are mainly  
800 made up of volcanic and sedimentary rocks, unrelated to ophiolites. Volcanic-sedimentary  
801 melange can shed light on both oceanic and emplacement processes.

802 Volcanic-sedimentary melange is well represented in the northeast of the region  
803 studied (Hekimhan area) (Fig. 2), where it is made up of short (10s of m), dismembered  
804 sequences of basalt, pelagic limestone and radiolarite (e.g. Yeşildere Melange). A local  
805 section comprises pillow basalt (80 m) with intercalations of ribbon radiolarite (c. 20 m),  
806 then alternations of radiolarite and pelagic limestone, followed by siliceous pelagic  
807 limestone (9 m). Radiolarite from the upper part of this interval was dated as Late Albian-  
808 Early Cenomanian (see Table 1). In the Dağlıca area (Area 2), short sections of basaltic lavas  
809 (<10s m) are interbedded with, and overlain by Middle Oxfordian-Early Tithonian radiolarian  
810 sediments (Robertson et al., 2013b). Geochemical data for the basalts from both areas  
811 indicate mid-ocean-ridge, to enriched intra-plate settings, although some samples have a

812 subduction-related influence (Robertson et al., 2013b; Robertson et al., in press a). A similar  
813 range of basaltic compositions has been identified within meta-volcanic-sedimentary  
814 melange farther west, including the Anatolides (Afyon zone) (Robertson et al., 2009; in press  
815 b).

816 The volcanic-sedimentary melange was sourced from oceanic crust, including MOR-  
817 type basalt, 'seamounts' and subduction-influenced crust, within an oceanic basin that  
818 existed at least from Late Jurassic-Late Cretaceous. The melange was accreted related to  
819 subduction, and was emplaced onto the Tauride platform together with the other  
820 allochthonous units.

821

## 822 **9. Ophiolite-related units**

823

824 Definitions: Ophiolites represent relatively coherent bodies of oceanic lithosphere, although  
825 commonly incomplete. Dismembered ophiolites are tectonically dissected. Ophiolitic  
826 melange has component lithologies derived from an ophiolite and directly associated deep-  
827 sea sediments. Ophiolite-related melange, in contrast, includes a mixture of ophiolitic rocks  
828 and other unrelated lithologies (e.g. neritic limestone). These three types of melange all  
829 occur within the eastern Taurides, related to sea-floor spreading and ophiolite  
830 emplacement.

831

### 832 **9. 1. Ophiolite-related melange and ophiolitic melange**

833

834 Ophiolite-related melange and ophiolitic melange are well exposed north of Elbistan (Area  
835 2, Dağlıca), where they are intergradational and structurally interleaved. Within the  
836 ophiolite-related melange, ophiolitic blocks/slices are embedded in a matrix of sheared  
837 mudrock. The ophiolitic melange is mainly sheared harzburgite but other ophiolitic  
838 lithologies are present including gabbro and diabase dykes (locally cut by plagiogranite  
839 veins), as exposed east of Elbistan (Area 5) (see Supplementary Fig. 5). In this area,  
840 dismembered ophiolitic rocks of the Dağlıca ophiolite (see below) are spatially associated  
841 with short (up to 10s of m), deformed successions of ophiolite-derived, matrix-supported  
842 conglomerates. In places, these clastic rocks occur above the Kemaliye Formation. The  
843 Kemaliye Formation, as related to the Munzur and Köseyahya thrust sheets, does not



844 usually contain ophiolitic material (in contrast to the type area, above the Keban  
845 metamorphics). However, locally in Area 2 (Dağlıca), the highest levels of the intact  
846 Kemaliye Formation contain ophiolitic debris (Fig. 19 log 4), suggesting a link with the  
847 tectonically associated ophiolitic rocks (Dağlıca ophiolite). However, no undeformed contact  
848 could be observed. The debris-flow deposits are crudely stratified (Fig. 20f), showing both  
849 normal and reverse grading. The clasts are mostly angular to subrounded and are dispersed  
850 randomly though a poorly sorted sand-granule-grade matrix (Fig. 20g). Most parts of an  
851 ophiolite pseudostratigraphy are represented as clasts, including gabbro (Fig. 20h) and  
852 basalt (Fig. 20i); siliceous pelagic carbonate is mostly preserved as diagenetic replacement  
853 chert (Fig. 20j).

854 Another excellent example of ophiolite-related melange, here termed the Divriği  
855 melange, is exposed in the northeast of the region (Area 5B) (Figs. 2, 23). This melange is  
856 located between the Munzur thrust sheet, below and the Divriği ophiolite, above (Aktimur,  
857 1988; Özgül and Turşucu, 1984; Öztürk and Öztunalı, 1993). This unit is otherwise known as  
858 the Yeşiltaşayla ophiolitic melange (Yılmaz and Yılmaz, 2004), the Refahiye ophiolite  
859 (Atabey and Aktimur, 1997), and the Eriç melange (Özer et al., 2004). The Divriği melange  
860 has undergone low-grade metamorphism and is cut by Eocene granites (Boztuğ et al., 2007;  
861 Kuşcu et al., 2013). The smaller Güneş ophiolite is exposed in the same area (Yılmaz, 2001).

862 The Divriği melange, up to several 100 m thick, directly overlies the Munzur thrust  
863 sheet in its type area, the Munzur Dağları (Aktimur et al., 1998; Fig. 24a, b; see also  
864 Supplementary Fig. 4). The highest stratigraphical levels of the Munzur thrust sheet are well  
865 dated to the east of our study area. In this area (Ayıkayası Dağı), Cenomanian-aged, rudist-  
866 bearing neritic limestones are overlain by a thin (4 m) interval of thin-bedded, reddish  
867 siliceous pelagic carbonate of Turonian-Campanian age (Özer et al., 2004). This interval can  
868 be correlated, broadly with the latest Cretaceous pelagic cover of the platform carbonates  
869 in the Elbistan area (Kızılkandil Formation). Where well exposed in our area, north of Divriği,  
870 well-bedded, unmetamorphosed neritic limestones of the Munzur thrust sheet dip regularly  
871 westwards and are over-ridden by ophiolite-related melange, with a low-angle thrust  
872 contact (Fig. 24b). The highest exposed levels of the Munzur succession (5 km SSE of Divriği)  
873 are locally dated as Middle Jurassic, using benthic foraminifera (Fig. 18d, e; see also  
874 Supplementary Table 1), suggesting that the Cretaceous part of the original succession is  
875 now absent. Dark neritic limestones in the lower levels of the succession in the Divriği area

876 are dated as Middle Triassic, based on benthic foraminifera (Fig. 18c). Similar platform  
877 lithologies are now present as blocks in the overlying ophiolite-related melange.

878 The Divriği melange overlies the succession in the Munzur thrust sheet. In places,  
879 neritic limestones are unconformably overlain by mudrocks that are similar to the matrix of  
880 the melange (Figs. 23, 24a-c). In places, the contact is faulted (see Supplementary Fig. 4).  
881 The lower part of the melange includes a neritic limestone block that was dated as Aptian-  
882 Albian, based on benthic foraminifera (Fig. 18f-i; see also Supplementary Table 1), similar to  
883 the age of the underlying intact platform succession. The mid to upper levels of the melange  
884 are dominated by elongate slices and blocks of recrystallised limestone, up to 100s m long  
885 and 10s m thick, set in a sheared shaly matrix (Figs. 24a-c, 25a). Benthic foraminifera within  
886 a packstone block gave an Aptian-Albian age (Fig. 18j-q), again suggesting that the missing  
887 interval at the top of the Munzur platform succession is represented by blocks in the  
888 melange. Other blocks include poorly sorted breccia-conglomerate, indicating a mass-flow  
889 (slope-related) setting, prior to emplacement into the melange. Some of the clasts are well-  
890 rounded suggesting exposure and reworking prior to redeposition, as in the Kemaliye  
891 Formation (see above). The blocks and terrigenous matrix are interspersed with  
892 anastomosing strands of highly sheared serpentinite, mostly harzburgitic (Figs. 24a-b; 25b;  
893 see Supplementary Fig. 4). In places, serpentinite melange reaches to within c. 80 (structural  
894 thickness) of the tectonic contact with the intact Munzur thrust sheet below. The melange  
895 as a whole has experienced polyphase deformation, with evidence of both southerly and  
896 northerly fold vergences (Fig. 25c, d).

897 Several additional areas provide supporting evidence. For example, an extensive  
898 outcrop of ophiolitic melange southeast of Divriği is dominated by sheared harzburgitic  
899 serpentinite, without limestone blocks (Fig. 25e, f). Similar serpentinite melange also occurs  
900 extensively, e.g. c. 70 km southwest of Divriği (around Kangal), where it overlies neritic  
901 limestones of the Munzur thrust sheet (locally dated as Jurassic; see Supplementary Table  
902 1). In addition, melange outcrops to the west of Divriği (Fig. 2) have been summarised  
903 elsewhere (e.g. Büyük Yılanlı Dağ) (Robertson et al., 2013b; see also Özgül et al., 1981; Özgül  
904 and Turşucu, 1984; Aktimur et al., 1988; Atabey et al., 1994). These include several types of  
905 melange associated with the Pınarbaşı ophiolite in the northeast of the region studied (i.e.  
906 Kireçlikyayla melange of Yılmaz et al., 1991, 1993; Pınarbaşı melange of Atabey and Aktimur,  
907 1997).

908

## 909 9.2. Ophiolites and related clastic deposits

910

911 Whereas, melanges are widely distributed throughout the eastern Taurides, coherent  
912 ophiolites are restricted to four main bodies, the Divriği (also Güneş), Hekimhan, Pınarbaşı  
913 and Kuluncak ophiolites, mainly in the north of the region studied (Fig. 2). Here we pay  
914 particular attention to the dismembered Dağlıca ophiolite and its associated debris-flow  
915 units (Area 2) which shed light on emplacement processes.

916 In the northeast, the Divriği (Sivas) ophiolite (Area 5B), dated at 93-94 Ma by zircon U-  
917 Pb, is partially dismembered and lacks extrusives rocks (Parlak et al., 2006, 2017). A locally  
918 exposed metamorphic sole (Fig. 24a, bii), dated at 93-94 Ma by Ar-Ar (Parlak et al., 2017),  
919 includes amphibolite, with subordinate, greenschist, marble and metachert, all cut by post-  
920 metamorphic diabase/microgabbro dykes. The protoliths of the amphibolite are within-  
921 plate basalts (seamount-type) and island-arc-type basalts, whereas the protoliths of the  
922 dykes are within-plate basalts (Parlak et al., 2006). Listwaenite is widespread in the Divriği  
923 (Sivas) ophiolite (Uçurum, 2000).

924 Farther southwest (c. 40 km), the dismembered Kuluncak-Hekimhan (Malatya) ophiolite  
925 (Fig. 2) comprises variably altered mantle harzburgite (tectonites), cut by isolated basaltic  
926 dykes, together with ultramafic cumulates (mainly dunite, wehrlite and pyroxenite), mafic  
927 cumulates (olivine-gabbro and normal gabbro), isotropic gabbro, diorite and quartz diorite,  
928 a sheeted dyke complex, plagiogranite and extrusive rocks. The basaltic extrusive rocks are  
929 associated with radiolarite, chert, pelagic limestone and hemipelagic mudstone (Metin et  
930 al., 2013; Camuzcuoğlu et al., 2017). Listwaenite again occurs (Uçurum, 2000). In the  
931 northeast, the Pınarbaşı ophiolite, dated as 93-94 Ma by zircon U-Pb (Parlak et al., 2017)  
932 (Fig. 2) exposes mantle tectonites, cut by isolated basaltic dykes, together with ultramafic to  
933 mafic cumulates, all above an amphibolitic sole (90-93 Ma by zircon U-Pb) (Parlak et al.,  
934 2017). These sole rocks are chemically similar to those of the Divriği ophiolite (Vergili and  
935 Parlak, 2005).

936 In addition, the dismembered Dağlıca ophiolite (Fig. 7; sections a, d, e) is restricted  
937 to thrust slices and blocks (up to km to km-sized). The lithologies were previously termed  
938 the Dağlıca complex (Kozlu et al., 1990; Perinçek and Kozlu, 1984), and the Dağlıca ophiolite  
939 (Robertson et al., 2013b). The lithologies include basalt, diabase, diabase dykes in

940 harzburgite, gabbro, gabbro pegmatite, harzburgite, pyroxenite, wehrlite and dunite (see  
941 Supplementary Fig. 5). The metamorphic sole is represented by rare blocks of amphibolite-  
942 greenschist within adjacent ophiolite-related melange. The basaltic rocks of the Dağlıca  
943 ophiolite are chemically indicative of a supra-subduction zone origin (Robertson et al.,  
944 2006).

945

### 946 9.3. Interpretation of the ophiolites, melanges and related mass-flow units

947

948 The ophiolites formed in a Late Cretaceous (c. 92-93 Ma), supra-subduction zone setting  
949 (Parlak et al., 2013, 2019). They represent different parts of a regional-scale thrust sheet of  
950 oceanic lithosphere, with a metamorphic sole that is only now locally preserved. The  
951 presence of all of the units of a complete ophiolite, taken regionally, suggests that a typical  
952 supra-subduction zone ophiolite initially formed with all of the expected lithological units;  
953 however, this was variably dismembered during emplacement.

954 During emplacement, related to flexural loading by advancing oceanic lithosphere,  
955 the Mesozoic carbonate platforms (Munzur and Köseyahya) subsided to create the regional-  
956 scale foredeep mentioned above (Kemaliye Formation; see above). In proximal (northerly)  
957 areas, represented by the Divriği melange, the upper stratigraphic (Cretaceous) levels of the  
958 Munzur platform were partly removed. Most likely, they were detached, bulldozed ahead  
959 and collapsed as debris-flows and blocks into the northern part of the regional foredeep.  
960 During southward emplacement, serpentinite derived from the over-riding ophiolite  
961 harzburgite was tectonically incorporated into the foredeep.

962 During emplacement, the East Tauride ophiolites were variably dismembered. The  
963 Dağlıca ophiolite was strongly dismembered to form thrust sheets and broken formation,  
964 and also underwent mass-wasting to form ophiolite-derived debris flows. Ophiolitic material  
965 was initially sand-sized (within the Kemaliye Formation), then became clast/block sized (i.e.  
966 more proximal) and culminated in the emplacement of large ophiolitic blocks and thrust  
967 sheets. Gravity emplacement was therefore an important process for the melange units.  
968 Ophiolite-related melange covered all parts of the region (including south of Elbistan; Area  
969 4). However, the ordered ophiolites are restricted to the north of the region, closest to their  
970 inferred origin and there is no field evidence that they were emplaced southwards over the  
971 entire region.

972

973 **10. Latest Cretaceous-Paleogene cover sediments**

974

975 Cover sediments provide important constraints on the nature of the substratum, the timing  
976 of emplacement and the tectonic conditions soon afterwards. The Divriği ophiolite is  
977 unconformably overlain by conglomerates, sandstone, mudstone, marl, limestone and  
978 volcanoclastic sediments, dated as Campanian-Maastrichtian (Yılmaz and Yılmaz, 2004; Bilgiç  
979 et al., 2008a, b). Approximately 50 km farther west (Tecer Dağı and Büyük Yılanlı Dağ),  
980 ophiolitic rocks, similar to the Divriği ophiolite (Kavak et al., 2017), are unconformably  
981 overlain by conglomeratic facies (Tecer Formation) (İnan and İnan, 1988), passing upwards  
982 into Late Maastrichtian shallow-marine, mixed carbonate-clastic facies (Atabey and Aktimur,  
983 1997; İnan and İnan, 1988; Robertson et al., 2013b). Both the Kuluncak and Hekimhan  
984 ophiolites (and related melange units) are unconformably overlain by ophiolite-derived  
985 conglomerates, passing upwards into Late Maastrichtian shallow-water carbonates,  
986 including rudist limestones (Booth et al., 2013; Robertson et al., 2013b; Bedi and Yusufoglu,  
987 2018). In addition, the Pınarbaşı ophiolite is unconformably overlain by non-marine clastics  
988 and minor carbonates, of inferred Palaeocene age (Erkan et al., 1978).

989         The widespread deposition of latest Cretaceous, typically late Maastrichtian, cover  
990 sediments show that, after short-lived emergence and erosion, the emplaced continental  
991 margin and ophiolitic units, were rapidly transgressed by non-marine to shallow-marine  
992 sediments, and that this was followed by a return to relatively stable tectonic conditions.  
993 The clast composition reflects the nearby units beneath, typically ophiolitic rocks. The  
994 timing of regional ophiolite emplacement is constrained as coeval with the syn-tectonic  
995 Kemaliye Formation (late Campanian-late Maastrichtian) but prior to the transgressive  
996 sediments regionally (probably late Maastrichtian). The emplacement of the allochthonous  
997 units therefore took place during a relatively short period of time (c. 75-70 Ma).

998

999 **11. Structural relationships**

1000

1001 11.1. Outcrop-scale structures

1002

1003 To shed additional light on the tectonic emplacement, bedding and fold data (fold axial  
1004 planes and fold hinges) were measured throughout the study area and plotted on  
1005 stereonet according to sub-area and tectono-stratigraphic unit (see also Supplementary  
1006 Fig. 6).

1007 Bedding in the Malatya and/or Keban metamorphics (Areas 1 and 5A) is generally  
1008 orientated NE-SW (see supplementary Fig. 7). Fold axial planes mainly plot in the northern  
1009 and southern quadrants, consistent with dominantly E-W folding with variably dipping axial  
1010 planes (c. 10-80°) (Fig. 26ai-aii).

1011 Structural measurement from the allochthonous Tauride units are relatively variable.  
1012 North of Elbistan (Area 2), the bedding strike is regionally c. E-W. Bedding orientations are  
1013 variable in all units, with a slight NW-SE trend, consistent with large-scale symmetrical  
1014 folding (see Supplementary Fig. 7). Fold axial planes are broadly east-west and commonly  
1015 west-dipping (Fig. 26bi). Many fold hinges trend c. E-W, with axial planes dipping both N and  
1016 S at moderate angles, suggesting refolding (Fig. 26bii). A local swing in fold hinge direction  
1017 (south to west) in the relatively autochthonous Gürün outcrop (see Supplementary Fig. 8)  
1018 could represent refolding (or possibly local block rotation). Farther east (Area 3A; E of  
1019 Elbistan), the bedding is more NW-SE. Fold axial planes and fold hinges are broadly east-  
1020 west, mainly at moderate angles (Fig. 26ci-ii; see Supplementary Fig. 9). In the Kemaliye  
1021 area in the northeast (Area 5A), bedding data from both the Malatya Metamorphics and the  
1022 Kemaliye Formation have a slight NW-SE strike, mainly at moderately angles (see  
1023 Supplementary Fig. 10). Fold axial planes (mostly in the Keban metamorphics) mainly dip  
1024 southwest at variable angles. Fold hinges have a dominant NW-SE trend. Opposing NW vs.  
1025 SE directions hint at re-folding (Fig. 26 di-dii).

1026 The relatively coherent data set from the Malatya Metamorphics (Fig. 26 ai-aii) is  
1027 consistent with N-S compression (without preferred vergence). The fold data from Area 2  
1028 (Dağlıca) are consistent with two-phase emplacement along c. E-W axes (with opposing  
1029 directions). The more NW-SE fold trend in the Kemaliye area farther northeast (Area 5A),  
1030 mainly in the Malatya (Keban) Metamorphics, represent a different compression direction  
1031 or possibly bulk rotation.

1032

1033 11.2. Inter-relations of regional tectono-stratigraphic units

1034 The mutual relations are mainly indicated by a combination of sedimentary, metamorphic,  
1035 igneous and structural evidence.

1036

1037 11.2.1. Relation of the Malatya metamorphics to the Göksun ophiolite: sedimentary  
1038 evidence

1039

1040 In the south, the Malatya Metamorphics (Bodrum nappe) are thrust over the post-  
1041 emplacement sedimentary cover of the Göksun ophiolite (Harami Formation), shedding  
1042 light on its timing of emplacement. South of Afşin (Area 1), the Göksun ophiolite is  
1043 unconformably overlain by conglomerate, sandstone, sandy/shaly limestone and marl (un-  
1044 named unit of Perinçek and Kozlu, 1984) that is correlated with the Harami Formation in its  
1045 type area (Elazığ) (Perinçek and Kozlu, 1984; Robertson et al., 2007; Bedi et al., 2009). The  
1046 succession south of Afşin begins with polymictic conglomerates with schist and marble,  
1047 radiolarite, pelagic limestone, chert, ophiolitic rocks (including diabase and basalt), and fines  
1048 upwards into sandstone, limestone and microconglomerates with clasts of similar  
1049 composition (Yılmaz et al., 1987; Bedi et al., 2009; this study). Thin sections include  
1050 monocrystalline (plutonic) quartz, polycrystalline (metamorphic) quartz, sericitic schist,  
1051 marble, micritic limestone, biotite and muscovite, in generally decreasing order of  
1052 abundance (Fig. 6k, l). The matrix is biomicrite with a mixture of planktic and benthic  
1053 foraminifera. The succession is dated as latest Cretaceous using planktic and benthic  
1054 foraminifera, and also calcareous nannofossils (Perinçek and Kozlu, 1984; Yılmaz et al., 1987,  
1055 1993; Robertson et al., 2007; Bedi et al., 2009). The basal conglomerates include pelagic  
1056 limestone pebbles of Santonian age, similar to the Kızılkandil Formation of the Munzur and  
1057 also the Köseyahya successions (Bedi et al., 2009). During this work, samples of calcarenite  
1058 yielded Late Campanian-Maastrichtian ages (see Supplementary Table 1). Samples from the  
1059 upper part of the formation (Sarıkaya member) have been dated as late Maastrichtian  
1060 based on planktic foraminifera and nannofossils (Bedi et al., 2009), of which the key taxa are  
1061 *Gansserina gansseri* (72.35-66 Ma, latest Campanian-Maastrichtian) and *Globostruncanita*  
1062 *angulata* (66.04-72.05 Ma, top Maastrichtian).

1063 The post-emplacement sedimentary cover of the Göksun ophiolite accumulated in a  
1064 shelf sea of moderate water depth (>10s m), with clastic sediment supply both from the  
1065 Munzur and/or Köseyahya platform units and also from already exhumed Malatya

1066 metamorphic rocks. The Malatya metamorphic thrust sheet was, therefore, tectonically  
1067 juxtaposed with the underlying Göksun ophiolite during the latest Cretaceous.

1068

1069 11.2.2. Post-exhumation imbrication of the Malatya Metamorphics: sedimentary and  
1070 structural evidence

1071

1072 SW of Elbistan (Area 4), the Neritic-pelagic (Köseyahya) thrust sheet is thrust southwards  
1073 over the Malatya Metamorphics (Fig. 9, section A). However, elsewhere the contact is  
1074 steeply dipping and is likely to be a strike-slip fault (Fig. 9, section A). In this area, near  
1075 Kalaycık (Fig. 9 section A; locality E), Triassic Malatya metamorphic rocks (exposed on  
1076 Medetsizdağı) are underlain by a small slice (>40 m thick) of unmetamorphosed debris-flow  
1077 deposits that include gabbro, basalt, pelagic limestone (with volcanic debris) and radiolarite.  
1078 This facies is similar to the Kemaliye Formation, as exposed c. 12 km to the NE (near Sokullu;  
1079 Fig. 9 map). A sample from a block of pelagic limestone contains Campanian-Maastrichtian  
1080 planktic foraminifera, as in the Kemaliye Formation (Fig. 21a-d). However, an additional  
1081 sample includes Globigerinidae (Fig. 21e, f) and also Rotaliidae, indicating a post-Cretaceous  
1082 (Cenozoic) age. Two other samples contain a rich Middle Palaeocene (Selandian) planktic  
1083 foraminiferal assemblage (see Supplementary Table 1). Relatively deep-water pelagic  
1084 conditions therefore existed during the Palaeogene, followed by reworking of pelagic  
1085 carbonates within debris-flow deposits. Elsewhere (e.g. west of Afşin), the Malatya  
1086 Metamorphics are internally imbricated with Eocene shelf-depth Nummulitic limestones  
1087 (Robertson et al., 2006; Fig. 4 a). The inter-slicing took place during Mid-Late Eocene  
1088 regional deformation (see below). However, the distance of Eocene thrust transport is likely  
1089 to have been limited (a few kms at most) because the Göksun ophiolite and the Malatya  
1090 Metamorphics are mutually intruded by the 88-82 Ma Baskil Granitoids, without major  
1091 thrust dislocation of the contact relations (Karaođlan et al., 2012, 2016; Bedi and Yusufoglu,  
1092 2018).

1093

1094 11.2.3. Contact relations between the Munzur and Köseyahya thrust sheets: sedimentary  
1095 and structural evidence

1096



1097 The Munzur thrust sheet is subdivided into the main, lower thrust sheet that encompasses  
1098 the entire succession and the much thinner, internally disrupted, upper thrust sheets  
1099 (mainly Cretaceous), as exposed in the north, in Area 2 (Dağlıca) (Figs. 7; Fig. 20c-e). The  
1100 upper and lower thrust sheets are separated by the Kemaliye Formation, which has  
1101 widespread inclusions of the dismembered Dağlıca ophiolite, related melange (Fig. 7) and,  
1102 locally, of the Pelagic (Gülbahar) unit (Fig. 7f). In places, limestones of upper thrust sheet  
1103 directly overlie the southern margin of the Gürün autochthon (Fig. 7c).

1104 NE of Elbistan (Area 3A), the Munzur thrust sheet is thrust southwards over the  
1105 Neritic-pelagic (Köseyahya) thrust sheet (Fig. 8 sections a, e). The two thrust sheets are  
1106 separated by mass-flow units, correlated with the Kemaliye Formation (see Supplementary  
1107 Fig. 7). Poorly bedded calcarenites form the matrix of debris-flow deposits; these include  
1108 large foraminifera and calcareous algae of Late Palaeozoic (Carboniferous-Permian) age (see  
1109 Supplementary Table 1), hinting at derivation from an original but now missing Late  
1110 Palaeozoic substratum to the Munzur limestones. The imbrication of the two major  
1111 platform carbonate/slope thrust sheets therefore took place after formation of the latest  
1112 Cretaceous Kemaliye Formation, probably during the latest Cretaceous.

1113 In the same area, NE of Elbistan (Area 3A), the Neritic-pelagic (Köseyahya) thrust sheet  
1114 beneath the Munzur thrust sheet is relatively thin (100s m) and highly disrupted. Pelagic  
1115 limestones of the Neritic-pelagic (Köseyahya) thrust sheet are repeatedly imbricated with  
1116 the latest Cretaceous Kemaliye Formation (Fig. 8). The Pelagic (Gülbahar) unit that is locally  
1117 exposed beneath both the Neritic-pelagic (Köseyahya) thrust sheet and the Munzur thrust  
1118 sheet are both tightly folded and, in places, intensely imbricated, indicating intense  
1119 compressional deformation during emplacement (see Supplementary Fig. 6). On the other  
1120 hand, the widespread presence of conjugate fault blocks indicates extension (see  
1121 Supplementary Fig. 6). One explanation is that the Neritic-pelagic (Köseyahya) sheets were  
1122 emplaced by gravity sliding into the Kemaliye foredeep, followed by imbrication during  
1123 regional emplacement into the latest Cretaceous thrust stack.

1124 In the south (south of Elbistan; Area 4), a Munzur thrust sheet is mapped as  
1125 underlying a Köseyahya thrust sheet (Bedi et al., 2009) (Fig. 9, section A). This points to  
1126 complex and variable re-imbrication because to the northeast (e.g. Area 3A; Fig. 8) the  
1127 Munzur thrust sheet regionally overlies the Köseyahya thrust sheet. All of this imbrication  
1128 and re-imbrication is inferred to be latest Cretaceous in age.

1129 In addition, to the NW of Elbistan (N of Afşin, near İncirli, Area 2), the Malatya  
1130 Metamorphics are thrust northwards over the Southern allochthon, including the Kemaliye  
1131 Formation, above a sharp south-dipping contact (Figs. 2; 4l; Supplementary Fig. 2). This  
1132 indicates an important, but localised, phase of backthrusting after the initial latest  
1133 Cretaceous emplacement. Northward vergence is also observed within the adjacent  
1134 Southern allochthon (Perinçek and Kozlu, 1984; Robertson et al., 2013).

1135

1136 11.2.4. Contact relations between the Gürün autochthon and the allochthonous units

1137

1138 Along the southern margin of the Gürün autochthon (Area 2; Dağlıca; Figs. 7, 20k), the  
1139 relatively autochthonous succession culminates with Middle Eocene (Lutetian) calcareous  
1140 mudstones, rich in large foraminifera. Interbedded sandstones and debris-flow deposits  
1141 contain ophiolitic detritus. Several km to the south (Hurman Çayı-Kalesi area) (Fig. 7, marked  
1142 in red), ophiolitic rocks and Munzur limestones are thrust over an isolated Early-Mid Eocene  
1143 succession (with no exposed base) (Robertson et al., 2013b). This begins with limestones  
1144 that are rich in large foraminifera (e.g. *Alveolina* sp., *Assilina* sp.) and passes upwards into  
1145 argillaceous and silty limestones (Demirogluk Formation of Bedi et al., 2009). This is  
1146 interpreted as a fragment of an Eocene shelf succession that was later incorporated into the  
1147 thrust stack. In the west of Area 2 (e.g. NW of Tavla), the Munzur limestones are  
1148 unconformably overlain by non-marine conglomerates, with well-rounded clasts that  
1149 include *Nummulites* sp. suggesting a post-Eocene age of accumulation (Early-Mid  
1150 Miocene(?)) (Fig. 7b; 20l). These conglomerates are also incorporated into the thrust stack.  
1151 Farther east, within the Gürün autochthon (near Akdere), Cenomanian rudist-bearing  
1152 limestones are unconformably overlain by thick-bedded to massive non-marine  
1153 conglomerates, of inferred Early-Mid Miocene age (Gövdelidağ Formation of Perinçek and  
1154 Kozlu, 1984). The conglomerates are in high-angle fault contact with Munzur limestones.  
1155 Slickensides indicate right-lateral strike-slip displacement (Robertson et al., 2013a). In the  
1156 far east of Area 2 (near Sarız), a moderate-angle (30-50°) south-dipping thrust (reverse fault)  
1157 separates the Paleogene Gürün autochthonous succession from the allochthonous units  
1158 above, pointing to northward displacement (i.e. backthrusting) (Robertson et al., 2013b),  
1159 which affected the Southern Allochthon as a whole. The outcrop bordering the Gürün  
1160 autochthon in the south is folded on a large scale along c. E-W axes. The timing of the

1161 folding is inferred to be pre-Pliocene, post-dating the inferred Miocene non-marine  
1162 conglomerates (Yılmaz et al., 1993; Perinçek and Kozlu, 1984; Kozlu et al., 1990; Robertson et  
1163 al., 2013b). In summary, within the Southern allochthon there is evidence of latest  
1164 Cretaceous southward thrust-stacking, Eocene re-imbrication and Late (?) Miocene back-  
1165 thrusting, reverse faulting and large-scale folding.

1166         Along the northern margin of the Gürün autochthon (Fig. 2), the relatively  
1167 autochthonous succession culminates in Middle Eocene shelf facies, similar to those in the  
1168 south. The Northern allochthon begins with an equivalent of the neritic Munzur thrust  
1169 sheet, followed upwards by the Pelagic nappe, equivalent to the Neritic-pelagic (Köseyahya)  
1170 thrust sheet, but more coherent stratigraphically. Overlying units include the Pınarbaşı  
1171 ophiolite and related melange units in the northwest (Robertson et al., 2013b). The  
1172 northern allochthon is overlain by Eocene marine clastic sediments. Although mapped as an  
1173 unconformable relationship (Yılmaz et al., 1997; MTA 2011; Bedi and Yusufaglu, 2018), field  
1174 observations in the northeast of the area suggest a thrust relationship (Robertson et al.,  
1175 2013b). In the southwest, near Pınarbaşı, the contact relations are mainly concealed by  
1176 numerous neotectonic strike-slip faults.

1177

### 1178 11.3. Effects of neotectonic faulting

1179

1180 Neotectonic displacements need to be back-stripped to interpret the preceding  
1181 emplacement history in detail.

1182         Previously published fault data, specifically from the generally NE-SW to ENE-WSW-  
1183 trending Göksu fault lineament of Kozlu et al. (1990) (Tavla-Sarız area; Figs. 2, 7), indicate  
1184 dominantly right-lateral displacement, with either reverse or normal components  
1185 (Robertson et al., 2013b). This is surprising because the dominant offset along neotectonic  
1186 faults in the region is left-lateral (e.g. Duman and Emre, 2013). During this study, additional  
1187 faults were measured, mainly farther east (e.g. Hurman Kalesi area). Of the new fault data  
1188 (see Supplementary Fig. 11), there are six NW-SE trending faults, one of which is left-lateral  
1189 and the remainder right-lateral. Of 10 NE-SW trending faults, seven are dextral, two have no  
1190 slickenlines to determine movement sense and one is an oblique reverse fault. The new  
1191 data support significant right-lateral displacement along a generally NE-SW to ENE-WSW-  
1192 trending lineament, possibly representing more than one phase of movement. The

1193 rectilinear right-lateral faulting appears to post-date the inferred Mid-Late Miocene folding  
1194 and reverse faulting/backthrusting that affects the Southern allochthon and the adjacent  
1195 Gürün autochthon (see above).

1196 Neotectonic faults are widely mapped further south, in the general Elbistan area, as  
1197 follows: (1) NW-SE trending faults (Kışlaköy and Hurman Faults), inferred to be normal  
1198 faults with dextral strike-slip components (strike N35°E; dip 81°SW; (2) NE-SW trending fault  
1199 (Sarıyatak Fault), a normal fault with a sinistral component (strike N15°E dip 78°SE; lineation  
1200 plunges 75°S); (3) ENE-WSW faults (Türkören Fault and Afşin-Elbistan Fault), of which four  
1201 fault planes on the left-lateral Afşin-Elbistan Fault have allowed calculation of principal  
1202 stress directions ( $\sigma_1$  51°/170°;  $\sigma_2$  30°/307°;  $\sigma_3$  22°/050°). The NE-SW  
1203 trending fault is inferred to have influenced the Pliocene-Quaternary clastic deposition  
1204 within the adjacent depocentre that forms part of the overall Afşin-Elbistan basin (Yusufoglu  
1205 et al., 2005; Bedi et al., 2009). Regional c. ENE-WSW left-lateral faulting generated overall  
1206 NW-SE trending fault-controlled depocentres that infilled with Pleistocene sediments. Some  
1207 of the neotectonic faults in the Elbistan region are reported to be covered by conglomerates  
1208 suggesting a switching of faults with time and/or a changing stress regime (Bedi et al.,  
1209 2009).

1210 The region to the west of the Malatya-Ovacık Fault Zone is transected by numerous  
1211 Plio-Quaternary left-lateral strike-slip faults, including the Afşin-Elbistan Fault and the  
1212 generally NNE-SSW Sarız and Gürün faults (MTA, 2011). Some of these faults are interpreted  
1213 to have active left-lateral movements (i.e. Beyyurdu and Gürün faults of Emre et al. (2018);  
1214 Türkören fault of Bedi et al. (2009)). The left-lateral faults relate to displacements along the  
1215 regional northern strand of the East Anatolian Fault System (Sürgü–Misis Fault system). The  
1216 Pliocene-Pleistocene westward tectonic escape of Anatolia (Şengör et al., 1985; Duman and  
1217 Emre, 2013) was partially accommodated by displacements along these faults.

1218 In the east, the Malatya-Ovacık Fault Zone delimits the western margin of the large  
1219 Malatya Basin. Early-Middle Miocene NW–SE extension there was followed by Mid-Late  
1220 Miocene volcanism ( $11.99 \pm 0.49$ - $4.82 \pm 0.57$ ) (Yamadağ volcanics) (Kaymakçı et al., 2006;  
1221 Kürüm et al., 2008). NNW-SSE left-lateral transpression is inferred along the Malatya-Ovacık  
1222 Fault Zone during Late Miocene-Early Pliocene, coupled with widespread Pliocene volcanism  
1223 (Ekici et al., 2007). Active left-lateral displacement began during the Late Pliocene,  
1224 influenced by variable NNE–SSW transpression (Kaymakçı et al., 2006). In summary, most of

1225 the neotectonic faults in the region studied have relatively small displacements (several  
1226 kms) that do not fundamentally change the regional tectono-stratigraphy; however, the  
1227 Sürgü–Misis Fault and Malatya-Ovacık Fault have tens of km of fault displacement that need  
1228 to be restored in any tectonic reconstruction.

1229

## 1230 **12. Discussion**

1231

1232 Below, we utilise the assembled body of evidence and interpretation to test and develop  
1233 several alternative tectonic hypotheses for the relationships between the main tectonic  
1234 units in the region.

1235

### 1236 12.1. Relation between the Northern and Southern allochthons and the Gürün autochthon

1237

1238 There are three main hypotheses for the emplacement of the northern and southern  
1239 allochthons in relation to the Gürün autochthon (Fig. 2). All three assume that the  
1240 allochthonous units cannot have been emplaced over the intact succession of the Gürün  
1241 autochthon, at least until the Mid-Late Eocene because of its intact stratigraphical  
1242 succession (Aziz et al., 1982; Perinçek and Kozlu, 1984; Robertson et al., 2013b).

1243 The first hypothesis is that the Southern allochthon was emplaced southwards over  
1244 the Gürün autochthon after deposition ended in the Early-Mid Eocene (Aziz et al., 1982).

1245 This is consistent with the evidence of southward thrusting during the Mid-Late Eocene in  
1246 the central Taurides (Özgül, 1984, 1997; Monod, 1977; Gutnic et al., 1979; Görür et al.,  
1247 1998; Demirtaşlı et al., 1984; Andrew and Robertson, 2002; Mackintosh and Robertson,  
1248 2012; McPhee et al., 2018b), and also in the western Taurides (De Graciansky, 1972;  
1249 Poisson, 1977; Şenel et al., 1989; Collins and Robertson, 1997, 1998, 1999; Robertson et al.,  
1250 2013a; Pourteau et al., 2016). However, a similar interpretation is problematic in the  
1251 eastern Taurides for three main reasons: (1) Thrust relations: A thrust is not mapped  
1252 regionally along the northern margin of the Gürün autochthon, between the Eocene  
1253 succession and the Northern allochthon (MTA, 2011; Bedi and Yusufoglu, 2018), although as  
1254 noted above, a thrust contact has been observed locally (Robertson et al., 2016). (2)

1255 Regional melange distribution: The Kemaliye Formation, as exposed above the Malatya

1256 (Keban) metamorphics in the Nurhak Dağ area (Area 3b), includes clasts and blocks derived

1257 from the Malatya and/or Köseyahya thrust sheets, strongly suggesting that allochthon  
1258 reached quite far south (10s km) of the Gürün autochthon during the latest Cretaceous. In  
1259 this case, the allochthon cannot have remained to the north of the Gürün autochthon until  
1260 the Eocene. (3) Cover relations: In the east, the Southern allochthon is locally covered and  
1261 sealed by late Maastrichtian-Eocene sediments of the Darende Basin (Fig. 2). Along the  
1262 western margin of the Darende basin (E of the bounding neotectonic Gürün fault)  
1263 specifically, allochthonous units, correlated with the Dağlıca ophiolite, are unconformably  
1264 overlain by conglomerates that pass upwards into Maastrichtian marls and limestones,  
1265 together with lenticular rudist build-ups (Kirankaya Formation). Further north, along the  
1266 western margin of the Darende basin, Maastrichtian sediments unconformably overlie the  
1267 Munzur limestone thrust sheet. Also, the Darende basin is transgressive on an equivalent of  
1268 the Munzur thrust sheet and related ophiolitic melange around its eastern margin (Booth et  
1269 al., 2013). After a Palaeocene-Early Eocene hiatus, the sedimentary succession passes into  
1270 Middle Eocene mixed siliciclastic/shallow-marine carbonates, with localised lenticular  
1271 volcanics, and then into Bartonian-early Priabonian regressive facies (Gürbüz and Gül, 2005;  
1272 Bedi et al., 2009; Booth et al., 2013). There is no evidence of increasing deformation  
1273 upwards that could relate to regional overthrusting. Any post-Cretaceous southward  
1274 emplacement of the Southern allochthon would instead need to entrain the Darende Basin  
1275 as a whole above an unexposed deeper-level regional-scale thrust. This requirement would  
1276 probably also apply to the Hekimhan Basin farther northeast (Booth et al., 2014). However,  
1277 there is no evidence that the Darende and Hekimhan basins are parts of a regional-scale  
1278 Eocene thrust sheet; e.g. no frontal thrust is exposed to the south. In summary, southward  
1279 emplacement of the Southern allochthon over the Gürün platform succession during, or  
1280 after, the Eocene seems unlikely.

1281 The second hypothesis is that the southern and northern allochthons were emplaced  
1282 from opposite directions during the latest Cretaceous, with the Gürün autochthon in  
1283 between (van Hinsbergen et al., 2020) (Fig. 27bi-bii). This is problematic for several reasons:  
1284 (1) The tectono-stratigraphy of both allochthons is very similar and does not indicate  
1285 different palaeogeographic origins; (2) The northward thrusting of the Malatya  
1286 Metamorphics that affects the Southern allochthon (e.g. İncirlik area) took place during the  
1287 Cenozoic because post-Cretaceous sediments are structurally interleaved; (3) The tectono-  
1288 stratigraphy of the E Tauride allochthons, combined, differs markedly from the South-

1289 Tauride allochthonous units; e.g. in the Adiyaman and Antalya areas (Robertson et al.,  
1290 2012).

1291         The third hypothesis is that both of the allochthonous units were assembled by  
1292 southward thrusting during the latest Cretaceous but in separate areas; subsequently the  
1293 Gürün autochthon and the already emplaced Northern allochthon were displaced  
1294 northeastwards (> 60 km) along the Güksu fault zone of Kozlu et al. (1990) to their present  
1295 positions, probably during the Mid-Late Eocene (Robertson et al., 2013b). This hypothesis is  
1296 consistent with the southwestward lateral passage of the Gürün autochthon into the Geyik  
1297 Dağ (Tauride platform) (e.g. in the Tufanbeyli-Saimbeyli-Feke-Kozan area) (MTA, 2011).  
1298 However, there are also problems with the right-lateral strike-slip hypothesis: (1) There is no  
1299 single clear-cut fault (terrane boundary fault) separating the Gürün autochthon from the  
1300 Southern allochthon; instead, strike-slip faults transect both the northern part of the  
1301 Southern allochthon and the southern part of the Gürün autochthon (Robertson et al.,  
1302 2013b; (2) Right-lateral strike-slip faults of appropriate c. NE-SW orientation are indeed  
1303 present (Robertson et al., 2013a; Supplementary Fig. 11) but these appear to post-date the  
1304 northward-directed displacement and folding of probable Mid-Late Miocene age. A possible  
1305 explanation is that eastward displacement of the Gürün autochthon/northern allochthon,  
1306 relative to the Southern allochthon, did indeed take place along the Eocene Göksu fault  
1307 zone of Kozlu et al. (1990) but this lineament was over-ridden and concealed during the  
1308 later folding and thrusting. The documented right-lateral neotectonic strike-slip faulting  
1309 along this lineament could have reactivated such a buried lineament. The dextral strike-slip  
1310 faults were overprinted by the dominantly Plio-Quaternary left-lateral faults affecting the  
1311 region in this interpretation.

1312         In summary, both the southern and the northern allochthons were emplaced  
1313 southwards onto the Tauride platform during latest Cretaceous time. The right-lateral  
1314 ‘terrane displacement’ interpretation is the most promising of the three options and could  
1315 also help to explain the regional east-directed Gürün curl (see Supplementary Fig. 1). In this  
1316 case the regional-scale ‘tectonic escape’ buckled the regional tectono-stratigraphy to form  
1317 the ‘curl’.

1318

1319 12.2. Relation between the Malatya Metamorphics and the Southern allochthon

1320

1321 Malatya Metamorphics encompass a Late Palaeozoic-Late Cretaceous stratigraphy,  
1322 consistent with a relatively internal part of the Tauride continent. No marginal (slope) units  
1323 are exposed. Assuming regional in-sequence thrusting, the Triassic-Late Cretaceous  
1324 successions of the Munzur and Köseyahya thrust sheets appear to represent northerly parts  
1325 of the Tauride continent that detached from their basement and were emplaced  
1326 southwards (Fig. 27a-c). During the Late Cretaceous, the more southerly located (Malatya)  
1327 platform (>75 km wide) was deeply underthrust northwards and metamorphosed under up  
1328 to amphibolite, or possibly low HP-LT conditions. This was associated with the intrusion of  
1329 the unmetamorphosed Baskil granitoids (88-82 Ma) (Bozkaya et al., 2007; Bedi et al., 2009;  
1330 Oberhansli et al., 2012; Rolland et al., 2012; Bedi and Yusufoglu, 2018) (Fig. 27d).

1331 In the northeast of the region, c. 100 km north of the main Malatya metamorphic  
1332 outcrop) there is a small outcrop that comprises Late Palaeozoic schist, overlain by Late  
1333 Permian meta-carbonates, Middle Triassic-Jurassic meta-platform carbonates and Late  
1334 Cretaceous meta-clastics/carbonates with meta-carbonate blocks (c. 40 km SW of Divriği;  
1335 Alacahan-Çetinkaya area; M on Fig. 2)) (Atabey and Aktimur, 1997; MTA, 2011; Robertson et  
1336 al., 2013b; Beyazpirinç and Akçay, 2013). The succession is comparable to the Malatya  
1337 Metamorphics, including the Late Cretaceous Karaböğürtlen Formation, suggesting that  
1338 Malatya metamorphic crust may extend far northwards beneath the Mesozoic  
1339 allochthonous units. However, it is also possible that the above outcrop represents the  
1340 metamorphosed northern margin of the Munzur platform (otherwise not exposed).

1341 In the northeast of the region (NW of Pınarbaşı), Hınzır Dağı and Korumaz Dağı (E of  
1342 Kayseri) there is an additional, sizeable outcrop of high-grade metamorphic rocks including  
1343 schist, gneiss and meta-platform carbonates, ranging in age from Carboniferous to  
1344 Cretaceous (Özer et al., 1984; Pourteau et al., 2010; MTA, 2011; unpublished data). These  
1345 rocks may correlate with the HP-LT Tavşanlı zone and/or the Afyon zone of the Anatolides  
1346 (Oberhansli et al., 2012; Pourteau et al., 2013), although more study is needed to confirm  
1347 this correlation.

1348 The Malatya Metamorphics exhumed rapidly (Robertson et al., 2013b), at least  
1349 partially, as indicated by the latest Cretaceous transgressive cover in the Malatya area  
1350 (Gündüzbey Formation) (Bedi and Yusufoglu, 2018). The Kemaliye Formation, extending  
1351 southwards from its type area near Kemaliye (Area 5A) for at least c. 120 km to Nurhak Dağı  
1352 (Area 3B), includes metamorphic debris from the Malatya Metamorphics and



1353 unmetamorphosed material from the Tauride allochthons, indicating that these two units  
1354 were juxtaposed during the latest Cretaceous. The Kemaliye Formation in its type area  
1355 accumulated during and/or very soon after exhumation of the Malatya Metamorphics. The  
1356 basal unconformity is interpreted as an eroded extensional detachment, explaining the  
1357 presence of high-strain lithologies (e.g. calc-schist; mylonite) near the top of the Malatya  
1358 metamorphics (Fig. 16i), and also as clasts in the overlying Kemaliye Formation. The Munzur  
1359 and Köseyahya thrust sheets were later re-activated and thrust farther south over the  
1360 Kemaliye Formation in the above areas, probably during the Mid-Late Eocene (Figs. 22a).

1361         The exposure of serpentinised harzburgite with small granitic intrusions that is sliced  
1362 between the Malatya metamorphics and the Kemaliye Formation ENE of Begre (Fig. 22a) is  
1363 interpreted as a fragment of the Göksun ophiolite and its granitic intrusions, as widely  
1364 exposed farther south. Compressional deformation (Mid-Late Miocene?) caused the cross-  
1365 cutting cleavage and cataclasis observed within the siliciclastic matrix of the Kemaliye  
1366 Formation in the south (Nurhak Dağı; Area 3B; see above). The overall evidence points to  
1367 complex multiphase displacement involving both the Malatya (Keban) metamorphics and  
1368 the Munzur-Köseyahya carbonate platform, during Late Cretaceous, Mid-Late Eocene and  
1369 Mid-Late Miocene (?).

1370

### 1371 12.3. Reconstruction of the allochthonous Tauride platform

1372

1373 Alternatives are: First, the Neritic-pelagic (Köseyahya) unit represents a basin within the  
1374 Munzur shelf. Secondly, the Munzur carbonate platform succession passed northwards into  
1375 the Neritic-pelagic (Köseyahya) platform (i.e. half-ramp) and then into the ocean (Fig. 26  
1376 a,b ) (preferred reconstruction).

1377         The first alternative (intra-platform basin) is hinted by the structural position of the  
1378 Neritic-pelagic (Köseyahya) succession beneath the main Munzur thrust sheet in the  
1379 Southern allochthon (Area 4; Fig. 9). However, against this: (1) No marginal facies of an  
1380 intra-platform basin are exposed; (2) The Neritic-pelagic thrust sheet also occurs above the  
1381 Munzur thrust sheet in the Northern allochthon suggesting that it restores to the north,  
1382 regionally (MTA, 2011; Robertson et al., 2013b). In the second, preferred option, initial  
1383 southward emplacement of the Tauride platform units during the latest Cretaceous (see  
1384 above) was accompanied by complex out-of-sequence thrusting, explaining why the Neritic-

1385 pelagic (Köseyahya) thrust sheet is locally above the main Munzur thrust sheet (e.g. Area 4;  
1386 Fig. 9). The distal edge of the Neritic-pelagic (Köseyahya) platform is therefore represented  
1387 by the Pelagic (Gülbahar) unit, with oceanic crust, including inferred seamounts to the north  
1388 (Fig. 28c,d).

1389

#### 1390 12.4. Ophiolite and melange emplacement; relation to units farther north

1391

1392 The East Tauride SSZ-type ophiolites were emplaced southwards onto the Tauride platform,  
1393 represented by the Munzur and Neritic-pelagic (Köseyahya) successions, together with  
1394 passive margin slope units (Pelagic (Gülbahar) unit) and oceanic sediments and igneous  
1395 rocks (accretionary melanges) (Figs. 28 e; 29 a-c). The driving force in the southward  
1396 emplacement was the collision of the regional-scale supra-subduction zone Tauride  
1397 ophiolite with the Tauride passive margin (Robertson et al., 2013b). The inferred tectonic  
1398 organisation at the end of the Cretaceous is summarised in Figure 30. By the late  
1399 Maastrichtian, the Malatya metamorphics were partially exhumed and eroded, while the  
1400 ophiolites were also partially eroded, producing a variable palaeotopography that was  
1401 smoothed by clastic debris and transgressed by a shallow sea; this deepened in places  
1402 during the Palaeocene, as indicated by fragmentary pelagic carbonates (Fig. 21e, f).

1403 Alternatives for the source of the ophiolites are:

1404 Option 1: All of the ophiolites, including those overlying the Arabian continent were derived  
1405 from a single Mesozoic Tethys to the north (Ricou et al., 1984) (Fig. 31 ai-aii), although this is  
1406 generally discounted nowadays (Robertson and Dixon, 1984; Stampfli and Borel, 2002;  
1407 Sosson et al., 2010; Rolland et al., 2012; van Hinsbergen et al., 2020);

1408 Option 2: The ophiolites in the area studied (e.g. Pınarbaşı, Divriği) and those to the south of  
1409 the Malatya Metamorphics (Göksun (N Berit), Kömürhan, İspendere) were derived from a  
1410 single oceanic basin located within Neotethys to the east and northeast (Stampfli et al.,  
1411 2001; Stampfli and Borel, 2002; Moix et al., 2008; Sosson et al., 2010; Rolland et al., 2012,  
1412 2016, 2020; van Hinsbergen et al., 2020; see Fig. 31 bi-bii).

1413 In one such scenario (Maffione et al., 2017), oceanic lithosphere was generated by  
1414 intra-oceanic SSZ-spreading, followed by generally southwestward roll-back and c. 90°  
1415 anticlockwise rotation of the subducting oceanic plate. Collision with continental blocks  
1416 emplaced ophiolites both southwards (i.e. Southern allochthon) and also northwards (i.e.

1417 Göksun (N Berit), Kömürhan, İspendere) onto the Malatya metamorphic crust. The  
1418 metamorphism relates to attempted bidirectional subduction during ophiolite emplacement  
1419 (Fig. 30). An Inner Tauride basin (rift or small ocean) did not exist or, if present, sutured  
1420 prior to overthrusting by the late Cretaceous ophiolites (Poisson et al., 1996; Hinsbergen et  
1421 al., 2016).

1422 In another, related scenario, the ophiolites were emplaced generally towards the  
1423 south-west, over a single Anatolide-Tauride-S Armenian continent (i.e. without an Inner  
1424 Tauride ocean) during the late Cretaceous (c. 75 Ma), all derived from the northern  
1425 Neotethys. The ophiolites of the northern Neotethys (İzmir-Ankara-Erzincan suture zone)  
1426 correlate with those of the Lesser Caucasus in Armenian and Georgia to the east,  
1427 representing remnants of an enormous (700 km long x 1-200 km wide) slab of oceanic  
1428 lithosphere that was emplaced onto continental crust during latest Cretaceous time (Sosson  
1429 et al., 2010; Rolland et al., 2012, 2016, 2020; Rolland, 2017; Hässig et al., 2013a, b).  
1430 Metamorphic soles of all of the ophiolites are similar in age (to within 10 Ma) suggesting  
1431 that the ophiolites were emplaced together. Subduction of the ocean was either  
1432 northwards, away from the continent (Sosson et al., 2010; Rolland et al., 2012, 2020), or  
1433 southwards, towards the continent (Hässig et al., 2015). Southward obduction was  
1434 facilitated by Cretaceous within-plate magmatism, documented in the Lesser Caucasus; this  
1435 rendered the ophiolitic lithosphere relatively hot and mobile at the time of emplacement  
1436 (Hässig et al., 2016). Syn-post emplacement extensional core-complex development thinned  
1437 the oceanic lithosphere and facilitated southward emplacement of ophiolites and related  
1438 continental margin units in this interpretation (Rolland et al., 2020).

1439 The above option (in its variants) is also problematic: (1) The allochthonous Tauride  
1440 units restore as a Permian-Triassic to Late Cretaceous rift/passive margin to an oceanic  
1441 basin further north. The emplacement of the continental margin, oceanic crust (melange)  
1442 and ophiolitic units are intimately related, coeval, and cannot be separated into a sutured  
1443 Inner Tauride Basin and overthrust ophiolites (relevant to the Maffione et al., 2017 model);  
1444 (2) the ophiolites in the E Taurides (e.g. Pınarbaşı and Divriği) are Late Cretaceous (Parlak et  
1445 al., 2013), whereas ophiolites further north within the Ankara-Erzincan suture zone  
1446 (northern Neotethys) are Early- Late Jurassic (Dilek and Thy, 2006; Robertson et al., 2013c;  
1447 Çelik et al., 2013; Hässig et al., 2013). Both ophiolites formed in a supra-subduction setting,  
1448 apparently related to northward subduction and cannot be treated as a single ophiolite of

1449 the similar age and tectonic setting (cf. Rolland et al., 2020); (3) Regional mapping (Bedi and  
1450 Yusufoglu, 2018) and our structural data (Fig. 26) are consistent with generally N to S  
1451 emplacement of the allochthonous Tauride units (in present coordinates) during the latest  
1452 Cretaceous (e.g. Area 2), without evidence of thrust sheets traversing the area obliquely, as  
1453 suggested by hypothesis two (cf. van Hinsbergen et al., 2016; Maffione et al., 2017); (4)  
1454 Evidence was not observed in our present field area to support emplacement of the Late  
1455 Cretaceous ophiolites by core complex-related gravity sliding (Hässig et al., 2016; Rolland et  
1456 al., 2020). Instead, the field evidence suggests that the ophiolites were relatively intact  
1457 when emplaced but were thinned in response to later multi-phase deformation and erosion.

1458         Option 3. The Tauride and Pontide-Lesser Caucasus ophiolites represent different  
1459 supra-subduction spreading events, which both culminated in Late Cretaceous regional  
1460 ophiolite emplacement (Parlak et al., 2012; Robertson et al., 2013c) (Fig. 31ci, cii). During  
1461 the Triassic, sea-floor spreading created oceanic lithosphere to the north of the Tauride-  
1462 Anatolide continental block. The Kırşehir continental unit represents a rifted continental  
1463 fragment with oceanic lithosphere potentially to the south and the north (e.g. Görür, et al.,  
1464 1984; Robertson et al., 2012; Barrier et al., 2018). The Jurassic Pontide-Lesser Caucasus  
1465 ophiolite formed in the Early-Mid Jurassic when oceanic lithosphere to the north of the  
1466 Kırşehir continental unit started to subduct northwards (Dilek and Thy, 2006; Robertson et  
1467 al., 2013c; Topuz et al., 2013a). During the Late Cretaceous, plate convergence triggered the  
1468 genesis of the Late Cretaceous Tauride ophiolites above a N-dipping subduction zone. To the  
1469 west and east of the Kırşehir continental unit Jurassic and Cretaceous oceanic crust were  
1470 effectively contiguous with no exposed intervening suture. The Tauride ophiolites were  
1471 obducted by regional trench-passive margin collision during the latest Cretaceous, which  
1472 emplaced the Late Cretaceous ophiolites and related melanges throughout the eastern,  
1473 central and western Taurides as a whole (Görür et al., 1984; Andrew and Robertson, 2002;  
1474 Clark and Robertson, 2002; Okay et al., 2001; Kadioğlu et al., 2006; Nairn et al., 2013,  
1475 Robertson et al., 2013c; Lefebvre et al., 2013b; Darin et al., 2018; Scleiffarth et al., 2018;  
1476 Legeay et al., 2019). The leading of the colliding Tauride passive margin, represented by the  
1477 Anatolide crustal block, subducted and underwent HP-LT metamorphism (Pourteau et al.,  
1478 2010, 2013). Uncertainties with the above option include: i) The absence of an exposed  
1479 suture between the E Taurides and Pontide ophiolites, although one may exist subsurface;  
1480 ii) The lack of definitive evidence that Late Cretaceous ophiolites farther west (i.e. Pozanti-

1481 Karsanti and Alihoca ophiolites) originated to the south of the Kirşehir crustal block. In  
1482 summary, the evidence discussed in this paper is consistent with, but not definitive of,  
1483 ophiolite emplacement from an Inner Tauride ocean that was located to the south of the  
1484 Mid-Late Jurassic oceanic crust that characterises the İzmir-Ankara-Erzincan suture zone.

1485

1486 14.5. Malatya metamorphics: relation to adjacent crustal units

1487

1488 There are three main options:

1489 A first option is that the Malatya metamorphics directly correlate with the Afyon zone  
1490 (Anatolides). The Afyon zone (Bolkar nappe) is restored to a northerly position relative to  
1491 the unmetamorphosed Aladağ nappe (Özgül, 1984; Pourteau et al., 2010, 2013; Mackintosh  
1492 and Robertson, 2012). By extension, the Munzur-Köseyahya platform originated as the  
1493 southward extension of the Malatya carbonate platform. Problems, however, with this are:  
1494 (1) The Malatya metamorphics are cut by the c. 88-82 Ma Baskil granitoids, which are  
1495 attributed to northward subduction from an oceanic basin to the south (Berit ocean),  
1496 suggesting a relatively southerly location (Rızaoğlu et al., 2006, 2009; Karaoğlu et al., 2012,  
1497 2016) (Fig. 30); (2) In contrast, the Afyon zone lacks comparable intrusives suggesting a  
1498 different palaeogeographic setting; (3) Option 1 implies northward deep-level  
1499 underthrusting of the Malatya platform, followed by exhumation, large-scale out-of-  
1500 sequence southward thrusting to place the metamorphics in their present structural order  
1501 beneath the allochthonous Tauride platform units (van Hinsbergen et al., 2020). However,  
1502 there is no obvious evidence of such regional-scale re-thrusting during either the latest  
1503 Cretaceous or the Eocene regional tectonic events (e.g. metamorphic klippen or foredeeps  
1504 with metamorphic detritus are absent). Regional southward emplacement of the northerly  
1505 ophiolites (Göksun (N Berit), Kömürhan, İspendere) over the entire Tauride platform,  
1506 followed by re-imbrication beneath, as proposed by van Hinsbergen et al. (2020), is also  
1507 problematic. The base of the tectonic contact between the Malatya metamorphics and the  
1508 Göksun ophiolite beneath is cut and sealed by the 83-81 Ma (Santonian-Campanian) Esence  
1509 granites (Karaoğlu et al., 2016), whereas the northerly ophiolites were emplaced  
1510 southwards only after deposition of the Albian-Santonian Kızılkandil Formation and the  
1511 overlying late Campanian-late Maastrichtian Kemaliye Formation (based on nannofossil  
1512 dating).

1513 A second option is that the Afyon zone and the Malatya metamorphics do indeed  
1514 correlate laterally but that the Munzur-Köseyahya platform units represent a separate  
1515 platform that was located to the northeast of the Geyik Dağ (Tauride autochthon). The  
1516 main problem with this interpretation is the absence of any preserved platform-slope facies  
1517 (e.g., deep-water slope facies and radiolarites) that could indicate the presence of a rifted  
1518 margin to the Malatya platform in the north (Perinçek and Kozlu, 1984; Kozlu et al., 1990;  
1519 Bedi et al., 2009; Robertson et al., 2013b; Bedi and Yusufoglu, 2018). Also, there is no  
1520 evidence of a southern rifted margin to the Munzur-Köseyahya platform in the south, which  
1521 would be expected in this alternative. However, it is possible that such margin units existed  
1522 but are not exposed.

1523 A third option is that the present regional-scale tectono-stratigraphy retains the latest  
1524 Cretaceous emplacement organisation. In this case, the Malatya and Afyon units, despite  
1525 undergoing similar metamorphism, did not form a continuous litho-tectonic unit. The Afyon  
1526 zone originated further northwest, whereas the Malatya metamorphic originated further  
1527 southeast (possibly offset by a c. N-S transform). The Munzur-Köseyahya platform formed a  
1528 separate crustal block to the northeast. The Malatya metamorphics originated by collapse of  
1529 the putative basin between the separate Malatya and Munzur Köseyahya platforms (see  
1530 above). Such a basin might have formed during Triassic rifting. Collapse of the inferred intra-  
1531 platform basin might have been driven by compression between two N-dipping subduction  
1532 zones (Berit/Göksun in the S; Inner Tauride in the N).

1533 In the absence of field evidence of major tectonic re-ordering as required in options 1  
1534 and 2, we favour option 3, which implies major palaeogeographic changes between the  
1535 central and eastern Taurides. It seems likely that the central Tauride platform (Geyik Dağ)  
1536 narrowed eastwards (Fig. 30), close to the future position of the neotectonic Sürgü-Misis  
1537 fault zone. To the west, the southern part of the Tauride platform (Geyik Dağ) was not  
1538 covered by the late Cretaceous south-moving allochthons. In contrast, farther east part of  
1539 the Tauride platform represented by the Malatya metamorphics, underthrust/subducted  
1540 northwards beneath more northerly Tauride crust (Munzur-Köseyahya platfors) (Fig. 30cii).

1541 Restoring the reported c. 29 km left-lateral offset along the neotectonic Malatya-  
1542 Ovacık Fault Zone (Westaway and Arger, 2001) still leaves the type outcrop of the Munzur  
1543 platform in the Munzur Dağları (Fig. 2) c. 80 km to the north of its counterpart within the  
1544 Southern allochthon (Munzur thrust sheets). The Tauride (Munzur) platform could,

1545 therefore, have stepped northwards towards the northeast, bounded by one or more c. N-S  
1546 transcurrent faults. However, it is unclear whether this would be entirely a Mesozoic  
1547 palaeogeographic feature or if it could relate to latest Cretaceous-Eocene (pre-Neogene)  
1548 tectonics. In either case, pre-existing faults are likely to have been re-activated to form  
1549 many of the major neotectonic faults seen today. In the absence of continuous exposure, or  
1550 subsurface evidence (e.g., borehole or seismic reflection) it is, therefore, uncertain as to  
1551 whether or not the South Armenian platform in the Lesser Caucasus simply represents the  
1552 eastward extension of the Tauride continent. Previously, the two platform exposures were  
1553 inferred to be parts of a single large continental unit mainly because of similar late  
1554 Cretaceous ophiolite emplacement in both areas (Sosson et al., 2010; Rolland et al., 2012).  
1555 However, an origin as two separate platforms is not precluded.

1556 The Malatya and Bitlis-Pütürge metamorphic units (Fig. 1) have also been considered to  
1557 represent, respectively westerly and more easterly segments of a single southerly active  
1558 margin of the Tauride continent, with the Southern Neotethys to the south (Barrier et al.,  
1559 2018). However, the Malatya and Bitlis-Pütürge continental units are separated by the Late  
1560 Cretaceous supra-subduction Göksun (N Berit), Kömürhan, İspendere and Yüksekova  
1561 ophiolites, interpreted as an intervening ocean basin (Robertson et al., 2006, 2012; Rolland  
1562 et al., 2012; Candan et al., 2014; Çetinkaplan et al., 2016; Barrier et al., 2018). The available  
1563 evidence is consistent with the existence of a southerly oceanic basin (Berit, or Göksun  
1564 ocean) that subducted northwards beneath the Malatya-Tauride platform during latest  
1565 Cretaceous (Fig. 30). The ophiolites (Göksun, İspendere and Kömürhan), dated at c. 87-85  
1566 Ma, formed above a subduction zone and include immature arc volcanics (Parlak et al.,  
1567 2009). The volcanics of the above ophiolites can also be broadly correlated with the Late  
1568 Cretaceous Yüksekova complex (dated at c. 83-75 Ma) (Karaoğlan et al., 2013), which is  
1569 traditionally interpreted as an immature oceanic arc (e.g. Ural et al., 2015 and references).

1570 As noted above, the Göksun SSZ-type lithosphere was emplaced beneath the Malatya  
1571 Metamorphic crust, where both were intruded by subduction-related granitic rocks (88-82  
1572 Ma Baskil intrusives) (Karaoğlan et al., 2016; Parlak, 2006; Rızaoğlu et al., 2009). The Baskil  
1573 intrusives include shoshonitic compositions (dated at 74–72 Ma), suggestive of collisional  
1574 and/or post-collisional settings (Ertürk et al., 2018; Kuşcu et al., 2013; Sar et al., 2019). This  
1575 is consistent with the collision of the Bitlis-Pütürge continental units to the south with the  
1576 Tauride continent to the north (Malatya Metamorphics) thereby closing the Berit ocean. In

1577 many reconstructions, some oceanic crust (Southern Neotethys) existed between the Bitlis-  
1578 Pütürge continental units and the Arabian continent. The initial closure of this ocean basin  
1579 and collision with Arabia may have occurred during the Mid-Late Eocene, but the main  
1580 collision took place during the Mid-Late Miocene (Aktaş and Robertson, 1984; Yılmaz, 1993;  
1581 Robertson et al., 2012a; Rolland et al., 2012, 2020; Barrier et al., 2018; van Hinsbergen et  
1582 al., 2020).

1583

## 1584 **Conclusions**

1585

1586 -The well-exposed eastern Taurides provide important insights into Tethyan  
1587 palaeogeography and tectonic development, including the unusual Gürün curl structure.

1588 -The region is restored as part of the northern rifted margin of the Tauride continent.

1589 -Rifting took place during the Triassic, separating a shallow-water carbonate platform to the  
1590 south from a deep-water proximal to distal slope and ocean basin to the north (Inner  
1591 Tauride ocean).

1592 -The regional Tauride carbonate platform (Geyik Dağ) is proposed to have narrowed and  
1593 become more palaeogeographically varied towards the eastwards, mainly represented, in  
1594 the E Taurides, by the Malatya Metamorphics and the unmetamorphosed Munzur and  
1595 Köseyahya platform units.

1596 -The restored northern part of the shallow-water combined Munzur-Köseyahya platform  
1597 subsided during the Mid-Jurassic to form a gently sloping, deeper-water ramp near, or  
1598 beneath, the carbonate compensation depth.

1599 -The Munzur-Köseyahya platform slope was covered by pelagic carbonate during the Late  
1600 Cretaceous, probably related to regional tectonic subsidence (rather than global sea-level  
1601 rise).

1602 -Dismembered deep-sea sedimentary and volcanic units exposed over a wide area are  
1603 restored as the former Triassic-Cretaceous deep-water passive margin slope/base of slope  
1604 of the Mesozoic carbonate platform (Pelagic (Gülbahar) unit).

1605 -Oceanic lithosphere formed above a subduction zone in the ocean (Inner Tauride ocean),  
1606 generally to the north (Pınarbaşı, Dağlıca, Hekimhan, Kuluncak and Divriği (and Güneş)  
1607 ophiolites), with associated formation of ophiolite metamorphic sole (although only locally  
1608 preserved).



1609 -Local, fragmentary successions of mainly within-plate-type basalts and radiolarian  
1610 cherts/pelagic limestones are interpreted as accreted/emplaced Jurassic-Cretaceous  
1611 oceanic seamounts.

1612 - Associated with emplacement of the Late Cretaceous ophiolites, the Tauride passive  
1613 margin underwent flexural loading and collapse to form a foredeep (late Campanian-  
1614 Maastrichtian). Talus in the form of gravity flows, blocks and disrupted sheets was shed into  
1615 the basin, mainly from the platform/slope units, and the advancing ophiolites/accretionary  
1616 melanges.

1617 -During the latest Cretaceous (late Campanian-late Maastrichtian), the SSZ ophiolites were  
1618 emplaced generally southwards onto the Tauride platform, in some areas as relatively intact  
1619 sheets (c. 6 km thick) (e.g. Pınarbaşı ophiolite), but elsewhere as dismembered units,  
1620 melanges and ophiolite-related debris flows (i.e. Dağlıca ophiolite and melange).

1621 -During its late Cretaceous southward tectonic transport, the allochthonous carbonate  
1622 platform was locally re-thrust, in places putting the restored southerly neritic carbonate  
1623 platform (Munzur thrust sheet) over the more northerly-derived deeper water facies  
1624 (Köseyahya thrust sheet).

1625 -Mixing of clastic debris (Kemaliye Formation) that derived from both the over-riding  
1626 Tauride allochthons and the Malatya Metamorphics shows that both were tectonically  
1627 juxtaposed (in close proximity) during the latest Cretaceous regional emplacement.

1628 -The Malatya Metamorphics were at least partially exhumed by the late Maastrichtian as  
1629 they are covered and sealed by latest Cretaceous sediments, that include metamorphic and  
1630 granitoid debris.

1631 -The Malatya Metamorphics were tectonically juxtaposed with the Göksun (and related  
1632 ophiolites) to the south during the latest Cretaceous. Both are cut and sealed by the 88-82  
1633 Ma Baskil granitoids. The latest Cretaceous marine sedimentary cover of the Göksun  
1634 ophiolite includes detritus from both the metamorphics and the unmetamorphosed Tauride  
1635 units, pointing to rapid exhumation.

1636 - Following Eocene shelf-depth deposition, folding and re-thrusting took place widely during  
1637 the Mid-Late Eocene. However, the co-intrusion of the Güksun ophiolite and Malatya  
1638 Metamorphics by the Late Cretaceous granites (Baskil granites) shows that these two  
1639 regional-scale crustal units were not displaced a large distance relative to each other (i.e.  
1640 >several km) after the latest Cretaceous.

1641 -Allochthonous units were first juxtaposed with the relatively autochthonous Gürün  
1642 platform succession (as presently exposed) during Mid-Late Eocene. In the absence of clear  
1643 evidence that the allochthonous Tauride units to the north (Northern allochthon) were  
1644 emplaced southwards over the autochthonous Gürün platform during this time, an  
1645 alternative is that the Southern allochthon and the Gürün platform/Northern allochthon  
1646 were brought together by >60 km of right-lateral transport during Mid-Late Eocene (i.e. as a  
1647 result of collision-related 'tectonic escape').

1648 -The Mid-Late Eocene deformation (folding and thrusting) is explained by thick-skinned  
1649 deformation, driven by suturing of the İzmir-Ankara-Erzincan ocean (northern Neotethys).

1650 - Mid-Late Miocene folding and thrusting (northwards in several areas) is explained by  
1651 suturing of the Southern Neotethys and collision with Arabia.

1652 -The available evidence is mainly consistent with the former existence of an Inner Tauride  
1653 ocean, comprising Late Cretaceous supra-subduction zone oceanic crust, that was separate  
1654 from more northerly supra-subduction zone oceanic crust, of Mid-Late Jurassic age, within  
1655 the İzmir-Ankara-Erzincan suture zone farther north.

1656

## 1657 **Acknowledgements**

1658

1659 We thank the DARIUS programme for financial support to carry out the fieldwork.  
1660 Additional funding from the John Dixon Memorial Fund assisted with the laboratory-based  
1661 studies. Güzide Önal assisted with drawing the diagrams. We thank Tumur Ustaömer and  
1662 Rolland Oberhansli for discussion. The manuscript benefitted from reviews by Aral Okay and  
1663 Yann Rolland, and advice from the editor, Ibrahim Uysal.

1664

1665 (This research did not receive any specific grant from funding agencies in the public,  
1666 commercial, or not-for-profit sectors.)

1667

1668

1669 **References**

1670

1671 Aktaş, G., Robertson, A.H.F., 1984. The Maden Complex, S E Turkey: Evolution of a  
1672 Neotethyan continental margin. In: Dixon, J.E., Robertson, A.H.F. (Eds.), The  
1673 Geological Evolution of the Eastern Mediterranean. Geological Society, London,  
1674 Special Publications, 17, 375–402.

1675 Aktimur, H.T., 1988. 1:100,000-scale Turkish geological map series, Divriği-F26 map. Mineral  
1676 Research and Exploration Institute of Turkey (MTA), Ankara (in Turkish).

1677

1678 Aktimur, H.T., Atalay, Z., Ateş, S., Tekerli, M.E., Yurdakul, M.E., 1988. Geology of the area  
1679 between Munzur Mountains and Çavuşdağı. Mineral Research and Exploration  
1680 Institute of Turkey (MTA), Report No. 301, 102p. (in Turkish).

1681 Andrew, T., Robertson, A.H.F., 2002. The Beyşehir–Hoyran–Hadim Nappes: genesis and  
1682 emplacement of Mesozoic marginal and oceanic units of the northern Neotethys  
1683 in southern Turkey. *Journal of the Geological Society, London* 159, 529–543.

1684 Atabey, E., 1993. Stratigraphy of Gürün autochthonous (Gürün-Sarız arası), Doğu Toroslar-GB  
1685 Sivas. *Türkiye Jeoloji Bülteni* 36/2, 99-113 (in Turkish).

1686

1687 Atabey, E., 1995. Geological evolution and sedimentology of the Gürün autochthone,  
1688 Department of Geological Engineering, Ankara University, Unpublished PhD thesis  
1689 (in Turkish).

1690

1691 Atabey, E., Aktimur, H.T., 1997. 1:100,000 Geological Map of Turkey, 48 (Sivas-G24), Mineral  
1692 Research and Exploration Institute of Turkey (MTA), Ankara (in Turkish).

1693

1694 Atabey, E., Bağırşakçı, S., Canpolat, M., Gökkaya, K.Y., Günal, S., Kılıç, N., 1994. Geology of  
1695 the area between Gürün-Kangal (Sivas) and Darende-Hasançelebi. Mineral  
1696 Research and Exploration Institute of Turkey (MTA), Report 9760 (unpublished) (in  
1697 Turkish).

1698

- 1699 Atabey, E., Bağırsakçı, K.Y., Gökkaya, S., Günal, S., Kılıç, N., Canpolat, M., 1997. 1:100,000  
1700 Geological Map of Turkey, 49 (Elbistan-H24), Mineral Research and Exploration  
1701 Institute of Turkey (MTA), Ankara (in Turkish).  
1702
- 1703 Aziz, A., Eraman, B., Kurt, G., Meşhur, M., 1982. Geological report for the area of Pınarbaşı-  
1704 Sarız-Gürün. Turkish Petroleum Company, Unpublished Report, 1601p. (in  
1705 Turkish).  
1706
- 1707 Barrier, E., Vrielynck, B., Brouillet, J.F., Brunet, M.F., 2018. Paleotectonic Reconstruction of  
1708 the Central Tethyan Realm. Tectono-Sedimentary-Palinspastic Maps from Late  
1709 Permian to Pliocene. CCGM/CGMW, Paris, Atlas of 20 maps (scale: 1/15.000.000).  
1710
- 1711 Bedi, Y., Usta, D., 2006. Palaeozoic stratigraphy of Tufanbeyli-Feke-Kozan regions (Eastern  
1712 Taurides). 6<sup>th</sup> Workshop of Stratigraphy Committee of Turkey: Lithostratigraphic  
1713 Nomenclature of PreCambrian - Palaeozoic units of the Taurides and SE Anatolia,  
1714 abstract book, p. 22-23, Ankara (in Turkish).  
1715
- 1716 Bedi, Y., Yusufoglu, H., 2018. 1:000,000 scale Türkiye Jeoloji Haritaları Serisi (Turkish  
1717 geological map series), Malatya-L49 Parftası, No. 261 (in Turkish).  
1718
- 1719 Bedi, Y., Senel, M., Usta, D., Özkan, M. K., Beyazpınar, M., 2004. The geological properties of  
1720 Binboğa Mountains and their correlation with similar units in west-central  
1721 Taurides. 57<sup>th</sup> Geological Congress of Turkey, Abstracts, 270-271.  
1722
- 1723 Bedi, Y., Usta D., Özkan, M.K., Beyazpınar, M., Yıldız, H., Yusufoglu, H., 2005. The tectono-  
1724 stratigraphic characteristics of allochthonous sequences in Eastern Taurides. 58<sup>th</sup>  
1725 Geological Congress of Turkey, Abstracts, 262-263.  
1726
- 1727 Bedi Y., Yusufoglu, H., Beyazpınar, M., Özkan, M.K., Usta D., Yıldız, H., 2009. Geodynamical  
1728 evolution of the Eastern Taurides (Afşin-Elbistan-Göksun-Sarız area). Mineral  
1729 Research and Exploration Institute of Turkey (MTA), Report No. 11150, 388 p. (in  
1730 Turkish).

- 1731
- 1732 Bedi, Y., Yusufoglu, H., Usta, D., Okuyucu, C., 2012. The presence of the Aladağ and Yahyalı  
1733 Nappes in the Eastern Taurides (Afşin-Malatya) and their tectonostratigraphic  
1734 characteristics. In: Paleozoic of Northern Gondwana and its petroleum potential a  
1735 field workshop, Sept. 9<sup>th</sup> European Association of Geoscientists and Engineers, p.  
1736 cp-367.
- 1737
- 1738 Bedi, Y., Krystyn, K., Tekin, U.K., Okuyucu, C., Demiray, D.G.S., 2016. A geosite area:  
1739 ammonoid assemblages of late Carnian age in the Domuzdağ Nappe (Eastern  
1740 Taurides, Elbistan, Kahramanmaraş), 69<sup>th</sup> Geological Congress of Turkey, 11-15  
1741 April 2016, Ankara, 215-215.
- 1742 Bedi, Y., Yusufoglu, H., Tekin, U.K., Usta, D., 2017. The tectonostratigraphic characteristics of  
1743 autochthonous and allochthonous sequences exposed among Tufanbeyli (Adana),  
1744 Elbistan (K.Maraş) and Malatya, eastern Taurides. Abstracts of the 70<sup>th</sup> Geological  
1745 Congress of Turkey, 10-14 April, Ankara, 22-23.
- 1746 Beyazpıncı, M., Akçay, A.E., 2013. The tectono-stratigraphic features of metamorphites in  
1747 Alacahan-Çetinkaya region (Kangal, Sivas). Bulletin of Mineral Research and  
1748 Exploration Institute of Turkey (MTA), 147, 19-29 (in Turkish).
- 1749 Bilgiç, T., 2008a. 1:100,000 Türkiye Jeoloji Haritaları, No: 85. Divriği-J39 Paftası (Divriği area),  
1750 Mineral Research and Exploration Institute of Turkey (MTA) (in Turkish).  
1751
- 1752 Bilgiç, T., 2008b. 1:100,000 Türkiye Jeoloji Haritaları, No: 85. Divriği-J40 Paftası (Divriği area),  
1753 Mineral Research and Exploration Institute of Turkey (MTA) (in Turkish).  
1754
- 1755 Bilgiç, T., 2008c 1:100,000 Türkiye Jeoloji Haritaları, No: 85. Divriği-J41 Paftası (Kemaliye  
1756 area), Mineral Research and Exploration Institute of Turkey (MTA) (in Turkish).  
1757
- 1758 Booth, M.G., Robertson, A.H.F., Taslı, K., İnan, N., Ünlügenç, U.C., Vincent, S., 2013. Two-  
1759 stage development of the Late Cretaceous to Late Eocene Darende Basin  
1760 implications for closure of Neotethys in central eastern Anatolia (Turkey). In:

- 1761 Robertson, A.H.F., Parlak, O., Ünlügenç, U.C. (Eds.), Geological Development of  
1762 Anatolia and the Easternmost Mediterranean Region. Geological Society, London,  
1763 Special Publications 372, pp. 385-420.  
1764
- 1765 Booth, M.G., Robertson, A.H.F., Taslı, K., İnan, N., 2014. Late Cretaceous to Late Eocene  
1766 Hekimhan Basin (Central eastern Turkey), as a supra-ophiolite  
1767 sedimentary/magmatic basin related to the latest stages of closure of Neotethys.  
1768 Cenozoic extensional tectonics in western Anatolia, Turkey. *Tectonophysics* 635,  
1769 6–32.  
1770
- 1771 Bosellini, A., Winterer, E.L., 1975. Pelagic limestone and radiolarite of the Tethyan Mesozoic:  
1772 a genetic model. *Geology* 3, 279-282.  
1773
- 1774 Bozkaya, Ö., Yalçın, H., Başbüyük, Z., Özfirat, O., Yılmaz, H., 2007. Origin and evolution of the  
1775 Southeast Anatolian metamorphic complex (Turkey). *Geologica Carpathica* 58,  
1776 197-210.  
1777
- 1778 Boztuğ, D., Harlavan, Y., Arehart, G.B., Satır, M., Avcık, N., 2007. K-Ar age, whole-rock and  
1779 isotope geochemistry of A-type granitoids in the Divriği-Sivas region, eastern-  
1780 central Anatolia, Turkey. *Lithos* 97, 193-218.  
1781
- 1782 Camuzcuoğlu, M., Bağcı, U., Koepke, J., Wolff, P.E., 2017. Tectonic significance of the  
1783 cumulate gabbros within Kuluncak ophiolitic suite (Malatya, SE Turkey) inferred  
1784 from geochemical data. *Ofioliti* 42, 81-103.  
1785
- 1786 Candan, O., Koralya, E., Çetinkaplan, M., Ersoy, Y., Topuz, G., Oberhaensli, R., Lid, Q.,  
1787 Yiğitbaş, E., 2014. Late Cretaceous-Eocene tectonometamorphic evolution of the  
1788 Berit meta-ophiolites and continental crustal units, north of  
1789 Kahramanmaraş/Turkey, 67<sup>th</sup> Geological Congress of Turkey, April, 560-561.  
1790
- 1791 Çelik, Ö.F., Chiaradia, M., marzoli, A., Billor, Z., Marschik, R., 2013. The Eldivan ophiolite and  
1792 volcanic rocks in the İzmir–Ankara–Erzincan suture zone, Northern Turkey:

1793 Geochronology, whole-rock geochemical and Nd–Sr–Pb isotope characteristics. *Lithos*  
1794 172-173, 31-46.  
1795  
1796 Çetinkaplan, M., Pourteau, A., Candan, O., Koralay, O.E., Oberhänsli, R., Okay, A.İ., 2016. P-T-  
1797 t evolution of eclogite/blueschist facies metamorphism in Alanya Massif: Time and  
1798 Space relations with HP event in Bitlis Massif, Turkey. *International Journal of Earth*  
1799 *Sciences* 105, 247–281.  
1800  
1801 Clark, M.S., Robertson, A.H.F., 2002. The role of the early Cenozoic Ulukışla Basin, southern  
1802 Turkey in suturing of the Mesozoic Tethys ocean. *Journal of the Geological Society,*  
1803 *London* 159, 673–690.  
1804  
1805 Cohen, K.M., Harper, D.A.T., Gibbard, P.L., 2020. ICS International Chronostratigraphic Chart,  
1806 2020/01. International Commission on Stratigraphy, IUGS. [www.stratigraphy.org](http://www.stratigraphy.org)  
1807  
1808 Collins, A.S., Robertson, A.H.F., 1997. Lycian melange, southwestern Turkey: an emplaced  
1809 Late Cretaceous accretionary complex. *Geology* 25, 25–258.  
1810  
1811 Collins, A., Robertson, A.H.F., 1998. Processes of Late Cretaceous to Late Miocene episodic  
1812 thrust-sheet translation in the Lycian Taurides, southwestern Turkey. *Journal of*  
1813 *the Geological Society, London* 155, 759-772.  
1814  
1815 Collins, A., Robertson, A.H.F., 1999. Evolution of the Lycian allochthon, western Turkey, as a  
1816 north-facing Late Palaeozoic–Mesozoic rift and passive continental margin.  
1817 *Geological Journal* 34, 107–138.  
1818  
1819 Darin, M., Umhoefer, P.J., Thomson, S., 2018. Rapid late Eocene Exhumation of the Sivas  
1820 Basin (Central Anatolia) driven by initial Arabia-Eurasia collision. *Tectonics* 37,  
1821 3805-3833.  
1822  
1823 Demirtaşlı, E., Turhan, N., Bilgin, A.Z., Selim, M., 1984. Geology of the Bolkar Mountains, In:  
1824 Tekeli, O., Göncüoğlu, M.C. (Eds.), *Geology of the Taurus Belt. Proceedings*

- 1825 International Symposium on the Geology of the Taurus Belt, Ankara, Turkey.  
1826 Mineral Resources and Exploration Institute of Turkey, pp. 125-141.  
1827
- 1828 Dilek, Y., Moores, E.M., 1990, Regional tectonics of the Eastern Mediterranean ophiolites, In:  
1829 Moores, E.M., Panayiotou, A., Xenophontos, C., Ophiolites, Oceanic Crustal  
1830 Analogues, Proceedings of the Symposium "Troodos 1987," Geological Survey  
1831 Department, Nicosia, Cyprus, pp. 295–309.  
1832
- 1833 Dilek, Y., Whitney, D.L., 1997. Counterclockwise P–T–t trajectory from the metamorphic sole  
1834 of a Neotethyan ophiolite (Turkey). *Tectonophysics* 280, 295–310.  
1835
- 1836 Dilek, Y., Thy, P., 2006. Age and petrogenesis of plagiogranite intrusions in the Ankara  
1837 melange, central Turkey. *Island Arc* 15, 44–57.  
1838
- 1839 Duman, T.Y., Emre, Ö., 2013. The East Anatolian fault: geometry, segmentation and jog  
1840 characteristics, In: Robertson, A.H.F., Parlak, O., Ünlügenç, U.C. (Eds.), *Geological*  
1841 *Society, London Special Publication* 372, pp. 495–529.  
1842
- 1843 Dumitrica, P., Tekin, U.K, Bedi, Y., 2013. Taxonomic study of spongy spumellarian Radiolaria  
1844 with three and four coplanar spines or arms from the middle Carnian (Late  
1845 Triassic) of the Köseyahya nappe (Elbistan, SE Turkey) and other Triassic localities.  
1846 *Paläontologische Zeitschrift Scientific Contributions to Palaeontology* 87, 345-395.  
1847
- 1848 Ekici, T., Alpaslan, M., Parlak, O., Temel, A., 2007. Geochemistry of the Pliocene basalts  
1849 erupted along the Malatya-Ovacık fault zone (MOFZ), eastern Anatolia, Turkey:  
1850 implications for source characteristics and partial melting processes. *Chemie der*  
1851 *Erde-Geochemistry* 67, 201–212.  
1852
- 1853 Emre, Ö., Duman, T.Y., Özalp, S., Çan, T., Olgun, Ş., Elmacı, H., Şaroğlu, F., 2018. Active fault  
1854 database of Turkey. *Bulletin of Earthquake Engineering* 16, 3229–3275.  
1855
- 1856 Erdoğan, B., 1975. Geology of Gölbaşı region. TPAO Report No. 917 (unpublished) (in



- 1857 Turkish).
- 1858
- 1859 Erkan, E.N., Özer, S., Sümengen, M., Terlemez, İ., 1978. Geology of Sarız, Şarkışla, Gemerek,
- 1860 Tomarza regions. Mineral Research and Exploration Institute of Turkey (MTA) Report
- 1861 No: 5641, Ankara (unpublished), (in Turkish).
- 1862
- 1863 Ertürk, M.A., Beyarslan, M., Chung, S.L., Lin, T.H., 2018. Eocene magmatism (Maden
- 1864 Complex) in the Southeast Anatolian Orogenic Belt: magma genesis and tectonic
- 1865 implications. *Geoscience Frontiers* 9, 1829–1847.
- 1866
- 1867 Genç, Ş.C., Yiğitbaş, E., Yılmaz, Y., 1993. The geology of the Berit Metaophiolite. A. Suat Erk
- 1868 Jeoloji Sempozyumu, Bildiriler Kitabı, pp. 37-52 (In Turkish with English abstract).
- 1869
- 1870 Göncüoğlu, M.C., Göncüoğlu, Y., Kozur, H.W., Kozlu, H., 2004. Paleozoic stratigraphy of the
- 1871 Geyik Dağ unit in the Eastern Taurides and implications for Gondwanian evolution.
- 1872 *Geologica Carpathica* 55, 433-447.
- 1873
- 1874 Görür, N., Oktay, F.Y., Seymen, İ., Şengör, A.M.C., 1984. Paleotectonic evolution of Tuz Gölü
- 1875 Basin complex, central Turkey, In: Dixon, J.E. & Robertson, A.H.F. (Eds.), *The*
- 1876 *Geological Evolution of the Eastern Mediterranean*. Geological Society Special
- 1877 Publication, London 17, pp. 81-96.
- 1878
- 1879 Görür, N., Şengör, A.M.C., Okay, A.İ., Tüysüz, O., Sakıncı, M., Yiğitbaş, E., Akkök, R., Özgül, N.,
- 1880 Genç, T., Örcen, S., Ercan, T., Akyürek, B. Şaroğlu, F., 1998. Triassic to Miocene
- 1881 Palaeogeographic Atlas of Turkey. İTÜ Maden Fak. Genel Anabilimdalı, Tübitak
- 1882 Global Tektonik Araştırma Ünitesi), MTA Genel Müdürlüğü, Ankara (in Turkish).
- 1883
- 1884 Graciansky, P.C. de, 1972. *Recherches géologiques dans le Taurus Lycien Occidental*. Thèse
- 1885 Doctorat d'Etat, Université de Paris-Sud, Orsay, France.
- 1886
- 1887 Gürbüz, K., Gül, M., 2005. Evolution of and factors controlling Eocene sedimentation in the
- 1888 Darende-Balaban Basin, Malatya (Eastern Turkey). *Turkish Journal of Earth*

1889 Sciences 14, 311-335.

1890

1891 Gutnic, M., Monod, O., Poisson, A., Dumont, J.-F., 1979. Géologie des Taurides Occidentales  
1892 (Turquie). Mémoires de La Société Géologique de France 137, 1-112.

1893

1894 Haq, B.U., 2014. Cretaceous eustasy revisited. Global and Planetary Change 113, 44-58.

1895

1896 Hässig, M., Rolland, Y., Sosson, M., Galoyan, G., Sahakyan, L., Topuz, G., Çelik, Ö.F., Avagyan,  
1897 A., Müller, C., 2013a. Linking the NE Anatolian and Lesser Caucasus ophiolites:  
1898 evidence for large scale obduction of oceanic crust and implications for the  
1899 formation of the Lesser Caucasus-Pontides Arc. Geodinamica Acta 26, 311–330.

1900

1901 Hässig, M., Rolland, Y., Sosson, M., Galoyan, G., Müller, C., Avagyan, A., Sahakyan, L., 2013b.  
1902 New structural and petrological data on the Amasia ophiolites (NW Sevan-Akera  
1903 suture zone, Lesser Caucasus): insights for a large-scale obduction in Armenia and  
1904 NE Turkey. Tectonophysics 588, 135-153.

1905

1906 Hässig, M., Rolland, Y., Sosson, M., 2017. From seafloor spreading to obduction: Jurassic–  
1907 Cretaceous evolution of the northern branch of the Neotethys in the Northeastern  
1908 Anatolian and Lesser Caucasus regions. In: Sosson, M., Stephenson, R. A., Adamia,  
1909 S.A. (Eds), Geological society, London, Special Publications, 428, 41-60.

1910

1911 Hässig, M., Rolland, Y., Sahakyan, L., Sosson, M., Galoyan, G., Avagyan, A., Bosch, D., Müller,  
1912 C., 2015. Multi-stage metamorphism in the South Armenian block during the Late  
1913 Jurassic to early Cretaceous: tectonics over south-dipping subduction of Northern  
1914 branch of Neotethys. Journal of Asian Earth Sciences 102, 4-23.

1915

1916 Hässig, M., Rolland, Y., Duretz, T., Sosson, M., 2016. Obduction triggered by regional heating  
1917 during plate reorganization. Terra Nova 28, 76-82.

1918

- 1919 Hayward, A.B., Robertson, A.H.F., 1982. Direction of ophiolite emplacement inferred from  
1920 Cretaceous and Tertiary sediments of an adjacent autochthon, the Bey Dağları,  
1921 southwest Turkey. Geological Society of America Bulletin 93, 68-75.  
1922
- 1923 İnan, S., İnan, N., 1988. Tecer limestone formation based on facies features. 42. Türkiye  
1924 Jeoloji Kurultayı, 15-19 Şubat, Ankara, Bildiri Özleri, p. 45 (in Turkish).  
1925
- 1926 Juteau, T., 1980. Ophiolites of Turkey. *Ophioliti* 2, 199–238.  
1927
- 1928 Kadioğlu, Y.K., Dilek, Y., Foland, K.A., 2006. Slab breakoff and syncollisional origin of the Late  
1929 Cretaceous magmatism in the Central Anatolian Crystalline Complex, Turkey, In:  
1930 Dilek, Y., Pavlides, S. (Eds.), *Postcollisional Tectonics and Magmatism in the*  
1931 *Mediterranean Region and Asia*. Geological Society of America Special Paper 409,  
1932 pp. 381–415.  
1933
- 1934 Karaman T., Poyraz N., Bakırhan B., Alan İ., Kadıncık G., Yılmaz H., Kılınc F., 1993. Geology of  
1935 the Malatya-Doğuşehir-Çelikhan area. Mineral Research and Exploration  
1936 Institute, Turkey. Report 9587, pp. 1-54 (in Turkish).  
1937
- 1938 Karaoğlu, F., Parlak, O., Klötzli, U., Thoni, M., Koller, F., 2012. U–Pb and Sm–Nd  
1939 geochronology of the ophiolites from the SE Turkey: implications for the  
1940 Neotethyan evolution. *Geodinamica Acta* 25, 146-161.  
1941
- 1942 Karaoğlu, F., Parlak, O., Klötzli, U., Koller, F., Rızaoğlu, T., 2013. Age and duration of intra-  
1943 oceanic arc volcanism built on a suprasubduction zone type oceanic crust in  
1944 southern Neotethys, SE Anatolia. *Geoscience Frontiers* 4, 399-408.  
1945
- 1946 Karaoğlu, F., Parlak, O., Hejl, E., Neubauer, F., Klötzli, U., 2016. Temporal evolution of the  
1947 active margin along the Southeast Anatolian Orogenic Belt (SE Turkey): Evidence  
1948 from U-Pb, Ar-Ar and fission track chronology. *Gondwana Research* 33, 190–208.  
1949

- 1950 Kavak, K.S., Parlak, O., Temiz, H., 2017. Geochemical characteristics of ophiolitic rocks from  
1951 the southern margin of the Sivas basin and their implications for the Inner Tauride  
1952 Ocean, Central-Eastern Turkey. *Geodinamica Acta* 29, 160-180.  
1953
- 1954 Kaya, A., 2016. Tectono-stratigraphic reconstruction of the Keban metamorphites based on  
1955 new fossil findings, Eastern Turkey. *Journal of African Earth Sciences* 124, 245-257.  
1956
- 1957 Kaymakçı, N., İnceöz, M., Ertepinar, P., 2006. 3D-architecture and Neogene evolution of the  
1958 Malatya Basin: inferences for the kinematics of the Malatya and Ovacık fault  
1959 zones. *Turkish Journal of Earth Science* 15, 123–154.  
1960
- 1961 Kozlu, H., Dercourt, J., Fourcade, E., Cros, P., Günay, Y., Bellier, J. P., 1990. The organisation  
1962 of Neo-Tethys in the Eastern Taurus region. 8<sup>th</sup> Petroleum Congress, Turkey,  
1963 Ankara, pp. 387–402 (in Turkish with English abstract).  
1964
- 1965 Kozlu, H., Göncüoğlu, M.C., 1997. Stratigraphy of the infra-Cambrian rock-units in the  
1966 eastern Taurides and their correlation with similar units in southern Anatolia. In:  
1967 Göncüoğlu, M.C., Derman, A.S. (Eds), *Early Palaeozoic Evolution of NW Gondwana*.  
1968 Turkish Association of Petroleum Geologists, Special Publications 3, pp. 50- 60.  
1969
- 1970 Kuşçu, İ., Tosdal, R.M., Gençalioglu-Kuşçu, G., Friedman, R., Ulrich, T.D., 2013. Late  
1971 Cretaceous to Middle Eocene magmatism and metallogeny of a portion of the  
1972 Southeastern Anatolian Orogenic Belt, East-Central Turkey. *Economic Geology*  
1973 108, 641–666.  
1974
- 1975 Kürüm, S., Önal, A., Boztuğ, D., Spell, T., Arslan, M., 2008. <sup>40</sup>Ar/<sup>39</sup>Ar age and geochemistry of  
1976 the post-collisional Miocene Yamadağ volcanics in the Arapkir area (Malatya  
1977 Province), eastern Anatolia, Turkey. *Journal of Asian Earth Sciences* 33, 229-251.  
1978
- 1979 Lefebvre, C., Umhoefer, P., Kaymakçı, N., Meijers, M., Teyssier, C., Whitney, D., Reid, M.,  
1980 Gençalioglu Kuşçu, G., Cosca, M., Brocard, G., 2013a. The Gürün Curl, SE Turkey: a

1981 potential link from crustal tectonics to mantle dynamics in the Arabia-Eurasia  
1982 collision-escape zone. American Geophysical Union Fall Meeting Abstracts.  
1983  
1984 Lefebvre, C., Meijers, M.J.M., Kaymakçı, N., Peynircioğlu, A., Langereis, C.G., van Hinsbergen,  
1985 D.J.J., 2013b. Reconstructing the geometry of central Anatolia during the late  
1986 Cretaceous: large-scale Cenozoic rotations and deformation between the Pontides  
1987 and Taurides. Earth Planetary Science Letters 366, 83-98.  
1988  
1989 Legeay, E., Pichat, A., Kergaravat, C., Ribes, C., Callot, J.-P., Ringenbach, J.-C.,  
1990 Bonnel, C., Hoareau, G., Poisson, A., Mohn, G., 2019. Geology of the Central Sivas  
1991 Basin (Turkey). Journal of Maps 15, 406-417.  
1992  
1993 Mackintosh, P.W., Robertson, A.H.F., 2012. Sedimentary and structural evidence for two-  
1994 phase Upper Cretaceous and Eocene emplacement of the Tauride thrust sheets in  
1995 central southern Turkey, In: Robertson, A.H.F., Parlak, O., Ünlügenç, U.C. (Eds.),  
1996 Geological Development of Anatolia and the Easternmost Mediterranean Region.  
1997 Geological Society, London, Special Publications 372, pp. 299-322.  
1998  
1999  
2000 Maffione, M., van Hinsbergen, D.J.J., de Gelder, G.I., van der Goes, F.C., Morris, A., 2017.  
2001 Kinematics of Late Cretaceous subduction initiation in the Neo-Tethys Ocean  
2002 reconstructed from ophiolites of Turkey, Cyprus, and Syria. Journal of Geophysical  
2003 Research: Solid Earth 122, 3953-3976.  
2004  
2005 Marcoux, J., Ricou, L.E., Burg, J.P., Brunn, J., 1989. Shear sense criteria in the Antalya and  
2006 Alanya thrust system (southwestern Turkey): evidence for a southward  
2007 emplacement. Tectonophysics 161, 81–91.  
2008  
2009 McPhee, P.J., van Hinsbergen, D.J.J., Maffione, M., Altıner, D., 2018a. Palinspastic  
2010 reconstruction versus cross-section balancing: how complete is the Central  
2011 Taurides fold-thrust belt (Turkey)? Tectonics 37, 4535-4566.  
2012

2013 McPhee, P.J., Altiner, D., van Hinsbergen, D.J.J., 2018b. First Balanced Cross Section Across  
2014 the Taurides Fold-Thrust Belt: geological constraints on the subduction history of  
2015 the Antalya slab in southern Anatolia. *Tectonics* 37, 3738-3759.  
2016  
2017 Metin, Y., Öcal, H., Çobankaya, M., Tunçdemir, V., Bağcı, U., Uçar, L., Çörekçioğlu, E., Taptık,  
2018 M.A., Duygu, L., Duran, S., Rızaoğlu, T., Sevimli, U.İ., 2013. Geodynamic evolution of  
2019 the northern part of the Eastern Taurus (Hekimhan-Darende-Kuluncak). Mineral  
2020 Research Exploration Institute of Turkey, Report no. 11685 (in Turkish).  
2021  
2022 Metin, S., Ayhan, A., Papak, İ., 1986. Geology of the western part of the Eastern Taurides  
2023 (SSE Turkey). Mineral Research Exploration Institute of Turkey, Bulletin 107, 1-12.  
2024  
2025 Miller, K.G., Kominz, M.A., Browning, J.V., Wright, J.D., Mountain, G.S., Katz, M.E., Sugarman,  
2026 P.J., Cramer, B.S., Christie-Blick, N., Pekar, S.F., 2005. The Phanerozoic record of  
2027 global sea-level change. *Science* 310 (5752), 1293–1298.  
2028  
2029 Moix, P., Beccaletto, L., Kozur, H.W., Hochard, C., Rossetti F., Stampfli, G.M., 2008. A new  
2030 classification of the Turkish terranes and sutures and its implication for the  
2031 paleotectonic history of the region. *Tectonophysics* 451, 7-39.  
2032  
2033 Monod, O., 1977. *Récherches Géologique dans les Taurus occidental au sud de Beyşehir*  
2034 (Turquie). Thèse de Doctorat de Science, Université de Paris-Sud, Orsay, France.  
2035  
2036 MTA, 2011. Geological map of Turkey 1:250,000 Mineral Research Exploration Institute of  
2037 Turkey (MTA), Ankara.  
2038  
2039 Nairn, S., Robertson, A.H.F., Taslı, K., İnan, N., Ünlügenç, U.C., 2013. Tectonostratigraphic  
2040 evolution of the Upper Cretaceous–Cenozoic Central Anatolian basins: an integrated  
2041 study of diachronous ocean basin closure and continental collision, In: Robertson,  
2042 A.H.F., Parlak, O., Ünlügenç, U.C. (Eds.), *Geological Development of Anatolia and the*  
2043 *Easternmost Mediterranean Region*. Geological Society, London, Special Publications  
2044 372, pp. 383-384.

- 2045
- 2046 Oberhänsli, R., Candan, O., Koralay, E., Bousquet, R., Okay, A., 2012. Dating subduction  
2047 events in East Anatolia, Turkey. *Turkish Journal of Earth Science* 21, 1-17.
- 2048
- 2049 Okay, A.İ., Şahintürk, Ö., 1997. Geology of the eastern Pontides. In: Robinson, A. G. (Ed.),  
2050 Regional and Petroleum Geology of the Black Sea and Surrounding Region. American  
2051 Association of Petroleum Geologists, Memoirs 68, 291–311.
- 2052
- 2053 Okay, A.İ., Tansel, İ., Tüysüz, O., 2001. Obduction, subduction and collision as reflected in the  
2054 Upper Cretaceous-Lower Eocene sedimentary record of western Turkey. *Geological  
2055 Magazine* 138, 117-142.
- 2056
- 2057 Özer, S., Terlemez, İ., Sümengen, M., Erkan, E., 1984. Stratigraphy and structural position of  
2058 the allochthonous units around Pınarbaşı (Kayseri) 27, 61-68 (in Turkish with an  
2059 English abstract).
- 2060
- 2061 Özer, S., 1998. Rudist bearing Upper Cretaceous metamorphic sequences of the Menderes  
2062 Massif (Western Turkey). *Geobios* 31, 235-249.
- 2063
- 2064 Özer, E., Koç, H., Özsayar, T., 2004. Stratigraphical evidence for the depression of the  
2065 northern margin of the Menderes-Tauride Block (Turkey) during the Late  
2066 Cretaceous. *Journal of Asian Earth Sciences* 22, 401-412.
- 2067
- 2068 Özgül, N., 1984. Stratigraphy and tectonic evolution of the central Taurides. In: Tekeli, O.,  
2069 Göncüoğlu, M.C. (Eds.), *Geology of the Taurus Belt. Proceedings of the Tauride  
2070 Symposium, Mineral Research Exploration Institute of Turkey (MTA), Ankara*, pp.  
2071 77-90.
- 2072

- 2073 Özgül, N., 1997. Stratigraphy of the tectono-stratigraphic units in the region Bozkır-Hadim-  
2074 Taşkent (northern central Taurides) (in Turkish). Mineral Research Exploration  
2075 Institute of Turkey, Bulletin 119, 113-174.  
2076
- 2077 Özgül, N., Turşucu, A., 1984. Stratigraphy of the Mesozoic carbonate sequence of the  
2078 Munzur Mountains (Eastern Taurides), In: Tekeli, O., Göncüoğlu, M.C. (Eds.),  
2079 International Symposium on the Geology of the Taurus Belt. Mineral Research and  
2080 Exploration Institute (MTA), Ankara, pp. 173-180.  
2081
- 2082 Özgül, N., Kozlu, H., 2002. Data on the stratigraphy and tectonics of the Kozan-Feke region  
2083 (Eastern Taurides). Bulletin of Turkish Association of Petroleum Geologists 14, 1-  
2084 36.  
2085
- 2086 Özgül, N., Metin, S., Göğer, E. Bingöl, İ., Baydar, O., Erdoğan, B., 1973. Cambrian to Tertiary  
2087 units around Tufanbeyli. Türkiye Kurultayı Bülteni 16/1, 82-100 (in Turkish).  
2088
- 2089 Özgül N., Turşucu A., Özyardımcı, N., Şenol, M., Bingöl, İ., Uysal, Ş., 1981. Geology of Munzur  
2090 Mountains. MTA Report No: 6995 (in Turkish).  
2091
- 2092 Öztürk, H., Öztunalı, Ö., 1993. Effects of young tectonics and results on the Divriği iron ores.  
2093 Türkiye Jeoloji Kurumu Bülteni 8, 97-106 [in Turkish with English abstract].  
2094
- 2095 Parlak, O., 2006. Geodynamic significance of granitoid magmatism in the southeast  
2096 Anatolian orogen: geochemical and geochronological evidence from Göksun–Afşin  
2097 (Kahramanmaraş, Turkey) region. International Journal of Earth Sciences 95, 609-627.  
2098
- 2099 Parlak, O., 2016. The Tauride ophiolites of Anatolia (Turkey): A review. Journal of Earth  
2100 Science 27, 901-934.  
2101
- 2102 Parlak, O., Bağcı, U., Rızaoğlu, T., Ionescu, C., Önal, G., Höck, V., Kozlu, H., 2020. Petrology of  
2103 ultramafic to mafic cumulate rocks from the Göksun (Kahramanmaraş) ophiolite,  
2104 southeast Turkey. Geoscience Frontiers 11, 109-128.



2105  
2106 Parlak, O., Çolakoğlu, A., Dönmez, C., Sayak, H., Yıldırım, N., Türkel, A., Odabaşı, İ., 2013. Geo-  
2107 chemistry and tectonic significance of ophiolites along the Ankara – Erzincan suture  
2108 zone in northeastern Anatolia. In: Robertson, A.H.F., Parlak, O., Ünlügenç, U.C. (Eds.),  
2109 Geological Development of Anatolia and the Easternmost Mediterranean Region.  
2110 Geological Society, London, Special Publications 372, pp. 75 – 105.  
2111  
2112 Parlak, O., Dunkl, I., Karaoğlan, F., Kusky, T.M., Zhang, C., Wang, L., Köpke, J., Billor, Z.,  
2113 Hames, W.E., Şimşek, E., Şimşek, G., Şimşek, T., Öztürk, S.E., 2019. Rapid cooling history  
2114 of a Neotethyan ophiolite: Evidence for contemporaneous subduction and  
2115 metamorphic sole formation. Geological Society of America Bulletin 131, 2011–2038.  
2116  
2117 Parlak, O., Höck, V., Kozlu, H., Delaloye, M., 2004. Oceanic crust generation in an island arc  
2118 tectonic setting, SE Anatolian Orogenic Belt (Turkey). Geological Magazine 141,  
2119 583–603.  
2120  
2121 Parlak, ORızaoğlu, T., Bağcı, U., Karaoğlan, F., Höck, V., 2009. Tectonic significance of the  
2122 geochemistry and petrology of ophiolites in southeast Anatolia, Turkey.  
2123 Tectonophysics 473, 173-187.  
2124  
2125 Parlak, O., Karaoğlan, F., Rızaoğlu, T., Klötzli, U., Koller, K., Billor, Z., 2013. U–Pb and <sup>40</sup>Ar–  
2126 <sup>39</sup>Ar geochronology of the ophiolites and granitoids from the Tauride belt:  
2127 Implications for the evolution of the Inner Tauride suture. Journal of Geodynamics  
2128 65, 22–37.  
2129  
2130 Parlak, O., Karaoğlan, F., Şimşek, E., Şimşek, G., Şimşek, T., Öztürk, S.E., Baydan, M., 2017.  
2131 Examination of spatial and temporal relations of the Tauride ophiolites and their  
2132 metamorphic soles by U-Pb SIMS and <sup>40</sup>Ar/<sup>39</sup>Ar methods. TÜBİTAK Project (Project no:  
2133 113Y412), 583 pp.  
2134

2135 Parlak. O., Yılmaz, H., Boztuğ, D., 2006. Origin and significance of the metamorphic sole of  
2136 the Divriği Ophiolite (Sivas, Turkey): evidence for slab break-off prior to ophiolite  
2137 emplacement. *Turkish Journal of Earth Sciences* 15, 25-45.  
2138

2139 Parlak, O., Robertson, A.H.F., 2004. The ophiolite-related Mersin Melange, southern Turkey:  
2140 Its role in the tectono-sedimentary setting of Tethys in the Eastern Mediterranean  
2141 region. *Geological Magazine* 141, 257–286.  
2142

2143 Pehlivan, Ş., Barkurt, M.Y., Bilginer, E., Kurt, Z., Sütçü, Y.F., Can, B., Bilgi, C., Örçen, S., Süer,  
2144 T., Karabıyıköğlü, M., 1991. Elbistan-Nurhak (Kahramanmaraş) dolayının jeolojisi.  
2145 Mineral Research Exploration Institute of Turkey, Report No. 9423 (unpublished) (in  
2146 Turkish).  
2147

2148 Perinçek, D., Kozlu, H., 1984. Stratigraphical and structural relations of the units in the Afşin-  
2149 Elbistan-Doğanşehir region (Eastern Taurus), In: Tekeli, O., Göncüoğlu, M.C. (Eds.),  
2150 *Geology of the Taurus Belt. Proceedings of International Symposium MTA, Ankara,*  
2151 *pp. 181-198.*  
2152

2153 Poisson, A., 1977. *Recherches géologiques dans les Taurus occidentales (Turquie). These,*  
2154 *D.Sc thesis, Université de Paris-Sud Orsay, 1-795.*  
2155

2156 Poisson, A., 1984. The extension of the Ionian trough into southwestern Turkey, In:  
2157 Dixon, J.E., Robertson, A.H.F. (Eds), *Geological Evolution of the Eastern*  
2158 *Mediterranean. Geological Society London, Special Publication 17, pp. 241-250.*  
2159

2160 Poisson, A., Guezou, J.C., Öztürk, A., İnan, S., Temiz, T., Gürsoy, H., Kavak, K.S., Özden, S.,  
2161 1996. Tectonic setting and evolution of the Sivas Basin, Central Anatolia,  
2162 Turkey. *International Geology Review* 38, 838-853.  
2163

2164 Pourteau, A., Candan, O., Oberhänsli, R., 2010. High-Pressure metasediments in central  
2165 Turkey: constraints on the Neotethyan closure history. *Tectonics* 29, TC5004, 18 p.  
2166

- 2167 Pourteau, A., Oberhänsli, R., Candan, O., Barrier, E., Vrielynck, B., 2016. Neotethyan closure  
2168 history of western Anatolia: a geodynamic discussion. *International Journal of Earth*  
2169 *Science* 105, 203-224.
- 2170
- 2171 Pourteau, L., Sudo, M., Candan, O., Lanari, P., Vidal, O., Oberhänsli, O., 2013. Neotethys  
2172 closure history of Anatolia: insights from  $^{40}\text{Ar}$ – $^{39}\text{Ar}$  geochronology and P–T  
2173 estimation in high pressure metasedimentary rocks. *Journal of Metamorphic*  
2174 *Geology* 31, 585-606.
- 2175
- 2176 Raymond, L.A., 1984. (Ed.) *Melanges: Their Nature, Origin and Significance*. Geological  
2177 Society of America Special Paper 198.
- 2178
- 2179 Rice, S.P., Robertson, A.H.F., Ustaömer, T., İnan, N., Taslı, K., 2009. Late Cretaceous-early  
2180 Eocene tectonic development of the Tethyan suture zone in the Erzincan area,  
2181 eastern Pontides, Turkey. *Geological Magazine* 146, 567-590.
- 2182
- 2183 Ricou, L.E., Marcoux, J., Whitechurch, H., 1984. The Mesozoic organization of the Taurides:  
2184 one or several ocean basins? In: Dixon, J.E., Robertson, A.H.F. (Eds.), *The Geological*  
2185 *Evolution of the Eastern Mediterranean*. Geological Society, London Special 17, pp.  
2186 349-359.
- 2187
- 2188 Rızaoğlu, T., Parlak, O., Hoeck, V., İşler, F., 2006. Nature and significance of Late Cretaceous  
2189 ophiolitic rocks and its relation to the Baskil granitoid in Elaziğ region, SE Turkey,  
2190 In: Robertson, A.H.F., Mountrakis, D. (Eds), *Tectonic Development of the Eastern*  
2191 *Mediterranean Region*. Geological Society, London, Special Publications, 260, pp.  
2192 327–350.
- 2193
- 2194 Rızaoğlu, T., Parlak, O., Hoeck, V., Koller, F., Hames, W.E., Billor, Z., 2009. Andean-type active  
2195 margin formation in the eastern Taurides: Geochemical and geochronological  
2196 evidence from the Baskil granitoid (Elaziğ, SE Turkey). *Tectonophysics* 473, 188-  
2197 207.
- 2198

- 2199 Robertson, A.H.F., 2002. Overview of the genesis and emplacement of Mesozoic ophiolites in  
2200 the Eastern Mediterranean Tethyan region. *Lithos* 65, 1-67.  
2201
- 2202 Robertson, A.H.F., Dixon, J.E., 1984. Introduction: aspects of the geological evolution of the  
2203 Eastern Mediterranean, In: Dixon, J.E., Robertson, A.H.F. (Eds), *The Geological*  
2204 *Evolution of the Eastern Mediterranean*. Geological Society, London Special  
2205 Publications 17, pp. 1-74.  
2206
- 2207 Robertson, A.H.F., Parlak, O., Dumitrica, P. Role of volcanic-sedimentary melanges, especially  
2208 the Aladağ melange, in the rift-drift-subduction-accretion-emplacement history of  
2209 the Mesozoic Inner Tauride ocean. *International Geology Review* (in press b).  
2210
- 2211 Robertson, A.H.F., Parlak, O., Metin, Y., Vergili, Ö., Taslı, K., İnan, N., Soycan, H., 2013b. Late  
2212 Palaeozoic–Cenozoic tectonic development of carbonate platform, margin and oceanic  
2213 units in the Eastern Taurides, Turkey, In: Robertson, A.H.F., Parlak, O., Ünlügenç, U.C.  
2214 (Eds), *Geological Development of Anatolia and the Easternmost Mediterranean Region*.  
2215 Geological Society, London, Special Publications 372, pp. 167-218.  
2216
- 2217 Robertson, A.H.F., Parlak, O., Rızaoğlu, T., Ünlügenç, U.C., İnan, N., Taslı, K., Ustaömer, T.,  
2218 2007. Tectonic evolution of the South Tethyan ocean: evidence from the Eastern  
2219 Taurus Mountains (Elazığ region, SE Turkey), In: *Deformation of Continental Crust:*  
2220 *The Legacy of Mike Coward*. Geological Society of London Special Publication 272,  
2221 pp. 231-270.  
2222
- 2223 Robertson, A.H.F., Parlak, O., Ustaömer, T., 2009. Melange genesis and ophiolite  
2224 emplacement related to subduction of the northern margin of the Tauride-  
2225 Anatolide continent, central and western Turkey, In: Van Hinsbergen, D.J.J.,  
2226 Edwards, M. A., Govers, R. (Eds.), *Collision and Collapse at the Africa–Arabia–*  
2227 *Eurasia Subduction Zone*. Geological Society, London, Special Publications 311, pp.  
2228 9–66.  
2229

- 2230 Robertson, A.H.F., Palak, O., Ustaömer, T., 2012. Overview of the Palaeozoic–Neogene  
2231 evolution of Neotethys in the Eastern Mediterranean region (southern Turkey,  
2232 Cyprus, Syria). *Petroleum Geoscience* 18, 381-404.  
2233
- 2234 Robertson, A.H.F., Palak, O., Ustaömer, T., 2013a. Mesozoic–Early Cenozoic palaeogeographic  
2235 development of Southern Turkey and the easternmost Mediterranean region:  
2236 evidence from the inter-relations of continental and carbonate platform units, In:  
2237 Robertson, A.H.F., Palak, O., Ünlügenç, U.C. (Eds.), *Geological Development of the*  
2238 *Anatolian Continent and the Easternmost Mediterranean Basin*. Geological  
2239 Society, London, Special Publications 372, pp. 167-218.  
2240
- 2241 Robertson, A.H.F., Palak, O., Ustaömer, T. Late Palaeozoic extensional volcanism along the  
2242 northern margin of Gondwana in southern Turkey: implications for Palaeotethyan  
2243 development. *International Journal of Earth Science* (in press a).  
2244
- 2245 Robertson, A.H.F., Parlak, O., Ustaömer, T., Taslı, K., İnan, N., Dumitrica, P., Karaoğlan, F.,  
2246 2013c. Subduction, ophiolite genesis and collision history of Tethys adjacent to the  
2247 Eurasian continental margin: new evidence from the Eastern Pontides, Turkey.  
2248 *Geodinamica Acta* 26, 230-293.  
2249
- 2250 Robertson, A.H.F., Ustaömer, T., Parlak, O., Ünlügenç, U.C., Taslı, K., İnan, N., 2006. The Berit  
2251 transect of the Tauride thrust belt, S. Turkey: Late Cretaceous–Early Cenozoic  
2252 accretionary/collisional processes related to closure of the southern Neotethys.  
2253 *Journal of Asian Earth Sciences* 27, 108–145.  
2254
- 2255 Rolland, Y., 2017. Caucasus collisional history: review of data from East Anatolia to West  
2256 Iran. *Gondwana Research* 49, 130-146.  
2257
- 2258 Rolland, Y., Perinçek, D., Kaymakçı, N., Sosson, M., Barrier, E., Avagyne, A., 2012. Evidence  
2259 for ~80–75 Ma subduction jump during Anatolide–Tauride–Armenian block  
2260 accretion and ~48 Ma Arabia–Eurasia collision in Lesser Caucasus–East Anatolia.  
2261 *Journal of Geodynamics* 56-57, 76-85.

2262

2263 Rolland, Y., Hässig, M., Bosch, D., Bruguier, O., Melis, R., Galoyan, G., Sosson, M., 2020. The  
2264 East Anatolia–Lesser Caucasus ophiolite: An exceptional case of large-scale  
2265 obduction, synthesis of data and numerical modelling. *Geoscience Frontiers* 11,  
2266 83-108.

2267

2268 Rolland, Y., Hässig, M., Bosch, D., Meijers, M.J.M., Sosson, M., Bruguier, O., Adamia,  
2269 S., Sadradze, N., 2016. A review of the plate convergence history of the East  
2270 Anatolia–Transcaucasus region during the Variscan: insights from the Georgian  
2271 basement and its connection to the Eastern Pontides. *Journal of*  
2272 *Geodynamics* 96, 131-145.

2273

2274 Sancar, T., Zabcı, C., Karabacak, V., Yazıcı, M., Akyüz, H.S., 2019. Geometry and  
2275 Paleoseismology of the Malatya Fault (Malatya-Ovacık Fault Zone), Eastern Turkey:  
2276 Implications for intraplate deformation of the Anatolian Scholle. *Journal of*  
2277 *Seismology* 23, 319-340.

2278

2279 Sar, A., Ertürk, M.A., Rizeli, M.E., 2019. Genesis of Late Cretaceous intra-oceanic arc  
2280 intrusions in the Pertek area of Tunceli Province, eastern Turkey, and implications  
2281 for the geodynamic evolution of the southern Neo-Tethys: results of zircon U–Pb  
2282 geochro- nology and geochemical and Sr–Nd isotopic analyses. *Lithos* 350–351,  
2283 105263. <https://doi.org/10.1016/j.lithos.2019.105263>.

2284

2285 Sarı, B., Özer, S., 2002. Upper Cretaceous stratigraphy of the Bey Dağları carbonate platform,  
2286 Korkuteli area (Western Taurides, Turkey). *Turkish Journal of Earth Sciences* 11,  
2287 39–59.

2288

2289 Sarı, B., Steuber, T., Özer, S., 2004. First record of Upper Turonian rudists (Mollusca,  
2290 Hippuritoidea) in the Bey Dağları carbonate platform, Western Taurides (Turkey):  
2291 Taxonomy and strontium isotope stratigraphy of *Vaccinites praegiganteus* (Toucas,  
2292 1904). *Cretaceous Research* 25, 235–248.

2293

- 2294 Sayıt, K., Göncüoğlu, M.C., Tekin, U.K., 2015. Middle Carnian Arc-Type Basalts from the  
2295 Lycian Nappes, Southwestern Anatolia: early Late Triassic Subduction in the  
2296 Northern Branch of Neotethys. *Journal of Geology* 123, 561-579.  
2297
- 2298 Scliffarth, W.K., Darin, M.H., Reind, M.R., Umhoeffer, P.J., 2018. Dynamics of episodic Late  
2299 Cretaceous–Cenozoic magmatism across Central to Eastern Anatolia: New insights  
2300 from an extensive geochronology compilation. *Geosphere* 14, 1990-2008.  
2301
- 2302 Şenel, M., 1984. Discussion on the Antalya nappes, In: Tekeli, O., Göncüoğlu, M.C. (Eds.),  
2303 International Symposium on the Geology of the Taurus Belt. General Directorate  
2304 of Mineral Research and Exploration, Ankara, pp. 41-52.  
2305
- 2306 Şenel, M., Selçuk, H., Bilgin, Z.R., Şen, A.M., Karaman, T., Dincer, M.A., Durukan, E., Arbas, A.,  
2307 Örcen, S., Bilgin, C., 1989. Geology of Çameli (Denizli)- Yesilova, (Burdur)- Elmalı  
2308 (Antalya) region. General Directorate of Mineral Research and Exploration, Report  
2309 No: 9429 (in Turkish).  
2310
- 2311 Şengör, A.M.C., Yılmaz, Y., 1981. Tethyan Evolution of Turkey: A plate tectonic approach.  
2312 *Tectonophysics* 75, 181-241.  
2313
- 2314 Şengör, A.M.C., Görür, N., Şaroğlu, F., 1985. Strike-slip faulting and related basin formation in  
2315 zones of tectonic escape: Turkey as a case study, In: Biddle KT, Christie-Blick N  
2316 (Eds.), *Strike-slip deformation, basin formation and sedimentation*. Society of  
2317 Economic Paleontologists and Mineralogists Special Publication 37, pp. 227–264.  
2318
- 2319 Solak, C., Taslı, K., Özer, S., Koç, H., 2017. Biostratigraphy and facies analysis of the Upper  
2320 Cretaceous-Danian? platform carbonate succession in the Kuyucak area, western  
2321 Central Taurides, S Turkey. *Cretaceous Research* 79, 43-63.  
2322
- 2323 Solak, C., Taslı, K., Özer, S., Koç, H., 2019. The Madenli (Central Taurides) Upper Cretaceous  
2324 platform carbonate succession: Benthic foraminiferal biostratigraphy and platform  
2325 evolution. *Geobios* 52, 67-93.

- 2326
- 2327 Sosson, M., Rolland, Y., Danelian, T., Muller, C., Melkonyan, R., Adamia, S., Babazadeh, V.,  
2328 Kangarli, T., Avagyan, A., Galoyan, G., Mosar, J., 2010. Subductions, obduction and  
2329 collision in the Lesser Caucasus (Armenia, Azerbaijan, Georgia), new insights, In:  
2330 Sosson, M., Kaymakçı, N., Stephenson, R.A., Bergerat, F., Starostenko, V. (Eds.),  
2331 Sedimentary Basin Tectonics from the Black Sea and Caucasus to the Arabian  
2332 Platform. Geological Society, London, Special Publications 340, 329-352.
- 2333
- 2334 Stampfli, G.M., Borel, G.D., 2002. A plate tectonic model for the Paleozoic and Mesozoic  
2335 constrained by dynamic plate boundaries and restored synthetic oceanic isochrons.  
2336 Earth and Planetary Science Letters 196, 17-33.
- 2337
- 2338 Stampfli, G., J. Mosar, P., Faure, A., Vannay, J.C., 2001. Permo-Mesozoic evolution of the  
2339 western Tethys realm: the Neotethys East Mediterranean basin connection, In:  
2340 Ziegler, P., Cavazza, W., Robertson, A.H.F., Crasquin-Soleau (Eds.), Peri-Tethys  
2341 Memoir 5 Peri-Tethyan Rift/Wrench Basins and Passive Margins. Memoirs du  
2342 Museum National D'Histoire Naturelle, pp. 51-108.
- 2343
- 2344 Tekin, U.K., Bedi Y., 2007a. Ruesticyrtiidae (Radiolaria) from the middle Carnian (Late  
2345 Triassic) of Köseyahya nappe, Elbistan, eastern Turkey. *Geologica Carpathica* 58,  
2346 153-167.
- 2347
- 2348 Tekin, U.K., Bedi, Y., 2007b. Middle Carnian (Late Triassic) Nassellaria (Radiolaria) of  
2349 Köseyahya nappe from eastern Tau-rides, eastern Turkey. *Rivista Italiana di*  
2350 *Paleontologia e Stratigrafia* 113, 167-190.
- 2351
- 2352 Topuz, G., Göçmengil, G., Rolland, Y., Çelik, Ö.F., Zack, T., Schmitt, A.K., 2013a. Jurassic  
2353 accretionary complex and ophiolite from northeast Turkey: no evidence for the  
2354 Cimmerian continental ribbon. *Geology* 41, 255-258.
- 2355
- 2356 Topuz, G., Çelik, Ö.F., Şengör, A.M.C., Altıntaş, I.E., Zack, T., Rolland, Y., Barth, M., 2013b.  
2357 Jurassic ophiolite formation and emplacement as back-stop to a subduction-



2358 accretion complex in Northeast Turkey, the Refahiye ophiolite, and relation to the  
2359 Balkan ophiolites. *American Journal of Science* 313, 1054 – 1087.  
2360  
2361 Uçurum, A., 2000. Geology, geochemistry, and evolution of the Divriği and Kuluncak  
2362 ophiolitic melanges, with reference to serpentinites in east-central Turkey.  
2363 *International Geology Review* 42, 172-191.  
2364  
2365 Ural, M., Arslan, M., Göncüoğlu, M.C., Tekin, U.K., Kürüm, S., 2015. Late Cretaceous arc and  
2366 back-arc formation within the southern Neotethys: whole rock, trace element and  
2367 Sr-Nd-Pb isotopic data from basaltic rocks of the Yüksekova complex (Malatya-  
2368 Elazığ, SE Turkey). *Ofioliti* 40, 57-72.  
2369  
2370 Ustaömer, T., Robertson, A.H.F., 2010. Late Palaeozoic – Early Cenozoic tectonic  
2371 development of the Eastern Pontides (Artvin area), Turkey: stages of clo- sure of  
2372 Tethys along the southern margin of Eurasia. In: Sosson, M., Kaymakçı, N.,  
2373 Stephenson, R.A., Bergerat, F., Starostenko, V. (Eds.), *Sedimentary Basin Tectonics*  
2374 *from the Black Sea and Caucasus to the Arabian Platform*. Geological Society,  
2375 London, Special Publications 340, 281 – 327.  
2376  
2377 Ustaömer, T., Robertson, A.H.F., Ustaömer, P.A., Gerdes, A., Peytcheva, I., 2013.  
2378 Constraints on Variscan and Cimmerian magmatism and metamorphism in the  
2379 Pontides (Yusufeli-Artvin area), NE Turkey from U-Pb dating and granite  
2380 geochemistry. In: Robertson, A.H.F., Parlak, O., Ünlügenç, U.C. (Eds.), *Geological*  
2381 *Development of Anatolia and the Easternmost Mediterranean Region*. Geological  
2382 Society, London, Special Publications 372, 49-74.  
2383  
2384 van Hinsbergen, D.J.J., Maffione, M., Plunder, A., Kaymakçı, N., Ganerød,  
2385 B., Hendriks, B.W.H., Corfu, F., Gürer, D., Gelder, G.I.N.O. de,  
2386 Peters, K., McPhee, J., Brouwer, F.M., Advokaat, E.L., Vissers, R.L.M., 2016. Tectonic  
2387 evolution and paleogeography of the Kırşehir Block and the Central Anatolian  
2388 Ophiolites, Turkey. *Tectonics* 35, [10.1002/2015TC004018](https://doi.org/10.1002/2015TC004018)  
2389

- 2390 van Hinsbergen, D.J.J., Torsvig, T.H., Schmid, S.M., Matenco, L.C., Maffione, M., Vissers, L.M.,  
2391 Güreş, D., Spakman, W., 2020. Orogenic architecture of the Mediterranean region  
2392 and kinematic reconstruction of its tectonic evolution since the Triassic. *Gondwana*  
2393 *Research* 81, 79-229.
- 2394
- 2395 Vergili, Ö., Parlak, O., 2005. Geochemistry and tectonic setting of metamorphic sole rocks  
2396 and mafic dikes from the Pınarbaşı (Kayseri) ophiolite, Central Anatolia. *Ofioliti* 30,  
2397 37–52.
- 2398
- 2399 Westaway, R., Arger, J., 2001. Kinematics of the Malatya–Ovacık Fault Zone. *Geodinamica*  
2400 *Acta* 14, 103-131.
- 2401
- 2402 Woodcock, N.H., Robertson, A.H.F., 1982. Wrench and thrust tectonics along a Mesozoic-  
2403 Cenozoic continental margin; Antalya Complex, SW Turkey. *Journal of the Geological*  
2404 *Society, London* 139, 147-163.
- 2405
- 2406 Yazgan, E., 1984. Geodynamic evolution of the Eastern Taurus region. In: Tekeli, O.,  
2407 Göncüođlu, M.C. (Eds.), *International Symposium on the Geology of the Taurus Belt*.  
2408 *General Directorate of Mineral Research and Exploration, Ankara*, pp. 199-208.
- 2409 Yazgan, E., Chessex, R., 1991. Geology and tectonic evolution of the southeastern Taurides in  
2410 the region of Malatya. *Turkish Association of Petroleum Geologists* 3, 1–42.
- 2411 Yılmaz, A., Bedi, Y., Uysal, S., Yusufoglu, H., Aydın N., 1993. Geological structure of the area  
2412 between Uzunyayla and Beritdađ of the Eastern Taurides. *Turkish Association of*  
2413 *Petroleum Geologists Bulletin* 5, 69–87 (in Turkish with English abstract).
- 2414
- 2415 Yılmaz, A., Bedi, Y., Uysal, S., Yusufoglu, H., Aydın N., 1991. 1:100,000 map and report  
2416 Elbistan H23 (K37). *Mineral Research Exploration Institute of Turkey (MTA)*, (in  
2417 Turkish).
- 2418

- 2419 Yılmaz, A., Bedi, Y., Uysal, S., Aydın N., 1994. 1:100,000 map and report Elbistan İ23 (L37).  
2420 Mineral Research Exploration Institute of Turkey (MTA), (in Turkish).  
2421
- 2422 H., Yılmaz, A., 2004. Geology and structural evolution of Divriği (Sivas) region. Bulletin of  
2423 Geological Society of Turkey 47 (1), 13-45.
- 2424 Yılmaz, C., 1994. Evolution of the Munzur Carbonate Platform during the Mesozoic, Middle  
2425 Eastern Anatolia (Turkey). *Géologia Méditerranéenne* 21, 195-196
- 2426 Yılmaz, H., 2001. Geology of the Güneş ophiolite (Divriği-Sivas). Proceeding of the 54<sup>th</sup>  
2427 Geological Congress of Turkey, 7-10 May 2011, Ankara, pp. 54-65 (in Turkish).  
2428
- 2429 Yılmaz, P.O., Maxwell, J.C., 1984. An example of an obduction melange: the Alakır Çay unit,  
2430 Antalya Complex, Southwest Turkey. In: Raymond, L.A. (Ed.), *Melanges: Their Nature,*  
2431 *Origin, and Significance.* Geological Society of America Special Paper 198, pp. 139-  
2432 152.  
2433
- 2434 Yılmaz, Y., 1993. New evidence and model on the evolution of the southeast Anatolian  
2435 orogen. *Geological Society of America Bulletin* 105, 251-271.  
2436
- 2437 Yılmaz, Y., Gürpınar, O., Kozlu, H., Gül, M.A., Yiğitbaş, E., Yıldırım, M., Genç, S.C., Keskin, M.,  
2438 1987. Geology of the northern part of Kahramanmaraş (Andırın-Berit-Engizek-  
2439 Nurhak-Binboğa Mountains). Turkish Petroleum Company Report (No: 2028), pp  
2440 218 (unpublished).  
2441
- 2442 Yılmaz, Y., Gürpınar, O., Kozlu, H., Gül, M.A., Yiğitbaş, E., Yıldırım, M., Genç, C., Keskin, M.,  
2443 1987. Geology of the northern part of Maraş (Andırın, Berit, Engizek-Nurhak-Binboğa  
2444 Mountains) structural and geological evolution. Publication of İstanbul University  
2445 Engineering Faculty 6, 1-97 (in Turkish).  
2446
- 2447 Yılmaz, Y., Tüysüz, O., Yiğitbaş, E., Genç, S.C., Şengör, A.M.C., 1997. Geology and tectonic  
2448 evolution of the Pontides. In: Robinson, A.G. (Ed.). *Regional and Petroleum Geology*

2449 of the Black Sea and Surrounding Region. American Association of Petroleum  
2450 Geologists, Memoirs 68, 183–226.  
2451  
2452 Yılmaz, Y., Yiğitbaş, E., Genç, S.C., 1993. Ophiolitic and metamorphic assemblages of  
2453 southeast Anatolia and their significance in the geological evolution of the orogenic  
2454 belt. *Tectonics* 12, 1280-1297.  
2455

2456 Yusifođlu, H., Bedi, Y., Usta, D., Özkan, M.K., Beyazpirinç, M., Yıldız, H., 2005. The tectonic  
2457 evolution of the Afşin-Elbistan Neogene Basin, Eastern Taurides, Turkey. 58<sup>th</sup>  
2458 Geological Congress of Turkey, MTA Ankara, 11-17 April, 2005.  
2459  
2460  
2461

2462

2463

2464 **Figure captions**

2465

2466

2467 Fig. 1. Outline map of Turkey showing the main tectonic units and the study area (main data  
2468 source, MTA 2012).

2469

2470 Fig. 2. Simplified geological map and cross-section of part of central eastern Anatolia,  
2471 simplified from MTA 1:100,000 and 1:250,000 geological maps of Turkey (MTA, 2011). The  
2472 area studied is divided into 5 sub-areas, as indicated: Area 1-NE, i.e. mainly NW of Elbistan,  
2473 including the Afşin area; Area 2-Dağlıca area, farther NW of Elbistan; Area 3A-East of  
2474 Elbistan, 3B-farther east, near Nurhak Dağı; Area 4-S-mainly south of Elbistan; Area 5A-  
2475 Kemaliye area, 5B Divriği area (both in the far NE). Additional geological units mentioned in  
2476 the text: AE Afşin-Elbistan basin; DB Darende basin; GO Göksun ophiolite; GF Göksu Fault;  
2477 SGF Sürgü-Misis Fault; İO İspendere ophiolite; KO Kömürhan ophiolite; KU Kuluncak  
2478 ophiolite. Additional locations and settlements mentioned in the text: B Büyük Yılanlı Dağ; K  
2479 Kangal (off map in central N, as indicated); N Nurhak Dağı; S Saimbeyli (just off map in SW);  
2480 Y Yeşildere.

2481

2482 Fig. 3. Stratigraphical columns showing the age and lithologies of the main geological units  
2483 discussed in this paper. See text for explanation and data sources.

2484

2485 Fig. 4. Field photographs of key features of the Malatya metamorphics in the area north and  
2486 west of Elbistan (Area 1). a, Eocene shelf limestones (Seske Fm.) above Malatya  
2487 Metamorphics; in places the two units are intersliced, Kepez Mah. (in foreground); GPS 37S  
2488 0303484/4230790; b, Foliated amphibolite; Late Palaeozoic; 0.5 km S of Türkören; c,  
2489 Normal-graded debris-flow deposit with carbonate clasts in a coarse calcarenite matrix;  
2490 recrystallised to micaceous marble; Late Palaeozoic; near Kepez, W of Afşin; GPS 37S  
2491 0303518/4229825; d, Isoclinally folded limestone with replacement chert, Late Permian;  
2492 Saldilek Tepe, NE of Afşin; GPS 37S 0322749/4239163; e, Thin-bedded micritic limestone  
2493 and dolomite (stromatolitic); Late Triassic; west of Afşin GPS 37S 0303484/4230790; f,

2494 Network of tension cracks infilled with pink micrite (recrystallised); within upper c. 50 m of  
2495 mapped Late Permian meta-limestone succession; beneath the Karaböğürtlen Formation;  
2496 GPS 37S 0329702/4236079; g, Debris-flow deposit composed of platy limestone clasts,  
2497 recrystallised to marble; several m above mapped normal contact with Late Permian meta-  
2498 limestone; Karaböğürtlen Formation; GPS 37S 0329013/4236061; h, Debris-flow deposit  
2499 with flattened clasts in a calcareous mudstone matrix; recrystallised to marble;  
2500 Karaböğürtlen Formation; GPS 37S 0328678/4235639; i, Foliated pebbly conglomerate;  
2501 clasts mainly sub-rounded; mostly siliceous calc-schist; Malatya metamorphic unit; near  
2502 Kamalak köy, SSW of İncirli; Karaböğürtlen Formation (GPS 37S 0304287/4250123); j, Blocks  
2503 of recrystallised limestone (marble), interbedded with carbonate-rock debris-flow deposits  
2504 and phyllite (Karaböğürtlen Formation); represents the leading edge of the Malatya  
2505 metamorphic unit (backthrust to N); c. 1 km SE of İncirli (GPS 37S 0307627/4251659); k,  
2506 Recrystallised limestone (marble) with reworked Megalodont bivalves (Karaböğürtlen  
2507 Formation); NW of Afşin, GPS 37S 0322629/0239403; l, Kemaliye Formation (foreground),  
2508 with serpentinite above (Dağlıca ophiolite); overthrust (northwards) by the Malatya  
2509 Metamorphics (Karaböğürtlen Formation); NW of İncirli.

2510

2511 Fig. 5. Part of the northeast outcrop of the Malatya Metamorphics (Area 1; NW of Elbistan;  
2512 Fig. 2). Simplified geological map; note the relation of the Late Cretaceous syn-tectonic  
2513 Karaböğürtlen Formation to the underlying units; modified from Bedi et al. (2009).

2514 Logs: 1, Late Palaeozoic succession including meta-basic extrusive rocks (west of Afşin); 2,  
2515 Triassic siliciclastic-carbonate facies; 3, Late Cretaceous Karaböğürtlen Formation with  
2516 carbonate and siliciclastic intercalations. Rock-relations diagrams: a, Latest Cretaceous  
2517 sedimentary cover of the Göksun ophiolite (Harami Fm.), overthrust by the Malatya  
2518 Metamorphics; 3 km SE of Afşin; b, Jurassic-Cretaceous (?) succession, unconformably  
2519 overlain by the Late Cretaceous Karaböğürtlen Formation; 6 km E of Afşin; c, Permian  
2520 succession unconformably overlain by Late Cretaceous Karaböğürtlen Formation; NE of  
2521 Körkuyu.

2522

2523 Fig. 6. Photomicrographs of sandstone of the Late Cretaceous Karaböğürtlen and Kemaliye  
2524 formations. Stratigraphy: a-b Karaböğürtlen Formation (Malatya Metamorphics); c-g  
2525 Kemaliye Formation above the Malatya (Keban) Metamorphics (Areas 1 & 5A); h-i Kemaliye

2526 Formation related to the Munzur limestones; j, Kemaliye Formation beneath the Köseyahya  
2527 thrust sheet; k-l Maastrichtian cover of the Göksun ophiolite. Composition: a, Rounded  
2528 grains of monocrystalline quartz and polycrystalline quartz (quartzite) in a recrystallised  
2529 calcareous matrix; crossed polars; c. 10 km W of Elbistan; GPS 37S 0330991/4230104); b,  
2530 Note the large rounded, then fragmented quartz grain, with cracks infilled by calcite spar,  
2531 suggesting high-strain deformation; location as a; c, Poorly sorted sandstone with common  
2532 monocrystalline quartz, polycrystalline quartz and muscovite in a quartz-rich, granular  
2533 calcareous matrix; crossed polars; Area 3B (Nurhak Dağı, near Beğre); GPS 37S  
2534 0393334/4227050; d, Poorly sorted sandstones with abundant grains of neritic limestone  
2535 (partly recrystallised), polycrystalline quartz and muscovite (deformed); crossed polars;  
2536 location as c; e, Poorly sorted sandstones including grains of neritic limestone (partly  
2537 recrystallised) and basalt (relatively fresh and chloritised); plane-polarised light; location as  
2538 c; f, Granitic grain from conglomeratic lens; crossed polars; location as c; g, Large alkali  
2539 feldspar crystal (upper right), together with monocrystalline quartz, other feldspar and  
2540 microcrystalline quartz in a calcareous and quartz-rich matrix; crossed polars; location as c;  
2541 h, Sub-rounded clast of fine-grained meta-siltstone (central), together with muscovite (large  
2542 lath), polycrystalline quartz (left, central), and bioclastic limestone (e.g., upper left); crossed  
2543 polars; location as c; i, Sub-rounded grains of dark chert (veined and recrystallised) and  
2544 partly recrystallised siltstone in a quartz- and carbonate-rich matrix; crossed polars; location  
2545 as c; j, Micaceous sandstone with common monocrystalline quartz, polycrystalline quartz  
2546 and muscovite, cemented by sparry calcite; near Bakış, east of Elbistan; GPS 37S  
2547 0361782/4222559; k, Bioclastic limestone with common bivalve shell fragments, planktic  
2548 foraminifera and a dark, bituminous schistose grain; cover of the Göksun ophiolite; SW  
2549 slope of Aktaş Tepe; plane-polarised light; GPS 37S 0318668/4232060; l, Bioclastic  
2550 limestone, including large grain of relatively well-rounded microcrystalline quartz; crossed  
2551 polars; same sample as k. Key to letters: B Bioclastic carbonate, BA Basalt, BI Bivalve, C  
2552 Carbonate (calcite), CH Chert, F Feldspar (alkaline), G Granitic lithoclast, Mq Monocrystalline  
2553 quartz, M Muscovite, N Neritic limestone, PL Planktic foraminifer, Pq Polycrystalline quartz,  
2554 S Siltstone, SH Schistose lithoclast.

2555

2556 Fig. 7. Outline geological map and local sections (a-f) of Area (Dağlıca). Based on mapping by  
2557 Perinçek and Kozlu (1984), Bedi et al. (2013), Robertson et al. (2013b) and this study. The



2558 location of the rock-relations diagrams and the logs (roman numerals Va,b,c, VI, VIII and IX;  
2559 see Fig. 11 for I-IV) are indicated. a, The lower Munzur thrust sheet is overlain by the  
2560 Kemaliye Formation and the dismembered Dağlıca ophiolite. The Kırmızı Kandil Formation  
2561 and the Kemaliye Formation are exposed above the upper Munzur thrust sheet; NW of  
2562 İncirli; b, Munzur thrust sheet in the north, unconformably overlain by conglomerates  
2563 (Miocene?), with well-rounded clasts including Eocene nummulitic limestone; NW of Tavla;  
2564 c, Relatively autochthonous succession (Gürün autochthon), overthrust by a Munzur thrust  
2565 sheet; near Dallıkavak; d, Lower Munzur thrust sheet, overthrust by the dismembered  
2566 Dağlıca ophiolite and by an upper Munzur thrust sheet; e, Blocks of the Dağlıca ophiolite  
2567 within ophiolite-derived debris flows, overthrust by an upper Munzur thrust sheet; Tatlar  
2568 area; f, Lower Munzur thrust sheet including the Kırmızı Kandil Formation and the Kemaliye  
2569 Formation; near Elmalı.

2570

2571 Fig. 8. Outline geological map (simplified from Bedi et al., 2009) and local rock-relations  
2572 diagrams in Area 3A (E of Elbistan). Note: Rock-relations diagrams a-d are located north of  
2573 the map area (see top right). a, Lower Munzur thrust sheet overlain by the Kırmızı Kandil  
2574 Formation and the Kemaliye Formation and Pelagic (Gülbahar) unit limestone and chert;  
2575 near Erikli (c. 20 km NW of the map area); b, Lower Munzur thrust sheet, overlain by the  
2576 Kırmızı Kandil Formation and the Kemaliye Formation (with blocks of neritic limestone),  
2577 overthrust by upper Munzur thrust sheet; Gökçek area; 10 km WNW of the map area; c,  
2578 Contact relations with the Darende basin to the east. Mesozoic Tauride units are locally  
2579 emplaced eastwards over the basin margin, which is tilted and overturned near the base.  
2580 Note: in places (off this section) an intact unconformity is exposed between the emplaced  
2581 Mesozoic allochthonous units and Maastrichtian sediments of the intact Darende basin  
2582 succession (see text); N of Dağdamı; 12 km N of map area; d, Lower Munzur thrust sheet,  
2583 overlain by the Kırmızı Kandil Fm. and then the Kemaliye Fm. (with blocks of neritic  
2584 limestone); 2 km NE of Kapaklı; 7 km N of map area; e, Kemaliye Formation enclosing blocks  
2585 of Pelagic (Gülbahar) unit lithologies, overthrust by the lower Munzur thrust sheet. The  
2586 Munzur thrust sheet is mapped as being thrust (SW) over the Köseyahya thrust sheet; 3.5  
2587 km E of Türkören (Yumru Tepe); f, Lower Munzur thrust sheet, with the Kırmızı Kandil and  
2588 Kemaliye formations above (with block of limestone), overthrust by the Köseyahya thrust  
2589 sheet. Note the Fe-rich crust at the top of the Kırmızı Kandil Formation; NW of Şerefli.

2590  
2591  
2592  
2593  
2594  
2595  
2596  
2597  
2598  
2599  
2600  
2601  
2602  
2603  
2604  
2605  
2606  
2607  
2608  
2609  
2610  
2611  
2612  
2613  
2614  
2615  
2616  
2617  
2618  
2619  
2620

Fig. 9. Outline geological map (simplified from Bedi et al., 2009) and local rock-relations diagrams in Area 4 (S of Elbistan). A-A' Malatya Metamorphics in steep fault contact with the Kemaliye Formation (as mapped by Bedi et al. (2009)), overlain by the Kemaliye Formation including blocks of limestone and radiolarite; in turn overthrust by a Munzur thrust sheet and then by ophiolite-related melange with blocks of ophiolitic rocks and limestone; finally overthrust by a Köseyahya thrust sheet; B-B' folded Köseyahya thrust sheet, emplaced over the Malatya metamorphic succession. The syncline (truncated) formed prior to thrust emplacement.

Fig. 10. Field photographs showing key sedimentary features of the Munzur and Köseyahya thrust sheets. a-h Munzur thrust sheet; i-l Köseyahya thrust sheet. a, Oncolite (algal) within Late Triassic micritic limestone; upper part removed by dissolution along a stylolite; E of Elbistan; GPS 37S 0346331/4227793; b, Thin interbed of intraformational sedimentary breccia (near a); c, Thin, intra-formational slump sheet composed of pelagic micrite (also near a); d, U. Cretaceous rudist limestone; lower Munzur thrust sheet; Kaşanlı area; GPS 37S 0325809/4257928; e, Late Cretaceous limestone of upper Munzur thrust sheet, with Kemaliye Formation beneath (shale with limestone blocks) and ultramafic mafic ophiolitic lithologies above, Hurman kalesi; GPS 37S 0310858/4260897; f, Upper Cretaceous pelagic limestone (Kırmızı Kandil Fm., Kapaklı area; GPS 37S 0361390 / 4257247; loc. 4.4; g, Fe-Mn crust at the contact between Late Cretaceous pelagic limestone below and the Kemaliye Formation above, recording a hiatus; near İncirli; GPS 37S 0305831/4252443; i, Ammonite in red bioclastic limestone (Late Triassic), Köseyahya thrust sheet, near Sarıkaya Tepe; E of Elbistan; GPS 37S 0362757/4228355; j, Crinoidal bioclastic limestone (Late Triassic); Köseyahya thrust sheet; loc. as i; k, White crinoidal limestone with diagenetic chert lenticles (Late Triassic); Köseyahya thrust sheet; loc. As j; l, Bioturbated pelagic limestone (Early Cretaceous), between Özbek and Güçük (E of Elbistan); GPS 37S 036516/4229889.

Fig. 11. Measured sedimentary logs (roman numerals) of Permian-Cretaceous facies of the Pelagic (Gülbahar) unit; see Fig. 8 for I-IV and Fig. 7 for V-IX, and the text for explanation.

2621 Fig. 12. Field photographs of the pelagic (Gülbahar) unit in Area 2 (Dağlıca). a, Sandstone  
2622 and shale (Triassic), overthrust by thick-bedded limestone of the Köseyahya thrust sheet;  
2623 Bakış area; GPS 37S 036782/4222559; b, Calcareous mudrock, with thin limestone  
2624 interbeds; note the small load casts in redeposited limestone; small slice (c. 10 m thick),  
2625 below Köseyahya thrust sheet; Triassic; Aşağıgücük köy; GPS 37S 0362059/4222332; c,  
2626 Radiolarian chert and pelagic limestone (centre, pink), positionally intercalated with  
2627 pelagic carbonate, with minor replacement chert (grey); Late Jurassic-Early Cretaceous;  
2628 Ayrancı Tepe; 2 km S of Büyük Tatlı; GPS 37S 0324740/4263734; d, Regularly bedded  
2629 calciturbidites, largely replaced by quartzitic chert; location near c; e, Calciturbidite, mainly  
2630 replaced by quartzitic chert; Late Jurassic-Early Cretaceous; Kayseri (near Hurman kalesi);  
2631 GPS 37S 0302827/4266442; f, Well-cemented debris-flow deposit with angular clasts of  
2632 chert (red) and pelagic carbonate. The chert mainly formed by replacement of pelagic  
2633 carbonate, location near c; g, Debris-flow deposit made of sub-rounded clasts of pelagic  
2634 carbonate in a calcarenite matrix, rich in redeposited ooids; gravity emplaced before  
2635 completely lithified; Late Jurassic-Early Cretaceous; SE of Büyük Tatlı; GPS 37S  
2636 0325527/4262472; h, Debris-flow deposit composed of angular to sub-rounded clasts of  
2637 white pelagic limestone and red radiolarite; the well-cemented nature is typical of the  
2638 pelagic succession in contrast to the Kemaliye Fm.; Late Jurassic-Early Cretaceous; near  
2639 Yumru Tepe, E of Elbistan; GPS 37S 036620/423774; i, Debris-flow deposit made up of  
2640 angular to sub-rounded clasts of pelagic limestone and redeposited calcarenite in a coarse  
2641 calcarenite (oolitic) matrix; Late Jurassic-Early Cretaceous; near Topaktaş (Kırksrak area);  
2642 GPS 37S 0298744/4262995.

2643

2644 Fig. 13. Outline geological map of Area 5A, Kemaliye and Area 5B, Divriği. See text for  
2645 explanation and data sources.

2646

2647 Fig. 14. Geological map of the type, Kemaliye area including the Kemaliye Formation (Area  
2648 5A), simplified from 1:100,000 geological maps of Turkey (Bilgiç, 2008b, c), with additional  
2649 information from this study.

2650

2651 Fig. 15. Local cross-sections of the Kemaliye Formation in its type area (5A). a, East of Keban  
2652 Lake; b, West of Keban Lake (farther southeast). See Fig. 13 for location and the text for  
2653 explanation.

2654

2655 Fig. 16. Field photograph Kemaliye Formation and related units in the type area (5A) (a-f)  
2656 and in Area 3B (Nurhak Dağı) (g-l). a, View southwest over the Late Cretaceous Kemaliye  
2657 Formation, with lenticular blocks, mainly limestone conglomerate in a matrix of shale and  
2658 sandstone; S of Kemaliye town; b, Calc-mylonite locally exposed near the contact between  
2659 the Malatya Metamorphics and the Kemaliye Formation (E of Keban Lake); c, Stratiform  
2660 debris-flow deposits with sub-rounded to well-rounded clasts, mainly neritic limestone, in a  
2661 coarse-grained sandy matrix; Kemaliye Formation, lower part; d, Debris-flow deposits with  
2662 mainly angular clasts of micaschist in a coarse-grained sandy matrix; Kemaliye Formation,  
2663 lower part, near Yuva; e, Lenticular debris-flow conglomerate, dominated by well-rounded,  
2664 varicoloured clasts of red radiolarian chert in a coarse-grained sandy matrix; Kemaliye  
2665 Formation, lower part; near Beğre (Area 3B); f, Mainly sub-angular clasts of neritic limestone  
2666 (calcite-veined) in a coarse-grained sandy matrix; Kemaliye Formation, upper part; near  
2667 Beğre (Area 3B); g, Serpentinite cut by small granitic intrusions (foreground), overthrust by a  
2668 thin unit of the Kemaliye Formation, and then by the Köseyahya thrust sheet (pale; main  
2669 mountain above), near Beğre; h, Calc-mylonite in the uppermost levels of the Malatya  
2670 Metamorphics, near Beğre; i, Isoclinally folded calc-schist in the uppermost levels of the  
2671 Malatya Metamorphics, later brecciated, near Beğre; j, Isoclinally folded calc-schist in the  
2672 uppermost levels of the Malatya Metamorphics, cut by small granitic intrusions (centre-  
2673 right); fold limb is 5 m across in the foreground, near Beğre; k, Granitic intrusions (by pen)  
2674 and greenish serpentinite (upper), mutually brecciated, indicating high-strain deformation  
2675 after intrusion, near Beğre; l, Iron-rich crust at the top of the platform succession, below the  
2676 Kemaliye Fm., marking a hiatus.

2677

2678 Fig. 17. Sedimentary log of the lower part of the Kemaliye Formation in its type, Kemaliye  
2679 area (5A). See text for explanation.

2680

2681 Fig. 18. Photomicrographs of key age-diagnostic benthic microfossils. a: *Neoendothyra* sp.;  
2682 sample ET12.37; Triassic; Dark limestone block in Kemaliye Formation, Area 5A, near Yuva,

2683 GPS 37S 0456773/4345128; b: *Meandrospira* sp., sample ET12.37, as above, Triassic; c:  
2684 *Thaumatoporella parvovesiculifera* (Tp), *Bosniella fontainei* (Bf), *Siphovalvulina variabilis*  
2685 (Sv), *Glomospira* sp. (Gl), sample ET12.57; Middle Triassic; Bioclastic limestone from Munzur  
2686 thrust sheet, Area 5B, c. 8 km SSE of Divriği, Area 5B, GPS 37S 0426455/4351186; d:  
2687 *Siphovalvulina variabilis*, sample ET12.58 (location as c); Jurassic; e: *Bosniella fontainei*,  
2688 sample ET12.57, Middle Jurassic (location c, d); f-g: *Nezzazata isabellae*, sample ET12.54,  
2689 Aptian-Albian, limestone block in lower part of ophiolite-related melange, Area 5B (Divriği),  
2690 GPS 37S 0425452/4367406; h, i: *Mayncina bulgarica* (Laug et al., 1980), sample ET12.54;  
2691 Aptian-Albian (location as f-g); j-l: *Parakoskinolina* sp., sample ET12.56; Aptian-Albian;  
2692 limestone block in mid part of the ophiolite-related melange, Area 5B (Divriği), GPS 37S  
2693 0425280/436641; m-o: *Akcaya minuta*, sample ET12.56; Aptian-Albian (location j-o); p:  
2694 *Nezzazatinella* sp., sample ET12. 56; Aptian-Albian (location as j-p); q: *Vercorsella* sp.,  
2695 sample ET12. 56, Aptian-Albian (location as j-q). Scale bars= 0.2 mm.

2696

2697 Fig. 19. Measured sedimentary logs of the Late Cretaceous Kemaliye Formation in Area 2  
2698 (Dağlıca); see the text for explanation. Logs 1-5 in Area 3A (E of Elbistan) and farther north;  
2699 Log 1. Near Köseyahya; Log 2, 6 km N of map in Fig. 8; Log 3, 5 km WSW of log 2; Log 4, 7 km  
2700 NE of log 2; Logs 5 and 6 in Area 2 (Dağlıca), see Fig. 7.

2701

2702 Fig. 20. Field photographs in Area 2 (Dağlıca), particularly the Kemaliye Formation. a, Pebbly  
2703 debris-flow, with mostly well-rounded clasts of meta-sandstone (quartzite), with some  
2704 micaschist (centre left); Kemaliye Formation; 1 km N of İncirli GPS 37S 0308706/4255621; b,  
2705 Debris-flow dominated by sub-rounded clasts of limestone (some with rudist debris) in a  
2706 pebbly matrix; Kemaliye Formation; c. 1 km N of İncirli, GPS 37S 0303828/4254761; c,  
2707 Cenomanian rudist-bearing limestone (part of a block) within shale and sandstone; Kemaliye  
2708 Formation; near Hurman kalesi, GPS 37S 0311635/4261660; d, Blocks of neritic limestone  
2709 with rudist bivalves in highly deformed Kemaliye Formation; near Hurman kalesi, GPS  
2710 0307401/4259103; e, Mudrocks of the Kemaliye Formation, interspersed with blocks of  
2711 Mesozoic neritic limestone; overthrust by the upper Munzur thrust sheet; Hurman kalesi  
2712 area, GPS 37S 0314553/4260250; f, Crudely stratified, ophiolite-derived debris-flow units,  
2713 including clasts of basalt, diabase, gabbro, pelagic limestone and radiolarian chert,  
2714 associated with the Dağlıca ophiolite; near Kaşanlı köy, GPS 37S 0326709/4257612; g,

2715 Matrix-supported debris-flow unit with clasts of gabbro (lower left), diabase and basalt;  
2716 associated with the Dağlıca ophiolite; same locality as f; h, Ophiolite-derived debris flow,  
2717 locally dominated by basalt (centre right); associated with the Dağlıca ophiolite; 1.5 km W of  
2718 Kırkısrak, GPS 37S 0294299/4259724; i, as d, e with angular clast of pink pelagic limestone,  
2719 with red 'replacement' chert; j, Debris-flow conglomerate made up of ophiolitic clasts  
2720 including gabbro, diabase and basalt; associated with the Dağlıca ophiolite; İncirli area, GPS  
2721 37S 030015/425603); k, Late Cretaceous-Eocene succession of the relatively autochthonous  
2722 Gürün platform, overthrust by Mesozoic Munzur limestone; 2 km NE of Dallıkavak, GPS 37S  
2723 0293001/4261378; l, Clast-supported conglomerate including well-rounded clasts of Eocene  
2724 Nummulitic limestone; probably Miocene; 1.5 km NW Çağsak, GPS 37S 0286787/4257672.

2725

2726 Fig. 21. Photomicrographs of key age-diagnostic planktic microfossils. a, *Globotruncana* cf.  
2727 *G. mariei* Banner & Blow, 1960, sample M.13.35; Kemaliye Formation; Campanian-  
2728 Maastrichtian, near Kapaklı, Area 3A, NE of Elbistan, GPS 37S 0361390/4259247; b,  
2729 *Globigerinelloides* sp., sample M.13.35, Campanian-Maastrichtian (same location); c,  
2730 *Globotruncana linneiana* (D'Orbigny, 1839), sample M13.4, pelagic limestone block in  
2731 Kemaliye Formation, Campanian-Maastrichtian, Odunluk Tepe; Area 3A, E of Elbistan; GPS  
2732 37S 0366666/4225559; *Archaeoglobigerina cretacea* (D'Orbigny, 1840), Campanian-  
2733 Maastrichtian (same location); e, f: *Globigerinidae*, sample M13.60, Cenozoic. Pelagic  
2734 limestone block in debris-flow deposit, near İğde köyü (SE of Elbistan), GPS 37S  
2735 0335066/4223251. Scale bars= 0.2 mm.

2736

2737 Fig. 22. Structural relationships in Area 3B (Nurhak Dağı); a, Meta-carbonate rocks of the  
2738 Malatya Metamorphics, structurally overlain by serpentinitised harzburgite which is cut by  
2739 small granitic intrusions, and in then overthrust by a thin unit of the Kemaliye Formation,  
2740 with the Köseyahya thrust sheet above; near Beğre;  
2741 b, Malatya Metamorphics, structurally overlain by serpentinitised harzburgite, then by the  
2742 Kemaliye Formation, with the Köseyahya thrust sheet above, c. 10 km north-east of a. The  
2743 blocks in the Kemaliye Formation include Triassic red crinoidal limestone, similar to that in  
2744 the Köseyahya thrust sheet, in a matrix of terrigenous sandstone and mudrock.

2745

2746 Fig. 23. Simplified geological map of part of Area 5B, Divriği (simplified from MTA 1:100,000  
2747 geological maps of Turkey (Bilgiç, 2008a, b, c). Note the locations of the representative  
2748 sections shown in Fig 25. See text for explanation and data sources.

2749

2750 Fig. 24. Summary of the stratigraphy and structural relations in part of Area 5B, Divriği. a,  
2751 Stratigraphic column; b, Rock-relations (bi in the north; b-ii in the south). See the text for  
2752 explanation and data sources.

2753

2754 Fig. 25. Field photographs of Divriği ophiolite-related melange in Area 5B. a, Elongate blocks  
2755 of thick-bedded neritic limestone set in a matrix of serpentinite and sandstone/shale; c. 6  
2756 km NW of Divriği); b, Elongate blocks of Mesozoic neritic limestone embedded in sheared  
2757 serpentinite; c. 6 km NW of Divriği); c, Part of a large block of thick-bedded neritic  
2758 limestone, deformed into a SW-verging fold; c. 6 km NW of Divriği); d, Large block of  
2759 Mesozoic neritic limestone in the Divriği melange, deformed into a N-verging fold; c. 3 km  
2760 NW of Divriği); e, Serpentinite melange with a strongly sheared steeply dipping fabric; c. 7  
2761 km SE of Divriği); f, Large exposure of serpentinite melange, dominated by mantle  
2762 harzburgite; c. 10 km SE of Divriği.

2763

2764 Fig. 26. Summary of fold data (axial planes and hinges) collected during this study, plotted as  
2765 poles; equal-area lower hemisphere projection; N= number of measurements; ai-aiv, Fold  
2766 axial planes; bi-biv Fold hinges. Individual plots: ai-bi Malatya Metamorphics (Area 1. W of  
2767 Elbistan); aii-bii Allochthonous Tauride units (Area 2, Dağlıca); aiii-biii Allochthonous Tauride  
2768 units (Area 3A, E of Elbistan); aiv-biv Combined units: Malatya (Keban) metamorphics and  
2769 Kemaliye Formation (Area 1) (Kemaliye area). See Supplementary Figs. 7-10 for plots of all  
2770 data, including bedding.

2771

2772 Fig. 27. Geological development of the central and northern parts of the Tauride continent.  
2773 a, Late Triassic extensional faulting establishes the contiguous neritic Munzur platform, the  
2774 Neritic-pelagic Köseyahya platform and the Pelagic (Gülbahar) unit; b, Mid-Late Jurassic. N-  
2775 dipping ramp develops redepositing mainly oolitic facies into deeper water; c, Late  
2776 Cretaceous (Cenomanian). Rudist bivalve reefs develop on proximal (Munzur) platform

2777 while deeper-water slope conditions persist farther north; d, Campanian-Maastrichtian. The  
2778 southern part of the Tauride continent (Malatya platform) detaches and is deeply  
2779 underthrust northwards; ophiolite is emplaced southwards over the northern edge of the  
2780 Tauride continent which collapsed in advance to form a foredeep.

2781

2782 Fig. 28. Geological development of the Tauride continent in the E Taurides. a, Carboniferous;  
2783 includes rift-related volcanism; b, Mid-Late Triassic continental rifting; c, Mid-Late Jurassic  
2784 passive margin subsidence; d, Late Cretaceous (Cenomanian, c. 90 Ma); northward  
2785 subduction of oceanic crust; e, Late Cretaceous (Campanian-Maastrichtian); collision and  
2786 crustal imbrication of the Tauride continent. Note: it is uncertain whether the Malatya and  
2787 Munzur-Köseyahya units were either contiguous or separate platforms. See text for  
2788 discussion.

2789

2790 Fig. 29. Stages in the latest Cretaceous (late Campanian-Maastrichtian), southward  
2791 emplacement of oceanic crust and passive continental margin units in the E Taurides. a,  
2792 Flexural foredeep is imbricated during compressional emplacement; b, With further  
2793 emplacement, the relatively distal neritic-pelagic (Köseyahya) platform detaches and is  
2794 thrust over the more proximal neritic (Munzur) platform; c, With further convergence, part  
2795 of the neritic (Munzur) platform is locally re-thrust over the neritic-pelagic platform unit.

2796

2797 Fig. 30. Rock-relations diagram showing the inferred tectono-stratigraphy of the E Taurides  
2798 following latest Cretaceous emplacement/exhumation, restored to beneath the latest  
2799 Cretaceous transgressive shallow-marine sedimentary cover (south of the Gürün  
2800 autochthon). From the structural base upwards: Malatya (Tauride) continental unit; Late  
2801 Cretaceous Göksun (Berit) ophiolite; partially exhumed Malatya Metamorphics (both of the  
2802 latter are stitched by the Late Cretaceous Baskil granitoids); debris-flows ('olistostromes')  
2803 (e.g. Kemaliye Formation type area), with slices and blocks of the pelagic (Gülbahar) unit  
2804 and finally supra-subduction zone ophiolites and their metamorphic sole. Note: variable  
2805 internal deformation of the Munzur, Köseyahya and ophiolitic thrust sheets is not shown.

2806



2807 Fig. 31. Alternative tectonic models for the eastern Taurides. ai-aii, Assumes one ocean to  
2808 the north and one continent to the south. The allochthonous units are emplaced by complex  
2809 out-of-sequence thrusting (based on Ricou et al., 1984); bi-bii. Assumes a single Mesozoic  
2810 Neotethys. The Late Cretaceous ophiolites form above a subduction zone to the E-NE that  
2811 rotates and rolls-back, emplacing segments over the N and S margins of the Tauride  
2812 continent and over Arabia/N Africa. The Bitlis and Pütürge metamorphism relates to  
2813 attempted southward subduction. An Inner Tauride basin is assumed between the Tauride  
2814 continent and a combined Kırşehir-Tavşanlı crustal block in the north, but this basin is not  
2815 the source of the ophiolites (based on van Hinsbergen et al., 2020); ci-cii. (preferred model).  
2816 This assumes several microcontinents and small Mesozoic ocean basins. The Bitlis and  
2817 Pütürge continental units represent rifted fragments with ocean crust on either side. Supra-  
2818 subduction zone oceanic crust in the northerly basin (Berit ocean) subducts northwards  
2819 resulting in arc magmatism that intrudes the continental block to the north (Malatya  
2820 metamorphic unit). An Inner Tauride ocean was potentially the source of Late Cretaceous  
2821 supra-subduction zone ophiolites in the north. Supra-subduction zones are emplaced  
2822 separately, southwards onto the Arabian margin. Uncertain is whether the Tauride platform  
2823 links with the South Armenian platform at depth as there is no continuous surface exposure.  
2824 See text for discussion.

2825  
2826  
2827  
2828  
2829  
2830  
2831  
2832  
2833  
2834  
2835  
2836  
2837  
2838

2839

2840

[Click here to view linked References](#)

1

2 **Late Palaeozoic-Neogene sedimentary and tectonic development of the Tauride continent**

3 **and adjacent Tethyan ocean basins in eastern Turkey: new data and integrated**

4 **interpretation**

5

6

7

8

9 Alastair Harry Forbes Robertson<sup>1</sup>, Osman Parlak<sup>2</sup>, Timur Ustaömer<sup>3</sup>, Kemal Taslı<sup>4</sup>, Paulian  
10 Dumitrica<sup>5</sup>

11

12

13 <sup>1</sup>School of GeoSciences, University of Edinburgh, Grant Institute, West Mains Rd.,

14 Edinburgh, EH9 3JW, UK ([Alastair.Robertson@ed.ac.uk](mailto:Alastair.Robertson@ed.ac.uk); corresponding author)

15 <sup>2</sup>Çukurova Üniversitesi, Jeoloji Mühendisliği Bölümü, 01330 Balcalı, Adana, Turkey

16 <sup>3</sup>İstanbul Üniversitesi-Cerrahpaşa, Jeoloji Mühendisliği Bölümü, Büyükçekmece, İstanbul,

17 Turkey

18 <sup>4</sup>Mersin Üniversitesi, Jeoloji Mühendisliği Bölümü, Mersin, Turkey

19 <sup>5</sup>Dennigkofenweg 33, CH-3037 Guemligen, Switzerland

20

21

22 **Abstract**

23 The eastern Taurus exemplifies continental rifting, passive margin development, Late  
24 Cretaceous melange genesis and ophiolite emplacement. Following Triassic rifting, a  
25 carbonate platform developed near sea level in the south (Munzur unit), whereas its  
26 northern extension (Neritic-pelagic unit) subsided into deep water during Late Jurassic-Late  
27 Cretaceous. Triassic-Cretaceous deep-water sediments and volcanics restore as distal deep-  
28 water slope/base of slope units. Jurassic-Cretaceous basic volcanics, interbedded with  
29 pelagic sediments, represent emplaced oceanic seamounts. Supra-subduction zone  
30 ophiolites formed to the north (c. 93 Ma), probably within an Inner Tauride ocean, and were  
31 emplaced southwards by trench-margin collision during latest Cretaceous (c. 75-66 Ma). The  
32 margin underwent flexural uplift/erosion and then subsidence/foredeep-infill. Part of the  
33 Tauride continent in the south (Malatya Metamorphics) deeply underthrust/subducted  
34 northwards, then exhumed rapidly by the late Maastrichtian (c. 65 Ma). To the south,  
35 oceanic lithosphere (e.g. Göksun ophiolite) was thrust northward beneath Tauride (Malatya)  
36 crust from a more southerly oceanic basin (Berit ocean), and intruded by Late Cretaceous  
37 subduction-related granitic rocks (88-82 Ma). Allochthonous units were assembled during  
38 the latest Cretaceous, followed by thick-skinned folding/thrusting, generally southwards,  
39 related to regional collision tectonics during Mid-Late Eocene. Part of the  
40 unmetamorphosed Tauride platform and its over-riding Late Cretaceous allochthon were  
41 apparently displaced >60 km northeastwards. Mid-Late Miocene regional collision drove  
42 variable folding and re-thrusting, in places northwards. Regional comparisons suggest that  
43 the Tauride carbonate platform (Geyik Dağ) narrowed eastwards, such that the  
44 palaeogeography of the E Taurides differed from farther west, influencing the late  
45 Mesozoic-Cenozoic structural development.

46

47

48 Key words: E Anatolia, Tethys, palaeogeography, tectonics, ophiolites, melange, deep-sea  
49 sediments

50

51

## 52 **1. Introduction**

53

54 The geological development of Tethys within and around Anatolia remains of current  
55 interest, with several alternative tectonic models being recently proposed (Moix et al.,  
56 2008; Robertson et al., 2012, 2013a; Rolland et al., 2012, 2020; Maffione et al., 2017; Parlak  
57 et al., 2019; Hinsbergen et al., 2020). In addition to ophiolites, continental margin units and  
58 melanges need to be taken into account. The Taurides represent a key part of Anatolia (Fig.  
59 1), where ophiolites were emplaced onto a regional-scale carbonate platform during latest  
60 Cretaceous time (Juteau, 1980; Şengör and Yılmaz, 1981; Robertson and Dixon, 1984; Ricou  
61 et al., 1984; Dilek and Moores, 1990; Robertson, 2002; Parlak, 2016; Barrier et al., 2018).  
62 There have been several attempts to explain the emplacement of the ophiolites and related  
63 continental margin units as a whole in the western Taurides (Hayward and Robertson, 1982;  
64 Woodcock and Robertson, 1982; Yılmaz and Maxwell, 1984; Şenel, 1984; Marcoux et al.,  
65 1989; Collins and Robertson, 1998), in the central Taurides (Demirtaşlı et al., 1984; Özgül,  
66 1997; Dilek and Whitney, 1997; Andrew and Robertson, 2002; Parlak and Robertson, 2004;  
67 McPhee et al., 2018a), and also in the eastern Taurides (Yılmaz, 1993; Yılmaz et al., 1993,  
68 Robertson et al., 2006, 2007, Robertson et al., 2013a b; Rolland et al., 2012, 2020).

69 The ophiolites, melanges and related continental units of the İzmir-Ankara-Erzincan  
70 (northern Neotethyan) suture zone in the Eastern Turkey have also received a considerable  
71 amount of attention in recent years (e.g., Yılmaz et al., 1997; Okay and Şahintürk, 1997; Rice  
72 et al., 2009; Ustaömer and Robertson, 2010, 2013; Robertson et al., 2013c; Topuz et al.,  
73 2013a, b; Rolland et al., 2012, 2020; Hässig et al., 2013, 2017). However, there have been  
74 few integrated studies that focus on the carbonate platforms, slope/basin facies and the  
75 related melange units in the Eastern Taurides (Fig. 2). These units are located in a critical  
76 position between the Arabian Platform (African plate) to the south and the Pontides  
77 (Eurasian plate) to the north. The eastern Tauride region has some distinctive features,  
78 notably an extraordinary NE-verging fold-like structure, up to 200 km long x 250 km wide  
79 (MTA, 2011), termed the Gürün curl after a town in the core of this structure (Lefebvre et  
80 al., 2013a) (Fig. 2; Supplementary Fig. 1). Is this a primary palaeogeographic feature, or  
81 related to tectonic emplacement, or to some combination of both?

82 A synthesis of the Tethyan geology of the Eastern Taurides is given here, utilising a  
83 combination of new data and also the available literature on this region (Perinçek and Kozlu,

84 1984; Robertson et al., 2013b; Bedi et al., 2004, 2005; Bedi and Yusufoglu, 2018). The region  
85 studied includes a Late Palaeozoic-Mesozoic metamorphosed carbonate platform, an  
86 unmetamorphosed carbonate platform and deeper-water marginal units, several types of  
87 melange, and also Late Cretaceous ophiolites with their metamorphic soles. Latest  
88 Cretaceous-Miocene cover successions help to constrain the distribution and timing of  
89 tectonic events, especially the exhumation of the metamorphic rocks. The assembled  
90 information will be used to test alternative tectonic models for the wider region (Kozlu et  
91 al., 1990; Robertson et al., 2013a, b; Barrier et al., 2018; van Hinsbergen et al., 2020; Rolland  
92 et al., 2012, 2020). We will demonstrate that the geology of eastern Anatolia represents a  
93 unique combination of palaeogeographic and tectonic features. The palaeogeography  
94 differs significantly from that of the central and western Taurides. Also, the Late Cretaceous  
95 ophiolites and related melange units differ significantly from Jurassic counterparts farther  
96 north in the E Pontide-Lesser Caucasus region.

97 In this paper, we use the time scale of Cohen et al. (2020).

98

## 99 **2. Regional tectono-stratigraphy**

100 We utilise a modified version of the tectono-stratigraphy based on mapping by the Turkish  
101 Petroleum Company (TPAO) (Perinçek and Kozlu, 1984), including changes and additions  
102 based on mapping by the Maden Tektik ve Arama (MTA) (Bedi et al., 2009; Bedi and  
103 Yusufoglu, 2018), related studies (Robertson et al., 2013b) and this work.

104 Moving northwards, the Arabian platform is tectonically overlain by a Miocene  
105 imbricate thrust belt, with, to the north of this, the Bitlis and Pütürge allochthonous  
106 continental units (Yılmaz, 1993; Yılmaz et al., 1993; Yazgan, 1984) (Fig. 1). These units are  
107 tectonically overlain by Late Cretaceous ophiolitic rocks, variously known as the Göksun  
108 (Berit), Kömürhan, İspendere or Yüksekova ophiolites. Our study effectively begins in the  
109 south with the Late Palaeozoic-Mesozoic Malatya Metamorphics (including the Keban and  
110 Binboğa metamorphic rocks; see below). To the north, these metamorphic rocks are over-  
111 ridden by allochthonous, unmetamorphosed Tauride carbonate platform, melanges and  
112 ophiolitic units. The allochthonous outcrop in the west of the region is split into two parts,  
113 termed the Northern and the Southern allochthon (Robertson et al., 2013b). Both the  
114 Northern and the Southern allochthon include emplaced thrust sheets of Mesozoic  
115 carbonate platform, slope and deeper-water facies, melanges and ophiolitic rocks. The

116 relationships between the two allochthonous assemblages is debatable as they are  
117 separated by a relatively autochthonous Tauride platform succession, termed the Gürün  
118 autochthon (Kozlu et al., 1990; Atabey, 1993; Atabey et al., 1994, 1997; Robertson et al.,  
119 2013b) (Fig. 2).

120 The Mesozoic-Paleogene units within our study area are unconformably overlain by  
121 two geographically and temporarily distinct types of sedimentary basin. The first is  
122 represented by latest Cretaceous-latest Eocene basins, including the Darende, Hekimhan  
123 and Malatya basins; the second comprises Neogene-Recent sediments (Salyan Formation)  
124 and volcanics (Kepezdağ volcanics), notably within the Afşin-Elbistan basin, the Pınarbaşı-  
125 Kangal basin and the upper part of the large Malatya basin (Fig. 2). The area is dissected by  
126 through-going neotectonic faults, principally the westward-curving Sürgü-Misis Fault  
127 (Duman and Emre, 2013), and also three main NNE-SSW-trending faults, the Sarız, Gürün  
128 and Malatya-Ovacık faults. Of the latter, by far the largest is the Malatya-Ovacık fault, which  
129 is estimated to have accommodated 29 km of left-lateral movement (Fig. 2) (Westaway and  
130 Arger, 2001; Kaymakçı et al., 2006; Sancar et al., 2019). In addition, part of the area is  
131 transected by lesser known, c. SSW-NNE to SW-NE trending faults (Göksu faults of Kozlu et  
132 al., 1990) that are important because they straddle the contact between the Gürün  
133 autochthon and the Southern allochthon (Robertson et al., 2013b)

134 To facilitate description and interpretation, we subdivide our study region into 5 sub-  
135 areas (Fig. 2). *Area 1*, NW of Elbistan (Afşin); *Area 2*, Dağlıca; *Area 3*, E of Elbistan  
136 (subdivided into *Area 3A* in the west and *Area 3B* (Nurhak Dağı) in the east; *Area 4*, S of  
137 Elbistan, and finally, Divriği-Kemaliye in the north-east (subdivided into *Area 5A*, Kemaliye  
138 and *Area 5B*, Divriği farther north).

139

### 140 **3. Tauride carbonate platform**

141

142 To the SW of our study area (Tufanbeyli-Saimbeyli-Sarız) (Fig. 2), the autochthonous Tauride  
143 platform succession encompasses Precambrian sediments (Emirgazi Formation), Cambrian  
144 shelf siliciclastics (Feke Quartzites) and mixed carbonate-siliciclastic sediments (Çal Tepe  
145 Formation), which are overlain by Ordovician mainly argillaceous and silty shelf sediments  
146 (Seydişehir, Bedivan and Halit Yaylası formations) including some glacial deposits. Fine-  
147 grained siliciclastic sediments with calcareous intervals (e.g. Nautiloid limestones) dominate

148 the Silurian (Puşçu Tepe Shale and Yukarı Yayla formations). The Devonian is mainly shelf  
149 carbonates, with minor basaltic volcanics, including a reef-bearing horizon (Şafak Tepe  
150 Formation). The lower interval (Alitepesi Formation) and the upper interval (Gümüşali and  
151 Naltaş formations) are relatively quartz rich. Above a quartz-rich base, the Permian is  
152 dominated by algal carbonates (Yığılı Tepe Formation) (Özgül et al., 1973; Metin et al., 1986;  
153 Kozlu and Göncüoğlu, 1997; Özgül and Kozlu, 2002; Göncüoğlu et al., 2004; Bedi and Usta,  
154 2006; Bedi et al., 2017).

155 The Palaeozoic succession accumulated on a continental platform, punctuated by  
156 unconformities that were probably tectonically influenced; i.e. at the Precambrian-  
157 Cambrian boundary (?), the Early-Late Ordovician boundary, the Silurian-Devonian  
158 boundary, the Early-Middle Devonian boundary and the Carboniferous-Permian boundary.  
159 There was an increased sedimentation rate during the late Carboniferous (Göncüoğlu et al.,  
160 2004). This represents a period of enhanced tectonic subsidence that may relate to Variscan  
161 collisional orogeny farther west, in the Aegean-Balkan region.

162 The Mesozoic succession is dominated by shelf carbonates, with stratigraphic breaks  
163 that are likely to have been tectonically controlled; i.e. during the Middle Triassic, the Early-  
164 Mid Jurassic, the Late Cretaceous ( Turonian-Santonian(?)), and the Early Eocene (Kozlu et  
165 al., 1990). Devonian to Permian, and locally also Triassic, siliciclastic and carbonate rocks  
166 crop out in the northwest of the Gürün autochthon, where they are unconformably overlain  
167 by Early Jurassic to Late Cretaceous shelf carbonates. The Cretaceous carbonates pass  
168 upwards into Cenozoic facies without a structural break (Özgül et al., 1973). The succession  
169 continues with deeper-water (but still shelf-depth) hemipelagic carbonates, siltstones,  
170 mudrocks and sparse sandstones, dated as Maastrichtian-Middle Eocene (Lutetian) (Aziz et  
171 al., 1982; Perinçek and Kozlu, 1984; Yılmaz et al., 1991, 1994; Atabey, 1995; Robertson et al.,  
172 2013b). Locally, Eocene or older sediments in the Gürün autochthon are unconformably  
173 overlain by Miocene sediments (e.g. non-marine conglomerates), and also by Plio-  
174 Quaternary volcanics and sediments (Perinçek and Kozlu, 1984; MTA, 2011). There is no  
175 evidence of any major structural break or suture zone within, or between, the outcrops that  
176 extend northeastwards from the Saimbeyli-Tufanbeyli-Sarız region to the Gürün autochthon  
177 (MTA, 2011). This whole crustal unit can, therefore, be correlated with the relatively  
178 autochthonous Tauride carbonate platform in the central Taurides (Geyik Dağ).



179 The Jurassic-Cretaceous carbonates accumulated on a gently subsiding shelf,  
180 followed by accelerated subsidence that was probably tectonically controlled during the  
181 latest Cretaceous and Palaeocene-Early Eocene. There is no evidence of emplacement of  
182 any allochthonous units over the Gürün autochthon, at least until the Mid-Late Eocene  
183 (Perinçek and Kozlu, 1984; Kozlu et al., 1990; Robertson et al., 2013b); this observation is  
184 critical to any tectonic reconstruction.

185

#### 186 **4. Malatya metamorphics**

187 The regionally extensive Late Palaeozoic (Devonian?) to Late Cretaceous Malatya  
188 Metamorphics (Figs. 2, 3) are widely exposed in the south of the study area (Karaman et al.,  
189 1993; Yılmaz et al., 1991, 1994; MTA, 2011; Bedi and Yusufoglu, 2018). The outcrops are  
190 variously referred to as the Malatya Metamorphics in the type area (S of Elbistan), the  
191 Binboğa Metamorphics (NW of the Sürgü-Misis Fault; i.e. west of Afşin) and the Keban  
192 Metamorphics (east of the Malatya-Ovacık Fault) (Perinçek and Kozlu, 1984; Bedi et al.,  
193 2005, Bedi and Usta, 2006; Kaya, 2016). The Keban Metamorphics have been locally dated  
194 (south of Keban Lake) as  $73.8 \pm 0.3$  Ma (Campanian) based on  $^{40}\text{Ar}/^{39}\text{Ar}$  dating of muscovite  
195 within fluorite-bearing marble (Rolland et al., 2012). However, it is unclear whether this age  
196 is representative of the Malatya Metamorphics as a whole (see below).

197 The outcrop to the east of the Malatya-Ovacık Fault was recently remapped as three  
198 different units, separated by thrusts (Bedi and Yusufoglu 2018). The first unit, termed the  
199 Bodrum nappe (named after a type area in the western Taurides) is a metamorphosed  
200 Middle Devonian to Late Cretaceous succession (Fig. 3). The mineral assemblages in this unit  
201 (Bodrum nappe) are mainly suggestive of greenschist facies metamorphism (Perinçek and  
202 Kozlu, 1984). Local intercalations of basic metavolcanics rock (west of Afşin) are indicative of  
203 amphibolite facies conditions (Robertson et al., in press b). However, reported occurrences  
204 of glaucophane (Bedi et al., 2009) hint at high pressure-low temperature (HP-LT)  
205 metamorphism. The second, structurally overlying, unit is a metamorphosed Carboniferous  
206 to Late Cretaceous succession that is exposed SW of Malatya. This is correlated with the  
207 Yahyalı nappe, which has its type area further west, near Yahyalı. The Yahyalı nappe in its  
208 type area has undergone HP-LT metamorphism, based on the occurrence of carpholite

209 (Pourteau et al., 2010). Structurally above comes as third unit with a Late Devonian to Late  
210 Cretaceous succession, which is correlated with the Aladağ (Hadim) nappe in the central  
211 Taurides (Bedi and Yusufoglu 2018).

212 The thrust sheets, as summarised above, are intruded by Late Cretaceous arc-type  
213 granitoid rocks (Baskil Granitoids). These are mainly I-type, calc-alkaline hornblende-biotite  
214 granodiorites and 'normal' granites, with both mantle and crustal-derived chemical  
215 features. The granitoid rocks are dated, radiometrically, as 88-82 Ma (Santonian-  
216 Campanian) (Parlak, 2006; Yazgan and Chessex, 1991; Rızaoğlu et al., 2009; Karaoğlu et al.,  
217 2016). The Malatya Metamorphics are structurally underlain, directly, by the relatively  
218 intact Göksun ophiolite (Parlak, 2006; Parlak et al., 2004, 2020), also known in this area as  
219 the Berit meta-ophiolite (Genç et al., 1993; Yılmaz et al., 1987; Yılmaz, 1993), the North Berit  
220 ophiolite (Robertson et al., 2006), and the Kömürhan ophiolite (Bedi et al., 2005, 2009).

221 The Malatya Metamorphics (Bodrum nappe) are unconformably overlain by Middle  
222 Palaeocene to Middle Eocene shallow-water calcareous sediments (Seske Formation), as  
223 exposed near, and to the west of Afşin (Perinçek and Kozlu, 1984; Yılmaz et al., 1991, 1994;  
224 Robertson et al., 2006) (Fig. 4a). The succession begins with conglomerate, with clasts  
225 including schist and marble and then passes upwards into shallow-water limestones,  
226 commonly rich in large foraminifera (e.g. *Alveolina* sp.) and ooids (see below).

227 The protoliths of the Malatya Metamorphics (Bodrum nappe) within our main study  
228 area, namely the Binboğa Mountains west of Afşin (Area 1) and the Doğanşehir and  
229 Kemaliye areas farther east (Areas 3B, 5A) (Fig. 2), are dated with variable precision, mainly  
230 using benthic foraminifera and some small gastropods (Bedi et al., 2005, 2009). The overall  
231 succession (Fig. 3) begins with mixed meta-clastic and meta-carbonate rocks (Yoncayolu  
232 Formation) that are dated as Middle Devonian-mid Carboniferous. Meta-volcanic rocks (Fig.  
233 4b) and meta-rudites (Fig. 4c) are intercalated in places (Fig. 5 logs 1, 2). Within the Keban  
234 metamorphics farther east, basic meta-dykes cut the Late Palaeozoic succession; also,  
235 foliated meta-dyabase occurs within the upper part of the early Carboniferous (?) succession  
236 (Kaya, 2016). Overlying meta-limestones and meta-dolomitic carbonates (Çayderesi  
237 Formation) (Fig. 4d) contain a relatively rich, well-dated Late Permian fauna and flora.  
238 Above a meta-bauxite, representing a hiatus, calc-schist and meta-carbonate alternations

239 (Alıçlı Formation) are dated as Early-Mid(?) Triassic (Özgül et al., 1981). Meta-carbonates,  
240 commonly dolomitic, of Mid-Triassic to Early Jurassic age, follow above this (Kayaköy  
241 Formation) (Figs. 5 log 2, 4e). The succession passes upwards into shelf carbonates, with  
242 common nodular chert of diagenetic replacement origin (Ulu Formation), dated as Mid-  
243 Jurassic and Early Cretaceous. There is then a prominent unconformity, followed by meta-  
244 siliceous limestone, meta-mudrock and meta-conglomerate, termed the Karaböğürtlen  
245 Formation (Bedi et al., 2005, 2009). This unit is named after a Late Cretaceous chaotic  
246 'blocky flysch' in the western Taurides (Denizli-Burdur area) (Özgül et al., 1981; Şenel et al.,  
247 1989).

248

#### 249 4.1. Late Cretaceous syn-tectonic sediments

250

251 The succession in the Malatya Metamorphics (Bodrum nappe) extends through the  
252 Cretaceous in the form of mainly siliceous meta-limestones, meta-mudrocks and  
253 subordinate meta-conglomerates (Bedi and Yusufoglu, 2018). Within Area 1 (east of Afşin),  
254 the meta-carbonates are mapped as locally ending in the Triassic (e.g. at Ballık Tepe), or in  
255 the Late Permian (e.g. at Abaz Tepe) (Fig. 5 section b) (Bedi et al., 2009). In several sections,  
256 the platform carbonate succession ends with an unconformity, marked by fissuring with red  
257 iron-oxide infills (Fig. 4f) and an iron-rich layer (up to several cm thick). An intact succession  
258 of mixed meta-carbonate and meta-siliciclastic rocks follows above this, with subordinate  
259 metadeposits (Figs. 4g-i; 5 log 3), representing the Karaböğürtlen Formation.  
260 Clasts and blocks of Jurassic-Cretaceous meta-neritic limestone are present, and also, rarely,  
261 clasts of metabasalt. The matrix includes abundant monocrystalline and polycrystalline  
262 quartz, muscovite, carbonate and, locally, basaltic detritus (Fig. 6a-c). A Late Cretaceous  
263 (Cenomanian age) is inferred, at least for the lower part of this formation, based on local  
264 occurrences of rudist bivalves (Fig. 4k). Similar metamorphosed rudists occur in the  
265 Menderes Massif (Özer, 1998).

266 Thick-bedded meta-debris-flow deposits (calcirudites) are well exposed in a key  
267 section, c. 16 km north of Afşin (3 km S of Tanır) (Fig. 2; also Supplementary Fig. 2), where  
268 they include abundant deformed and fragmented recrystallised rudist bivalves. The meta-  
269 limestones pass into a thin (1m) interval of green meta-chert, formed by diagenetic  
270 replacement of carbonate, followed by reddish-brown meta-conglomerate (several m thick),

271 with abundant rounded pebbles (<10 cm in size) of red radiolarian meta-chert and also  
272 meta-limestone (recrystallised), set in a sandy matrix. After further meta-limestone  
273 conglomerate, with rounded clasts (<10 cm in size), there is a return to thick-bedded detrital  
274 meta-carbonates before the section ends. This section is important as it indicates that  
275 relatively deep-water facies (radiolarian cherts) were redeposited onto the Malatya  
276 carbonate platform during the Late Cretaceous (see below).

277 In another key section, c. 20 km to the NW (near İncirli), where the Malatya  
278 Metamorphics (Bodrum nappe) are thrust northwards over the Southern allochthon (see  
279 below), the Karaböğürtlen Formation (up to 300 m thick) comprises lenses (up to >100 m  
280 long by 20 m thick) of medium-thick bedded meta-limestone (marble), alternating with  
281 sheared and folded meta-mudrock (phyllite.) Both the blocks and the matrix have  
282 undergone similar metamorphism. Near the thrust contact there are marble blocks (tens of  
283 cm-to m-sized) within sheared matrix-supported conglomerates (Fig. 4j). This section  
284 confirms that the Karaböğürtlen Formation includes meta-debris-flow ('olistostromes')  
285 related to Late Cretaceous tectonic instability.

286

#### 287 4.2. Interpretation of the Malatya Metamorphics

288

289 During Middle Devonian to Carboniferous, the Malatya Metamorphics (Bodrum nappe)  
290 accumulated on a mixed carbonate-clastic-depositing shelf, punctuated by tectonic  
291 instability, basaltic volcanism and localised mass-flow deposition. Marine transgression  
292 characterised the Late Permian, followed by rift-related tectonic instability and subsidence  
293 during the Early-Mid Triassic. A relatively stable, gently subsiding carbonate platform  
294 developed during the Late Triassic-Cretaceous, deepening during the Early Cretaceous, as  
295 suggested by increased chert content. The rudist reefs signify shallowing during the  
296 Cenomanian. The carbonate platform was uplifted and variably eroded, in places down to  
297 the Late Permian, resulting in a regional unconformity that was capped by metalliferous  
298 oxides during a hiatus in deposition. The unconformity was then covered by a Late  
299 Cretaceous (but poorly dated), mixed carbonate-siliciclastic succession, including local  
300 debris flow-deposits. The siliciclastic detritus, largely derived from metamorphic and  
301 plutonic igneous rocks, was probably recycled from the underlying Malatya succession. The  
302 well-rounded nature of many of the pebbles, especially meta-chert (Fig. 6a, b) is indicative

303 or reworking in a high-energy shallow-marine or fluvial setting prior to redeposition as  
304 debris flows. The pebbly conglomerates with red chert (near Tanır) show that deep-sea  
305 material, typical of the Southern allochthon to the north, was redeposited into the subsided  
306 Malatya platform.

307 The Late Cretaceous Karaböğürtlen Formation is interpreted as the proximal  
308 (southerly) part of a regional-scale, flexurally-controlled foredeep related to Late Cretaceous  
309 emplacement of continental margin and ophiolitic rocks. However, ophiolitic material is  
310 absent from the Karaböğürtlen Formation, in contrast to structurally higher units (see  
311 Discussion).

312 The timing of metamorphism of the Malatya Metamorphics is stratigraphically  
313 constrained as postdating the youngest deposition (Late Cretaceous (?) Karaböğürtlen  
314 Formation) but predating the Eocene sedimentary cover (Seske Formation) (Özgül et al.,  
315 1981; Perinçek and Kozlu, 1984; Kozlu et al., 1990; Robertson et al., 2006; Bedi et al., 2009).  
316 East of the Malatya-Ovacık Fault, the Keban metamorphics are locally dated radiometrically  
317 as  $73.8 \pm 0.3$  Ma (Campanian) (Rolland et al., 2012). In this area the metamorphics are  
318 unconformably overlain by latest Cretaceous sediments, known as the Gündüzbey  
319 Formation, which correlates with the regional Harami Formation (Erdoğan, 1975). The  
320 Gündüzbey Formation begins with polymictic conglomerates, followed by sandstone-shale-  
321 conglomerate alternations (generally Santonian-Campanian in age) and then shelf  
322 carbonates (Campanian-Maastrichtian) (Bedi and Yusufoglu, 2018). Along the eastern  
323 margin of the Malatya basin, the late Cretaceous sediments are unconformably overlain,  
324 directly, by Eocene conglomerates, limestones and turbidites (Yeşilyurt Formation) (Bedi et  
325 al., 2017; Bedi and Yusufoglu, 2018). The 88-82 Ma (Santonian-Campanian) Baskil Granitoids  
326 that cut the Malatya Metamorphics are inferred to have taken 6–10 Ma to cool below 300  
327 °C, based on  $^{39}\text{Ar}$ – $^{40}\text{Ar}$  dating of amphibole, biotite and K-feldspar (Karaoglan et al., 2016).

328 The Malatya metamorphics as a whole are intruded by the Baskil granites  
329 (unmetamorphosed). The long period of time (6-10 Ma) taken to cool below 300° suggests  
330 that the granites were intruded into crust with a high heat flow, presumably related to arc  
331 magmatism. The U-Pb age (88-83 Ma) of the granitoid intrusions is significantly older than  
332 the reported age of metamorphism ( $73.8 \pm 0.3$  Ma) (Rolland et al., 2012). However, the  
333 fluorite-bearing marble that was dated by these authors could represent a late-stage  
334 metasomatic event. The Malatya Metamorphics including the granite-bearing units were

335 tectonically imbricated after intrusion (e.g. E of Doğanşehir) (Bedi and Yusufoglu, 2018),  
336 probably during the Eocene.

337

## 338 **5. Late Triassic-Late Cretaceous unmetamorphosed platform carbonates**

339

### 340 5.1. Neritic thrust sheets

341

342 The mainly neritic Munzur thrust sheet (Fig. 2) is equivalent to the Munzur nappe of Özgül  
343 et al. (1981) and Bedi et al. (2004, 2009), to the Andırın Limestone of Perinçek and Kozlu  
344 (1984) and to the Neritic nappe of Robertson et al. (2013b). Similar successions are exposed  
345 in both the Northern allochthon and the Southern allochthon, respectively, to the north and  
346 the south of the Gürün autochthon (Fig. 2). South of the Gürün autochthon, in Area 2  
347 (Dağlıca), the Munzur thrust sheet comprises two main units; first, an extensive, relatively  
348 intact, lower Munzur thrust sheet, and secondly a thinner, internally disrupted upper  
349 Munzur thrust sheet (transitional to broken formation). The succession in the lower Munzur  
350 thrust sheet is widely exposed in Area 2 (Dağlıca) (Fig. 7 sections a-f), in Area 3A (E of  
351 Elbistan) (Fig. 8 sections a-e) and in Area 4 (S of Elbistan (Fig. 9). The Munzur thrust sheets  
352 are entirely Mesozoic, with no preserved Late Palaeozoic substratum, in contrast to the  
353 Malatya Metamorphics (Bodrum nappe). The complete Late Triassic to Late Cretaceous  
354 succession is exposed in the lower Munzur thrust sheet (Bedi et al., 2004, 2009; Bedi and  
355 Yusufoglu, 2018), whereas Cretaceous facies are commonly exposed in the more localised  
356 upper Munzur thrust sheet, mainly in Area 2 (Fig. 7) and Area 3A (Fig. 8). During this study,  
357 bioclastic limestones in the upper Munzur thrust sheet were dated as late Barremian-early  
358 Aptian (near Küçük Tatlar) (see Supplementary table 1). Higher stratigraphic levels are rich  
359 in Cenomanian rudist bivalves.

360 Taking the Munzur thrust sheets together, the succession begins with Norian thick-  
361 bedded neritic limestone, rich in calcareous algae (Fig. 10a) and Megalodonts, with local  
362 evidence of intraformational reworking and tectonic instability (Fig. 10b, c). Above an  
363 unconformity, the Early Jurassic begins with a conglomerate, overlain by pinkish nodular  
364 micritic limestone, up to 40 m thick, rich in crinoids, algae, ammonites and gastropods. The  
365 Middle Jurassic to Early Cretaceous interval is neritic, commonly oolitic and/or rich in  
366 benthic foraminifera. The neritic succession typically culminates in a Cenomanian interval

367 rich in rudist bivalves (Fig. 10d), as well-exposed in the upper Munzur thrust sheet in Area 2  
368 (Dağlıca) (Fig. 10e).

369 The neritic limestones are covered by Albian-Santonian pinkish pelagic carbonates,  
370 with sparse thin-bedded bioclastic calcarenites, known as the Kızılkandil Formation  
371 (equivalent to the Kırmızı Kandil Formation of Perinçek and Kozlu 1984) (Fig. 10 f). In places  
372 (e.g. Küçük tepe-Gerdekes yayla), rudist-bearing neritic limestones are reported to grade  
373 laterally and vertically into *Globotruncana*-bearing pelagic limestones (Bedi et al., 2009).  
374 The pelagic carbonates include thin (several cm) interbeds of fine to medium-grained,  
375 neritic-derived calciturbidites; locally (e.g. near Erikli) these include redeposited Late  
376 Jurassic-Early Cretaceous benthic foraminifera (see Supplementary Table 1). The succession  
377 ends with an unconformity, which is covered by a ferruginous oxide crust in some sections  
378 (Fig. 10g); this is overlain by latest Cretaceous syn-emplacement facies (Kemaliye Formation;  
379 see below).

380 In one area (e.g. E of Tavla), a small thrust sheet is dominated by limestone breccia-  
381 conglomerate (mass-flow accumulations) and calciturbidites (c. 150 m thick) (Fig. 10h). This  
382 unit is tentatively interpreted as proximal platform-slope facies.

383 For the Late Triassic, there is widespread evidence of tectonic instability related to  
384 regional rifting. The Jurassic-Cenomanian succession accumulated on the inner part of a  
385 gently subsiding carbonate platform (Yılmaz, 1994), mainly influenced by global sea-level  
386 change. The Albian-Santonian pelagic carbonates (Kızılkandil Formation) accumulated  
387 during a time of overall relatively high global sea level (Miller et al., 2005). However, the  
388 presence of interbedded bioclastic calciturbidites points to sub-aqueous erosion that was  
389 probably triggered by contemporaneous tectonic instability. There was then a hiatus (up to  
390 c. 8 Ma), allowing local precipitation of ferruginous oxide from seawater, before syn-  
391 emplacement facies (Kemaliye Formation) began to accumulate. The hiatus is likely to be  
392 coeval with the break in deposition that affected the adjacent Malatya Metamorphics, and  
393 is interpreted to represent the southward passage of an emplacement-related flexural bulge  
394 (see below).

395

396 5.2. Late Triassic-Late Cretaceous Neritic-pelagic (Köseyahya) thrust sheet

397

398 The traditional Munzur nappe (Perinçek and Kozlu, 1984) is made up of two separate  
399 regional-scale thrust units. The first comprises the Munzur thrust sheets, which are neritic  
400 throughout Late Triassic-Cenomanian, as summarised above. The second is the Köseyahya  
401 thrust sheet, as defined near Köseyahya, to the south of the Gürün autochthon (Bedi et al.,  
402 2005, 2009) (Fig. 8). A similar succession, termed the Neritic-pelagic nappe is exposed to  
403 the north of the Gürün autochthon (Robertson et al., 2013b). The successions in both areas  
404 can be correlated and are here referred to as the Neritic-pelagic (Köseyahya) thrust sheet.

405 The most complete succession (Fig. 3) through the Neritic-pelagic (Köseyahya) thrust  
406 sheet is exposed in the type area, near Köseyahya (Area 3A, near log III) (Fig. 8 sections a, e,  
407 f) (Bedi et al., 2009), with an additional outcrop in Area 4, south of Elbistan (Fig. 9 sections a,  
408 b) and Area 4B, Nurhak Dağı). The type section is located 750 m south of Köseyahya (near  
409 Burmakaya Tepe) (Tekin and Bedi, 2007a, b; Dumitrica et al., 2013). There, the succession  
410 begins in the Middle Carnian, as dated by radiolarians, with alternations of fine-grained  
411 sandstone, calcareous siltstone, marl, mudstone and micritic limestones. Volcaniclastic  
412 interbeds and chert of diagenetic replacement origin are also present, mainly in the higher  
413 levels. The succession continues with Late Carnian pink to red calcilutites (4.6 m thick), rich  
414 in ammonoids, crinoids, conodonts and pelagic bivalves (*Halobia* sp.) ('Hallstatt limestone')  
415 (Fig. 10i, j) (Bedi et al., 2016). Medium to thick-bedded Norian white limestones above  
416 ('Dachstein limestones') (Fig. 10k) include abundant Megalodonts and benthic foraminifera  
417 (Tekin and Bedi, 2007a, b). Above a discontinuity, the Early Jurassic is made up of relatively  
418 thin, stratigraphically condensed (c. 20 m), nodular, ammonite-rich micritic limestone  
419 ('Ammonitico Rosso'). The Mid-Late Jurassic is dominated by redeposited limestones  
420 (calciturbidites), with pelagic carbonate interbeds that are commonly silicified. The  
421 redeposited limestones are rich in neritic grains, especially ooids and are extensively  
422 silicified. Radiolarian chert increases in abundance during the Tithonian-Cenomanian  
423 interval. The Early Cretaceous (Tithonian-Berriasian) is dated using calpionellids within  
424 pelagic interbeds (Area 3A, E of Elbistan) (Fig. 10l) (see Supplementary table 1).

425 The upper part of the succession (Özbey Formation), where exposed, is  
426 positionally overlain by pinkish pelagic carbonates with radiolarian chert intercalations.  
427 The pinkish pelagic carbonates are similar to those of the Munzur thrust sheets (see above)  
428 and have been given the same name (Kızılkandil Formation), although only those in the  
429 Neritic-pelagic (Köseyahya) thrust sheet are siliceous. The type section (near Kızılkandil



430 mezası), c. 40-50 m thick, depositionally overlies a layer of redeposited oolitic limestone  
431 (Özbey Formation). In a nearby succession, the Kızılkandil Formation unconformably overlies  
432 older neritic facies (Demirlitepe Formation), and includes both planktic foraminifera of  
433 Turonian-Santonian age and also radiolarians of Turonian-Santonian age. Another section,  
434 which is faulted against Late Triassic neritic facies (Ortakandil Tepe), contains Turonian  
435 planktic foraminifera and radiolarians; a further section (Han tepe-Toklu tepe) contains  
436 Turonian-Santonian radiolarians (Bedi et al., 2009).

437         The Kızılkandil Formation has been variously dated as Turonian-early Campanian  
438 (Perinçek and Kozlu, 1984), Coniacian-Campanian (Pehlivan et al., 1991), or Albian-  
439 Santonian, using a combination of nannofossils, radiolarians and planktic foraminifera (Bedi  
440 et al., 2009). The shortest-ranging planktic foraminifera, determined by Dr. A. Hakyemez,  
441 are *Rotalipora ticinensis*, *Rotalipora apenninica* (upper Albian), *Helvetoglobotruncana*  
442 *helvetica* (lower-middle Turonian) and *Dicarinella asymetrica* (Santonian) (Robaszynski and  
443 Caron, 1995). Radiolaria range from Albian-Santonian (Bedi et al., 2009). The pelagic  
444 limestones are unconformably overlain by the syn-emplacement Kemaliye Formation (see  
445 below).

446         The succession in the Neritic-pelagic (Köseyahya) thrust sheet began to accumulate  
447 during the Carnian on a submerged shelf, in the form of stratigraphically condensed,  
448 hemipelagic limestones and siliceous sediments, which are variably rich in ammonites,  
449 crinoids, foraminifera, calcareous algae and radiolarians. Condensed ammonite-rich, red  
450 pelagic carbonate deposition persisted during the Early Jurassic. During the Late Jurassic,  
451 the carbonate platform developed into a gently sloping carbonate ramp on which  
452 redeposited ooid-rich facies accumulated. The probable source was the adjacent shallow-  
453 water Munzur carbonate platform. The greatly increased abundance of chert in the  
454 Tithonian-Albian interval points to further deepening. This probably resulted from tectonic  
455 subsidence because global sea-level rise is not inferred during this time interval (Haq, 2014).  
456 Where the pelagic limestones (Kızılkandil Formation) overlie older parts of the succession  
457 (Demirlitepe Formation), tectonically induced uplift and submarine erosion are inferred. The  
458 pelagic carbonates accumulated during the mid-Late Cretaceous (Albian-Santonian), as in  
459 the Munzur thrust-sheet succession. The sea floor was already deep, favouring continuing  
460 radiolarian deposition. The appearance of pelagic carbonate probably represents increased  
461 planktic productivity (Bosellini and Winterer, 1975).

462 The Late Cretaceous pelagic carbonates in both the Munzur and Köseyahya  
463 successions are similar to those overlying the Tauride carbonate platform elsewhere,  
464 including the Bey Dağları (Poisson, 1977, 1984) and the Geyik Dağ (Sarı and Özer, 2002; Sarı  
465 et al., 2004). In the Geyik Dağ (central Taurides), Cenomanian rudist-rich facies are overlain  
466 by pelagic carbonates that accumulated until the Eocene (Solak et al., 2017, 2019), similar to  
467 the Gürün autochthon (Fig. 2).

468

## 469 **6. Late Permian-Late Cretaceous Pelagic (Gülbahar) unit**

470

471 Widely distributed, dismembered Late Permian to Late Cretaceous deep-water successions,  
472 including both pelagic and coarser-grained redeposited facies, and also basaltic rocks were  
473 previously included within the Dağlıca Complex ('flysch with blocks'), together with  
474 dismembered ophiolitic rocks (Kozlu et al., 1990; Perinçek and Kozlu, 1984). However, more  
475 recent mapping and stratigraphical studies indicate the presence of an originally intact  
476 Triassic to Late Cretaceous deep-water platform-margin succession. This has been named  
477 the Gülbahar Nappe (Bedi et al., 2009, 2018), based on a proposed correlation with  
478 comparable deep-sea successions including basaltic volcanics in the western Taurides (Şenel  
479 et al., 1989; Collins and Robertson, 1998; Sayit et al., 2015). The deep-sea platform-margin  
480 succession in the Eastern Taurides has also been termed, informally, as the Pelagic nappe, in  
481 contrast to the traditional Munzur thrust-sheet neritic succession (Robertson et al., 2013b).

482 No complete succession of the Pelagic (Gülbahar) unit is known in any one section,  
483 although an overall stratigraphy can be pieced together (Fig. 3). Local sections show  
484 considerable facies variation and may represent combinations of lateral variation and/or  
485 proximal-distal changes. The most intact sequences are mainly located to the south of the  
486 Gürün autochthon in Area 2 (e.g. Büyük Tatlı), whereas, within the Northern allochthon, the  
487 Pelagic unit is mainly represented by blocks of Mesozoic deep-water facies within melange  
488 (Robertson et al., 2013b).

489 During the present study, local sequences of the Pelagic (Gülbahar) unit were  
490 studied in Areas 2-4 (Figs. 7-9). Relatively intact and continuous sequences (up to c. 80 m  
491 thick) are exposed between the lower and the upper Munzur thrust sheets in Area 2  
492 (Dağlıca) (Fig. 7; e.g. near Tatlar, specifically Büyük Tatlı), although these are too small and  
493 localised to show effectively on regional-scale maps. Up to tens of m-thick sequences are

494 widely exposed beneath the Köseyahya thrust sheets in Area 3A (E of Elbistan) (Fig. 8), and  
495 also occur beneath both the Munzur and Köseyahya thrust sheets in Area 4 (south of  
496 Elbistan) (Fig. 9). In addition, variable-sized, isolated blocks of similar lithologies are strewn  
497 through the late Cretaceous syn-tectonic Kemaliye Formation, as exposed in each of the  
498 above areas (see below).

499         The oldest known lithologies in the Pelagic (Gülbahar) unit are Late Permian  
500 siltstones, marls, siliceous limestones and thin-bedded limestones, including fusulinids and  
501 benthic foraminifera (Bedi et al., 2009) (Fig. 11, logs II, III; see Fig. 8 for locations). There are  
502 also short, highly deformed intervals of Triassic sandstone and shale (Fig. 12a, b). Jurassic-  
503 Cretaceous facies are mainly non-calcareous radiolarites and radiolarian mudstones,  
504 interbedded with pelagic carbonates (Fig. 12c), variably silicified calciturbidites (Fig. 12 d, e)  
505 and carbonate debris flow-deposits, variably rich in chert clasts (Fig. 12 f-i). The redeposited  
506 limestones are rich in redeposited ooids, oolitic limestone, pisoliths, benthic foraminifera  
507 (with oolitic coatings) and calcareous algae. Reworked pelagic limestone, radiolarian chert,  
508 monocrystalline quartz and muscovite are also present.

509         Variably preserved radiolarians, identified during this study (see Table 1), yielded the  
510 following Late Triassic to Late Cretaceous ages for local sections or blocks: Late Norian  
511 (block in serpentinite, near Yoksullu mezra (Area 4; Fig. 11, log I); Middle Jurassic (Bajocian),  
512 near Büyük Tatlı (Area 2) and near Yoksullu mezra; Late Oxfordian near Yoksullu mezra; Late  
513 Oxfordian-Tithonian near Kayseri (Area 2, log VII) and near Topaktaş (Area 2, log VIII);  
514 Kimmeridgian-early Tithonian near Büyük Tatlı and near Yoksullu mezra; Late Tithonian-  
515 Berriasian near Büyük Tatlı); Late Valanginian-Hauterivian (block in debris-flow deposit) near  
516 Kabaktepe; Early Albian at Kırandere (near İncelik köy; Area 2); Aptian at Kırandere; and Late  
517 Albian-Cenomanian also at Kırandere. In addition, redeposited benthic foraminifera are  
518 dated more generally as Late Jurassic-Early Cretaceous (at Kaşanlı, Küçük Tatlı and Büyük  
519 Tatlı, all in Area 2 (see Supplementary Table 1).

520         An overall deep-marine, lower slope to base of-slope setting is inferred for the  
521 Pelagic (Gülbahar) unit. Late Permian pelagic carbonates with relatively fine-grained  
522 siliciclastic turbidites were followed by Early to Middle Triassic hemipelagic mudrocks, fine-  
523 grained sandstone turbidites and thin-bedded hemipelagic carbonates. Middle to Late  
524 Triassic hemipelagic limestones (Halobia limestones), radiolarian sediments, calciturbidites,  
525 quartzose sandstone/siltstone turbidites and, locally redeposited conglomerates, followed

526 above this. The Jurassic-Early Cretaceous encompassed non-calcareous radiolarian muds,  
527 variably silicified calciturbidites and also debris-flow deposits with reworked neritic clasts  
528 (e.g. oolitic limestone) and/or pelagic clasts (radiolarite; pelagic limestone). Deposition  
529 locally culminated in large-scale gravity collapse of slope facies, leading to redeposition,  
530 with clasts of neritic/pelagic limestone and radiolarite in a matrix of lithoclastic debris-flow  
531 deposits, sandstone turbidites, ophiolite-derived debris-flow deposits, calciturbidites and  
532 muds. The ophiolite-bearing mass-flow units represent a depositional-tectonic link between  
533 the passive margin slope lithologies and the emplacement-related mass-flow units which  
534 are located higher in the tectono-stratigraphy (see below).

535 In places (e.g. Dağlıca, Area 2), short, highly deformed sequences of basalt,  
536 volcanoclastic sandstone and/or hyaloclastite are interbedded with Middle-Late Triassic  
537 deep-water calcareous and siliceous facies (Kozlu et al., 1990; Bedi et al., 2009; Robertson et  
538 al., 2013b). Chemically, the basalts are of enriched, alkaline, within-plate type (Robertson et  
539 al., 2013b). A sample of radiolarian chert from Area 2 (Bakış) gave a Norian (Late Triassic)  
540 age (Fig. 11 log II; see Table 1). In addition, in Area 5A (Kemaliye) (Fig. 2) basaltic lavas of the  
541 Pelagic (Gülbahar) unit are interbedded with Late Triassic pelagic limestones (dated) and  
542 radiolarian cherts (see Supplementary Table 1).

543 The Pelagic (Gülbahar) unit accumulated adjacent to the Munzur and Köseyahya  
544 thrust sheet successions, taken together. The Permian siliciclastic material is likely to have  
545 been derived from an original, but now tectonically detached, substratum of the carbonate  
546 platform units. The Triassic records subsidence, localised alkaline basaltic volcanism (rift-  
547 related), terrigenous sand/silt gravity input, hemipelagic carbonate deposition (periplatform  
548 ooze) and radiolarian accumulation in a fertile sea. The Jurassic-Cretaceous was  
549 characterised by 'background' radiolarian and siliceous pelagic carbonate deposition  
550 (diagenetically altered to chert), beneath (or near) the carbonate compensation depth  
551 (CCD). The calciturbidites and carbonate debris-flow deposits accumulated on an unstable  
552 slope, derived from the adjacent carbonate platform. The Late Cretaceous is characterised  
553 by pelagic limestone, marl and chert that accumulated above the CCD, with *Globotrunca* sp.,  
554 as in the adjacent carbonate platform units (equivalent to the Kızılkandil Formation). The  
555 presence of ophiolite-derived debris-flows within a sequence affected by slumping and soft-  
556 sediment deposition suggests that the distal platform slope over-steepened and collapsed  
557 related to ophiolite emplacement.

558

## 559 **7. Late Cretaceous emplacement-related Kemaliye Formation**

560

561 In different areas, the Malatya Metamorphics and both the Munzur and Köseyahya platform  
562 units are positionally overlain by Late Cretaceous syn-tectonic lithologies that provide key  
563 information concerning the nature and timing of both tectonic emplacement and  
564 exhumation in the region. In general, the lithologies form coherent to highly disrupted  
565 successions, which are characterised by matrix-supported conglomerates, blocks, or  
566 dismembered thrust sheets, all set within an argillaceous and/or sandy matrix. The syn-  
567 tectonic units occur at two different structural levels in the regional thrust stack. The  
568 higher-level unit overlies the Munzur/Köseyahya platform units, whereas the lower-level  
569 unit overlies the Malatya (Keban) metamorphics.

570 In the northeast of the region studied, near Kemaliye (Figs. 13, 14 Area 5A), meta-  
571 carbonate rocks (Kaletepesi limestone) that are correlated with the lower part of the Keban  
572 metamorphics (Bilgiç, 2008b, c) are mapped as being unconformably overlain by  
573 'olistostromes', named the Kemaliye Formation, after the town in this area (Figs. 13, 14)  
574 (Özgül et al., 1981; Özgül and Turşucu, 1984; Perinçek and Kozlu, 1984; Bilgiç, 2008b, c). The  
575 formation has been inferred to be Late Senonian (Özgül et al., 1981), or more specifically  
576 Late Campanian-Early Maastrichtian (Bilgiç, 2008b, c), based on the youngest datable  
577 fossiliferous material (i.e. *Globotruncana*-bearing pelagic limestone). In general, the  
578 succession has been described as beginning with localised conglomerates, with clasts of  
579 dark grey limestone, chert and diabase, passing into sandstone, with common basic igneous  
580 rock and limestone grains, and also interbeds of sandstone and marl (Perinçek and Kozlu,  
581 1984). In its type area, the Kemaliye Formation is locally overlain, unconformably, by Early  
582 Eocene lithologies (Subaşı formation) (Bilgiç, 2008b, c). The Kemaliye Formation appears to  
583 correlate with the latest Cretaceous Gündüzbey Formation, to the south of Malatya.

584 The term, Kemaliye Formation was later adopted for all of the Late Cretaceous  
585 unmetamorphosed syn-tectonic facies in the region, including those associated with the  
586 allochthonous Munzur and Köseyahya successions (Bedi and Yusufoglu, 2018). However,  
587 this is problematic for several reasons: (1) The underlying units differ strongly in different  
588 areas (i.e. Malatya (Keban) Metamorphics in the type area, versus Munzur-Köseyahya  
589 unmetamorphosed carbonate platform elsewhere); (2) The Kemaliye Formation in its type

590 area includes lithologies (e.g. basalt-pelagic limestone-radiolarite) that are assigned to the  
591 Pelagic (Gülbahar) unit elsewhere (i.e. it is a composite unit); (3) The Kemaliye Formation, as  
592 previously mapped, is, in part, tectonically assembled rather than an intact sedimentary  
593 succession.

594         Although we retain the general name, Kemaliye Formation here for consistency with  
595 previous work, the occurrences in three different tectono-stratigraphic settings are  
596 discussed separately below. These are: (1) Unconformably overlying the Malatya (Keban)  
597 Metamorphics in Area 5A (Kemaliye) (Figs. 15a, 16a); (2) Unconformably overlying the  
598 Munzur and/or the Köseyahya thrust sheets, and also underlying the Munzur and Köseyahya  
599 thrust sheets where no basement is exposed. Consideration of these two main contrasting  
600 settings allows a more refined interpretation in terms of syn- versus post-emplacement  
601 tectonics.

602

#### 603 7.1. Late Cretaceous Kemaliye Formation overlying the Malatya (Keban) Metamorphics

604

605 An unconformity is mapped between the Kemaliye Formation and the Malatya (Keban)  
606 Metamorphics west of Keban Lake (Bilgiç, 2008b, c) (Fig. 14). The meta-carbonate rocks  
607 near the contact are in places converted to calc-mylonite, indicating high-strain conditions  
608 (Fig. 16b). In some areas, the lower part of the formation is dominated by crudely bedded  
609 debris-flow conglomerates (Fig. 15a; 16c), as logged locally (Fig. 17). These contain  
610 abundant clasts of metamorphic rocks (Fig. 16d), together with radiolarian chert (Fig. 16e),  
611 deformed limestone (Fig. 16f), granite (locally), coral and large bivalves (rudists). Above this,  
612 much of the outcrop is dominated by blocks and dismembered thrust sheets (Fig. 16a).  
613 Many of the blocks are well-bedded, commonly dark, organic-rich limestones (typically 10s  
614 of m in size). Short, intact sequences of well-bedded limestones are intercalated with  
615 limestone conglomerates (calcirudites) that locally include well-rounded clasts and rudist  
616 debris of probable Cenomanian age. Neritic limestones of Triassic-Cretaceous age, chert  
617 (undated) and Late Cretaceous pelagic limestones are also present. A neritic limestone block  
618 (near Yuva; Fig. 14) is dated as Triassic based on benthic foraminifera (Fig. 18a, b; see also  
619 Supplementary Table 1). In one area, slices and/or large blocks of basaltic lava are exposed  
620 above the contact with the metamorphics (Fig. 15b). The lavas are interbedded with pelagic  
621 limestones that contain a typical Triassic fauna, including *Halobia* sp. and radiolarians (see

622 Supplementary Table 1). Although mapped as Kemaliye Formation (Bilgiç, 2008b, c) this  
623 volcanogenic unit belongs to the Pelagic (Gülbahar) unit (see above).

624 The matrix of the Kemaliye Formation in the type area is extremely heterogeneous,  
625 including variable abundances of monocrystalline quartz, polycrystalline quartz, plagioclase  
626 (altered), muscovite, biotite, epidote, clinopyroxene, hornblende, chlorite (including blue  
627 chlorite), zircon, apatite and opaque grains, in generally decreasing order of abundance.  
628 Lithoclasts are mainly micaschist, quartzite, chert, neritic limestone, basalt (with orientated  
629 microphenocrysts), altered basic volcanic glass (palagonite), felsic volcanics (recrystallised),  
630 dacite (with plagioclase phenocrysts), granite, bioclastic carbonate, marble, dolomite,  
631 sandstone (with parallel-orientated muscovite laths), siltstone (locally iron-rich), shale  
632 (partly recrystallised), serpentinite, gabbro, diabase, phyllite, phyllonite and mylonite (Fig.  
633 6d-g). Bioclasts include micritic grains with shell fragments, pellets, benthic foraminifera,  
634 algal grains (pisoliths) and/or oolitic limestone (with clear, plutonic quartz cores). The matrix  
635 is either calcareous (partly recrystallised), or siliciclastic (with fine quartz and muscovite).  
636 Most grains are angular although a few are well-rounded. Some samples have a calcite spar  
637 cement.

638 In the northeast, where the Kemaliye Formation is mainly covered by younger  
639 volcanics (Fig. 14; NE of Yaka), small exposures of debris-flow deposits include clasts and  
640 blocks of altered lava, serpentinite and platy grey-pink Triassic pelagic limestone (see  
641 Supplementary Table 1). Farther northeast again, towards Ovacık (Fig. 13), the formation  
642 includes a large (c. 5 km-long) tabular body of Permian limestone that is tectonically  
643 overlain by serpentinised ultramafic rocks (Bilgiç, 2008b, c; MTA, 2011).

644

## 645 7.2. Kemaliye Formation associated with the Munzur and Köseyahya thrust sheets

646

647 Previous authors reported that the Munzur limestones, including the Late Cretaceous  
648 pelagic limestones (Kızılkandil Formation), pass unconformably upwards into syn-tectonic  
649 calcareous siltstones and sandstones, followed by an incoming of limestone blocks. This unit  
650 was termed the Binboğa Formation by Perincek and Kozlu (1984), named after the Binboğa  
651 Mountains 20 km west of Afşin. However, the term Binboğa Formation was later applied to  
652 the entire Early Triassic-Early Cretaceous succession of the Munzur thrust sheet (Kozlu et al.,  
653 1990), complicating the use of this name. The latest Cretaceous syn-tectonic interval was

654 later correlated with the Kemaliye Formation (Bedi et al., 2009; Robertson et al., 2013b;  
655 Bedi and Yusufoglu, 2018), although, as noted above, this unit differs strongly from the type  
656 Kemaliye area.

657 Planktic foraminifera from the Kemaliye Formation above the Munzur limestones  
658 (Bedi et al., 2009) are long-ranging throughout Campanian-Maastrichtian. The shortest-  
659 ranged taxon is *Globotruncana dupeublei*, whose first occurrence (base) is within the  
660 *Gansserina gansseri* Zone (71.75-72.97 Ma; late Campanian-early Maastrichtian), whereas  
661 the last occurrence (top) is within the *Abatomphalus mayaroensis* Zone (67.30-69.18Ma; top  
662 of Maastrichtian stage) ([microtax.org/pforams/index.php](http://microtax.org/pforams/index.php)). In addition, nannoplankton data  
663 support a late Campanian-late Maastrichtian age for the Kemaliye Formation within the  
664 Munzur and Köseyahya thrust sheets (Bedi et al., 2009).

665 During this study, six sections of the Kemaliye Formation within the main Munzur  
666 thrust sheet were logged in Area 2 (Dağlıca), where they show considerable facies variation  
667 (Fig. 19 logs 1-6). The formation is typically dominated by alternations of calcareous  
668 mudstone-siltstone-sandstone (Fig. 19 logs 1, 2, 4). In places, sandstone, limestone  
669 conglomerates (calcirudites) and limestone breccias appear near the base of the succession  
670 (Fig. 19; logs 3, 5, 6; Fig. 20a, b). During this study, intervals of pinkish pelagic limestone  
671 were dated as Campanian-Maastrichtian (near Kapaklı; see Supplementary Table 1). Benthic  
672 foraminifera within a limestone block, near Kaşanlı, yielded an Early Cretaceous age  
673 (Supplementary Table 1). Other blocks are rich in rudist bivalves (Fig. 20c, d).

674 The upper levels of the succession are commonly tectonically disrupted and include  
675 neritic and pelagic limestone blocks (Fig. 19 log 6; Fig. 20d, e). Clasts of bioclastic calcarenite  
676 yielded reworked Middle-Late Jurassic benthic foraminifera (see Supplementary Table 1). In  
677 places, the outcrop is chaotic with limestone blocks strewn through a sheared mudstone-  
678 sandstone matrix.

679 The sandstone interbeds are heterogeneous and include both monocrystalline and  
680 polycrystalline quartz, muscovite, neritic carbonate, chert, quartzose siltstone and basalt  
681 (Fig. 6h-i). The calcarenites comprise variable mixtures of platform-derived material (e.g.  
682 pisoliths, shells, echinoderm debris, ooids), chert (microcrystalline quartz), altered basalt,  
683 vesicular volcanic glass (with plagioclase microphenocrysts), serpentinite, microgabbro and  
684 dolerite, together with rare monocrystalline quartz, siltstone (terrigenous), phyllite,



685 plagiogranite, amphibolite, muscovite, altered plagioclase and pyroxene. Many grains are  
686 well-rounded. Planktic foraminifera (e.g. *Globotrunca* sp.) occur rarely.

687         Comparable sequences of the Kemaliye Formation are also exposed unconformably  
688 overlying the Late Cretaceous pelagic carbonates of the Köseyahya platform/proximal slope  
689 succession (Kızılkandil Fm.), as well exposed in Area 3A (E of Elbistan) and Area 4 (S of  
690 Elbistan). The succession in Area 3A encompasses interbedded mudstones, siltstones,  
691 sandstones and clasts of limestone (Triassic-Cretaceous), chert and serpentinite (Fig. 6j).  
692 Overlying debris-flow deposits ('blocky flysch') include clasts and blocks that can be  
693 correlated with the platform succession beneath, including micritic, oolitic and pisolitic  
694 limestone, and also pelagic limestones (Kızılkandil Formation). Other lithologies can be  
695 correlated with the over-riding Pelagic (Gülbahar) unit (e.g. radiolarite and volcanic  
696 material). Blocks of pink, chert-bearing pelagic limestone in Area 3A, east of Elbistan (near  
697 Odunluk Tepe and Yumru Tepe) are dated as Campanian-Maastrichtian based on planktic  
698 foraminifera (see Supplementary Table 1). A chalky debris flow-deposit farther northeast  
699 (near Dağdam) includes Late Cretaceous planktic foraminifera (see Supplementary Table 1).  
700 Facies equivalents of the Kemaliye Formation are also well exposed south of Elbistan (Area  
701 4), beneath the Köseyahya thrust sheet and/or the Munzur thrust sheet, with no exposed  
702 stratigraphic base (Fig. 8). In the southern part of Area 4, pelagic limestone blocks contain  
703 Campanian-Maastrichtian planktic foraminifera, as in the Kemaliye Formation generally (Fig.  
704 21a-d). However, a sample from the same local outcrop contains Globigerinidae (Fig. 21e, f),  
705 and also Rotaliidae, indicating a post-Cretaceous (Cenozoic) age, and thus that the Kemaliye  
706 Formation underwent post-depositional reworking in this area (see below).

707         The Kemaliye Formation is also exposed farther east, as a narrow c. NE-SW-trending  
708 strip in Area 3B, Nurhak Dağı which exhibits some critical additional field relationships (Figs.  
709 2, 16g, 22a, b). The uppermost exposed levels of the Malatya Metamorphics there are  
710 represented by well-bedded calc-schists, in places transformed to calc-mylonite (Fig. 16h),  
711 or are isoclinally folded (Fig. 16i). Above a low-angle tectonic contact, meta-carbonate rocks  
712 are overlain by meta-serpentinite (Fig. 22a, b). Both the calc-schist and the meta-  
713 serpentinite are cut by small granitic intrusions (Figs. 22a). The Malatya Metamorphics were  
714 isoclinally folded prior to intrusion (Fig. 16j). The contact between the meta-serpentinite  
715 and the granitic intrusion is brecciated indicating subsequent brittle deformation (Fig. 16k).  
716 Although not dated specifically, these intrusions are likely to form part of the Eocene

717 Doğanşehir granitoids (MTA, 2011; Kuşcu et al., 2013; Karaoğlu et al., 2012, 2016; Bedi and  
718 Yusufoglu, 2018). The serpentinite is overlain, with a low-angle thrust contact, by a thin  
719 facies equivalent of the Kemaliye Formation that includes blocks of Triassic red crinoidal  
720 limestone, similar to the Köseyahya platform/slope succession (see above), and also blocks  
721 of limestone and limestone breccia set in a sandy matrix (Fig. 22b). Further south (near  
722 Beğre), the serpentinite is overthrust by a thin slice of neritic limestone and limestone  
723 debris-flow deposits with rudist debris, of probable Cenomanian age, capped by Fe-oxide  
724 (Figs. 16l; 22a; see also Supplementary Fig. 3). This unit is interpreted as a small thrust slice  
725 of the contact between the Köseyahya platform/slope succession and the overlying  
726 Kemaliye Formation.

727 In thin section, some of the matrix sandstones of the Kemaliye Formation in Area 3B  
728 (Nurhak Dağı) have a well-developed shear fabric, in which large quartz grains are fractured  
729 and veined, with a calcite spar infill at right angles to the shear fabric. Foliated muscovite is  
730 present along shear bands indicating partial recrystallisation. Two phases of deformation  
731 are indicated by the presence of extensional calcite veins orientated at right angles to each  
732 other. *En echelon* cracks are interpreted as riedel shears.

733

### 734 7.3. Interpretation of the syn-tectonic Kemaliye Formation

735

736 The type area of the Kemaliye Formation (near Kemaliye; Area 5A) is a composite unit,  
737 dominated by gravity-controlled deposition, mainly by mass-flow processes. The rudist  
738 bivalves and *Globotruncana*-bearing limestones within slices and blocks indicate a Late  
739 Cretaceous age, although the matrix remains poorly dated. The lower part of the succession  
740 includes debris-flow conglomerates ('olistostromes'), sandstones, shales and exotic blocks  
741 that covered the Malatya metamorphic rocks. The metamorphic and local granitic detritus  
742 were derived from the subjacent Malatya (or Keban) Metamorphics, confirming that they  
743 were exhumed prior to deposition (see Discussion). However, the dominant sources of the  
744 exotic material were the over-riding Munzur thrust sheet, the Pelagic (Gülbahar) unit, and  
745 ophiolitic rocks (e.g. serpentinite). The limestone conglomerates with well-rounded clasts  
746 and rudist debris were sourced from the Munzur platform. The Triassic basalts with Halobia-  
747 limestone and radiolarite are correlated with the Pelagic (Gülbahar) lower slope/basinal

748 unit, as noted above. Ophiolitic rocks are exposed to the northeast of the Kemaliye  
749 Formation type area.

750 The Late Cretaceous pelagic carbonate deposition (Kızılkandil Formation) of both the  
751 Munzur and Köseyahya thrust sheets ended with a hiatus (early Campanian (?); c. 83-78  
752 Ma), commonly marked by iron-oxide accumulation. The likely cause of the hiatus, similar to  
753 that in the Malatya metamorphic succession, was flexural uplift related to the regional  
754 ophiolite emplacement. The hiatus was followed by mixed siliciclastic-carbonate  
755 redeposition during late Campanian-Maastrichtian, forming the Kemaliye Formation. Talus,  
756 ranging from sand-sized, to blocks (up to many-metre-sized), were shed into the basin,  
757 largely derived from the upper levels of the adjacent Mesozoic carbonate platform and/or  
758 slope units (e.g. Cenomanian rudist limestone). The likely cause of basin formation was  
759 regional-scale downflexure ahead of the advancing thrust load, which was dominantly  
760 ophiolitic. The presence of Triassic-Cretaceous clasts suggests that, in places, all levels of the  
761 stratigraphy were exposed and eroded. This, in turn, suggests that platform and slope units  
762 were imbricated and uplifted, eroded, and then collapsed as debris into the flexural  
763 foredeep. Permian limestone is inferred to have existed beneath the Mesozoic platform  
764 and/or slope units, as supported by the presence of the large (km-sized) body of Permian  
765 limestone, as associated with the Kemaliye Formation in the northeast of the type area  
766 (Area 5A; Fig. 13). In addition, the pelagic lithologies (e.g. radiolarian chert, siliceous pelagic  
767 limestone) and also alkaline within plate-type basalt were derived from the Pelagic  
768 (Gülbahar) unit. Ophiolitic material is also variably present in the form of basalt, diabase,  
769 gabbro and/or serpentinite, sourced from the over-riding ophiolitic units. The succession  
770 accumulated in relatively deep water (100s m), as suggested by intercalations of pelagic  
771 carbonate containing Campanian-Maastrichtian planktic foraminifera.

772 Slices of the Munzur limestone were emplaced over the Kemaliye Formation in places,  
773 complicating the local tectono-stratigraphy. For example, in Area 3B (Nurhak Dağı), a slice of  
774 the highest levels of the neritic Munzur platform, complete with its iron-oxide coating (see  
775 above), was imbricated beneath the over-riding Köseyahya thrust sheet. Since the Mesozoic  
776 limestones (Munzur and Köseyahya) now structurally overlie the Kemaliye Formation it can  
777 be inferred that the Malatya-Keban metamorphics were exhumed, eroded to form clastic  
778 material (Kemaliye Formation), and later over-riden by the regional limestone thrust sheet  
779 in this area.

780 The Kemaliye Formation above the Munzur and Köseyahya platform/slope  
781 successions is comparable with the widespread late Cretaceous syn-tectonic Yavça  
782 Formation (and facies equivalents) that intervene between platform carbonates, below and  
783 ophiolitic rock, above throughout the Taurides, for example in the Aladağ Unit  
784 (Maastrichtian Zekeriya Formation) and in the Bolkar Dağ Unit (late Campanian-  
785 Maastrichtian Söğüt Formation). These units unconformably overlie units of different age  
786 and facies in different areas and are generally interpreted as olistostromes or sedimentary  
787 melanges related to regional ophiolite emplacement (Özgül, 1997; Andrew and Robertson,  
788 2002; Parlak and Robertson, 2004; Mackintosh and Robertson, 2012; Bedi and Yusufoglu,  
789 2018). In summary, the Kemaliye Formation in its type area (Area 5A) is a composite unit  
790 which formed above the Malatya (Keban) metamorphics during or after their exhumation.  
791 In contrast, the Kemaliye Formation as mapped regionally above the Tauride platform units  
792 is an intact succession, interpreted as a foredeep related to ophiolite obduction.

793

794

## 795 **8. Volcanic-sedimentary melange**

796

797 Definitions: Melanges comprise disorganised blocks of single, or multiple lithologies, with or  
798 without a matrix, and may be either sedimentary or tectonic origin, or both (see Raymond,  
799 1984). Volcanic-sedimentary melange is a variety of melange in which the blocks are mainly  
800 made up of volcanic and sedimentary rocks, unrelated to ophiolites. Volcanic-sedimentary  
801 melange can shed light on both oceanic and emplacement processes.

802 Volcanic-sedimentary melange is well represented in the northeast of the region  
803 studied (Hekimhan area) (Fig. 2), where it is made up of short (10s of m), dismembered  
804 sequences of basalt, pelagic limestone and radiolarite (e.g. Yeşildere Melange). A local  
805 section comprises pillow basalt (80 m) with intercalations of ribbon radiolarite (c. 20 m),  
806 then alternations of radiolarite and pelagic limestone, followed by siliceous pelagic  
807 limestone (9 m). Radiolarite from the upper part of this interval was dated as Late Albian-  
808 Early Cenomanian (see Table 1). In the Dağlıca area (Area 2), short sections of basaltic lavas  
809 (<10s m) are interbedded with, and overlain by Middle Oxfordian-Early Tithonian radiolarian  
810 sediments (Robertson et al., 2013b). Geochemical data for the basalts from both areas  
811 indicate mid-ocean-ridge, to enriched intra-plate settings, although some samples have a

812 subduction-related influence (Robertson et al., 2013b; Robertson et al., in press a). A similar  
813 range of basaltic compositions has been identified within meta-volcanic-sedimentary  
814 melange farther west, including the Anatolides (Afyon zone) (Robertson et al., 2009; in press  
815 b).

816 The volcanic-sedimentary melange was sourced from oceanic crust, including MOR-  
817 type basalt, 'seamounts' and subduction-influenced crust, within an oceanic basin that  
818 existed at least from Late Jurassic-Late Cretaceous. The melange was accreted related to  
819 subduction, and was emplaced onto the Tauride platform together with the other  
820 allochthonous units.

821

## 822 **9. Ophiolite-related units**

823

824 Definitions: Ophiolites represent relatively coherent bodies of oceanic lithosphere, although  
825 commonly incomplete. Dismembered ophiolites are tectonically dissected. Ophiolitic  
826 melange has component lithologies derived from an ophiolite and directly associated deep-  
827 sea sediments. Ophiolite-related melange, in contrast, includes a mixture of ophiolitic rocks  
828 and other unrelated lithologies (e.g. neritic limestone). These three types of melange all  
829 occur within the eastern Taurides, related to sea-floor spreading and ophiolite  
830 emplacement.

831

### 832 **9. 1. Ophiolite-related melange and ophiolitic melange**

833

834 Ophiolite-related melange and ophiolitic melange are well exposed north of Elbistan (Area  
835 2, Dağlıca), where they are intergradational and structurally interleaved. Within the  
836 ophiolite-related melange, ophiolitic blocks/slices are embedded in a matrix of sheared  
837 mudrock. The ophiolitic melange is mainly sheared harzburgite but other ophiolitic  
838 lithologies are present including gabbro and diabase dykes (locally cut by plagiogranite  
839 veins), as exposed east of Elbistan (Area 5) (see Supplementary Fig. 5). In this area,  
840 dismembered ophiolitic rocks of the Dağlıca ophiolite (see below) are spatially associated  
841 with short (up to 10s of m), deformed successions of ophiolite-derived, matrix-supported  
842 conglomerates. In places, these clastic rocks occur above the Kemaliye Formation. The  
843 Kemaliye Formation, as related to the Munzur and Köseyahya thrust sheets, does not

844 usually contain ophiolitic material (in contrast to the type area, above the Keban  
845 metamorphics). However, locally in Area 2 (Dağlıca), the highest levels of the intact  
846 Kemaliye Formation contain ophiolitic debris (Fig. 19 log 4), suggesting a link with the  
847 tectonically associated ophiolitic rocks (Dağlıca ophiolite). However, no undeformed contact  
848 could be observed. The debris-flow deposits are crudely stratified (Fig. 20f), showing both  
849 normal and reverse grading. The clasts are mostly angular to subrounded and are dispersed  
850 randomly though a poorly sorted sand-granule-grade matrix (Fig. 20g). Most parts of an  
851 ophiolite pseudostratigraphy are represented as clasts, including gabbro (Fig. 20h) and  
852 basalt (Fig. 20i); siliceous pelagic carbonate is mostly preserved as diagenetic replacement  
853 chert (Fig. 20j).

854 Another excellent example of ophiolite-related melange, here termed the Divriği  
855 melange, is exposed in the northeast of the region (Area 5B) (Figs. 2, 23). This melange is  
856 located between the Munzur thrust sheet, below and the Divriği ophiolite, above (Aktimur,  
857 1988; Özgül and Turşucu, 1984; Öztürk and Öztunalı, 1993). This unit is otherwise known as  
858 the Yeşiltaşayla ophiolitic melange (Yılmaz and Yılmaz, 2004), the Refahiye ophiolite  
859 (Atabey and Aktimur, 1997), and the Eriç melange (Özer et al., 2004). The Divriği melange  
860 has undergone low-grade metamorphism and is cut by Eocene granites (Boztuğ et al., 2007;  
861 Kuşcu et al., 2013). The smaller Güneş ophiolite is exposed in the same area (Yılmaz, 2001).

862 The Divriği melange, up to several 100 m thick, directly overlies the Munzur thrust  
863 sheet in its type area, the Munzur Dağları (Aktimur et al., 1998; Fig. 24a, b; see also  
864 Supplementary Fig. 4). The highest stratigraphical levels of the Munzur thrust sheet are well  
865 dated to the east of our study area. In this area (Ayıkayası Dağı), Cenomanian-aged, rudist-  
866 bearing neritic limestones are overlain by a thin (4 m) interval of thin-bedded, reddish  
867 siliceous pelagic carbonate of Turonian-Campanian age (Özer et al., 2004). This interval can  
868 be correlated, broadly with the latest Cretaceous pelagic cover of the platform carbonates  
869 in the Elbistan area (Kızılkandil Formation). Where well exposed in our area, north of Divriği,  
870 well-bedded, unmetamorphosed neritic limestones of the Munzur thrust sheet dip regularly  
871 westwards and are over-ridden by ophiolite-related melange, with a low-angle thrust  
872 contact (Fig. 24b). The highest exposed levels of the Munzur succession (5 km SSE of Divriği)  
873 are locally dated as Middle Jurassic, using benthic foraminifera (Fig. 18d, e; see also  
874 Supplementary Table 1), suggesting that the Cretaceous part of the original succession is  
875 now absent. Dark neritic limestones in the lower levels of the succession in the Divriği area

876 are dated as Middle Triassic, based on benthic foraminifera (Fig. 18c). Similar platform  
877 lithologies are now present as blocks in the overlying ophiolite-related melange.

878 The Divriği melange overlies the succession in the Munzur thrust sheet. In places,  
879 neritic limestones are unconformably overlain by mudrocks that are similar to the matrix of  
880 the melange (Figs. 23, 24a-c). In places, the contact is faulted (see Supplementary Fig. 4).  
881 The lower part of the melange includes a neritic limestone block that was dated as Aptian-  
882 Albian, based on benthic foraminifera (Fig. 18f-i; see also Supplementary Table 1), similar to  
883 the age of the underlying intact platform succession. The mid to upper levels of the melange  
884 are dominated by elongate slices and blocks of recrystallised limestone, up to 100s m long  
885 and 10s m thick, set in a sheared shaly matrix (Figs. 24a-c, 25a). Benthic foraminifera within  
886 a packstone block gave an Aptian-Albian age (Fig. 18j-q), again suggesting that the missing  
887 interval at the top of the Munzur platform succession is represented by blocks in the  
888 melange. Other blocks include poorly sorted breccia-conglomerate, indicating a mass-flow  
889 (slope-related) setting, prior to emplacement into the melange. Some of the clasts are well-  
890 rounded suggesting exposure and reworking prior to redeposition, as in the Kemaliye  
891 Formation (see above). The blocks and terrigenous matrix are interspersed with  
892 anastomosing strands of highly sheared serpentinite, mostly harzburgitic (Figs. 24a-b; 25b;  
893 see Supplementary Fig. 4). In places, serpentinite melange reaches to within c. 80 (structural  
894 thickness) of the tectonic contact with the intact Munzur thrust sheet below. The melange  
895 as a whole has experienced polyphase deformation, with evidence of both southerly and  
896 northerly fold vergences (Fig. 25c, d).

897 Several additional areas provide supporting evidence. For example, an extensive  
898 outcrop of ophiolitic melange southeast of Divriği is dominated by sheared harzburgitic  
899 serpentinite, without limestone blocks (Fig. 25e, f). Similar serpentinite melange also occurs  
900 extensively, e.g. c. 70 km southwest of Divriği (around Kangal), where it overlies neritic  
901 limestones of the Munzur thrust sheet (locally dated as Jurassic; see Supplementary Table  
902 1). In addition, melange outcrops to the west of Divriği (Fig. 2) have been summarised  
903 elsewhere (e.g. Büyük Yılanlı Dağ) (Robertson et al., 2013b; see also Özgül et al., 1981; Özgül  
904 and Turşucu, 1984; Aktimur et al., 1988; Atabey et al., 1994). These include several types of  
905 melange associated with the Pınarbaşı ophiolite in the northeast of the region studied (i.e.  
906 Kireçlikyayla melange of Yılmaz et al., 1991, 1993; Pınarbaşı melange of Atabey and Aktimur,  
907 1997).

908

## 909 9.2. Ophiolites and related clastic deposits

910

911 Whereas, melanges are widely distributed throughout the eastern Taurides, coherent  
912 ophiolites are restricted to four main bodies, the Divriği (also Güneş), Hekimhan, Pınarbaşı  
913 and Kuluncak ophiolites, mainly in the north of the region studied (Fig. 2). Here we pay  
914 particular attention to the dismembered Dağlıca ophiolite and its associated debris-flow  
915 units (Area 2) which shed light on emplacement processes.

916 In the northeast, the Divriği (Sivas) ophiolite (Area 5B), dated at 93-94 Ma by zircon U-  
917 Pb, is partially dismembered and lacks extrusives rocks (Parlak et al., 2006, 2017). A locally  
918 exposed metamorphic sole (Fig. 24a, bii), dated at 93-94 Ma by Ar-Ar (Parlak et al., 2017),  
919 includes amphibolite, with subordinate, greenschist, marble and metachert, all cut by post-  
920 metamorphic diabase/microgabbro dykes. The protoliths of the amphibolite are within-  
921 plate basalts (seamount-type) and island-arc-type basalts, whereas the protoliths of the  
922 dykes are within-plate basalts (Parlak et al., 2006). Listwaenite is widespread in the Divriği  
923 (Sivas) ophiolite (Uçurum, 2000).

924 Farther southwest (c. 40 km), the dismembered Kuluncak-Hekimhan (Malatya) ophiolite  
925 (Fig. 2) comprises variably altered mantle harzburgite (tectonites), cut by isolated basaltic  
926 dykes, together with ultramafic cumulates (mainly dunite, wehrlite and pyroxenite), mafic  
927 cumulates (olivine-gabbro and normal gabbro), isotropic gabbro, diorite and quartz diorite,  
928 a sheeted dyke complex, plagiogranite and extrusive rocks. The basaltic extrusive rocks are  
929 associated with radiolarite, chert, pelagic limestone and hemipelagic mudstone (Metin et  
930 al., 2013; Camuzcuoğlu et al., 2017). Listwaenite again occurs (Uçurum, 2000). In the  
931 northeast, the Pınarbaşı ophiolite, dated as 93-94 Ma by zircon U-Pb (Parlak et al., 2017)  
932 (Fig. 2) exposes mantle tectonites, cut by isolated basaltic dykes, together with ultramafic to  
933 mafic cumulates, all above an amphibolitic sole (90-93 Ma by zircon U-Pb) (Parlak et al.,  
934 2017). These sole rocks are chemically similar to those of the Divriği ophiolite (Vergili and  
935 Parlak, 2005).

936 In addition, the dismembered Dağlıca ophiolite (Fig. 7; sections a, d, e) is restricted  
937 to thrust slices and blocks (up to km to km-sized). The lithologies were previously termed  
938 the Dağlıca complex (Kozlu et al., 1990; Perinçek and Kozlu, 1984), and the Dağlıca ophiolite  
939 (Robertson et al., 2013b). The lithologies include basalt, diabase, diabase dykes in



940 harzburgite, gabbro, gabbro pegmatite, harzburgite, pyroxenite, wehrlite and dunite (see  
941 Supplementary Fig. 5). The metamorphic sole is represented by rare blocks of amphibolite-  
942 greenschist within adjacent ophiolite-related melange. The basaltic rocks of the Dağlıca  
943 ophiolite are chemically indicative of a supra-subduction zone origin (Robertson et al.,  
944 2006).

945

### 946 9.3. Interpretation of the ophiolites, melanges and related mass-flow units

947

948 The ophiolites formed in a Late Cretaceous (c. 92-93 Ma), supra-subduction zone setting  
949 (Parlak et al., 2013, 2019). They represent different parts of a regional-scale thrust sheet of  
950 oceanic lithosphere, with a metamorphic sole that is only now locally preserved. The  
951 presence of all of the units of a complete ophiolite, taken regionally, suggests that a typical  
952 supra-subduction zone ophiolite initially formed with all of the expected lithological units;  
953 however, this was variably dismembered during emplacement.

954 During emplacement, related to flexural loading by advancing oceanic lithosphere,  
955 the Mesozoic carbonate platforms (Munzur and Köseyahya) subsided to create the regional-  
956 scale foredeep mentioned above (Kemaliye Formation; see above). In proximal (northerly)  
957 areas, represented by the Divriği melange, the upper stratigraphic (Cretaceous) levels of the  
958 Munzur platform were partly removed. Most likely, they were detached, bulldozed ahead  
959 and collapsed as debris-flows and blocks into the northern part of the regional foredeep.  
960 During southward emplacement, serpentinite derived from the over-riding ophiolite  
961 harzburgite was tectonically incorporated into the foredeep.

962 During emplacement, the East Tauride ophiolites were variably dismembered. The  
963 Dağlıca ophiolite was strongly dismembered to form thrust sheets and broken formation,  
964 and also underwent mass-wasting to form ophiolite-derived debris flows. Ophiolitic material  
965 was initially sand-sized (within the Kemaliye Formation), then became clast/block sized (i.e.  
966 more proximal) and culminated in the emplacement of large ophiolitic blocks and thrust  
967 sheets. Gravity emplacement was therefore an important process for the melange units.  
968 Ophiolite-related melange covered all parts of the region (including south of Elbistan; Area  
969 4). However, the ordered ophiolites are restricted to the north of the region, closest to their  
970 inferred origin and there is no field evidence that they were emplaced southwards over the  
971 entire region.

972

973 **10. Latest Cretaceous-Paleogene cover sediments**

974

975 Cover sediments provide important constraints on the nature of the substratum, the timing  
976 of emplacement and the tectonic conditions soon afterwards. The Divriği ophiolite is  
977 unconformably overlain by conglomerates, sandstone, mudstone, marl, limestone and  
978 volcanoclastic sediments, dated as Campanian-Maastrichtian (Yılmaz and Yılmaz, 2004; Bilgiç  
979 et al., 2008a, b). Approximately 50 km farther west (Tecer Dağı and Büyük Yılanlı Dağ),  
980 ophiolitic rocks, similar to the Divriği ophiolite (Kavak et al., 2017), are unconformably  
981 overlain by conglomeratic facies (Tecer Formation) (İnan and İnan, 1988), passing upwards  
982 into Late Maastrichtian shallow-marine, mixed carbonate-clastic facies (Atabey and Aktimur,  
983 1997; İnan and İnan, 1988; Robertson et al., 2013b). Both the Kuluncak and Hekimhan  
984 ophiolites (and related melange units) are unconformably overlain by ophiolite-derived  
985 conglomerates, passing upwards into Late Maastrichtian shallow-water carbonates,  
986 including rudist limestones (Booth et al., 2013; Robertson et al., 2013b; Bedi and Yusufoglu,  
987 2018). In addition, the Pınarbaşı ophiolite is unconformably overlain by non-marine clastics  
988 and minor carbonates, of inferred Palaeocene age (Erkan et al., 1978).

989         The widespread deposition of latest Cretaceous, typically late Maastrichtian, cover  
990 sediments show that, after short-lived emergence and erosion, the emplaced continental  
991 margin and ophiolitic units, were rapidly transgressed by non-marine to shallow-marine  
992 sediments, and that this was followed by a return to relatively stable tectonic conditions.  
993 The clast composition reflects the nearby units beneath, typically ophiolitic rocks. The  
994 timing of regional ophiolite emplacement is constrained as coeval with the syn-tectonic  
995 Kemaliye Formation (late Campanian-late Maastrichtian) but prior to the transgressive  
996 sediments regionally (probably late Maastrichtian). The emplacement of the allochthonous  
997 units therefore took place during a relatively short period of time (c. 75-70 Ma).

998

999 **11. Structural relationships**

1000

1001 11.1. Outcrop-scale structures

1002

1003 To shed additional light on the tectonic emplacement, bedding and fold data (fold axial  
1004 planes and fold hinges) were measured throughout the study area and plotted on  
1005 stereonet according to sub-area and tectono-stratigraphic unit (see also Supplementary  
1006 Fig. 6).

1007 Bedding in the Malatya and/or Keban metamorphics (Areas 1 and 5A) is generally  
1008 orientated NE-SW (see supplementary Fig. 7). Fold axial planes mainly plot in the northern  
1009 and southern quadrants, consistent with dominantly E-W folding with variably dipping axial  
1010 planes (c. 10-80°) (Fig. 26ai-aii).

1011 Structural measurement from the allochthonous Tauride units are relatively variable.  
1012 North of Elbistan (Area 2), the bedding strike is regionally c. E-W. Bedding orientations are  
1013 variable in all units, with a slight NW-SE trend, consistent with large-scale symmetrical  
1014 folding (see Supplementary Fig. 7). Fold axial planes are broadly east-west and commonly  
1015 west-dipping (Fig. 26bi). Many fold hinges trend c. E-W, with axial planes dipping both N and  
1016 S at moderate angles, suggesting refolding (Fig. 26bii). A local swing in fold hinge direction  
1017 (south to west) in the relatively autochthonous Gürün outcrop (see Supplementary Fig. 8)  
1018 could represent refolding (or possibly local block rotation). Farther east (Area 3A; E of  
1019 Elbistan), the bedding is more NW-SE. Fold axial planes and fold hinges are broadly east-  
1020 west, mainly at moderate angles (Fig. 26ci-ii; see Supplementary Fig. 9). In the Kemaliye  
1021 area in the northeast (Area 5A), bedding data from both the Malatya Metamorphics and the  
1022 Kemaliye Formation have a slight NW-SE strike, mainly at moderately angles (see  
1023 Supplementary Fig. 10). Fold axial planes (mostly in the Keban metamorphics) mainly dip  
1024 southwest at variable angles. Fold hinges have a dominant NW-SE trend. Opposing NW vs.  
1025 SE directions hint at re-folding (Fig. 26 di-dii).

1026 The relatively coherent data set from the Malatya Metamorphics (Fig. 26 ai-aii) is  
1027 consistent with N-S compression (without preferred vergence). The fold data from Area 2  
1028 (Dağlıca) are consistent with two-phase emplacement along c. E-W axes (with opposing  
1029 directions). The more NW-SE fold trend in the Kemaliye area farther northeast (Area 5A),  
1030 mainly in the Malatya (Keban) Metamorphics, represent a different compression direction  
1031 or possibly bulk rotation.

1032

1033 11.2. Inter-relations of regional tectono-stratigraphic units

1034 The mutual relations are mainly indicated by a combination of sedimentary, metamorphic,  
1035 igneous and structural evidence.

1036

1037 11.2.1. Relation of the Malatya metamorphics to the Göksun ophiolite: sedimentary  
1038 evidence

1039

1040 In the south, the Malatya Metamorphics (Bodrum nappe) are thrust over the post-  
1041 emplacement sedimentary cover of the Göksun ophiolite (Harami Formation), shedding  
1042 light on its timing of emplacement. South of Afşin (Area 1), the Göksun ophiolite is  
1043 unconformably overlain by conglomerate, sandstone, sandy/shaly limestone and marl (un-  
1044 named unit of Perinçek and Kozlu, 1984) that is correlated with the Harami Formation in its  
1045 type area (Elazığ) (Perinçek and Kozlu, 1984; Robertson et al., 2007; Bedi et al., 2009). The  
1046 succession south of Afşin begins with polymictic conglomerates with schist and marble,  
1047 radiolarite, pelagic limestone, chert, ophiolitic rocks (including diabase and basalt), and fines  
1048 upwards into sandstone, limestone and microconglomerates with clasts of similar  
1049 composition (Yılmaz et al., 1987; Bedi et al., 2009; this study). Thin sections include  
1050 monocrystalline (plutonic) quartz, polycrystalline (metamorphic) quartz, sericitic schist,  
1051 marble, micritic limestone, biotite and muscovite, in generally decreasing order of  
1052 abundance (Fig. 6k, l). The matrix is biomicrite with a mixture of planktic and benthic  
1053 foraminifera. The succession is dated as latest Cretaceous using planktic and benthic  
1054 foraminifera, and also calcareous nannofossils (Perinçek and Kozlu, 1984; Yılmaz et al., 1987,  
1055 1993; Robertson et al., 2007; Bedi et al., 2009). The basal conglomerates include pelagic  
1056 limestone pebbles of Santonian age, similar to the Kızılkandil Formation of the Munzur and  
1057 also the Köseyahya successions (Bedi et al., 2009). During this work, samples of calcarenite  
1058 yielded Late Campanian-Maastrichtian ages (see Supplementary Table 1). Samples from the  
1059 upper part of the formation (Sarıkaya member) have been dated as late Maastrichtian  
1060 based on planktic foraminifera and nannofossils (Bedi et al., 2009), of which the key taxa are  
1061 *Gansserina gansseri* (72.35-66 Ma, latest Campanian-Maastrichtian) and *Globostruncanita*  
1062 *angulata* (66.04-72.05 Ma, top Maastrichtian).

1063 The post-emplacement sedimentary cover of the Göksun ophiolite accumulated in a  
1064 shelf sea of moderate water depth (>10s m), with clastic sediment supply both from the  
1065 Munzur and/or Köseyahya platform units and also from already exhumed Malatya

1066 metamorphic rocks. The Malatya metamorphic thrust sheet was, therefore, tectonically  
1067 juxtaposed with the underlying Göksun ophiolite during the latest Cretaceous.

1068

1069 11.2.2. Post-exhumation imbrication of the Malatya Metamorphics: sedimentary and  
1070 structural evidence

1071

1072 SW of Elbistan (Area 4), the Neritic-pelagic (Köseyahya) thrust sheet is thrust southwards  
1073 over the Malatya Metamorphics (Fig. 9, section A). However, elsewhere the contact is  
1074 steeply dipping and is likely to be a strike-slip fault (Fig. 9, section A). In this area, near  
1075 Kalaycık (Fig. 9 section A; locality E), Triassic Malatya metamorphic rocks (exposed on  
1076 Medetsizdağı) are underlain by a small slice (>40 m thick) of unmetamorphosed debris-flow  
1077 deposits that include gabbro, basalt, pelagic limestone (with volcanic debris) and radiolarite.  
1078 This facies is similar to the Kemaliye Formation, as exposed c. 12 km to the NE (near Sokullu;  
1079 Fig. 9 map). A sample from a block of pelagic limestone contains Campanian-Maastrichtian  
1080 planktic foraminifera, as in the Kemaliye Formation (Fig. 21a-d). However, an additional  
1081 sample includes Globigerinidae (Fig. 21e, f) and also Rotaliidae, indicating a post-Cretaceous  
1082 (Cenozoic) age. Two other samples contain a rich Middle Palaeocene (Selandian) planktic  
1083 foraminiferal assemblage (see Supplementary Table 1). Relatively deep-water pelagic  
1084 conditions therefore existed during the Palaeogene, followed by reworking of pelagic  
1085 carbonates within debris-flow deposits. Elsewhere (e.g. west of Afşin), the Malatya  
1086 Metamorphics are internally imbricated with Eocene shelf-depth Nummulitic limestones  
1087 (Robertson et al., 2006; Fig. 4 a). The inter-slicing took place during Mid-Late Eocene  
1088 regional deformation (see below). However, the distance of Eocene thrust transport is likely  
1089 to have been limited (a few kms at most) because the Göksun ophiolite and the Malatya  
1090 Metamorphics are mutually intruded by the 88-82 Ma Baskil Granitoids, without major  
1091 thrust dislocation of the contact relations (Karaođlan et al., 2012, 2016; Bedi and Yusufoglu,  
1092 2018).

1093

1094 11.2.3. Contact relations between the Munzur and Köseyahya thrust sheets: sedimentary  
1095 and structural evidence

1096

1097 The Munzur thrust sheet is subdivided into the main, lower thrust sheet that encompasses  
1098 the entire succession and the much thinner, internally disrupted, upper thrust sheets  
1099 (mainly Cretaceous), as exposed in the north, in Area 2 (Dağlıca) (Figs. 7; Fig. 20c-e). The  
1100 upper and lower thrust sheets are separated by the Kemaliye Formation, which has  
1101 widespread inclusions of the dismembered Dağlıca ophiolite, related melange (Fig. 7) and,  
1102 locally, of the Pelagic (Gülbahar) unit (Fig. 7f). In places, limestones of upper thrust sheet  
1103 directly overlie the southern margin of the Gürün autochthon (Fig. 7c).

1104 NE of Elbistan (Area 3A), the Munzur thrust sheet is thrust southwards over the  
1105 Neritic-pelagic (Köseyahya) thrust sheet (Fig. 8 sections a, e). The two thrust sheets are  
1106 separated by mass-flow units, correlated with the Kemaliye Formation (see Supplementary  
1107 Fig. 7). Poorly bedded calcarenites form the matrix of debris-flow deposits; these include  
1108 large foraminifera and calcareous algae of Late Palaeozoic (Carboniferous-Permian) age (see  
1109 Supplementary Table 1), hinting at derivation from an original but now missing Late  
1110 Palaeozoic substratum to the Munzur limestones. The imbrication of the two major  
1111 platform carbonate/slope thrust sheets therefore took place after formation of the latest  
1112 Cretaceous Kemaliye Formation, probably during the latest Cretaceous.

1113 In the same area, NE of Elbistan (Area 3A), the Neritic-pelagic (Köseyahya) thrust sheet  
1114 beneath the Munzur thrust sheet is relatively thin (100s m) and highly disrupted. Pelagic  
1115 limestones of the Neritic-pelagic (Köseyahya) thrust sheet are repeatedly imbricated with  
1116 the latest Cretaceous Kemaliye Formation (Fig. 8). The Pelagic (Gülbahar) unit that is locally  
1117 exposed beneath both the Neritic-pelagic (Köseyahya) thrust sheet and the Munzur thrust  
1118 sheet are both tightly folded and, in places, intensely imbricated, indicating intense  
1119 compressional deformation during emplacement (see Supplementary Fig. 6). On the other  
1120 hand, the widespread presence of conjugate fault blocks indicates extension (see  
1121 Supplementary Fig. 6). One explanation is that the Neritic-pelagic (Köseyahya) sheets were  
1122 emplaced by gravity sliding into the Kemaliye foredeep, followed by imbrication during  
1123 regional emplacement into the latest Cretaceous thrust stack.

1124 In the south (south of Elbistan; Area 4), a Munzur thrust sheet is mapped as  
1125 underlying a Köseyahya thrust sheet (Bedi et al., 2009) (Fig. 9, section A). This points to  
1126 complex and variable re-imbrication because to the northeast (e.g. Area 3A; Fig. 8) the  
1127 Munzur thrust sheet regionally overlies the Köseyahya thrust sheet. All of this imbrication  
1128 and re-imbrication is inferred to be latest Cretaceous in age.

1129 In addition, to the NW of Elbistan (N of Afşin, near İncirli, Area 2), the Malatya  
1130 Metamorphics are thrust northwards over the Southern allochthon, including the Kemaliye  
1131 Formation, above a sharp south-dipping contact (Figs. 2; 4l; Supplementary Fig. 2). This  
1132 indicates an important, but localised, phase of backthrusting after the initial latest  
1133 Cretaceous emplacement. Northward vergence is also observed within the adjacent  
1134 Southern allochthon (Perinçek and Kozlu, 1984; Robertson et al., 2013).

1135

1136 11.2.4. Contact relations between the Gürün autochthon and the allochthonous units

1137

1138 Along the southern margin of the Gürün autochthon (Area 2; Dağlıca; Figs. 7, 20k), the  
1139 relatively autochthonous succession culminates with Middle Eocene (Lutetian) calcareous  
1140 mudstones, rich in large foraminifera. Interbedded sandstones and debris-flow deposits  
1141 contain ophiolitic detritus. Several km to the south (Hurman Çayı-Kalesi area) (Fig. 7, marked  
1142 in red), ophiolitic rocks and Munzur limestones are thrust over an isolated Early-Mid Eocene  
1143 succession (with no exposed base) (Robertson et al., 2013b). This begins with limestones  
1144 that are rich in large foraminifera (e.g. *Alveolina* sp., *Assilina* sp.) and passes upwards into  
1145 argillaceous and silty limestones (Demirogluk Formation of Bedi et al., 2009). This is  
1146 interpreted as a fragment of an Eocene shelf succession that was later incorporated into the  
1147 thrust stack. In the west of Area 2 (e.g. NW of Tavla), the Munzur limestones are  
1148 unconformably overlain by non-marine conglomerates, with well-rounded clasts that  
1149 include *Nummulites* sp. suggesting a post-Eocene age of accumulation (Early-Mid  
1150 Miocene(?)) (Fig. 7b; 20l). These conglomerates are also incorporated into the thrust stack.  
1151 Farther east, within the Gürün autochthon (near Akdere), Cenomanian rudist-bearing  
1152 limestones are unconformably overlain by thick-bedded to massive non-marine  
1153 conglomerates, of inferred Early-Mid Miocene age (Gövdelidağ Formation of Perinçek and  
1154 Kozlu, 1984). The conglomerates are in high-angle fault contact with Munzur limestones.  
1155 Slickensides indicate right-lateral strike-slip displacement (Robertson et al., 2013a). In the  
1156 far east of Area 2 (near Sarız), a moderate-angle (30-50°) south-dipping thrust (reverse fault)  
1157 separates the Paleogene Gürün autochthonous succession from the allochthonous units  
1158 above, pointing to northward displacement (i.e. backthrusting) (Robertson et al., 2013b),  
1159 which affected the Southern Allochthon as a whole. The outcrop bordering the Gürün  
1160 autochthon in the south is folded on a large scale along c. E-W axes. The timing of the

1161 folding is inferred to be pre-Pliocene, post-dating the inferred Miocene non-marine  
1162 conglomerates (Yılmaz et al., 1993; Perinçek and Kozlu, 1984; Kozlu et al., 1990; Robertson et  
1163 al., 2013b). In summary, within the Southern allochthon there is evidence of latest  
1164 Cretaceous southward thrust-stacking, Eocene re-imbrication and Late (?) Miocene back-  
1165 thrusting, reverse faulting and large-scale folding.

1166         Along the northern margin of the Gürün autochthon (Fig. 2), the relatively  
1167 autochthonous succession culminates in Middle Eocene shelf facies, similar to those in the  
1168 south. The Northern allochthon begins with an equivalent of the neritic Munzur thrust  
1169 sheet, followed upwards by the Pelagic nappe, equivalent to the Neritic-pelagic (Köseyahya)  
1170 thrust sheet, but more coherent stratigraphically. Overlying units include the Pınarbaşı  
1171 ophiolite and related melange units in the northwest (Robertson et al., 2013b). The  
1172 northern allochthon is overlain by Eocene marine clastic sediments. Although mapped as an  
1173 unconformable relationship (Yılmaz et al., 1997; MTA 2011; Bedi and Yusufaglu, 2018), field  
1174 observations in the northeast of the area suggest a thrust relationship (Robertson et al.,  
1175 2013b). In the southwest, near Pınarbaşı, the contact relations are mainly concealed by  
1176 numerous neotectonic strike-slip faults.

1177

### 1178 11.3. Effects of neotectonic faulting

1179

1180 Neotectonic displacements need to be back-stripped to interpret the preceding  
1181 emplacement history in detail.

1182         Previously published fault data, specifically from the generally NE-SW to ENE-WSW-  
1183 trending Göksu fault lineament of Kozlu et al. (1990) (Tavla-Sarız area; Figs. 2, 7), indicate  
1184 dominantly right-lateral displacement, with either reverse or normal components  
1185 (Robertson et al., 2013b). This is surprising because the dominant offset along neotectonic  
1186 faults in the region is left-lateral (e.g. Duman and Emre, 2013). During this study, additional  
1187 faults were measured, mainly farther east (e.g. Hurman Kalesi area). Of the new fault data  
1188 (see Supplementary Fig. 11), there are six NW-SE trending faults, one of which is left-lateral  
1189 and the remainder right-lateral. Of 10 NE-SW trending faults, seven are dextral, two have no  
1190 slickenlines to determine movement sense and one is an oblique reverse fault. The new  
1191 data support significant right-lateral displacement along a generally NE-SW to ENE-WSW-  
1192 trending lineament, possibly representing more than one phase of movement. The



1193 rectilinear right-lateral faulting appears to post-date the inferred Mid-Late Miocene folding  
1194 and reverse faulting/backthrusting that affects the Southern allochthon and the adjacent  
1195 Gürün autochthon (see above).

1196 Neotectonic faults are widely mapped further south, in the general Elbistan area, as  
1197 follows: (1) NW-SE trending faults (Kışlaköy and Hurman Faults), inferred to be normal  
1198 faults with dextral strike-slip components (strike N35°E; dip 81°SW; (2) NE-SW trending fault  
1199 (Sarıyatak Fault), a normal fault with a sinistral component (strike N15°E dip 78°SE; lineation  
1200 plunges 75°S); (3) ENE-WSW faults (Türkören Fault and Afşin-Elbistan Fault), of which four  
1201 fault planes on the left-lateral Afşin-Elbistan Fault have allowed calculation of principal  
1202 stress directions ( $\sigma_1$  51°/170°;  $\sigma_2$  30°/307°;  $\sigma_3$  22°/050°). The NE-SW  
1203 trending fault is inferred to have influenced the Pliocene-Quaternary clastic deposition  
1204 within the adjacent depocentre that forms part of the overall Afşin-Elbistan basin (Yusufoglu  
1205 et al., 2005; Bedi et al., 2009). Regional c. ENE-WSW left-lateral faulting generated overall  
1206 NW-SE trending fault-controlled depocentres that infilled with Pleistocene sediments. Some  
1207 of the neotectonic faults in the Elbistan region are reported to be covered by conglomerates  
1208 suggesting a switching of faults with time and/or a changing stress regime (Bedi et al.,  
1209 2009).

1210 The region to the west of the Malatya-Ovacık Fault Zone is transected by numerous  
1211 Plio-Quaternary left-lateral strike-slip faults, including the Afşin-Elbistan Fault and the  
1212 generally NNE-SSW Sarız and Gürün faults (MTA, 2011). Some of these faults are interpreted  
1213 to have active left-lateral movements (i.e. Beyyurdu and Gürün faults of Emre et al. (2018);  
1214 Türkören fault of Bedi et al. (2009)). The left-lateral faults relate to displacements along the  
1215 regional northern strand of the East Anatolian Fault System (Sürgü–Misis Fault system). The  
1216 Pliocene-Pleistocene westward tectonic escape of Anatolia (Şengör et al., 1985; Duman and  
1217 Emre, 2013) was partially accommodated by displacements along these faults.

1218 In the east, the Malatya-Ovacık Fault Zone delimits the western margin of the large  
1219 Malatya Basin. Early-Middle Miocene NW–SE extension there was followed by Mid-Late  
1220 Miocene volcanism ( $11.99 \pm 0.49$ – $4.82 \pm 0.57$ ) (Yamadağ volcanics) (Kaymakçı et al., 2006;  
1221 Kürüm et al., 2008). NNW-SSE left-lateral transpression is inferred along the Malatya-Ovacık  
1222 Fault Zone during Late Miocene-Early Pliocene, coupled with widespread Pliocene volcanism  
1223 (Ekici et al., 2007). Active left-lateral displacement began during the Late Pliocene,  
1224 influenced by variable NNE–SSW transpression (Kaymakçı et al., 2006). In summary, most of

1225 the neotectonic faults in the region studied have relatively small displacements (several  
1226 kms) that do not fundamentally change the regional tectono-stratigraphy; however, the  
1227 Sürgü–Misis Fault and Malatya-Ovacık Fault have tens of km of fault displacement that need  
1228 to be restored in any tectonic reconstruction.

1229

## 1230 **12. Discussion**

1231

1232 Below, we utilise the assembled body of evidence and interpretation to test and develop  
1233 several alternative tectonic hypotheses for the relationships between the main tectonic  
1234 units in the region.

1235

### 1236 12.1. Relation between the Northern and Southern allochthons and the Gürün autochthon

1237

1238 There are three main hypotheses for the emplacement of the northern and southern  
1239 allochthons in relation to the Gürün autochthon (Fig. 2). All three assume that the  
1240 allochthonous units cannot have been emplaced over the intact succession of the Gürün  
1241 autochthon, at least until the Mid-Late Eocene because of its intact stratigraphical  
1242 succession (Aziz et al., 1982; Perinçek and Kozlu, 1984; Robertson et al., 2013b).

1243 The first hypothesis is that the Southern allochthon was emplaced southwards over  
1244 the Gürün autochthon after deposition ended in the Early-Mid Eocene (Aziz et al., 1982).

1245 This is consistent with the evidence of southward thrusting during the Mid-Late Eocene in  
1246 the central Taurides (Özgül, 1984, 1997; Monod, 1977; Gutnic et al., 1979; Görür et al.,  
1247 1998; Demirtaşlı et al., 1984; Andrew and Robertson, 2002; Mackintosh and Robertson,  
1248 2012; McPhee et al., 2018b), and also in the western Taurides (De Graciansky, 1972;  
1249 Poisson, 1977; Şenel et al., 1989; Collins and Robertson, 1997, 1998, 1999; Robertson et al.,  
1250 2013a; Pourteau et al., 2016). However, a similar interpretation is problematic in the  
1251 eastern Taurides for three main reasons: (1) Thrust relations: A thrust is not mapped  
1252 regionally along the northern margin of the Gürün autochthon, between the Eocene  
1253 succession and the Northern allochthon (MTA, 2011; Bedi and Yusufoglu, 2018), although as  
1254 noted above, a thrust contact has been observed locally (Robertson et al., 2016). (2)

1255 Regional melange distribution: The Kemaliye Formation, as exposed above the Malatya

1256 (Keban) metamorphics in the Nurhak Dağ area (Area 3b), includes clasts and blocks derived

1257 from the Malatya and/or Köseyahya thrust sheets, strongly suggesting that allochthon  
1258 reached quite far south (10s km) of the Gürün autochthon during the latest Cretaceous. In  
1259 this case, the allochthon cannot have remained to the north of the Gürün autochthon until  
1260 the Eocene. (3) Cover relations: In the east, the Southern allochthon is locally covered and  
1261 sealed by late Maastrichtian-Eocene sediments of the Darende Basin (Fig. 2). Along the  
1262 western margin of the Darende basin (E of the bounding neotectonic Gürün fault)  
1263 specifically, allochthonous units, correlated with the Dağlıca ophiolite, are unconformably  
1264 overlain by conglomerates that pass upwards into Maastrichtian marls and limestones,  
1265 together with lenticular rudist build-ups (Kırankaya Formation). Further north, along the  
1266 western margin of the Darende basin, Maastrichtian sediments unconformably overlie the  
1267 Munzur limestone thrust sheet. Also, the Darende basin is transgressive on an equivalent of  
1268 the Munzur thrust sheet and related ophiolitic melange around its eastern margin (Booth et  
1269 al., 2013). After a Palaeocene-Early Eocene hiatus, the sedimentary succession passes into  
1270 Middle Eocene mixed siliciclastic/shallow-marine carbonates, with localised lenticular  
1271 volcanics, and then into Bartonian-early Priabonian regressive facies (Gürbüz and Gül, 2005;  
1272 Bedi et al., 2009; Booth et al., 2013). There is no evidence of increasing deformation  
1273 upwards that could relate to regional overthrusting. Any post-Cretaceous southward  
1274 emplacement of the Southern allochthon would instead need to entrain the Darende Basin  
1275 as a whole above an unexposed deeper-level regional-scale thrust. This requirement would  
1276 probably also apply to the Hekimhan Basin farther northeast (Booth et al., 2014). However,  
1277 there is no evidence that the Darende and Hekimhan basins are parts of a regional-scale  
1278 Eocene thrust sheet; e.g. no frontal thrust is exposed to the south. In summary, southward  
1279 emplacement of the Southern allochthon over the Gürün platform succession during, or  
1280 after, the Eocene seems unlikely.

1281 The second hypothesis is that the southern and northern allochthons were emplaced  
1282 from opposite directions during the latest Cretaceous, with the Gürün autochthon in  
1283 between (van Hinsbergen et al., 2020) (Fig. 27bi-bii). This is problematic for several reasons:  
1284 (1) The tectono-stratigraphy of both allochthons is very similar and does not indicate  
1285 different palaeogeographic origins; (2) The northward thrusting of the Malatya  
1286 Metamorphics that affects the Southern allochthon (e.g. İncirlik area) took place during the  
1287 Cenozoic because post-Cretaceous sediments are structurally interleaved; (3) The tectono-  
1288 stratigraphy of the E Tauride allochthons, combined, differs markedly from the South-

1289 Tauride allochthonous units; e.g. in the Adiyaman and Antalya areas (Robertson et al.,  
1290 2012).

1291         The third hypothesis is that both of the allochthonous units were assembled by  
1292 southward thrusting during the latest Cretaceous but in separate areas; subsequently the  
1293 Gürün autochthon and the already emplaced Northern allochthon were displaced  
1294 northeastwards (> 60 km) along the Güksu fault zone of Kozlu et al. (1990) to their present  
1295 positions, probably during the Mid-Late Eocene (Robertson et al., 2013b). This hypothesis is  
1296 consistent with the southwestward lateral passage of the Gürün autochthon into the Geyik  
1297 Dağ (Tauride platform) (e.g. in the Tufanbeyli-Saimbeyli-Feke-Kozan area) (MTA, 2011).  
1298 However, there are also problems with the right-lateral strike-slip hypothesis: (1) There is no  
1299 single clear-cut fault (terrane boundary fault) separating the Gürün autochthon from the  
1300 Southern allochthon; instead, strike-slip faults transect both the northern part of the  
1301 Southern allochthon and the southern part of the Gürün autochthon (Robertson et al.,  
1302 2013b; (2) Right-lateral strike-slip faults of appropriate c. NE-SW orientation are indeed  
1303 present (Robertson et al., 2013a; Supplementary Fig. 11) but these appear to post-date the  
1304 northward-directed displacement and folding of probable Mid-Late Miocene age. A possible  
1305 explanation is that eastward displacement of the Gürün autochthon/northern allochthon,  
1306 relative to the Southern allochthon, did indeed take place along the Eocene Göksu fault  
1307 zone of Kozlu et al. (1990) but this lineament was over-ridden and concealed during the  
1308 later folding and thrusting. The documented right-lateral neotectonic strike-slip faulting  
1309 along this lineament could have reactivated such a buried lineament. The dextral strike-slip  
1310 faults were overprinted by the dominantly Plio-Quaternary left-lateral faults affecting the  
1311 region in this interpretation.

1312         In summary, both the southern and the northern allochthons were emplaced  
1313 southwards onto the Tauride platform during latest Cretaceous time. The right-lateral  
1314 ‘terrane displacement’ interpretation is the most promising of the three options and could  
1315 also help to explain the regional east-directed Gürün curl (see Supplementary Fig. 1). In this  
1316 case the regional-scale ‘tectonic escape’ buckled the regional tectono-stratigraphy to form  
1317 the ‘curl’.

1318

1319 12.2. Relation between the Malatya Metamorphics and the Southern allochthon

1320

1321 Malatya Metamorphics encompass a Late Palaeozoic-Late Cretaceous stratigraphy,  
1322 consistent with a relatively internal part of the Tauride continent. No marginal (slope) units  
1323 are exposed. Assuming regional in-sequence thrusting, the Triassic-Late Cretaceous  
1324 successions of the Munzur and Köseyahya thrust sheets appear to represent northerly parts  
1325 of the Tauride continent that detached from their basement and were emplaced  
1326 southwards (Fig. 27a-c). During the Late Cretaceous, the more southerly located (Malatya)  
1327 platform (>75 km wide) was deeply underthrust northwards and metamorphosed under up  
1328 to amphibolite, or possibly low HP-LT conditions. This was associated with the intrusion of  
1329 the unmetamorphosed Baskil granitoids (88-82 Ma) (Bozkaya et al., 2007; Bedi et al., 2009;  
1330 Oberhansli et al., 2012; Rolland et al., 2012; Bedi and Yusufoglu, 2018) (Fig. 27d).

1331 In the northeast of the region, c. 100 km north of the main Malatya metamorphic  
1332 outcrop) there is a small outcrop that comprises Late Palaeozoic schist, overlain by Late  
1333 Permian meta-carbonates, Middle Triassic-Jurassic meta-platform carbonates and Late  
1334 Cretaceous meta-clastics/carbonates with meta-carbonate blocks (c. 40 km SW of Divriği;  
1335 Alacahan-Çetinkaya area; M on Fig. 2)) (Atabey and Aktimur, 1997; MTA, 2011; Robertson et  
1336 al., 2013b; Beyazpirinç and Akçay, 2013). The succession is comparable to the Malatya  
1337 Metamorphics, including the Late Cretaceous Karaböğürtlen Formation, suggesting that  
1338 Malatya metamorphic crust may extend far northwards beneath the Mesozoic  
1339 allochthonous units. However, it is also possible that the above outcrop represents the  
1340 metamorphosed northern margin of the Munzur platform (otherwise not exposed).

1341 In the northeast of the region (NW of Pınarbaşı), Hınzır Dağı and Korumaz Dağı (E of  
1342 Kayseri) there is an additional, sizeable outcrop of high-grade metamorphic rocks including  
1343 schist, gneiss and meta-platform carbonates, ranging in age from Carboniferous to  
1344 Cretaceous (Özer et al., 1984; Pourteau et al., 2010; MTA, 2011; unpublished data). These  
1345 rocks may correlate with the HP-LT Tavşanlı zone and/or the Afyon zone of the Anatolides  
1346 (Oberhansli et al., 2012; Pourteau et al., 2013), although more study is needed to confirm  
1347 this correlation.

1348 The Malatya Metamorphics exhumed rapidly (Robertson et al., 2013b), at least  
1349 partially, as indicated by the latest Cretaceous transgressive cover in the Malatya area  
1350 (Gündüzbey Formation) (Bedi and Yusufoglu, 2018). The Kemaliye Formation, extending  
1351 southwards from its type area near Kemaliye (Area 5A) for at least c. 120 km to Nurhak Dağı  
1352 (Area 3B), includes metamorphic debris from the Malatya Metamorphics and

1353 unmetamorphosed material from the Tauride allochthons, indicating that these two units  
1354 were juxtaposed during the latest Cretaceous. The Kemaliye Formation in its type area  
1355 accumulated during and/or very soon after exhumation of the Malatya Metamorphics. The  
1356 basal unconformity is interpreted as an eroded extensional detachment, explaining the  
1357 presence of high-strain lithologies (e.g. calc-schist; mylonite) near the top of the Malatya  
1358 metamorphics (Fig. 16i), and also as clasts in the overlying Kemaliye Formation. The Munzur  
1359 and Köseyahya thrust sheets were later re-activated and thrust farther south over the  
1360 Kemaliye Formation in the above areas, probably during the Mid-Late Eocene (Figs. 22a).

1361 The exposure of serpentinised harzburgite with small granitic intrusions that is sliced  
1362 between the Malatya metamorphics and the Kemaliye Formation ENE of Begre (Fig. 22a) is  
1363 interpreted as a fragment of the Göksun ophiolite and its granitic intrusions, as widely  
1364 exposed farther south. Compressional deformation (Mid-Late Miocene?) caused the cross-  
1365 cutting cleavage and cataclasis observed within the siliciclastic matrix of the Kemaliye  
1366 Formation in the south (Nurhak Dağı; Area 3B; see above). The overall evidence points to  
1367 complex multiphase displacement involving both the Malatya (Keban) metamorphics and  
1368 the Munzur-Köseyahya carbonate platform, during Late Cretaceous, Mid-Late Eocene and  
1369 Mid-Late Miocene (?).

1370

### 1371 12.3. Reconstruction of the allochthonous Tauride platform

1372

1373 Alternatives are: First, the Neritic-pelagic (Köseyahya) unit represents a basin within the  
1374 Munzur shelf. Secondly, the Munzur carbonate platform succession passed northwards into  
1375 the Neritic-pelagic (Köseyahya) platform (i.e. half-ramp) and then into the ocean (Fig. 26  
1376 a,b ) (preferred reconstruction).

1377 The first alternative (intra-platform basin) is hinted by the structural position of the  
1378 Neritic-pelagic (Köseyahya) succession beneath the main Munzur thrust sheet in the  
1379 Southern allochthon (Area 4; Fig. 9). However, against this: (1) No marginal facies of an  
1380 intra-platform basin are exposed; (2) The Neritic-pelagic thrust sheet also occurs above the  
1381 Munzur thrust sheet in the Northern allochthon suggesting that it restores to the north,  
1382 regionally (MTA, 2011; Robertson et al., 2013b). In the second, preferred option, initial  
1383 southward emplacement of the Tauride platform units during the latest Cretaceous (see  
1384 above) was accompanied by complex out-of-sequence thrusting, explaining why the Neritic-

1385 pelagic (Köseyahya) thrust sheet is locally above the main Munzur thrust sheet (e.g. Area 4;  
1386 Fig. 9). The distal edge of the Neritic-pelagic (Köseyahya) platform is therefore represented  
1387 by the Pelagic (Gülbahar) unit, with oceanic crust, including inferred seamounts to the north  
1388 (Fig. 28c,d).

1389

#### 1390 12.4. Ophiolite and melange emplacement; relation to units farther north

1391

1392 The East Tauride SSZ-type ophiolites were emplaced southwards onto the Tauride platform,  
1393 represented by the Munzur and Neritic-pelagic (Köseyahya) successions, together with  
1394 passive margin slope units (Pelagic (Gülbahar) unit) and oceanic sediments and igneous  
1395 rocks (accretionary melanges) (Figs. 28 e; 29 a-c). The driving force in the southward  
1396 emplacement was the collision of the regional-scale supra-subduction zone Tauride  
1397 ophiolite with the Tauride passive margin (Robertson et al., 2013b). The inferred tectonic  
1398 organisation at the end of the Cretaceous is summarised in Figure 30. By the late  
1399 Maastrichtian, the Malatya metamorphics were partially exhumed and eroded, while the  
1400 ophiolites were also partially eroded, producing a variable palaeotopography that was  
1401 smoothed by clastic debris and transgressed by a shallow sea; this deepened in places  
1402 during the Palaeocene, as indicated by fragmentary pelagic carbonates (Fig. 21e, f).

1403 Alternatives for the source of the ophiolites are:

1404 Option 1: All of the ophiolites, including those overlying the Arabian continent were derived  
1405 from a single Mesozoic Tethys to the north (Ricou et al., 1984) (Fig. 31 ai-aii), although this is  
1406 generally discounted nowadays (Robertson and Dixon, 1984; Stampfli and Borel, 2002;  
1407 Sosson et al., 2010; Rolland et al., 2012; van Hinsbergen et al., 2020);

1408 Option 2: The ophiolites in the area studied (e.g. Pınarbaşı, Divriği) and those to the south of  
1409 the Malatya Metamorphics (Göksun (N Berit), Kömürhan, İspendere) were derived from a  
1410 single oceanic basin located within Neotethys to the east and northeast (Stampfli et al.,  
1411 2001; Stampfli and Borel, 2002; Moix et al., 2008; Sosson et al., 2010; Rolland et al., 2012,  
1412 2016, 2020; van Hinsbergen et al., 2020; see Fig. 31 bi-bii).

1413 In one such scenario (Maffione et al., 2017), oceanic lithosphere was generated by  
1414 intra-oceanic SSZ-spreading, followed by generally southwestward roll-back and c. 90°  
1415 anticlockwise rotation of the subducting oceanic plate. Collision with continental blocks  
1416 emplaced ophiolites both southwards (i.e. Southern allochthon) and also northwards (i.e.

1417 Göksun (N Berit), Kömürhan, İspendere) onto the Malatya metamorphic crust. The  
1418 metamorphism relates to attempted bidirectional subduction during ophiolite emplacement  
1419 (Fig. 30). An Inner Tauride basin (rift or small ocean) did not exist or, if present, sutured  
1420 prior to overthrusting by the late Cretaceous ophiolites (Poisson et al., 1996; Hinsbergen et  
1421 al., 2016).

1422 In another, related scenario, the ophiolites were emplaced generally towards the  
1423 south-west, over a single Anatolide-Tauride-S Armenian continent (i.e. without an Inner  
1424 Tauride ocean) during the late Cretaceous (c. 75 Ma), all derived from the northern  
1425 Neotethys. The ophiolites of the northern Neotethys (İzmir-Ankara-Erzincan suture zone)  
1426 correlate with those of the Lesser Caucasus in Armenian and Georgia to the east,  
1427 representing remnants of an enormous (700 km long x 1-200 km wide) slab of oceanic  
1428 lithosphere that was emplaced onto continental crust during latest Cretaceous time (Sosson  
1429 et al., 2010; Rolland et al., 2012, 2016, 2020; Rolland, 2017; Hässig et al., 2013a, b).  
1430 Metamorphic soles of all of the ophiolites are similar in age (to within 10 Ma) suggesting  
1431 that the ophiolites were emplaced together. Subduction of the ocean was either  
1432 northwards, away from the continent (Sosson et al., 2010; Rolland et al., 2012, 2020), or  
1433 southwards, towards the continent (Hässig et al., 2015). Southward obduction was  
1434 facilitated by Cretaceous within-plate magmatism, documented in the Lesser Caucasus; this  
1435 rendered the ophiolitic lithosphere relatively hot and mobile at the time of emplacement  
1436 (Hässig et al., 2016). Syn-post emplacement extensional core-complex development thinned  
1437 the oceanic lithosphere and facilitated southward emplacement of ophiolites and related  
1438 continental margin units in this interpretation (Rolland et al., 2020).

1439 The above option (in its variants) is also problematic: (1) The allochthonous Tauride  
1440 units restore as a Permian-Triassic to Late Cretaceous rift/passive margin to an oceanic  
1441 basin further north. The emplacement of the continental margin, oceanic crust (melange)  
1442 and ophiolitic units are intimately related, coeval, and cannot be separated into a sutured  
1443 Inner Tauride Basin and overthrust ophiolites (relevant to the Maffione et al., 2017 model);  
1444 (2) the ophiolites in the E Taurides (e.g. Pınarbaşı and Divriği) are Late Cretaceous (Parlak et  
1445 al., 2013), whereas ophiolites further north within the Ankara-Erzincan suture zone  
1446 (northern Neotethys) are Early- Late Jurassic (Dilek and Thy, 2006; Robertson et al., 2013c;  
1447 Çelik et al., 2013; Hässig et al., 2013). Both ophiolites formed in a supra-subduction setting,  
1448 apparently related to northward subduction and cannot be treated as a single ophiolite of



1449 the similar age and tectonic setting (cf. Rolland et al., 2020); (3) Regional mapping (Bedi and  
1450 Yusufoglu, 2018) and our structural data (Fig. 26) are consistent with generally N to S  
1451 emplacement of the allochthonous Tauride units (in present coordinates) during the latest  
1452 Cretaceous (e.g. Area 2), without evidence of thrust sheets traversing the area obliquely, as  
1453 suggested by hypothesis two (cf. van Hinsbergen et al., 2016; Maffione et al., 2017); (4)  
1454 Evidence was not observed in our present field area to support emplacement of the Late  
1455 Cretaceous ophiolites by core complex-related gravity sliding (Hässig et al., 2016; Rolland et  
1456 al., 2020). Instead, the field evidence suggests that the ophiolites were relatively intact  
1457 when emplaced but were thinned in response to later multi-phase deformation and erosion.

1458         Option 3. The Tauride and Pontide-Lesser Caucasus ophiolites represent different  
1459 supra-subduction spreading events, which both culminated in Late Cretaceous regional  
1460 ophiolite emplacement (Parlak et al., 2012; Robertson et al., 2013c) (Fig. 31ci, cii). During  
1461 the Triassic, sea-floor spreading created oceanic lithosphere to the north of the Tauride-  
1462 Anatolide continental block. The Kırşehir continental unit represents a rifted continental  
1463 fragment with oceanic lithosphere potentially to the south and the north (e.g. Görür, et al.,  
1464 1984; Robertson et al., 2012; Barrier et al., 2018). The Jurassic Pontide-Lesser Caucasus  
1465 ophiolite formed in the Early-Mid Jurassic when oceanic lithosphere to the north of the  
1466 Kırşehir continental unit started to subduct northwards (Dilek and Thy, 2006; Robertson et  
1467 al., 2013c; Topuz et al., 2013a). During the Late Cretaceous, plate convergence triggered the  
1468 genesis of the Late Cretaceous Tauride ophiolites above a N-dipping subduction zone. To the  
1469 west and east of the Kırşehir continental unit Jurassic and Cretaceous oceanic crust were  
1470 effectively contiguous with no exposed intervening suture. The Tauride ophiolites were  
1471 obducted by regional trench-passive margin collision during the latest Cretaceous, which  
1472 emplaced the Late Cretaceous ophiolites and related melanges throughout the eastern,  
1473 central and western Taurides as a whole (Görür et al., 1984; Andrew and Robertson, 2002;  
1474 Clark and Robertson, 2002; Okay et al., 2001; Kadioğlu et al., 2006; Nairn et al., 2013,  
1475 Robertson et al., 2013c; Lefebvre et al., 2013b; Darin et al., 2018; Scleiffarth et al., 2018;  
1476 Legeay et al., 2019). The leading of the colliding Tauride passive margin, represented by the  
1477 Anatolide crustal block, subducted and underwent HP-LT metamorphism (Pourteau et al.,  
1478 2010, 2013). Uncertainties with the above option include: i) The absence of an exposed  
1479 suture between the E Taurides and Pontide ophiolites, although one may exist subsurface;  
1480 ii) The lack of definitive evidence that Late Cretaceous ophiolites farther west (i.e. Pozanti-

1481 Karsanti and Alihoca ophiolites) originated to the south of the Kirşehir crustal block. In  
1482 summary, the evidence discussed in this paper is consistent with, but not definitive of,  
1483 ophiolite emplacement from an Inner Tauride ocean that was located to the south of the  
1484 Mid-Late Jurassic oceanic crust that characterises the İzmir-Ankara-Erzincan suture zone.

1485

1486 14.5. Malatya metamorphics: relation to adjacent crustal units

1487

1488 There are three main options:

1489 A first option is that the Malatya metamorphics directly correlate with the Afyon zone  
1490 (Anatolides). The Afyon zone (Bolkar nappe) is restored to a northerly position relative to  
1491 the unmetamorphosed Aladağ nappe (Özgül, 1984; Pourteau et al., 2010, 2013; Mackintosh  
1492 and Robertson, 2012). By extension, the Munzur-Köseyahya platform originated as the  
1493 southward extension of the Malatya carbonate platform. Problems, however, with this are:  
1494 (1) The Malatya metamorphics are cut by the c. 88-82 Ma Baskil granitoids, which are  
1495 attributed to northward subduction from an oceanic basin to the south (Berit ocean),  
1496 suggesting a relatively southerly location (Rızaoğlu et al., 2006, 2009; Karaoğlu et al., 2012,  
1497 2016) (Fig. 30); (2) In contrast, the Afyon zone lacks comparable intrusives suggesting a  
1498 different palaeogeographic setting; (3) Option 1 implies northward deep-level  
1499 underthrusting of the Malatya platform, followed by exhumation, large-scale out-of-  
1500 sequence southward thrusting to place the metamorphics in their present structural order  
1501 beneath the allochthonous Tauride platform units (van Hinsbergen et al., 2020). However,  
1502 there is no obvious evidence of such regional-scale re-thrusting during either the latest  
1503 Cretaceous or the Eocene regional tectonic events (e.g. metamorphic klippen or foredeeps  
1504 with metamorphic detritus are absent). Regional southward emplacement of the northerly  
1505 ophiolites (Göksun (N Berit), Kömürhan, İspendere) over the entire Tauride platform,  
1506 followed by re-imbrication beneath, as proposed by van Hinsbergen et al. (2020), is also  
1507 problematic. The base of the tectonic contact between the Malatya metamorphics and the  
1508 Göksun ophiolite beneath is cut and sealed by the 83-81 Ma (Santonian-Campanian) Esence  
1509 granites (Karaoğlu et al., 2016), whereas the northerly ophiolites were emplaced  
1510 southwards only after deposition of the Albian-Santonian Kızılkandil Formation and the  
1511 overlying late Campanian-late Maastrichtian Kemaliye Formation (based on nannofossil  
1512 dating).

1513 A second option is that the Afyon zone and the Malatya metamorphics do indeed  
1514 correlate laterally but that the Munzur-Köseyahya platform units represent a separate  
1515 platform that was located to the northeast of the Geyik Dağ (Tauride autochthon). The  
1516 main problem with this interpretation is the absence of any preserved platform-slope facies  
1517 (e.g., deep-water slope facies and radiolarites) that could indicate the presence of a rifted  
1518 margin to the Malatya platform in the north (Perinçek and Kozlu, 1984; Kozlu et al., 1990;  
1519 Bedi et al., 2009; Robertson et al., 2013b; Bedi and Yusufoglu, 2018). Also, there is no  
1520 evidence of a southern rifted margin to the Munzur-Köseyahya platform in the south, which  
1521 would be expected in this alternative. However, it is possible that such margin units existed  
1522 but are not exposed.

1523 A third option is that the present regional-scale tectono-stratigraphy retains the latest  
1524 Cretaceous emplacement organisation. In this case, the Malatya and Afyon units, despite  
1525 undergoing similar metamorphism, did not form a continuous litho-tectonic unit. The Afyon  
1526 zone originated further northwest, whereas the Malatya metamorphic originated further  
1527 southeast (possibly offset by a c. N-S transform). The Munzur-Köseyahya platform formed a  
1528 separate crustal block to the northeast. The Malatya metamorphics originated by collapse of  
1529 the putative basin between the separate Malatya and Munzur Köseyahya platforms (see  
1530 above). Such a basin might have formed during Triassic rifting. Collapse of the inferred intra-  
1531 platform basin might have been driven by compression between two N-dipping subduction  
1532 zones (Berit/Göksun in the S; Inner Tauride in the N).

1533 In the absence of field evidence of major tectonic re-ordering as required in options 1  
1534 and 2, we favour option 3, which implies major palaeogeographic changes between the  
1535 central and eastern Taurides. It seems likely that the central Tauride platform (Geyik Dağ)  
1536 narrowed eastwards (Fig. 30), close to the future position of the neotectonic Sürgü-Misis  
1537 fault zone. To the west, the southern part of the Tauride platform (Geyik Dağ) was not  
1538 covered by the late Cretaceous south-moving allochthons. In contrast, farther east part of  
1539 the Tauride platform represented by the Malatya metamorphics, underthrust/subducted  
1540 northwards beneath more northerly Tauride crust (Munzur-Köseyahya platfors) (Fig. 30cii).

1541 Restoring the reported c. 29 km left-lateral offset along the neotectonic Malatya-  
1542 Ovacık Fault Zone (Westaway and Arger, 2001) still leaves the type outcrop of the Munzur  
1543 platform in the Munzur Dağları (Fig. 2) c. 80 km to the north of its counterpart within the  
1544 Southern allochthon (Munzur thrust sheets). The Tauride (Munzur) platform could,

1545 therefore, have stepped northwards towards the northeast, bounded by one or more c. N-S  
1546 transcurrent faults. However, it is unclear whether this would be entirely a Mesozoic  
1547 palaeogeographic feature or if it could relate to latest Cretaceous-Eocene (pre-Neogene)  
1548 tectonics. In either case, pre-existing faults are likely to have been re-activated to form  
1549 many of the major neotectonic faults seen today. In the absence of continuous exposure, or  
1550 subsurface evidence (e.g., borehole or seismic reflection) it is, therefore, uncertain as to  
1551 whether or not the South Armenian platform in the Lesser Caucasus simply represents the  
1552 eastward extension of the Tauride continent. Previously, the two platform exposures were  
1553 inferred to be parts of a single large continental unit mainly because of similar late  
1554 Cretaceous ophiolite emplacement in both areas (Sosson et al., 2010; Rolland et al., 2012).  
1555 However, an origin as two separate platforms is not precluded.

1556 The Malatya and Bitlis-Pütürge metamorphic units (Fig. 1) have also been considered to  
1557 represent, respectively westerly and more easterly segments of a single southerly active  
1558 margin of the Tauride continent, with the Southern Neotethys to the south (Barrier et al.,  
1559 2018). However, the Malatya and Bitlis-Pütürge continental units are separated by the Late  
1560 Cretaceous supra-subduction Göksun (N Berit), Kömürhan, İspendere and Yüksekova  
1561 ophiolites, interpreted as an intervening ocean basin (Robertson et al., 2006, 2012; Rolland  
1562 et al., 2012; Candan et al., 2014; Çetinkaplan et al., 2016; Barrier et al., 2018). The available  
1563 evidence is consistent with the existence of a southerly oceanic basin (Berit, or Göksun  
1564 ocean) that subducted northwards beneath the Malatya-Tauride platform during latest  
1565 Cretaceous (Fig. 30). The ophiolites (Göksun, İspendere and Kömürhan), dated at c. 87-85  
1566 Ma, formed above a subduction zone and include immature arc volcanics (Parlak et al.,  
1567 2009). The volcanics of the above ophiolites can also be broadly correlated with the Late  
1568 Cretaceous Yüksekova complex (dated at c. 83-75 Ma) (Karaoğlan et al., 2013), which is  
1569 traditionally interpreted as an immature oceanic arc (e.g. Ural et al., 2015 and references).

1570 As noted above, the Göksun SSZ-type lithosphere was emplaced beneath the Malatya  
1571 Metamorphic crust, where both were intruded by subduction-related granitic rocks (88-82  
1572 Ma Baskil intrusives) (Karaoğlan et al., 2016; Parlak, 2006; Rızaoğlu et al., 2009). The Baskil  
1573 intrusives include shoshonitic compositions (dated at 74–72 Ma), suggestive of collisional  
1574 and/or post-collisional settings (Ertürk et al., 2018; Kuşcu et al., 2013; Sar et al., 2019). This  
1575 is consistent with the collision of the Bitlis-Pütürge continental units to the south with the  
1576 Tauride continent to the north (Malatya Metamorphics) thereby closing the Berit ocean. In

1577 many reconstructions, some oceanic crust (Southern Neotethys) existed between the Bitlis-  
1578 Pütürge continental units and the Arabian continent. The initial closure of this ocean basin  
1579 and collision with Arabia may have occurred during the Mid-Late Eocene, but the main  
1580 collision took place during the Mid-Late Miocene (Aktaş and Robertson, 1984; Yılmaz, 1993;  
1581 Robertson et al., 2012a; Rolland et al., 2012, 2020; Barrier et al., 2018; van Hinsbergen et  
1582 al., 2020).

1583

## 1584 **Conclusions**

1585

1586 -The well-exposed eastern Taurides provide important insights into Tethyan  
1587 palaeogeography and tectonic development, including the unusual Gürün curl structure.

1588 -The region is restored as part of the northern rifted margin of the Tauride continent.

1589 -Rifting took place during the Triassic, separating a shallow-water carbonate platform to the  
1590 south from a deep-water proximal to distal slope and ocean basin to the north (Inner  
1591 Tauride ocean).

1592 -The regional Tauride carbonate platform (Geyik Dağ) is proposed to have narrowed and  
1593 become more palaeogeographically varied towards the eastwards, mainly represented, in  
1594 the E Taurides, by the Malatya Metamorphics and the unmetamorphosed Munzur and  
1595 Köseyahya platform units.

1596 -The restored northern part of the shallow-water combined Munzur-Köseyahya platform  
1597 subsided during the Mid-Jurassic to form a gently sloping, deeper-water ramp near, or  
1598 beneath, the carbonate compensation depth.

1599 -The Munzur-Köseyahya platform slope was covered by pelagic carbonate during the Late  
1600 Cretaceous, probably related to regional tectonic subsidence (rather than global sea-level  
1601 rise).

1602 -Dismembered deep-sea sedimentary and volcanic units exposed over a wide area are  
1603 restored as the former Triassic-Cretaceous deep-water passive margin slope/base of slope  
1604 of the Mesozoic carbonate platform (Pelagic (Gülbahar) unit).

1605 -Oceanic lithosphere formed above a subduction zone in the ocean (Inner Tauride ocean),  
1606 generally to the north (Pınarbaşı, Dağlıca, Hekimhan, Kuluncak and Divriği (and Güneş)  
1607 ophiolites), with associated formation of ophiolite metamorphic sole (although only locally  
1608 preserved).

1609 -Local, fragmentary successions of mainly within-plate-type basalts and radiolarian  
1610 cherts/pelagic limestones are interpreted as accreted/emplaced Jurassic-Cretaceous  
1611 oceanic seamounts.

1612 - Associated with emplacement of the Late Cretaceous ophiolites, the Tauride passive  
1613 margin underwent flexural loading and collapse to form a foredeep (late Campanian-  
1614 Maastrichtian). Talus in the form of gravity flows, blocks and disrupted sheets was shed into  
1615 the basin, mainly from the platform/slope units, and the advancing ophiolites/accretionary  
1616 melanges.

1617 -During the latest Cretaceous (late Campanian-late Maastrichtian), the SSZ ophiolites were  
1618 emplaced generally southwards onto the Tauride platform, in some areas as relatively intact  
1619 sheets (c. 6 km thick) (e.g. Pınarbaşı ophiolite), but elsewhere as dismembered units,  
1620 melanges and ophiolite-related debris flows (i.e. Dağlıca ophiolite and melange).

1621 -During its late Cretaceous southward tectonic transport, the allochthonous carbonate  
1622 platform was locally re-thrust, in places putting the restored southerly neritic carbonate  
1623 platform (Munzur thrust sheet) over the more northerly-derived deeper water facies  
1624 (Köseyahya thrust sheet).

1625 -Mixing of clastic debris (Kemaliye Formation) that derived from both the over-riding  
1626 Tauride allochthons and the Malatya Metamorphics shows that both were tectonically  
1627 juxtaposed (in close proximity) during the latest Cretaceous regional emplacement.

1628 -The Malatya Metamorphics were at least partially exhumed by the late Maastrichtian as  
1629 they are covered and sealed by latest Cretaceous sediments, that include metamorphic and  
1630 granitoid debris.

1631 -The Malatya Metamorphics were tectonically juxtaposed with the Göksun (and related  
1632 ophiolites) to the south during the latest Cretaceous. Both are cut and sealed by the 88-82  
1633 Ma Baskil granitoids. The latest Cretaceous marine sedimentary cover of the Göksun  
1634 ophiolite includes detritus from both the metamorphics and the unmetamorphosed Tauride  
1635 units, pointing to rapid exhumation.

1636 - Following Eocene shelf-depth deposition, folding and re-thrusting took place widely during  
1637 the Mid-Late Eocene. However, the co-intrusion of the Güksun ophiolite and Malatya  
1638 Metamorphics by the Late Cretaceous granites (Baskil granites) shows that these two  
1639 regional-scale crustal units were not displaced a large distance relative to each other (i.e.  
1640 >several km) after the latest Cretaceous.

1641 -Allochthonous units were first juxtaposed with the relatively autochthonous Gürün  
1642 platform succession (as presently exposed) during Mid-Late Eocene. In the absence of clear  
1643 evidence that the allochthonous Tauride units to the north (Northern allochthon) were  
1644 emplaced southwards over the autochthonous Gürün platform during this time, an  
1645 alternative is that the Southern allochthon and the Gürün platform/Northern allochthon  
1646 were brought together by >60 km of right-lateral transport during Mid-Late Eocene (i.e. as a  
1647 result of collision-related 'tectonic escape').

1648 -The Mid-Late Eocene deformation (folding and thrusting) is explained by thick-skinned  
1649 deformation, driven by suturing of the İzmir-Ankara-Erzincan ocean (northern Neotethys).

1650 - Mid-Late Miocene folding and thrusting (northwards in several areas) is explained by  
1651 suturing of the Southern Neotethys and collision with Arabia.

1652 -The available evidence is mainly consistent with the former existence of an Inner Tauride  
1653 ocean, comprising Late Cretaceous supra-subduction zone oceanic crust, that was separate  
1654 from more northerly supra-subduction zone oceanic crust, of Mid-Late Jurassic age, within  
1655 the İzmir-Ankara-Erzincan suture zone farther north.

1656

## 1657 **Acknowledgements**

1658

1659 We thank the DARIUS programme for financial support to carry out the fieldwork.

1660 Additional funding from the John Dixon Memorial Fund assisted with the laboratory-based  
1661 studies. Güzide Önal assisted with drawing the diagrams. We thank Tumur Ustaömer and

1662 Rolland Oberhansli for discussion. The manuscript benefitted from reviews by Aral Okay and  
1663 Yann Rolland, and advice from the editor, Ibrahim Uysal.

1664

1665 (This research did not receive any specific grant from funding agencies in the public,  
1666 commercial, or not-for-profit sectors.)

1667

1668

1669

1670 **References**

1671

1672 Aktaş, G., Robertson, A.H.F., 1984. The Maden Complex, S E Turkey: Evolution of a  
1673 Neotethyan continental margin. In: Dixon, J.E., Robertson, A.H.F. (Eds.), The  
1674 Geological Evolution of the Eastern Mediterranean. Geological Society, London,  
1675 Special Publications, 17, 375–402.

1676 Aktimur, H.T., 1988. 1:100,000-scale Turkish geological map series, Divriği-F26 map. Mineral  
1677 Research and Exploration Institute of Turkey (MTA), Ankara (in Turkish).

1678

1679 Aktimur, H.T., Atalay, Z., Ateş, S., Tekerli, M.E., Yurdakul, M.E., 1988. Geology of the area  
1680 between Munzur Mountains and Çavuşdağı. Mineral Research and Exploration  
1681 Institute of Turkey (MTA), Report No. 301, 102p. (in Turkish).

1682 Andrew, T., Robertson, A.H.F., 2002. The Beyşehir–Hoyran–Hadim Nappes: genesis and  
1683 emplacement of Mesozoic marginal and oceanic units of the northern Neotethys  
1684 in southern Turkey. *Journal of the Geological Society, London* 159, 529–543.

1685 Atabey, E., 1993. Stratigraphy of Gürün autochthonous (Gürün-Sarız arası), Doğu Toroslar-GB  
1686 Sivas. *Türkiye Jeoloji Bülteni* 36/2, 99-113 (in Turkish).

1687

1688 Atabey, E., 1995. Geological evolution and sedimentology of the Gürün autochthone,  
1689 Department of Geological Engineering, Ankara University, Unpublished PhD thesis  
1690 (in Turkish).

1691

1692 Atabey, E., Aktimur, H.T., 1997. 1:100,000 Geological Map of Turkey, 48 (Sivas-G24), Mineral  
1693 Research and Exploration Institute of Turkey (MTA), Ankara (in Turkish).

1694

1695 Atabey, E., Bağırşakçı, S., Canpolat, M., Gökkaya, K.Y., Günal, S., Kılıç, N., 1994. Geology of  
1696 the area between Gürün-Kangal (Sivas) and Darende-Hasançelebi. Mineral  
1697 Research and Exploration Institute of Turkey (MTA), Report 9760 (unpublished) (in  
1698 Turkish).



- 1699
- 1700 Atabey, E., Bağırsakçı, K.Y., Gökkaya, S., Günal, S., Kılıç, N., Canpolat, M., 1997. 1:100,000  
1701 Geological Map of Turkey, 49 (Elbistan-H24), Mineral Research and Exploration  
1702 Institute of Turkey (MTA), Ankara (in Turkish).  
1703
- 1704 Aziz, A., Eraman, B., Kurt, G., Meşhur, M., 1982. Geological report for the area of Pınarbaşı-  
1705 Sarız-Gürün. Turkish Petroleum Company, Unpublished Report, 1601p. (in  
1706 Turkish).  
1707
- 1708 Barrier, E., Vrielynck, B., Brouillet, J.F., Brunet, M.F., 2018. Paleotectonic Reconstruction of  
1709 the Central Tethyan Realm. Tectono-Sedimentary-Palinspastic Maps from Late  
1710 Permian to Pliocene. CCGM/CGMW, Paris, Atlas of 20 maps (scale: 1/15.000.000).  
1711
- 1712 Bedi, Y., Usta, D., 2006. Palaeozoic stratigraphy of Tufanbeyli-Feke-Kozan regions (Eastern  
1713 Taurides). 6<sup>th</sup> Workshop of Stratigraphy Committee of Turkey: Lithostratigraphic  
1714 Nomenclature of PreCambrian - Palaeozoic units of the Taurides and SE Anatolia,  
1715 abstract book, p. 22-23, Ankara (in Turkish).  
1716
- 1717 Bedi, Y., Yusufoglu, H., 2018. 1:000,000 scale Türkiye Jeoloji Haritaları Serisi (Turkish  
1718 geological map series), Malatya-L49 Parftası, No. 261 (in Turkish).  
1719
- 1720 Bedi, Y., Senel, M., Usta, D., Özkan, M. K., Beyazpırınç, M., 2004. The geological properties of  
1721 Binboğa Mountains and their correlation with similar units in west-central  
1722 Taurides. 57<sup>th</sup> Geological Congress of Turkey, Abstracts, 270-271.  
1723
- 1724 Bedi, Y., Usta D., Özkan, M.K., Beyazpırınç, M., Yıldız, H., Yusufoglu, H., 2005. The tectono-  
1725 stratigraphic characteristics of allochthonous sequences in Eastern Taurides. 58<sup>th</sup>  
1726 Geological Congress of Turkey, Abstracts, 262-263.  
1727
- 1728 Bedi Y., Yusufoglu, H., Beyazpırınç, M., Özkan, M.K., Usta D., Yıldız, H., 2009. Geodynamical  
1729 evolution of the Eastern Taurides (Afşin-Elbistan-Göksun-Sarız area). Mineral

- 1730 Research and Exploration Institute of Turkey (MTA), Report No. 11150, 388 p. (in  
1731 Turkish).
- 1732
- 1733 Bedi, Y., Yusufoglu, H., Usta, D., Okuyucu, C., 2012. The presence of the Aladağ and Yahyalı  
1734 Nappes in the Eastern Taurides (Afşin-Malatya) and their tectonostratigraphic  
1735 characteristics. In: Paleozoic of Northern Gondwana and its petroleum potential a  
1736 field workshop, Sept. 9<sup>th</sup> European Association of Geoscientists and Engineers, p.  
1737 cp-367.
- 1738
- 1739 Bedi, Y., Krystyn, K., Tekin, U.K., Okuyucu, C., Demiray, D.G.S., 2016. A geosite area:  
1740 ammonoid assemblages of late Carnian age in the Domuzdağ Nappe (Eastern  
1741 Taurides, Elbistan, Kahramanmaraş), 69<sup>th</sup> Geological Congress of Turkey, 11-15  
1742 April 2016, Ankara, 215-215.
- 1743 Bedi, Y., Yusufoglu, H., Tekin, U.K., Usta, D., 2017. The tectonostratigraphic characteristics of  
1744 autochthonous and allochthonous sequences exposed among Tufanbeyli (Adana),  
1745 Elbistan (K.Maraş) and Malatya, eastern Taurides. Abstracts of the 70<sup>th</sup> Geological  
1746 Congress of Turkey, 10-14 April, Ankara, 22-23.
- 1747 Beyazpırınç, M., Akçay, A.E., 2013. The tectono-stratigraphic features of metamorphites in  
1748 Alacahan-Çetinkaya region (Kangal, Sivas). Bulletin of Mineral Research and  
1749 Exploration Institute of Turkey (MTA), 147, 19-29 (in Turkish).
- 1750 Bilgiç, T., 2008a. 1:100,000 Türkiye Jeoloji Haritaları, No: 85. Divriği-J39 Paftası (Divriği area),  
1751 Mineral Research and Exploration Institute of Turkey (MTA) (in Turkish).
- 1752
- 1753 Bilgiç, T., 2008b. 1:100,000 Türkiye Jeoloji Haritaları, No: 85. Divriği-J40 Paftası (Divriği area),  
1754 Mineral Research and Exploration Institute of Turkey (MTA) (in Turkish).
- 1755
- 1756 Bilgiç, T., 2008c 1:100,000 Türkiye Jeoloji Haritaları, No: 85. Divriği-J41 Paftası (Kemaliye  
1757 area), Mineral Research and Exploration Institute of Turkey (MTA) (in Turkish).
- 1758

- 1759 Booth, M.G., Robertson, A.H.F., Taslı, K., İnan, N., Ünlügenç, U.C., Vincent, S., 2013. Two-  
1760 stage development of the Late Cretaceous to Late Eocene Darende Basin  
1761 implications for closure of Neotethys in central eastern Anatolia (Turkey). In:  
1762 Robertson, A.H.F., Parlak, O., Ünlügenç, U.C. (Eds.), Geological Development of  
1763 Anatolia and the Easternmost Mediterranean Region. Geological Society, London,  
1764 Special Publications 372, pp. 385-420.  
1765
- 1766 Booth, M.G., Robertson, A.H.F., Taslı, K., İnan, N., 2014. Late Cretaceous to Late Eocene  
1767 Hekimhan Basin (Central eastern Turkey), as a supra-ophiolite  
1768 sedimentary/magmatic basin related to the latest stages of closure of Neotethys.  
1769 Cenozoic extensional tectonics in western Anatolia, Turkey. *Tectonophysics* 635,  
1770 6–32.  
1771
- 1772 Bosellini, A., Winterer, E.L., 1975. Pelagic limestone and radiolarite of the Tethyan Mesozoic:  
1773 a genetic model. *Geology* 3, 279-282.  
1774
- 1775 Bozkaya, Ö., Yalçın, H., Başbüyük, Z., Özfırat, O., Yılmaz, H., 2007. Origin and evolution of the  
1776 Southeast Anatolian metamorphic complex (Turkey). *Geologica Carpathica* 58,  
1777 197-210.  
1778
- 1779 Boztuğ, D., Harlavan, Y., Arehart, G.B., Satır, M., Avcık, N., 2007. K-Ar age, whole-rock and  
1780 isotope geochemistry of A-type granitoids in the Divriği-Sivas region, eastern-  
1781 central Anatolia, Turkey. *Lithos* 97, 193-218.  
1782
- 1783 Camuzcuoğlu, M., Bağcı, U., Koepke, J., Wolff, P.E., 2017. Tectonic significance of the  
1784 cumulate gabbros within Kuluncak ophiolitic suite (Malatya, SE Turkey) inferred  
1785 from geochemical data. *Ofioliti* 42, 81-103.  
1786
- 1787 Candan, O., Koralaya, E., Çetinkaplan, M., Ersoy, Y., Topuz, G., Oberhaensli, R., Lid, Q.,  
1788 Yiğitbaş, E., 2014. Late Cretaceous-Eocene tectonometamorphic evolution of the  
1789 Berit meta-ophiolites and continental crustal units, north of  
1790 Kahramanmaraş/Turkey, 67<sup>th</sup> Geological Congress of Turkey, April, 560-561.

1791

1792 Çelik, Ö.F., Chiaradia, M., marzoli, A., Billor, Z., Marschik, R., 2013. The Eldivan ophiolite and  
1793 volcanic rocks in the İzmir–Ankara–Erzincan suture zone, Northern Turkey:  
1794 Geochronology, whole-rock geochemical and Nd–Sr–Pb isotope characteristics. *Lithos*  
1795 172-173, 31-46.

1796

1797 Çetinkaplan, M., Pourteau, A., Candan, O., Koralay, O.E., Oberhänsli, R., Okay, A.İ., 2016. P-T-  
1798 t evolution of eclogite/blueschist facies metamorphism in Alanya Massif: Time and  
1799 Space relations with HP event in Bitlis Massif, Turkey. *International Journal of Earth*  
1800 *Sciences* 105, 247–281.

1801

1802 Clark, M.S., Robertson, A.H.F., 2002. The role of the early Cenozoic Ulukışla Basin, southern  
1803 Turkey in suturing of the Mesozoic Tethys ocean. *Journal of the Geological Society,*  
1804 *London* 159, 673–690.

1805

1806 Cohen, K.M., Harper, D.A.T., Gibbard, P.L., 2020. ICS International Chronostratigraphic Chart,  
1807 2020/01. International Commission on Stratigraphy, IUGS. [www.stratigraphy.org](http://www.stratigraphy.org)

1808

1809 Collins, A.S., Robertson, A.H.F., 1997. Lycian melange, southwestern Turkey: an emplaced  
1810 Late Cretaceous accretionary complex. *Geology* 25, 25–258.

1811

1812 Collins, A., Robertson, A.H.F., 1998. Processes of Late Cretaceous to Late Miocene episodic  
1813 thrust-sheet translation in the Lycian Taurides, southwestern Turkey. *Journal of*  
1814 *the Geological Society, London* 155, 759-772.

1815

1816 Collins, A., Robertson, A.H.F., 1999. Evolution of the Lycian allochthon, western Turkey, as a  
1817 north-facing Late Palaeozoic–Mesozoic rift and passive continental margin.  
1818 *Geological Journal* 34, 107–138.

1819

1820 Darin, M., Umhoefer, P.J., Thomson, S., 2018. Rapid late Eocene Exhumation of the Sivas  
1821 Basin (Central Anatolia) driven by initial Arabia-Eurasia collision. *Tectonics* 37,  
1822 3805-3833.

1823

1824 Demirtaşlı, E., Turhan, N., Bilgin, A.Z., Selim, M., 1984. Geology of the Bolkar Mountains, In:

1825 Tekeli, O., Göncüoğlu, M.C. (Eds.), Geology of the Taurus Belt. Proceedings

1826 International Symposium on the Geology of the Taurus Belt, Ankara, Turkey.

1827 Mineral Resources and Exploration Institute of Turkey, pp. 125-141.

1828

1829 Dilek, Y., Moores, E.M., 1990, Regional tectonics of the Eastern Mediterranean ophiolites, In:

1830 Moores, E.M., Panayiotou, A., Xenophontos, C., Ophiolites, Oceanic Crustal

1831 Analogues, Proceedings of the Symposium "Troodos 1987," Geological Survey

1832 Department, Nicosia, Cyprus, pp. 295–309.

1833

1834 Dilek, Y., Whitney, D.L., 1997. Counterclockwise P–T–t trajectory from the metamorphic sole

1835 of a Neotethyan ophiolite (Turkey). *Tectonophysics* 280, 295–310.

1836

1837 Dilek, Y., Thy, P., 2006. Age and petrogenesis of plagiogranite intrusions in the Ankara

1838 melange, central Turkey. *Island Arc* 15, 44–57.

1839

1840 Duman, T.Y., Emre, Ö., 2013. The East Anatolian fault: geometry, segmentation and jog

1841 characteristics, In: Robertson, A.H.F., Parlak, O., Ünlügenç, U.C. (Eds.), Geological

1842 Society, London Special Publication 372, pp. 495–529.

1843

1844 Dumitrica, P., Tekin, U.K, Bedi, Y., 2013. Taxonomic study of spongy spumellarian Radiolaria

1845 with three and four coplanar spines or arms from the middle Carnian (Late

1846 Triassic) of the Köseyahya nappe (Elbistan, SE Turkey) and other Triassic localities.

1847 *Paläontologische Zeitschrift Scientific Contributions to Palaeontology* 87, 345-395.

1848

1849 Ekici, T., Alpaslan, M., Parlak, O., Temel, A., 2007. Geochemistry of the Pliocene basalts

1850 erupted along the Malatya-Ovacık fault zone (MOFZ), eastern Anatolia, Turkey:

1851 implications for source characteristics and partial melting processes. *Chemie der*

1852 *Erde-Geochemistry* 67, 201–212.

1853

- 1854 Emre, Ö., Duman, T.Y., Özalp, S., Çan, T., Olgun, Ş., Elmacı, H., Şaroğlu, F., 2018. Active fault  
1855 database of Turkey. *Bulletin of Earthquake Engineering* 16, 3229–3275.  
1856
- 1857 Erdoğan, B., 1975. Geology of Gölbaşı region. TPAO Report No. 917 (unpublished) (in  
1858 Turkish).  
1859
- 1860 Erkan, E.N., Özer, S., Sümengen, M., Terlemez, İ., 1978. Geology of Sarız, Şarkışla, Gemerek,  
1861 Tomarza regions. Mineral Research and Exploration Institute of Turkey (MTA) Report  
1862 No: 5641, Ankara (unpublished), (in Turkish).  
1863
- 1864 Ertürk, M.A., Beyarslan, M., Chung, S.L., Lin, T.H., 2018. Eocene magmatism (Maden  
1865 Complex) in the Southeast Anatolian Orogenic Belt: magma genesis and tectonic  
1866 implications. *Geoscience Frontiers* 9, 1829–1847.  
1867
- 1868 Genç, Ş.C., Yiğitbaş, E., Yılmaz, Y., 1993. The geology of the Berit Metaophiolite. A. Suat Erk  
1869 Jeoloji Sempozyumu, Bildiriler Kitabı, pp. 37-52 (In Turkish with English abstract).  
1870
- 1871 Göncüoğlu, M.C., Göncüoğlu, Y., Kozur, H.W., Kozlu, H., 2004. Paleozoic stratigraphy of the  
1872 Geyik Dağ unit in the Eastern Taurides and implications for Gondwanian evolution.  
1873 *Geologica Carpathica* 55, 433-447.  
1874
- 1875 Görür, N., Oktay, F.Y., Seymen, İ., Şengör, A.M.C., 1984. Paleotectonic evolution of Tuz Gölü  
1876 Basin complex, central Turkey, In: Dixon, J.E. & Robertson, A.H.F. (Eds.), *The  
1877 Geological Evolution of the Eastern Mediterranean*. Geological Society Special  
1878 Publication, London 17, pp. 81-96.  
1879
- 1880 Görür, N., Şengör, A.M.C., Okay, A.İ., Tüysüz, O., Sakıncı, M., Yiğitbaş, E., Akkök, R., Özgül, N.,  
1881 Genç, T., Örçen, S., Ercan, T., Akyürek, B. Şaroğlu, F., 1998. Triassic to Miocene  
1882 Palaeogeographic Atlas of Turkey. İTÜ Maden Fak. Genel Anabilimdalı, Tübitak  
1883 Global Tektonik Araştırma Ünitesi), MTA Genel Müdürlüğü, Ankara (in Turkish).  
1884
- 1885 Graciansky, P.C. de, 1972. *Recherches géologiques dans le Taurus Lycien Occidental*. Thèse

1886 Doctorat d'Etat, Université de Paris-Sud, Orsay, France.

1887

1888 Gürbüz, K., Gül, M., 2005. Evolution of and factors controlling Eocene sedimentation in the  
1889 Darende-Balaban Basin, Malatya (Eastern Turkey). *Turkish Journal of Earth  
1890 Sciences* 14, 311-335.

1891

1892 Gutnic, M., Monod, O., Poisson, A., Dumont, J.-F., 1979. Géologie des Taurides Occidentales  
1893 (Turquie). *Mémoires de La Société Géologique de France* 137, 1-112.

1894

1895 Haq, B.U., 2014. Cretaceous eustasy revisited. *Global and Planetary Change* 113, 44-58.

1896

1897 Hässig, M., Rolland, Y., Sosson, M., Galoyan, G., Sahakyan, L., Topuz, G., Çelik, Ö.F., Avagyan,  
1898 A., Müller, C., 2013a. Linking the NE Anatolian and Lesser Caucasus ophiolites:  
1899 evidence for large scale obduction of oceanic crust and implications for the  
1900 formation of the Lesser Caucasus-Pontides Arc. *Geodinamica Acta* 26, 311–330.

1901

1902 Hässig, M., Rolland, Y., Sosson, M., Galoyan, G., Müller, C., Avagyan, A., Sahakyan, L., 2013b.  
1903 New structural and petrological data on the Amasia ophiolites (NW Sevan-Akera  
1904 suture zone, Lesser Caucasus): insights for a large-scale obduction in Armenia and  
1905 NE Turkey. *Tectonophysics* 588, 135-153.

1906

1907 Hässig, M., Rolland, Y., Sosson, M., 2017. From seafloor spreading to obduction: Jurassic–  
1908 Cretaceous evolution of the northern branch of the Neotethys in the Northeastern  
1909 Anatolian and Lesser Caucasus regions. In: Sosson, M., Stephenson, R. A., Adamia,  
1910 S.A. (Eds), Geological society, London, Special Publications, 428, 41-60.

1911

1912 Hässig, M., Rolland, Y., Sahakyan, L., Sosson, M., Galoyan, G., Avagyan, A., Bosch, D., Müller,  
1913 C., 2015. Multi-stage metamorphism in the South Armenian block during the Late  
1914 Jurassic to early Cretaceous: tectonics over south-dipping subduction of Northern  
1915 branch of Neotethys. *Journal of Asian Earth Sciences* 102, 4-23.

1916

1917 Hässig, M., Rolland, Y., Duretz, T., Sosson, M., 2016. Obduction triggered by regional heating

- 1918 during plate reorganization. *Terra Nova* 28, 76-82.
- 1919
- 1920 Hayward, A.B., Robertson, A.H.F., 1982. Direction of ophiolite emplacement inferred from  
1921 Cretaceous and Tertiary sediments of an adjacent autochthon, the Bey Dağları,  
1922 southwest Turkey. *Geological Society of America Bulletin* 93, 68-75.
- 1923
- 1924 İnan, S., İnan, N., 1988. Tecer limestone formation based on facies features. 42. Türkiye  
1925 Jeoloji Kurultayı, 15-19 Şubat, Ankara, Bildiri Özleri, p. 45 (in Turkish).
- 1926
- 1927 Juteau, T., 1980. Ophiolites of Turkey. *Ophioliti* 2, 199–238.
- 1928
- 1929 Kadioğlu, Y.K., Dilek, Y., Foland, K.A., 2006. Slab breakoff and syncollisional origin of the Late  
1930 Cretaceous magmatism in the Central Anatolian Crystalline Complex, Turkey, In:  
1931 Dilek, Y., Pavlides, S. (Eds.), *Postcollisional Tectonics and Magmatism in the*  
1932 *Mediterranean Region and Asia*. Geological Society of America Special Paper 409,  
1933 pp. 381–415.
- 1934
- 1935 Karaman T., Poyraz N., Bakırhan B., Alan İ., Kadıncık G., Yılmaz H., Kılınc F., 1993. Geology of  
1936 the Malatya-Doğanşehir-Çelikhan area. Mineral Research and Exploration  
1937 Institute, Turkey. Report 9587, pp. 1-54 (in Turkish).
- 1938
- 1939 Karaoğlu, F., Parlak, O., Klötzli, U., Thoni, M., Koller, F., 2012. U–Pb and Sm–Nd  
1940 geochronology of the ophiolites from the SE Turkey: implications for the  
1941 Neotethyan evolution. *Geodinamica Acta* 25, 146-161.
- 1942
- 1943 Karaoğlu, F., Parlak, O., Klötzli, U., Koller, F., Rızaoğlu, T., 2013. Age and duration of intra-  
1944 oceanic arc volcanism built on a suprasubduction zone type oceanic crust in  
1945 southern Neotethys, SE Anatolia. *Geoscience Frontiers* 4, 399-408.
- 1946
- 1947 Karaoğlu, F., Parlak, O., Hejl, E., Neubauer, F., Klötzli, U., 2016. Temporal evolution of the  
1948 active margin along the Southeast Anatolian Orogenic Belt (SE Turkey): Evidence  
1949 from U-Pb, Ar-Ar and fission track chronology. *Gondwana Research* 33, 190–208.



- 1950
- 1951 Kavak, K.S., Parlak, O., Temiz, H., 2017. Geochemical characteristics of ophiolitic rocks from  
1952 the southern margin of the Sivas basin and their implications for the Inner Tauride  
1953 Ocean, Central-Eastern Turkey. *Geodinamica Acta* 29, 160-180.
- 1954
- 1955 Kaya, A., 2016. Tectono-stratigraphic reconstruction of the Keban metamorphites based on  
1956 new fossil findings, Eastern Turkey. *Journal of African Earth Sciences* 124, 245-257.
- 1957
- 1958 Kaymakçı, N., İnceöz, M., Ertepinar, P., 2006. 3D-architecture and Neogene evolution of the  
1959 Malatya Basin: inferences for the kinematics of the Malatya and Ovacık fault  
1960 zones. *Turkish Journal of Earth Science* 15, 123–154.
- 1961
- 1962 Kozlu, H., Dercourt, J., Fourcade, E., Cros, P., Günay, Y., Bellier, J. P., 1990. The organisation  
1963 of Neo-Tethys in the Eastern Taurus region. 8<sup>th</sup> Petroleum Congress, Turkey,  
1964 Ankara, pp. 387–402 (in Turkish with English abstract).
- 1965
- 1966 Kozlu, H., Göncüoğlu, M.C., 1997. Stratigraphy of the infra-Cambrian rock-units in the  
1967 eastern Taurides and their correlation with similar units in southern Anatolia. In:  
1968 Göncüoğlu, M.C., Derman, A.S. (Eds), *Early Palaeozoic Evolution of NW Gondwana*.  
1969 Turkish Association of Petroleum Geologists, Special Publications 3, pp. 50- 60.
- 1970
- 1971 Kuşçu, İ., Tosdal, R.M., Gençalioğlu-Kuşçu, G., Friedman, R., Ulrich, T.D., 2013. Late  
1972 Cretaceous to Middle Eocene magmatism and metallogeny of a portion of the  
1973 Southeastern Anatolian Orogenic Belt, East-Central Turkey. *Economic Geology*  
1974 108, 641–666.
- 1975
- 1976 Kürüm, S., Önal, A., Boztuğ, D., Spell, T., Arslan, M., 2008. <sup>40</sup>Ar/<sup>39</sup>Ar age and geochemistry of  
1977 the post-collisional Miocene Yamadağ volcanics in the Arapkir area (Malatya  
1978 Province), eastern Anatolia, Turkey. *Journal of Asian Earth Sciences* 33, 229-251.
- 1979
- 1980 Lefebvre, C., Umhoefer, P., Kaymakçı, N., Meijers, M., Teyssier, C., Whitney, D., Reid, M.,  
1981 Gençalioğlu Kuşçu, G., Cosca, M., Brocard, G., 2013a. The Gürün Curl, SE Turkey: a

1982 potential link from crustal tectonics to mantle dynamics in the Arabia-Eurasia  
1983 collision-escape zone. American Geophysical Union Fall Meeting Abstracts.  
1984  
1985 Lefebvre, C., Meijers, M.J.M., Kaymakçı, N., Peynircioğlu, A., Langereis, C.G., van Hinsbergen,  
1986 D.J.J., 2013b. Reconstructing the geometry of central Anatolia during the late  
1987 Cretaceous: large-scale Cenozoic rotations and deformation between the Pontides  
1988 and Taurides. Earth Planetary Science Letters 366, 83-98.  
1989  
1990 Legeay, E., Pichat, A., Kergaravat, C., Ribes, C., Callot, J.-P., Ringenbach, J.-C.,  
1991 Bonnel, C., Hoareau, G., Poisson, A., Mohn, G., 2019. Geology of the Central Sivas  
1992 Basin (Turkey). Journal of Maps 15, 406-417.  
1993  
1994 Mackintosh, P.W., Robertson, A.H.F., 2012. Sedimentary and structural evidence for two-  
1995 phase Upper Cretaceous and Eocene emplacement of the Tauride thrust sheets in  
1996 central southern Turkey, In: Robertson, A.H.F., Parlak, O., Ünlügenç, U.C. (Eds.),  
1997 Geological Development of Anatolia and the Easternmost Mediterranean Region.  
1998 Geological Society, London, Special Publications 372, pp. 299-322.  
1999  
2000  
2001 Maffione, M., van Hinsbergen, D.J.J., de Gelder, G.I., van der Goes, F.C., Morris, A., 2017.  
2002 Kinematics of Late Cretaceous subduction initiation in the Neo-Tethys Ocean  
2003 reconstructed from ophiolites of Turkey, Cyprus, and Syria. Journal of Geophysical  
2004 Research: Solid Earth 122, 3953-3976.  
2005  
2006 Marcoux, J., Ricou, L.E., Burg, J.P., Brunn, J., 1989. Shear sense criteria in the Antalya and  
2007 Alanya thrust system (southwestern Turkey): evidence for a southward  
2008 emplacement. Tectonophysics 161, 81–91.  
2009  
2010 McPhee, P.J., van Hinsbergen, D.J.J., Maffione, M., Altiner, D., 2018a. Palinspastic  
2011 reconstruction versus cross-section balancing: how complete is the Central  
2012 Taurides fold-thrust belt (Turkey)? Tectonics 37, 4535-4566.  
2013

2014 McPhee, P.J., Altiner, D., van Hinsbergen, D.J.J., 2018b. First Balanced Cross Section Across  
2015 the Taurides Fold-Thrust Belt: geological constraints on the subduction history of  
2016 the Antalya slab in southern Anatolia. *Tectonics* 37, 3738-3759.  
2017  
2018 Metin, Y., Öcal, H., Çobankaya, M., Tunçdemir, V., Bağcı, U., Uçar, L., Çörekçioğlu, E., Taptık,  
2019 M.A., Duygu, L., Duran, S., Rızaoğlu, T., Sevimli, U.İ., 2013. Geodynamic evolution of  
2020 the northern part of the Eastern Taurus (Hekimhan-Darende-Kuluncak). Mineral  
2021 Research Exploration Institute of Turkey, Report no. 11685 (in Turkish).  
2022  
2023 Metin, S., Ayhan, A., Papak, İ., 1986. Geology of the western part of the Eastern Taurides  
2024 (SSE Turkey). Mineral Research Exploration Institute of Turkey, Bulletin 107, 1-12.  
2025  
2026 Miller, K.G., Kominz, M.A., Browning, J.V., Wright, J.D., Mountain, G.S., Katz, M.E., Sugarman,  
2027 P.J., Cramer, B.S., Christie-Blick, N., Pekar, S.F., 2005. The Phanerozoic record of  
2028 global sea-level change. *Science* 310 (5752), 1293–1298.  
2029  
2030 Moix, P., Beccaletto, L., Kozur, H.W., Hochard, C., Rossetti F., Stampfli, G.M., 2008. A new  
2031 classification of the Turkish terranes and sutures and its implication for the  
2032 paleotectonic history of the region. *Tectonophysics* 451, 7-39.  
2033  
2034 Monod, O., 1977. *Récherches Géologique dans les Taurus occidental au sud de Beyşehir*  
2035 (Turquie). Thèse de Doctorat de Science, Université de Paris-Sud, Orsay, France.  
2036  
2037 MTA, 2011. Geological map of Turkey 1:250,000 Mineral Research Exploration Institute of  
2038 Turkey (MTA), Ankara.  
2039  
2040 Nairn, S., Robertson, A.H.F., Taslı, K., İnan, N., Ünlügenç, U.C., 2013. Tectonostratigraphic  
2041 evolution of the Upper Cretaceous–Cenozoic Central Anatolian basins: an integrated  
2042 study of diachronous ocean basin closure and continental collision, In: Robertson,  
2043 A.H.F., Parlak, O., Ünlügenç, U.C. (Eds.), *Geological Development of Anatolia and the*  
2044 *Easternmost Mediterranean Region*. Geological Society, London, Special Publications  
2045 372, pp. 383-384.

- 2046
- 2047 Oberhänsli, R., Candan, O., Koralay, E., Bousquet, R., Okay, A., 2012. Dating subduction  
2048 events in East Anatolia, Turkey. *Turkish Journal of Earth Science* 21, 1-17.
- 2049
- 2050 Okay, A.İ., Şahintürk, Ö., 1997. Geology of the eastern Pontides. In: Robinson, A. G. (Ed.),  
2051 Regional and Petroleum Geology of the Black Sea and Surrounding Region. American  
2052 Association of Petroleum Geologists, Memoirs 68, 291–311.
- 2053
- 2054 Okay, A.İ., Tansel, İ., Tüysüz, O., 2001. Obduction, subduction and collision as reflected in the  
2055 Upper Cretaceous-Lower Eocene sedimentary record of western Turkey. *Geological  
2056 Magazine* 138, 117-142.
- 2057
- 2058 Özer, S., Terlemez, İ., Sümengen, M., Erkan, E., 1984. Stratigraphy and structural position of  
2059 the allochthonous units around Pınarbaşı (Kayseri) 27, 61-68 (in Turkish with an  
2060 English abstract).
- 2061
- 2062 Özer, S., 1998. Rudist bearing Upper Cretaceous metamorphic sequences of the Menderes  
2063 Massif (Western Turkey). *Geobios* 31, 235-249.
- 2064
- 2065 Özer, E., Koç, H., Özsayar, T., 2004. Stratigraphical evidence for the depression of the  
2066 northern margin of the Menderes-Tauride Block (Turkey) during the Late  
2067 Cretaceous. *Journal of Asian Earth Sciences* 22, 401-412.
- 2068
- 2069 Özgül, N., 1984. Stratigraphy and tectonic evolution of the central Taurides. In: Tekeli, O.,  
2070 Göncüoğlu, M.C. (Eds.), *Geology of the Taurus Belt. Proceedings of the Tauride  
2071 Symposium, Mineral Research Exploration Institute of Turkey (MTA), Ankara*, pp.  
2072 77-90.
- 2073

- 2074 Özgül, N., 1997. Stratigraphy of the tectono-stratigraphic units in the region Bozkır-Hadim-  
2075 Taşkent (northern central Taurides) (in Turkish). Mineral Research Exploration  
2076 Institute of Turkey, Bulletin 119, 113-174.  
2077
- 2078 Özgül, N., Turşucu, A., 1984. Stratigraphy of the Mesozoic carbonate sequence of the  
2079 Munzur Mountains (Eastern Taurides), In: Tekeli, O., Göncüoğlu, M.C. (Eds.),  
2080 International Symposium on the Geology of the Taurus Belt. Mineral Research and  
2081 Exploration Institute (MTA), Ankara, pp. 173-180.  
2082
- 2083 Özgül, N., Kozlu, H., 2002. Data on the stratigraphy and tectonics of the Kozan-Feke region  
2084 (Eastern Taurides). Bulletin of Turkish Association of Petroleum Geologists 14, 1-  
2085 36.  
2086
- 2087 Özgül, N., Metin, S., Göğer, E. Bingöl, İ., Baydar, O., Erdoğan, B., 1973. Cambrian to Tertiary  
2088 units around Tufanbeyli. Türkiye Kurultayı Bülteni 16/1, 82-100 (in Turkish).  
2089
- 2090 Özgül N., Turşucu A., Özyardımcı, N., Şenol, M., Bingöl, İ., Uysal, Ş., 1981. Geology of Munzur  
2091 Mountains. MTA Report No: 6995 (in Turkish).  
2092
- 2093 Öztürk, H., Öztunalı, Ö., 1993. Effects of young tectonics and results on the Divriği iron ores.  
2094 Türkiye Jeoloji Kurumu Bülteni 8, 97-106 [in Turkish with English abstract].  
2095
- 2096 Parlak, O., 2006. Geodynamic significance of granitoid magmatism in the southeast  
2097 Anatolian orogen: geochemical and geochronological evidence from Göksun–Afşin  
2098 (Kahramanmaraş, Turkey) region. International Journal of Earth Sciences 95, 609-627.  
2099
- 2100 Parlak, O., 2016. The Tauride ophiolites of Anatolia (Turkey): A review. Journal of Earth  
2101 Science 27, 901-934.  
2102
- 2103 Parlak, O., Bağcı, U., Rızaoğlu, T., Ionescu, C., Önal, G., Höck, V., Kozlu, H., 2020. Petrology of  
2104 ultramafic to mafic cumulate rocks from the Göksun (Kahramanmaraş) ophiolite,  
2105 southeast Turkey. Geoscience Frontiers 11, 109-128.

2106  
2107 Parlak, O., Çolakoğlu, A., Dönmez, C., Sayak, H., Yıldırım, N., Türkel, A., Odabaşı, İ., 2013. Geo-  
2108 chemistry and tectonic significance of ophiolites along the Ankara – Erzincan suture  
2109 zone in northeastern Anatolia. In: Robertson, A.H.F., Parlak, O., Ünlügenç, U.C. (Eds.),  
2110 Geological Development of Anatolia and the Easternmost Mediterranean Region.  
2111 Geological Society, London, Special Publications 372, pp. 75 – 105.  
2112  
2113 Parlak, O., Dunkl, I., Karaoğlan, F., Kusky, T.M., Zhang, C., Wang, L., Köpke, J., Billor, Z.,  
2114 Hames, W.E., Şimşek, E., Şimşek, G., Şimşek, T., Öztürk, S.E., 2019. Rapid cooling history  
2115 of a Neotethyan ophiolite: Evidence for contemporaneous subduction and  
2116 metamorphic sole formation. Geological Society of America Bulletin 131, 2011–2038.  
2117  
2118 Parlak, O., Höck, V., Kozlu, H., Delaloye, M., 2004. Oceanic crust generation in an island arc  
2119 tectonic setting, SE Anatolian Orogenic Belt (Turkey). Geological Magazine 141,  
2120 583–603.  
2121  
2122 Parlak, ORızaoğlu, T., Bağcı, U., Karaoğlan, F., Höck, V., 2009. Tectonic significance of the  
2123 geochemistry and petrology of ophiolites in southeast Anatolia, Turkey.  
2124 Tectonophysics 473, 173-187.  
2125  
2126 Parlak, O., Karaoğlan, F., Rızaoğlu, T., Klötzli, U., Koller, K., Billor, Z., 2013. U–Pb and <sup>40</sup>Ar–  
2127 <sup>39</sup>Ar geochronology of the ophiolites and granitoids from the Tauride belt:  
2128 Implications for the evolution of the Inner Tauride suture. Journal of Geodynamics  
2129 65, 22–37.  
2130  
2131 Parlak, O., Karaoğlan, F., Şimşek, E., Şimşek, G., Şimşek, T., Öztürk, S.E., Baydan, M., 2017.  
2132 Examination of spatial and temporal relations of the Tauride ophiolites and their  
2133 metamorphic soles by U-Pb SIMS and <sup>40</sup>Ar/<sup>39</sup>Ar methods. TÜBİTAK Project (Project no:  
2134 113Y412), 583 pp.  
2135

2136 Parlak. O., Yılmaz, H., Boztuğ, D., 2006. Origin and significance of the metamorphic sole of  
2137 the Divriği Ophiolite (Sivas, Turkey): evidence for slab break-off prior to ophiolite  
2138 emplacement. *Turkish Journal of Earth Sciences* 15, 25-45.  
2139

2140 Parlak, O., Robertson, A.H.F., 2004. The ophiolite-related Mersin Melange, southern Turkey:  
2141 Its role in the tectono-sedimentary setting of Tethys in the Eastern Mediterranean  
2142 region. *Geological Magazine* 141, 257–286.  
2143

2144 Pehlivan, Ş., Barkurt, M.Y., Bilginer, E., Kurt, Z., Sütçü, Y.F., Can, B., Bilgi, C., Örçen, S., Süer,  
2145 T., Karabıyıköğlü, M., 1991. Elbistan-Nurhak (Kahramanmaraş) dolayının jeolojisi.  
2146 Mineral Research Exploration Institute of Turkey, Report No. 9423 (unpublished) (in  
2147 Turkish).  
2148

2149 Perinçek, D., Kozlu, H., 1984. Stratigraphical and structural relations of the units in the Afşin-  
2150 Elbistan-Doğanşehir region (Eastern Taurus), In: Tekeli, O., Göncüoğlu, M.C. (Eds.),  
2151 *Geology of the Taurus Belt. Proceedings of International Symposium MTA, Ankara,*  
2152 *pp. 181-198.*  
2153

2154 Poisson, A., 1977. *Recherches géologiques dans les Taurus occidentales (Turquie). These,*  
2155 *D.Sc thesis, Université de Paris-Sud Orsay, 1-795.*  
2156

2157 Poisson, A., 1984. The extension of the Ionian trough into southwestern Turkey, In:  
2158 Dixon, J.E., Robertson, A.H.F. (Eds), *Geological Evolution of the Eastern*  
2159 *Mediterranean. Geological Society London, Special Publication 17, pp. 241-250.*  
2160

2161 Poisson, A., Guezou, J.C., Öztürk, A., İnan, S., Temiz, T., Gürsoy, H., Kavak, K.S., Özden, S.,  
2162 1996. Tectonic setting and evolution of the Sivas Basin, Central Anatolia,  
2163 Turkey. *International Geology Review* 38, 838-853.  
2164

2165 Pourteau, A., Candan, O., Oberhänsli, R., 2010. High-Pressure metasediments in central  
2166 Turkey: constraints on the Neotethyan closure history. *Tectonics* 29, TC5004, 18 p.  
2167

- 2168 Pourteau, A., Oberhänsli, R., Candan, O., Barrier, E., Vrielynck, B., 2016. Neotethyan closure  
2169 history of western Anatolia: a geodynamic discussion. *International Journal of Earth*  
2170 *Science* 105, 203-224.
- 2171
- 2172 Pourteau, L., Sudo, M., Candan, O., Lanari, P., Vidal, O., Oberhänsli, O., 2013. Neotethys  
2173 closure history of Anatolia: insights from  $^{40}\text{Ar}$ – $^{39}\text{Ar}$  geochronology and P–T  
2174 estimation in high pressure metasedimentary rocks. *Journal of Metamorphic*  
2175 *Geology* 31, 585-606.
- 2176
- 2177 Raymond, L.A., 1984. (Ed.) *Melanges: Their Nature, Origin and Significance*. Geological  
2178 Society of America Special Paper 198.
- 2179
- 2180 Rice, S.P., Robertson, A.H.F., Ustaömer, T., İnan, N., Taslı, K., 2009. Late Cretaceous-early  
2181 Eocene tectonic development of the Tethyan suture zone in the Erzincan area,  
2182 eastern Pontides, Turkey. *Geological Magazine* 146, 567-590.
- 2183
- 2184 Ricou, L.E., Marcoux, J., Whitechurch, H., 1984. The Mesozoic organization of the Taurides:  
2185 one or several ocean basins? In: Dixon, J.E., Robertson, A.H.F. (Eds.), *The Geological*  
2186 *Evolution of the Eastern Mediterranean*. Geological Society, London Special 17, pp.  
2187 349-359.
- 2188
- 2189 Rızaoğlu, T., Parlak, O., Hoeck, V., İşler, F., 2006. Nature and significance of Late Cretaceous  
2190 ophiolitic rocks and its relation to the Baskil granitoid in Elaziğ region, SE Turkey,  
2191 In: Robertson, A.H.F., Mountrakis, D. (Eds), *Tectonic Development of the Eastern*  
2192 *Mediterranean Region*. Geological Society, London, Special Publications, 260, pp.  
2193 327–350.
- 2194
- 2195 Rızaoğlu, T., Parlak, O., Hoeck, V., Koller, F., Hames, W.E., Billor, Z., 2009. Andean-type active  
2196 margin formation in the eastern Taurides: Geochemical and geochronological  
2197 evidence from the Baskil granitoid (Elaziğ, SE Turkey). *Tectonophysics* 473, 188-  
2198 207.
- 2199



- 2200 Robertson, A.H.F., 2002. Overview of the genesis and emplacement of Mesozoic ophiolites in  
2201 the Eastern Mediterranean Tethyan region. *Lithos* 65, 1-67.  
2202
- 2203 Robertson, A.H.F., Dixon, J.E., 1984. Introduction: aspects of the geological evolution of the  
2204 Eastern Mediterranean, In: Dixon, J.E., Robertson, A.H.F. (Eds), *The Geological*  
2205 *Evolution of the Eastern Mediterranean*. Geological Society, London Special  
2206 Publications 17, pp. 1-74.  
2207
- 2208 Robertson, A.H.F., Parlak, O., Dumitrica, P. Role of volcanic-sedimentary melanges, especially  
2209 the Aladağ melange, in the rift-drift-subduction-accretion-emplacement history of  
2210 the Mesozoic Inner Tauride ocean. *International Geology Review* (in press b).  
2211
- 2212 Robertson, A.H.F., Parlak, O., Metin, Y., Vergili, Ö., Taslı, K., İnan, N., Soycan, H., 2013b. Late  
2213 Palaeozoic–Cenozoic tectonic development of carbonate platform, margin and oceanic  
2214 units in the Eastern Taurides, Turkey, In: Robertson, A.H.F., Parlak, O., Ünlügenç, U.C.  
2215 (Eds), *Geological Development of Anatolia and the Easternmost Mediterranean Region*.  
2216 Geological Society, London, Special Publications 372, pp. 167-218.  
2217
- 2218 Robertson, A.H.F., Parlak, O., Rızaoğlu, T., Ünlügenç, U.C., İnan, N., Taslı, K., Ustaömer, T.,  
2219 2007. Tectonic evolution of the South Tethyan ocean: evidence from the Eastern  
2220 Taurus Mountains (Elazığ region, SE Turkey), In: *Deformation of Continental Crust:*  
2221 *The Legacy of Mike Coward*. Geological Society of London Special Publication 272,  
2222 pp. 231-270.  
2223
- 2224 Robertson, A.H.F., Parlak, O., Ustaömer, T., 2009. Melange genesis and ophiolite  
2225 emplacement related to subduction of the northern margin of the Tauride-  
2226 Anatolide continent, central and western Turkey, In: Van Hinsbergen, D.J.J.,  
2227 Edwards, M. A., Govers, R. (Eds.), *Collision and Collapse at the Africa–Arabia–*  
2228 *Eurasia Subduction Zone*. Geological Society, London, Special Publications 311, pp.  
2229 9–66.  
2230

- 2231 Robertson, A.H.F., Palak, O., Ustaömer, T., 2012. Overview of the Palaeozoic–Neogene  
2232 evolution of Neotethys in the Eastern Mediterranean region (southern Turkey,  
2233 Cyprus, Syria). *Petroleum Geoscience* 18, 381-404.
- 2234
- 2235 Robertson, A.H.F., Palak, O., Ustaömer, T., 2013a. Mesozoic–Early Cenozoic palaeogeographic  
2236 development of Southern Turkey and the easternmost Mediterranean region:  
2237 evidence from the inter-relations of continental and carbonate platform units, In:  
2238 Robertson, A.H.F., Palak, O., Ünlügenç, U.C. (Eds.), *Geological Development of the*  
2239 *Anatolian Continent and the Easternmost Mediterranean Basin*. Geological  
2240 Society, London, Special Publications 372, pp. 167-218.
- 2241
- 2242 Robertson, A.H.F., Palak, O., Ustaömer, T. Late Palaeozoic extensional volcanism along the  
2243 northern margin of Gondwana in southern Turkey: implications for Palaeotethyan  
2244 development. *International Journal of Earth Science* (in press a).
- 2245
- 2246 Robertson, A.H.F., Parlak, O., Ustaömer, T., Taslı, K., İnan, N., Dumitrica, P., Karaoğlan, F.,  
2247 2013c. Subduction, ophiolite genesis and collision history of Tethys adjacent to the  
2248 Eurasian continental margin: new evidence from the Eastern Pontides, Turkey.  
2249 *Geodinamica Acta* 26, 230-293.
- 2250
- 2251 Robertson, A.H.F., Ustaömer, T., Parlak, O., Ünlügenç, U.C., Taslı, K., İnan, N., 2006. The Berit  
2252 transect of the Tauride thrust belt, S. Turkey: Late Cretaceous–Early Cenozoic  
2253 accretionary/collisional processes related to closure of the southern Neotethys.  
2254 *Journal of Asian Earth Sciences* 27, 108–145.
- 2255
- 2256 Rolland, Y., 2017. Caucasus collisional history: review of data from East Anatolia to West  
2257 Iran. *Gondwana Research* 49, 130-146.
- 2258
- 2259 Rolland, Y., Perinçek, D., Kaymakçı, N., Sosson, M., Barrier, E., Avagyne, A., 2012. Evidence  
2260 for ~80–75 Ma subduction jump during Anatolide–Tauride–Armenian block  
2261 accretion and ~48 Ma Arabia–Eurasia collision in Lesser Caucasus–East Anatolia.  
2262 *Journal of Geodynamics* 56-57, 76-85.

2263

2264 Rolland, Y., Hässig, M., Bosch, D., Bruguier, O., Melis, R., Galoyan, G., Sosson, M., 2020. The  
2265 East Anatolia–Lesser Caucasus ophiolite: An exceptional case of large-scale  
2266 obduction, synthesis of data and numerical modelling. *Geoscience Frontiers* 11,  
2267 83-108.

2268

2269 Rolland, Y., Hässig, M., Bosch, D., Meijers, M.J.M., Sosson, M., Bruguier, O., Adamia,  
2270 S., Sadradze, N., 2016. A review of the plate convergence history of the East  
2271 Anatolia–Transcaucasus region during the Variscan: insights from the Georgian  
2272 basement and its connection to the Eastern Pontides. *Journal of*  
2273 *Geodynamics* 96, 131-145.

2274

2275 Sancar, T., Zabcı, C., Karabacak, V., Yazıcı, M., Akyüz, H.S., 2019. Geometry and  
2276 Paleoseismology of the Malatya Fault (Malatya-Ovacık Fault Zone), Eastern Turkey:  
2277 Implications for intraplate deformation of the Anatolian Scholle. *Journal of*  
2278 *Seismology* 23, 319-340.

2279

2280 Sar, A., Ertürk, M.A., Rizeli, M.E., 2019. Genesis of Late Cretaceous intra-oceanic arc  
2281 intrusions in the Pertek area of Tunceli Province, eastern Turkey, and implications  
2282 for the geodynamic evolution of the southern Neo-Tethys: results of zircon U–Pb  
2283 geochro- nology and geochemical and Sr–Nd isotopic analyses. *Lithos* 350–351,  
2284 105263. <https://doi.org/10.1016/j.lithos.2019.105263>.

2285

2286 Sarı, B., Özer, S., 2002. Upper Cretaceous stratigraphy of the Bey Dağları carbonate platform,  
2287 Korkuteli area (Western Taurides, Turkey). *Turkish Journal of Earth Sciences* 11,  
2288 39–59.

2289

2290 Sarı, B., Steuber, T., Özer, S., 2004. First record of Upper Turonian rudists (Mollusca,  
2291 Hippuritoidea) in the Bey Dağları carbonate platform, Western Taurides (Turkey):  
2292 Taxonomy and strontium isotope stratigraphy of *Vaccinites praegiganteus* (Toucas,  
2293 1904). *Cretaceous Research* 25, 235–248.

2294

- 2295 Sayit, K., Göncüoğlu, M.C., Tekin, U.K., 2015. Middle Carnian Arc-Type Basalts from the  
2296 Lycian Nappes, Southwestern Anatolia: early Late Triassic Subduction in the  
2297 Northern Branch of Neotethys. *Journal of Geology* 123, 561-579.  
2298
- 2299 Sclieffarth, W.K., Darin, M.H., Reind, M.R., Umhoeffer, P.J., 2018. Dynamics of episodic Late  
2300 Cretaceous–Cenozoic magmatism across Central to Eastern Anatolia: New insights  
2301 from an extensive geochronology compilation. *Geosphere* 14, 1990-2008.  
2302
- 2303 Şenel, M., 1984. Discussion on the Antalya nappes, In: Tekeli, O., Göncüoğlu, M.C. (Eds.),  
2304 International Symposium on the Geology of the Taurus Belt. General Directorate  
2305 of Mineral Research and Exploration, Ankara, pp. 41-52.  
2306
- 2307 Şenel, M., Selçuk, H., Bilgin, Z.R., Şen, A.M., Karaman, T., Dincer, M.A., Durukan, E., Arbas, A.,  
2308 Örcen, S., Bilgin, C., 1989. Geology of Çameli (Denizli)- Yesilova, (Burdur)- Elmalı  
2309 (Antalya) region. General Directorate of Mineral Research and Exploration, Report  
2310 No: 9429 (in Turkish).  
2311
- 2312 Şengör, A.M.C., Yılmaz, Y., 1981. Tethyan Evolution of Turkey: A plate tectonic approach.  
2313 *Tectonophysics* 75, 181-241.  
2314
- 2315 Şengör, A.M.C., Görür, N., Şaroğlu, F., 1985. Strike-slip faulting and related basin formation in  
2316 zones of tectonic escape: Turkey as a case study, In: Biddle KT, Christie-Blick N  
2317 (Eds.), *Strike-slip deformation, basin formation and sedimentation*. Society of  
2318 Economic Paleontologists and Mineralogists Special Publication 37, pp. 227–264.  
2319
- 2320 Solak, C., Taslı, K., Özer, S., Koç, H., 2017. Biostratigraphy and facies analysis of the Upper  
2321 Cretaceous-Danian? platform carbonate succession in the Kuyucak area, western  
2322 Central Taurides, S Turkey. *Cretaceous Research* 79, 43-63.  
2323
- 2324 Solak, C., Taslı, K., Özer, S., Koç, H., 2019. The Madenli (Central Taurides) Upper Cretaceous  
2325 platform carbonate succession: Benthic foraminiferal biostratigraphy and platform  
2326 evolution. *Geobios* 52, 67-93.

2327

2328 Sossou, M., Rolland, Y., Danelian, T., Muller, C., Melkonyan, R., Adamia, S., Babazadeh, V.,  
2329 Kangarli, T., Avagyan, A., Galoyan, G., Mosar, J., 2010. Subductions, obduction and  
2330 collision in the Lesser Caucasus (Armenia, Azerbaijan, Georgia), new insights, In:  
2331 Sossou, M., Kaymakçı, N., Stephenson, R.A., Bergerat, F., Starostenko, V. (Eds.),  
2332 Sedimentary Basin Tectonics from the Black Sea and Caucasus to the Arabian  
2333 Platform. Geological Society, London, Special Publications 340, 329-352.

2334

2335 Stampfli, G.M., Borel, G.D., 2002. A plate tectonic model for the Paleozoic and Mesozoic  
2336 constrained by dynamic plate boundaries and restored synthetic oceanic isochrons.  
2337 Earth and Planetary Science Letters 196, 17-33.

2338

2339 Stampfli, G., J. Mosar, P., Faure, A., Vannay, J.C., 2001. Permo-Mesozoic evolution of the  
2340 western Tethys realm: the Neotethys East Mediterranean basin connection, In:  
2341 Ziegler, P., Cavazza, W., Robertson, A.H.F., Crasquin-Soleau (Eds.), Peri-Tethys  
2342 Memoir 5 Peri-Tethyan Rift/Wrench Basins and Passive Margins. Memoirs du  
2343 Museum National D'Histoire Naturelle, pp. 51-108.

2344

2345 Tekin, U.K., Bedi Y., 2007a. Ruesticyrtiidae (Radiolaria) from the middle Carnian (Late  
2346 Triassic) of Köseyahya nappe, Elbistan, eastern Turkey. *Geologica Carpathica* 58,  
2347 153-167.

2348

2349 Tekin, U.K., Bedi, Y., 2007b. Middle Carnian (Late Triassic) Nassellaria (Radiolaria) of  
2350 Köseyahya nappe from eastern Tau-rides, eastern Turkey. *Rivista Italiana di*  
2351 *Paleontologia e Stratigrafia* 113, 167-190.

2352

2353 Topuz, G., Göçmengil, G., Rolland, Y., Çelik, Ö.F., Zack, T., Schmitt, A.K., 2013a. Jurassic  
2354 accretionary complex and ophiolite from northeast Turkey: no evidence for the  
2355 Cimmerian continental ribbon. *Geology* 41, 255-258.

2356

2357 Topuz, G., Çelik, Ö.F., Şengör, A.M.C., Altıntaş, I.E., Zack, T., Rolland, Y., Barth, M., 2013b.  
2358 Jurassic ophiolite formation and emplacement as back-stop to a subduction-

2359 accretion complex in Northeast Turkey, the Refahiye ophiolite, and relation to the  
2360 Balkan ophiolites. *American Journal of Science* 313, 1054 – 1087.  
2361  
2362 Uçurum, A., 2000. Geology, geochemistry, and evolution of the Divriği and Kuluncak  
2363 ophiolitic melanges, with reference to serpentinites in east-central Turkey.  
2364 *International Geology Review* 42, 172-191.  
2365  
2366 Ural, M., Arslan, M., Göncüoğlu, M.C., Tekin, U.K., Kürüm, S., 2015. Late Cretaceous arc and  
2367 back-arc formation within the southern Neotethys: whole rock, trace element and  
2368 Sr-Nd-Pb isotopic data from basaltic rocks of the Yüksekova complex (Malatya-  
2369 Elazığ, SE Turkey). *Ofioliti* 40, 57-72.  
2370  
2371 Ustaömer, T., Robertson, A.H.F., 2010. Late Palaeozoic – Early Cenozoic tectonic  
2372 development of the Eastern Pontides (Artvin area), Turkey: stages of clo- sure of  
2373 Tethys along the southern margin of Eurasia. In: Sosson, M., Kaymakçı, N.,  
2374 Stephenson, R.A., Bergerat, F., Starostenko, V. (Eds.), *Sedimentary Basin Tectonics*  
2375 *from the Black Sea and Caucasus to the Arabian Platform*. Geological Society,  
2376 London, Special Publications 340, 281 – 327.  
2377  
2378 Ustaömer, T., Robertson, A.H.F., Ustaömer, P.A., Gerdes, A., Peytcheva, I., 2013.  
2379 Constraints on Variscan and Cimmerian magmatism and metamorphism in the  
2380 Pontides (Yusufeli-Artvin area), NE Turkey from U-Pb dating and granite  
2381 geochemistry. In: Robertson, A.H.F., Parlak, O., Ünlügenç, U.C. (Eds.), *Geological*  
2382 *Development of Anatolia and the Easternmost Mediterranean Region*. Geological  
2383 Society, London, Special Publications 372, 49-74.  
2384  
2385 van Hinsbergen, D.J.J., Maffione, M., Plunder, A., Kaymakçı, N., Ganerød,  
2386 B., Hendriks, B.W.H., Corfu, F., Gürer, D., Gelder, G.I.N.O. de,  
2387 Peters, K., McPhee, J., Brouwer, F.M., Advokaat, E.L., Vissers, R.L.M., 2016. Tectonic  
2388 evolution and paleogeography of the Kırşehir Block and the Central Anatolian  
2389 Ophiolites, Turkey. *Tectonics* 35, [10.1002/2015TC004018](https://doi.org/10.1002/2015TC004018)  
2390

- 2391 van Hinsbergen, D.J.J., Torsvig, T.H., Schmid, S.M., Matenco, L.C., Maffione, M., Vissers, L.M.,  
2392 Güreş, D., Spakman, W., 2020. Orogenic architecture of the Mediterranean region  
2393 and kinematic reconstruction of its tectonic evolution since the Triassic. *Gondwana*  
2394 *Research* 81, 79-229.
- 2395
- 2396 Vergili, Ö., Parlak, O., 2005. Geochemistry and tectonic setting of metamorphic sole rocks  
2397 and mafic dikes from the Pınarbaşı (Kayseri) ophiolite, Central Anatolia. *Ofioliti* 30,  
2398 37–52.
- 2399
- 2400 Westaway, R., Arger, J., 2001. Kinematics of the Malatya–Ovacık Fault Zone. *Geodinamica*  
2401 *Acta* 14, 103-131.
- 2402
- 2403 Woodcock, N.H., Robertson, A.H.F., 1982. Wrench and thrust tectonics along a Mesozoic-  
2404 Cenozoic continental margin; Antalya Complex, SW Turkey. *Journal of the Geological*  
2405 *Society, London* 139, 147-163.
- 2406
- 2407 Yazgan, E., 1984. Geodynamic evolution of the Eastern Taurus region. In: Tekeli, O.,  
2408 Göncüođlu, M.C. (Eds.), *International Symposium on the Geology of the Taurus Belt*.  
2409 *General Directorate of Mineral Research and Exploration, Ankara*, pp. 199-208.
- 2410 Yazgan, E., Chessex, R., 1991. Geology and tectonic evolution of the southeastern Taurides in  
2411 the region of Malatya. *Turkish Association of Petroleum Geologists* 3, 1–42.
- 2412 Yılmaz, A., Bedi, Y., Uysal, S., Yusufoglu, H., Aydın N., 1993. Geological structure of the area  
2413 between Uzunyayla and Beritdađ of the Eastern Taurides. *Turkish Association of*  
2414 *Petroleum Geologists Bulletin* 5, 69–87 (in Turkish with English abstract).
- 2415
- 2416 Yılmaz, A., Bedi, Y., Uysal, S., Yusufoglu, H., Aydın N., 1991. 1:100,000 map and report  
2417 Elbistan H23 (K37). *Mineral Research Exploration Institute of Turkey (MTA)*, (in  
2418 Turkish).
- 2419

- 2420 Yılmaz, A., Bedi, Y., Uysal, S., Aydın N., 1994. 1:100,000 map and report Elbistan İ23 (L37).  
2421 Mineral Research Exploration Institute of Turkey (MTA), (in Turkish).  
2422
- 2423 H., Yılmaz, A., 2004. Geology and structural evolution of Divriği (Sivas) region. Bulletin of  
2424 Geological Society of Turkey 47 (1), 13-45.
- 2425 Yılmaz, C., 1994. Evolution of the Munzur Carbonate Platform during the Mesozoic, Middle  
2426 Eastern Anatolia (Turkey). *Géologia Méditerranéenne* 21, 195-196
- 2427 Yılmaz, H., 2001. Geology of the Güneş ophiolite (Divriği-Sivas). Proceeding of the 54<sup>th</sup>  
2428 Geological Congress of Turkey, 7-10 May 2011, Ankara, pp. 54-65 (in Turkish).  
2429
- 2430 Yılmaz, P.O., Maxwell, J.C., 1984. An example of an obduction melange: the Alakır Çay unit,  
2431 Antalya Complex, Southwest Turkey. In: Raymond, L.A. (Ed.), *Melanges: Their Nature,*  
2432 *Origin, and Significance.* Geological Society of America Special Paper 198, pp. 139-  
2433 152.  
2434
- 2435 Yılmaz, Y., 1993. New evidence and model on the evolution of the southeast Anatolian  
2436 orogen. *Geological Society of America Bulletin* 105, 251-271.  
2437
- 2438 Yılmaz, Y., Gürpınar, O., Kozlu, H., Gül, M.A., Yiğitbaş, E., Yıldırım, M., Genç, S.C., Keskin, M.,  
2439 1987. Geology of the northern part of Kahramanmaraş (Andırın-Berit-Engizek-  
2440 Nurhak-Binboğa Mountains). Turkish Petroleum Company Report (No: 2028), pp  
2441 218 (unpublished).  
2442
- 2443 Yılmaz, Y., Gürpınar, O., Kozlu, H., Gül, M.A., Yiğitbaş, E., Yıldırım, M., Genç, C., Keskin, M.,  
2444 1987. Geology of the northern part of Maraş (Andırın, Berit, Engizek-Nurhak-Binboğa  
2445 Mountains) structural and geological evolution. Publication of İstanbul University  
2446 Engineering Faculty 6, 1-97 (in Turkish).  
2447
- 2448 Yılmaz, Y., Tüysüz, O., Yiğitbaş, E., Genç, S.C., Şengör, A.M.C., 1997. Geology and tectonic  
2449 evolution of the Pontides. In: Robinson, A.G. (Ed.). *Regional and Petroleum Geology*



2450 of the Black Sea and Surrounding Region. American Association of Petroleum  
2451 Geologists, Memoirs 68, 183–226.  
2452  
2453 Yılmaz, Y., Yiğitbaş, E., Genç, S.C., 1993. Ophiolitic and metamorphic assemblages of  
2454 southeast Anatolia and their significance in the geological evolution of the orogenic  
2455 belt. *Tectonics* 12, 1280-1297.  
2456

2457

2458 Yusifođlu, H., Bedi, Y., Usta, D., Özkan, M.K., Beyazpirinç, M., Yıldız, H., 2005. The tectonic  
2459 evolution of the Afşin-Elbistan Neogene Basin, Eastern Taurides, Turkey. 58<sup>th</sup>  
2460 Geological Congress of Turkey, MTA Ankara, 11-17 April, 2005.

2461

2462

2463

2464  
2465  
2466  
2467  
2468  
2469  
2470  
2471  
2472  
2473  
2474  
2475  
2476  
2477  
2478  
2479  
2480  
2481  
2482  
2483  
2484  
2485  
2486  
2487  
2488  
2489  
2490  
2491  
2492  
2493  
2494  
2495

**Figure captions**

Fig. 1. Outline map of Turkey showing the main tectonic units and the study area (main data source, MTA 2012).

Fig. 2. Simplified geological map and cross-section of part of central eastern Anatolia, simplified from MTA 1:100,000 and 1:250,000 geological maps of Turkey (MTA, 2011). The area studied is divided into 5 sub-areas, as indicated: Area 1-NE, i.e. mainly NW of Elbistan, including the Afşin area; Area 2-Dağlıca area, farther NW of Elbistan; Area 3A-East of Elbistan, 3B-farther east, near Nurhak Dağı; Area 4-S-mainly south of Elbistan; Area 5A-Kemaliye area, 5B Divriği area (both in the far NE). Additional geological units mentioned in the text: AE Afşin-Elbistan basin; DB Darende basin; GO Göksun ophiolite; GF Göksu Fault; SGF Sürgü-Misis Fault; İO İspendere ophiolite; KO Kömürhan ophiolite; KU Kuluncak ophiolite. Additional locations and settlements mentioned in the text: B Büyük Yılanlı Dağ; K Kangal (off map in central N, as indicated); N Nurhak Dağı; S Saimbeyli (just off map in SW); Y Yeşildere.

Fig. 3. Stratigraphical columns showing the age and lithologies of the main geological units discussed in this paper. See text for explanation and data sources.

Fig. 4. Field photographs of key features of the Malatya metamorphics in the area north and west of Elbistan (Area 1). a, Eocene shelf limestones (Seske Fm.) above Malatya Metamorphics; in places the two units are intersliced, Kepez Mah. (in foreground); GPS 37S 0303484/4230790; b, Foliated amphibolite; Late Palaeozoic; 0.5 km S of Türkören; c, Normal-graded debris-flow deposit with carbonate clasts in a coarse calcarenite matrix; recrystallised to micaceous marble; Late Palaeozoic; near Kepez, W of Afşin; GPS 37S 0303518/4229825; d, Isoclinally folded limestone with replacement chert, Late Permian; Saldilek Tepe, NE of Afşin; GPS 37S 0322749/4239163; e, Thin-bedded micritic limestone

2496 and dolomite (stromatolitic); Late Triassic; west of Afşin GPS 37S 0303484/4230790; f,  
2497 Network of tension cracks infilled with pink micrite (recrystallised); within upper c. 50 m of  
2498 mapped Late Permian meta-limestone succession; beneath the Karaböğürtlen Formation;  
2499 GPS 37S 0329702/4236079; g, Debris-flow deposit composed of platy limestone clasts,  
2500 recrystallised to marble; several m above mapped normal contact with Late Permian meta-  
2501 limestone; Karaböğürtlen Formation; GPS 37S 0329013/4236061; h, Debris-flow deposit  
2502 with flattened clasts in a calcareous mudstone matrix; recrystallised to marble;  
2503 Karaböğürtlen Formation; GPS 37S 0328678/4235639; i, Foliated pebbly conglomerate;  
2504 clasts mainly sub-rounded; mostly siliceous calc-schist; Malatya metamorphic unit; near  
2505 Kamalak köy, SSW of İncirli; Karaböğürtlen Formation (GPS 37S 0304287/4250123); j, Blocks  
2506 of recrystallised limestone (marble), interbedded with carbonate-rock debris-flow deposits  
2507 and phyllite (Karaböğürtlen Formation); represents the leading edge of the Malatya  
2508 metamorphic unit (backthrust to N); c. 1 km SE of İncirli (GPS 37S 0307627/4251659); k,  
2509 Recrystallised limestone (marble) with reworked Megalodont bivalves (Karaböğürtlen  
2510 Formation); NW of Afşin, GPS 37S 0322629/0239403; l, Kemaliye Formation (foreground),  
2511 with serpentinite above (Dağlıca ophiolite); overthrust (northwards) by the Malatya  
2512 Metamorphics (Karaböğürtlen Formation); NW of İncirli.

2513

2514 Fig. 5. Part of the northeast outcrop of the Malatya Metamorphics (Area 1; NW of Elbistan;  
2515 Fig. 2). Simplified geological map; note the relation of the Late Cretaceous syn-tectonic  
2516 Karaböğürtlen Formation to the underlying units; modified from Bedi et al. (2009).

2517 Logs: 1, Late Palaeozoic succession including meta-basic extrusive rocks (west of Afşin); 2,  
2518 Triassic siliciclastic-carbonate facies; 3, Late Cretaceous Karaböğürtlen Formation with  
2519 carbonate and siliciclastic intercalations. Rock-relations diagrams: a, Latest Cretaceous  
2520 sedimentary cover of the Göksun ophiolite (Harami Fm.), overthrust by the Malatya  
2521 Metamorphics; 3 km SE of Afşin; b, Jurassic-Cretaceous (?) succession, unconformably  
2522 overlain by the Late Cretaceous Karaböğürtlen Formation; 6 km E of Afşin; c, Permian  
2523 succession unconformably overlain by Late Cretaceous Karaböğürtlen Formation; NE of  
2524 Körkuyu.

2525

2526 Fig. 6. Photomicrographs of sandstone of the Late Cretaceous Karaböğürtlen and Kemaliye  
2527 formations. Stratigraphy: a-b Karaböğürtlen Formation (Malatya Metamorphics); c-g

2528 Kemaliye Formation above the Malatya (Keban) Metamorphics (Areas 1 & 5A); h-i Kemaliye  
 2529 Formation related to the Munzur limestones; j, Kemaliye Formation beneath the Köseyahya  
 2530 thrust sheet; k-l Maastrichtian cover of the Göksun ophiolite. Composition: a, Rounded  
 2531 grains of monocrystalline quartz and polycrystalline quartz (quartzite) in a recrystallised  
 2532 calcareous matrix; crossed polars; c. 10 km W of Elbistan; GPS 37S 0330991/4230104); b,  
 2533 Note the large rounded, then fragmented quartz grain, with cracks infilled by calcite spar,  
 2534 suggesting high-strain deformation; location as a; c, Poorly sorted sandstone with common  
 2535 monocrystalline quartz, polycrystalline quartz and muscovite in a quartz-rich, granular  
 2536 calcareous matrix; crossed polars; Area 3B (Nurhak Dağı, near Beğre); GPS 37S  
 2537 0393334/4227050; d, Poorly sorted sandstones with abundant grains of neritic limestone  
 2538 (partly recrystallised), polycrystalline quartz and muscovite (deformed); crossed polars;  
 2539 location as c; e, Poorly sorted sandstones including grains of neritic limestone (partly  
 2540 recrystallised) and basalt (relatively fresh and chloritised); plane-polarised light; location as  
 2541 c; f, Granitic grain from conglomeratic lens; crossed polars; location as c; g, Large alkali  
 2542 feldspar crystal (upper right), together with monocrystalline quartz, other feldspar and  
 2543 microcrystalline quartz in a calcareous and quartz-rich matrix; crossed polars; location as c;  
 2544 h, Sub-rounded clast of fine-grained meta-siltstone (central), together with muscovite (large  
 2545 lath), polycrystalline quartz (left, central), and bioclastic limestone (e.g., upper left); crossed  
 2546 polars; location as c; i, Sub-rounded grains of dark chert (veined and recrystallised) and  
 2547 partly recrystallised siltstone in a quartz- and carbonate-rich matrix; crossed polars; location  
 2548 as c; j, Micaceous sandstone with common monocrystalline quartz, polycrystalline quartz  
 2549 and muscovite, cemented by sparry calcite; near Bakış, east of Elbistan; GPS 37S  
 2550 0361782/4222559; k, Bioclastic limestone with common bivalve shell fragments, planktic  
 2551 foraminifera and a dark, bituminous schistose grain; cover of the Göksun ophiolite; SW  
 2552 slope of Aktaş Tepe; plane-polarised light; GPS 37S 0318668/4232060; l, Bioclastic  
 2553 limestone, including large grain of relatively well-rounded microcrystalline quartz; crossed  
 2554 polars; same sample as k. Key to letters: B Bioclastic carbonate, BA Basalt, BI Bivalve, C  
 2555 Carbonate (calcite), CH Chert, F Feldspar (alkaline), G Granitic lithoclast, Mq Monocrystalline  
 2556 quartz, M Muscovite, N Neritic limestone, PL Planktic foraminifer, Pq Polycrystalline quartz,  
 2557 S Siltstone, SH Schistose lithoclast.  
 2558

2559 Fig. 7. Outline geological map and local sections (a-f) of Area (Dağlıca). Based on mapping by  
2560 Perinçek and Kozlu (1984), Bedi et al. (2013), Robertson et al. (2013b) and this study. The  
2561 location of the rock-relations diagrams and the logs (roman numerals Va,b,c, VI, VIII and IX;  
2562 see Fig. 11 for I-IV) are indicated. a, The lower Munzur thrust sheet is overlain by the  
2563 Kemaliye Formation and the dismembered Dağlıca ophiolite. The Kırmızı Kandil Formation  
2564 and the Kemaliye Formation are exposed above the upper Munzur thrust sheet; NW of  
2565 İncirli; b, Munzur thrust sheet in the north, unconformably overlain by conglomerates  
2566 (Miocene?), with well-rounded clasts including Eocene nummulitic limestone; NW of Tavla;  
2567 c, Relatively autochthonous succession (Gürün autochthon), overthrust by a Munzur thrust  
2568 sheet; near Dallıkavak; d, Lower Munzur thrust sheet, overthrust by the dismembered  
2569 Dağlıca ophiolite and by an upper Munzur thrust sheet; e, Blocks of the Dağlıca ophiolite  
2570 within ophiolite-derived debris flows, overthrust by an upper Munzur thrust sheet; Tatlar  
2571 area; f, Lower Munzur thrust sheet including the Kırmızı Kandil Formation and the Kemaliye  
2572 Formation; near Elmalı.

2573

2574 Fig. 8. Outline geological map (simplified from Bedi et al., 2009) and local rock-relations  
2575 diagrams in Area 3A (E of Elbistan). Note: Rock-relations diagrams a-d are located north of  
2576 the map area (see top right). a, Lower Munzur thrust sheet overlain by the Kırmızı Kandil  
2577 Formation and the Kemaliye Formation and Pelagic (Gülbahar) unit limestone and chert;  
2578 near Erikli (c. 20 km NW of the map area); b, Lower Munzur thrust sheet, overlain by the  
2579 Kırmızı Kandil Formation and the Kemaliye Formation (with blocks of neritic limestone),  
2580 overthrust by upper Munzur thrust sheet; Gökçek area; 10 km WNW of the map area; c,  
2581 Contact relations with the Darende basin to the east. Mesozoic Tauride units are locally  
2582 emplaced eastwards over the basin margin, which is tilted and overturned near the base.  
2583 Note: in places (off this section) an intact unconformity is exposed between the emplaced  
2584 Mesozoic allochthonous units and Maastrichtian sediments of the intact Darende basin  
2585 succession (see text); N of Dağdamı; 12 km N of map area; d, Lower Munzur thrust sheet,  
2586 overlain by the Kırmızı Kandil Fm. and then the Kemaliye Fm. (with blocks of neritic  
2587 limestone); 2 km NE of Kapaklı; 7 km N of map area; e, Kemaliye Formation enclosing blocks  
2588 of Pelagic (Gülbahar) unit lithologies, overthrust by the lower Munzur thrust sheet. The  
2589 Munzur thrust sheet is mapped as being thrust (SW) over the Köseyahya thrust sheet; 3.5  
2590 km E of Türkören (Yumru Tepe); f, Lower Munzur thrust sheet, with the Kırmızı Kandil and

2591 Kemaliye formations above (with block of limestone), overthrust by the Köseyahya thrust  
2592 sheet. Note the Fe-rich crust at the top of the Kırmızı Kandil Formation; NW of Şerefli.

2593

2594 Fig. 9. Outline geological map (simplified from Bedi et al., 2009) and local rock-relations  
2595 diagrams in Area 4 (S of Elbistan). A-A' Malatya Metamorphics in steep fault contact with  
2596 the Kemaliye Formation (as mapped by Bedi et al. (2009)), overlain by the Kemaliye  
2597 Formation including blocks of limestone and radiolarite; in turn overthrust by a Munzur  
2598 thrust sheet and then by ophiolite-related melange with blocks of ophiolitic rocks and  
2599 limestone; finally overthrust by a Köseyahya thrust sheet; B-B' folded Köseyahya thrust  
2600 sheet, emplaced over the Malatya metamorphic succession. The syncline (truncated)  
2601 formed prior to thrust emplacement.

2602

2603 Fig. 10. Field photographs showing key sedimentary features of the Munzur and Köseyahya  
2604 thrust sheets. a-h Munzur thrust sheet; i-l Köseyahya thrust sheet. a, Oncolite (algal) within  
2605 Late Triassic micritic limestone; upper part removed by dissolution along a stylolite; E of  
2606 Elbistan; GPS 37S 0346331/4227793; b, Thin interbed of intraformational sedimentary  
2607 breccia (near a); c, Thin, intra-formational slump sheet composed of pelagic micrite (also  
2608 near a; d, U. Cretaceous rudist limestone; lower Munzur thrust sheet; Kaşanlı area; GPS 37S  
2609 0325809/4257928; e, Late Cretaceous limestone of upper Munzur thrust sheet, with  
2610 Kemaliye Formation beneath (shale with limestone blocks) and ultramafic mafic ophiolitic  
2611 lithologies above, Hurman kalesi; GPS 37S 0310858/4260897; f, Upper Cretaceous pelagic  
2612 limestone (Kırmızı Kandil Fm., Kapaklı area; GPS 37S 0361390 / 4257247; loc. 4.4; g, Fe-Mn  
2613 crust at the contact between Late Cretaceous pelagic limestone below and the Kemaliye  
2614 Formation above, recording a hiatus; near İncirli; GPS 37S 0305831/4252443; i, Ammonite in  
2615 red bioclastic limestone (Late Triassic), Köseyahya thrust sheet, near Sarıkaya Tepe; E of  
2616 Elbistan; GPS 37S 0362757/4228355; j, Crinoidal bioclastic limestone (Late Triassic);  
2617 Köseyahya thrust sheet; loc. as i; k, White crinoidal limestone with diagenetic chert lenticles  
2618 (Late Triassic); Köseyahya thrust sheet; loc. As j; l, Bioturbated pelagic limestone (Early  
2619 Cretaceous), between Özbek and Gücük (E of Elbistan); GPS 37S 036516/4229889.

2620

2621 Fig. 11. Measured sedimentary logs (roman numerals) of Permian-Cretaceous facies of the  
2622 Pelagic (Gülbahar) unit; see Fig. 8 for I-IV and Fig. 7 for V-IX, and the text for explanation.

2623

2624 Fig. 12. Field photographs of the pelagic (Gülbahar) unit in Area 2 (Dağlıca). a, Sandstone  
2625 and shale (Triassic), overthrust by thick-bedded limestone of the Köseyahya thrust sheet;  
2626 Bakış area; GPS 37S 036782/4222559; b, Calcareous mudrock, with thin limestone  
2627 interbeds; note the small load casts in redeposited limestone; small slice (c. 10 m thick),  
2628 below Köseyahya thrust sheet; Triassic; Aşağıgücük köy; GPS 37S 0362059/4222332; c,  
2629 Radiolarian chert and pelagic limestone (centre, pink), positionally intercalated with  
2630 pelagic carbonate, with minor replacement chert (grey); Late Jurassic-Early Cretaceous;  
2631 Ayrancı Tepe; 2 km S of Büyük Tatlı; GPS 37S 0324740/4263734; d, Regularly bedded  
2632 calciturbidites, largely replaced by quartzitic chert; location near c; e, Calciturbidite, mainly  
2633 replaced by quartzitic chert; Late Jurassic-Early Cretaceous; Kayseri (near Hurman kalesi);  
2634 GPS 37S 0302827/4266442; f, Well-cemented debris-flow deposit with angular clasts of  
2635 chert (red) and pelagic carbonate. The chert mainly formed by replacement of pelagic  
2636 carbonate, location near c; g, Debris-flow deposit made of sub-rounded clasts of pelagic  
2637 carbonate in a calcarenite matrix, rich in redeposited ooids; gravity emplaced before  
2638 completely lithified; Late Jurassic-Early Cretaceous; SE of Büyük Tatlı; GPS 37S  
2639 0325527/4262472; h, Debris-flow deposit composed of angular to sub-rounded clasts of  
2640 white pelagic limestone and red radiolarite; the well-cemented nature is typical of the  
2641 pelagic succession in contrast to the Kemaliye Fm.; Late Jurassic-Early Cretaceous; near  
2642 Yumru Tepe, E of Elbistan; GPS 37S 036620/423774; i, Debris-flow deposit made up of  
2643 angular to sub-rounded clasts of pelagic limestone and redeposited calcarenite in a coarse  
2644 calcarenite (oolitic) matrix; Late Jurassic-Early Cretaceous; near Topaktaş (Kırksrak area);  
2645 GPS 37S 0298744/4262995.

2646

2647 Fig. 13. Outline geological map of Area 5A, Kemaliye and Area 5B, Divriği. See text for  
2648 explanation and data sources.

2649

2650 Fig. 14. Geological map of the type, Kemaliye area including the Kemaliye Formation (Area  
2651 5A), simplified from 1:100,000 geological maps of Turkey (Bilgiç, 2008b, c), with additional  
2652 information from this study.

2653



2654 Fig. 15. Local cross-sections of the Kemaliye Formation in its type area (5A). a, East of Keban  
2655 Lake; b, West of Keban Lake (farther southeast). See Fig. 13 for location and the text for  
2656 explanation.

2657

2658 Fig. 16. Field photograph Kemaliye Formation and related units in the type area (5A) (a-f)  
2659 and in Area 3B (Nurhak Dağı) (g-l). a, View southwest over the Late Cretaceous Kemaliye  
2660 Formation, with lenticular blocks, mainly limestone conglomerate in a matrix of shale and  
2661 sandstone; S of Kemaliye town; b, Calc-mylonite locally exposed near the contact between  
2662 the Malatya Metamorphics and the Kemaliye Formation (E of Keban Lake); c, Stratiform  
2663 debris-flow deposits with sub-rounded to well-rounded clasts, mainly neritic limestone, in a  
2664 coarse-grained sandy matrix; Kemaliye Formation, lower part; d, Debris-flow deposits with  
2665 mainly angular clasts of micaschist in a coarse-grained sandy matrix; Kemaliye Formation,  
2666 lower part, near Yuva; e, Lenticular debris-flow conglomerate, dominated by well-rounded,  
2667 varicoloured clasts of red radiolarian chert in a coarse-grained sandy matrix; Kemaliye  
2668 Formation, lower part; near Beğre (Area 3B); f, Mainly sub-angular clasts of neritic limestone  
2669 (calcite-veined) in a coarse-grained sandy matrix; Kemaliye Formation, upper part; near  
2670 Beğre (Area 3B); g, Serpentinite cut by small granitic intrusions (foreground), overthrust by a  
2671 thin unit of the Kemaliye Formation, and then by the Köseyahya thrust sheet (pale; main  
2672 mountain above), near Beğre; h, Calc-mylonite in the uppermost levels of the Malatya  
2673 Metamorphics, near Beğre; i, Isoclinally folded calc-schist in the uppermost levels of the  
2674 Malatya Metamorphics, later brecciated, near Beğre; j, Isoclinally folded calc-schist in the  
2675 uppermost levels of the Malatya Metamorphics, cut by small granitic intrusions (centre-  
2676 right); fold limb is 5 m across in the foreground, near Beğre; k, Granitic intrusions (by pen)  
2677 and greenish serpentinite (upper), mutually brecciated, indicating high-strain deformation  
2678 after intrusion, near Beğre; l, Iron-rich crust at the top of the platform succession, below the  
2679 Kemaliye Fm., marking a hiatus.

2680

2681 Fig. 17. Sedimentary log of the lower part of the Kemaliye Formation in its type, Kemaliye  
2682 area (5A). See text for explanation.

2683

2684 Fig. 18. Photomicrographs of key age-diagnostic benthic microfossils. a: *Neoendothyra* sp.;  
2685 sample ET12.37; Triassic; Dark limestone block in Kemaliye Formation, Area 5A, near Yuva,

2686 GPS 37S 0456773/4345128; b: *Meandrospira* sp., sample ET12.37, as above, Triassic; c:  
2687 *Thaumatoporella parvovesiculifera* (Tp), *Bosniella fontainei* (Bf), *Siphovalvulina variabilis*  
2688 (Sv), *Glomospira* sp. (Gl), sample ET12.57; Middle Triassic; Bioclastic limestone from Munzur  
2689 thrust sheet, Area 5B, c. 8 km SSE of Divriği, Area 5B, GPS 37S 0426455/4351186; d:  
2690 *Siphovalvulina variabilis*, sample ET12.58 (location as c); Jurassic; e: *Bosniella fontainei*,  
2691 sample ET12.57, Middle Jurassic (location c, d); f-g: *Nezzazata isabellae*, sample ET12.54,  
2692 Aptian-Albian, limestone block in lower part of ophiolite-related melange, Area 5B (Divriği),  
2693 GPS 37S 0425452/4367406; h, i: *Mayncina bulgarica* (Laug et al., 1980), sample ET12.54;  
2694 Aptian-Albian (location as f-g); j-l: *Parakoskinolina* sp., sample ET12.56; Aptian-Albian;  
2695 limestone block in mid part of the ophiolite-related melange, Area 5B (Divriği), GPS 37S  
2696 0425280/436641; m-o: *Akcaya minuta*, sample ET12.56; Aptian-Albian (location j-o); p:  
2697 *Nezzazatinella* sp., sample ET12. 56; Aptian-Albian (location as j-p); q: *Vercorsella* sp.,  
2698 sample ET12. 56, Aptian-Albian (location as j-q). Scale bars= 0.2 mm.

2699

2700 Fig. 19. Measured sedimentary logs of the Late Cretaceous Kemaliye Formation in Area 2  
2701 (Dağlıca); see the text for explanation. Logs 1-5 in Area 3A (E of Elbistan) and farther north;  
2702 Log 1. Near Köseyahya; Log 2, 6 km N of map in Fig. 8; Log 3, 5 km WSW of log 2; Log 4, 7 km  
2703 NE of log 2; Logs 5 and 6 in Area 2 (Dağlıca), see Fig. 7.

2704

2705 Fig. 20. Field photographs in Area 2 (Dağlıca), particularly the Kemaliye Formation. a, Pebbly  
2706 debris-flow, with mostly well-rounded clasts of meta-sandstone (quartzite), with some  
2707 micaschist (centre left); Kemaliye Formation; 1 km N of İncirli GPS 37S 0308706/4255621; b,  
2708 Debris-flow dominated by sub-rounded clasts of limestone (some with rudist debris) in a  
2709 pebbly matrix; Kemaliye Formation; c. 1 km N of İncirli, GPS 37S 0303828/4254761; c,  
2710 Cenomanian rudist-bearing limestone (part of a block) within shale and sandstone; Kemaliye  
2711 Formation; near Hurman kalesi, GPS 37S 0311635/4261660; d, Blocks of neritic limestone  
2712 with rudist bivalves in highly deformed Kemaliye Formation; near Hurman kalesi, GPS  
2713 0307401/4259103; e, Mudrocks of the Kemaliye Formation, interspersed with blocks of  
2714 Mesozoic neritic limestone; overthrust by the upper Munzur thrust sheet; Hurman kalesi  
2715 area, GPS 37S 0314553/4260250; f, Crudely stratified, ophiolite-derived debris-flow units,  
2716 including clasts of basalt, diabase, gabbro, pelagic limestone and radiolarian chert,  
2717 associated with the Dağlıca ophiolite; near Kaşanlı köy, GPS 37S 0326709/4257612; g,

2718 Matrix-supported debris-flow unit with clasts of gabbro (lower left), diabase and basalt;  
2719 associated with the Dağlıca ophiolite; same locality as f; h, Ophiolite-derived debris flow,  
2720 locally dominated by basalt (centre right); associated with the Dağlıca ophiolite; 1.5 km W of  
2721 Kırkısrak, GPS 37S 0294299/4259724; i, as d, e with angular clast of pink pelagic limestone,  
2722 with red 'replacement' chert; j, Debris-flow conglomerate made up of ophiolitic clasts  
2723 including gabbro, diabase and basalt; associated with the Dağlıca ophiolite; İncirli area, GPS  
2724 37S 030015/425603); k, Late Cretaceous-Eocene succession of the relatively autochthonous  
2725 Gürün platform, overthrust by Mesozoic Munzur limestone; 2 km NE of Dallıkavak, GPS 37S  
2726 0293001/4261378; l, Clast-supported conglomerate including well-rounded clasts of Eocene  
2727 Nummulitic limestone; probably Miocene; 1.5 km NW Çağsak, GPS 37S 0286787/4257672.

2728

2729 Fig. 21. Photomicrographs of key age-diagnostic planktic microfossils. a, *Globotruncana* cf.  
2730 *G. mariei* Banner & Blow, 1960, sample M.13.35; Kemaliye Formation; Campanian-  
2731 Maastrichtian, near Kapaklı, Area 3A, NE of Elbistan, GPS 37S 0361390/4259247; b,  
2732 *Globigerinelloides* sp., sample M.13.35, Campanian-Maastrichtian (same location); c,  
2733 *Globotruncana linneiana* (D'Orbigny, 1839), sample M13.4, pelagic limestone block in  
2734 Kemaliye Formation, Campanian-Maastrichtian, Odunluk Tepe; Area 3A, E of Elbistan; GPS  
2735 37S 0366666/4225559; *Archaeoglobigerina cretacea* (D'Orbigny, 1840), Campanian-  
2736 Maastrichtian (same location); e, f: *Globigerinidae*, sample M13.60, Cenozoic. Pelagic  
2737 limestone block in debris-flow deposit, near İğde köyü (SE of Elbistan), GPS 37S  
2738 0335066/4223251. Scale bars= 0.2 mm.

2739

2740 Fig. 22. Structural relationships in Area 3B (Nurhak Dağı); a, Meta-carbonate rocks of the  
2741 Malatya Metamorphics, structurally overlain by serpentinitised harzburgite which is cut by  
2742 small granitic intrusions, and in then overthrust by a thin unit of the Kemaliye Formation,  
2743 with the Köseyahya thrust sheet above; near Beğre;  
2744 b, Malatya Metamorphics, structurally overlain by serpentinitised harzburgite, then by the  
2745 Kemaliye Formation, with the Köseyahya thrust sheet above, c. 10 km north-east of a. The  
2746 blocks in the Kemaliye Formation include Triassic red crinoidal limestone, similar to that in  
2747 the Köseyahya thrust sheet, in a matrix of terrigenous sandstone and mudrock.

2748

2749 Fig. 23. Simplified geological map of part of Area 5B, Divriği (simplified from MTA 1:100,000  
2750 geological maps of Turkey (Bilgiç, 2008a, b, c). Note the locations of the representative  
2751 sections shown in Fig 25. See text for explanation and data sources.

2752

2753 Fig. 24. Summary of the stratigraphy and structural relations in part of Area 5B, Divriği. a,  
2754 Stratigraphic column; b, Rock-relations (bi in the north; b-ii in the south). See the text for  
2755 explanation and data sources.

2756

2757 Fig. 25. Field photographs of Divriği ophiolite-related melange in Area 5B. a, Elongate blocks  
2758 of thick-bedded neritic limestone set in a matrix of serpentinite and sandstone/shale; c. 6  
2759 km NW of Divriği); b, Elongate blocks of Mesozoic neritic limestone embedded in sheared  
2760 serpentinite; c. 6 km NW of Divriği); c, Part of a large block of thick-bedded neritic  
2761 limestone, deformed into a SW-verging fold; c. 6 km NW of Divriği); d, Large block of  
2762 Mesozoic neritic limestone in the Divriği melange, deformed into a N-verging fold; c. 3 km  
2763 NW of Divriği); e, Serpentinite melange with a strongly sheared steeply dipping fabric; c. 7  
2764 km SE of Divriği); f, Large exposure of serpentinite melange, dominated by mantle  
2765 harzburgite; c. 10 km SE of Divriği.

2766

2767 Fig. 26. Summary of fold data (axial planes and hinges) collected during this study, plotted as  
2768 poles; equal-area lower hemisphere projection; N= number of measurements; ai-aiv, Fold  
2769 axial planes; bi-biv Fold hinges. Individual plots: ai-bi Malatya Metamorphics (Area 1. W of  
2770 Elbistan); aii-bii Allochthonous Tauride units (Area 2, Dağlıca); aiii-biii Allochthonous Tauride  
2771 units (Area 3A, E of Elbistan); aiv-biv Combined units: Malatya (Keban) metamorphics and  
2772 Kemaliye Formation (Area 1) (Kemaliye area). See Supplementary Figs. 7-10 for plots of all  
2773 data, including bedding.

2774

2775 Fig. 27. Geological development of the central and northern parts of the Tauride continent.  
2776 a, Late Triassic extensional faulting establishes the contiguous neritic Munzur platform, the  
2777 Neritic-pelagic Köseyahya platform and the Pelagic (Gülbahar) unit; b, Mid-Late Jurassic. N-  
2778 dipping ramp develops redepositing mainly oolitic facies into deeper water; c, Late  
2779 Cretaceous (Cenomanian). Rudist bivalve reefs develop on proximal (Munzur) platform

2780 while deeper-water slope conditions persist farther north; d, Campanian-Maastrichtian. The  
2781 southern part of the Tauride continent (Malatya platform) detaches and is deeply  
2782 underthrust northwards; ophiolite is emplaced southwards over the northern edge of the  
2783 Tauride continent which collapsed in advance to form a foredeep.

2784

2785 Fig. 28. Geological development of the Tauride continent in the E Taurides. a, Carboniferous;  
2786 includes rift-related volcanism; b, Mid-Late Triassic continental rifting; c, Mid-Late Jurassic  
2787 passive margin subsidence; d, Late Cretaceous (Cenomanian, c. 90 Ma); northward  
2788 subduction of oceanic crust; e, Late Cretaceous (Campanian-Maastrichtian); collision and  
2789 crustal imbrication of the Tauride continent. Note: it is uncertain whether the Malatya and  
2790 Munzur-Köseyahya units were either contiguous or separate platforms. See text for  
2791 discussion.

2792

2793 Fig. 29. Stages in the latest Cretaceous (late Campanian-Maastrichtian), southward  
2794 emplacement of oceanic crust and passive continental margin units in the E Taurides. a,  
2795 Flexural foredeep is imbricated during compressional emplacement; b, With further  
2796 emplacement, the relatively distal neritic-pelagic (Köseyahya) platform detaches and is  
2797 thrust over the more proximal neritic (Munzur) platform; c, With further convergence, part  
2798 of the neritic (Munzur) platform is locally re-thrust over the neritic-pelagic platform unit.

2799

2800 Fig. 30. Rock-relations diagram showing the inferred tectono-stratigraphy of the E Taurides  
2801 following latest Cretaceous emplacement/exhumation, restored to beneath the latest  
2802 Cretaceous transgressive shallow-marine sedimentary cover (south of the Gürün  
2803 autochthon). From the structural base upwards: Malatya (Tauride) continental unit; Late  
2804 Cretaceous Göksun (Berit) ophiolite; partially exhumed Malatya Metamorphics (both of the  
2805 latter are stitched by the Late Cretaceous Baskil granitoids); debris-flows ('olistostromes')  
2806 (e.g. Kemaliye Formation type area), with slices and blocks of the pelagic (Gülbahar) unit  
2807 and finally supra-subduction zone ophiolites and their metamorphic sole. Note: variable  
2808 internal deformation of the Munzur, Köseyahya and ophiolitic thrust sheets is not shown.

2809

2810 Fig. 31. Alternative tectonic models for the eastern Taurides. ai-aii, Assumes one ocean to  
2811 the north and one continent to the south. The allochthonous units are emplaced by complex  
2812 out-of-sequence thrusting (based on Ricou et al., 1984); bi-bii. Assumes a single Mesozoic  
2813 Neotethys. The Late Cretaceous ophiolites form above a subduction zone to the E-NE that  
2814 rotates and rolls-back, emplacing segments over the N and S margins of the Tauride  
2815 continent and over Arabia/N Africa. The Bitlis and Pütürge metamorphism relates to  
2816 attempted southward subduction. An Inner Tauride basin is assumed between the Tauride  
2817 continent and a combined Kırşehir-Tavşanlı crustal block in the north, but this basin is not  
2818 the source of the ophiolites (based on van Hinsbergen et al., 2020); ci-cii. (preferred model).  
2819 This assumes several microcontinents and small Mesozoic ocean basins. The Bitlis and  
2820 Pütürge continental units represent rifted fragments with ocean crust on either side. Supra-  
2821 subduction zone oceanic crust in the northerly basin (Berit ocean) subducts northwards  
2822 resulting in arc magmatism that intrudes the continental block to the north (Malatya  
2823 metamorphic unit). An Inner Tauride ocean was potentially the source of Late Cretaceous  
2824 supra-subduction zone ophiolites in the north. Supra-subduction zones are emplaced  
2825 separately, southwards onto the Arabian margin. Uncertain is whether the Tauride platform  
2826 links with the South Armenian platform at depth as there is no continuous surface exposure.  
2827 See text for discussion.

2828

2829

2830

2831

2832

2833

2834

2835

2836

2837

2838

2839

2840

2841

2842

2843

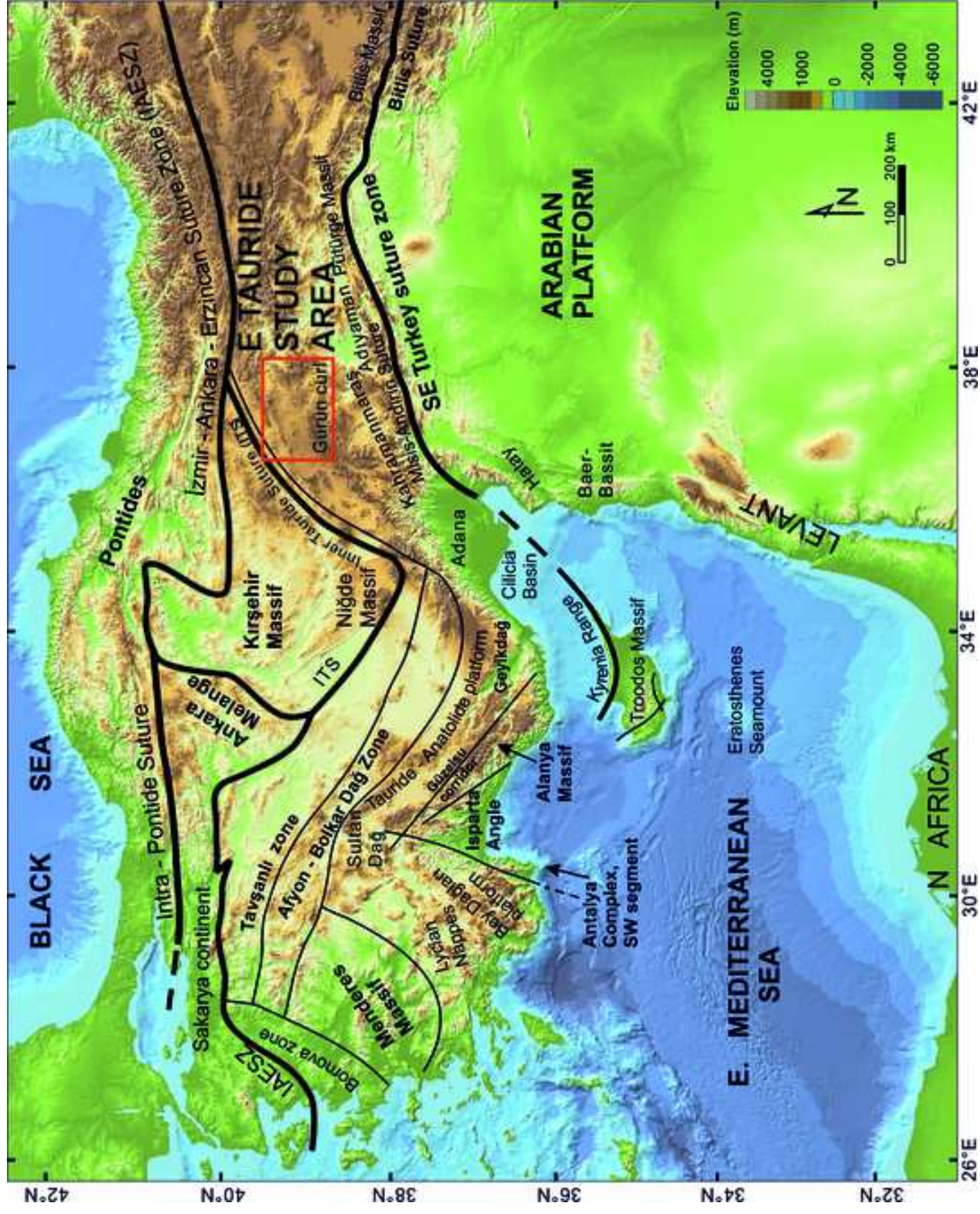
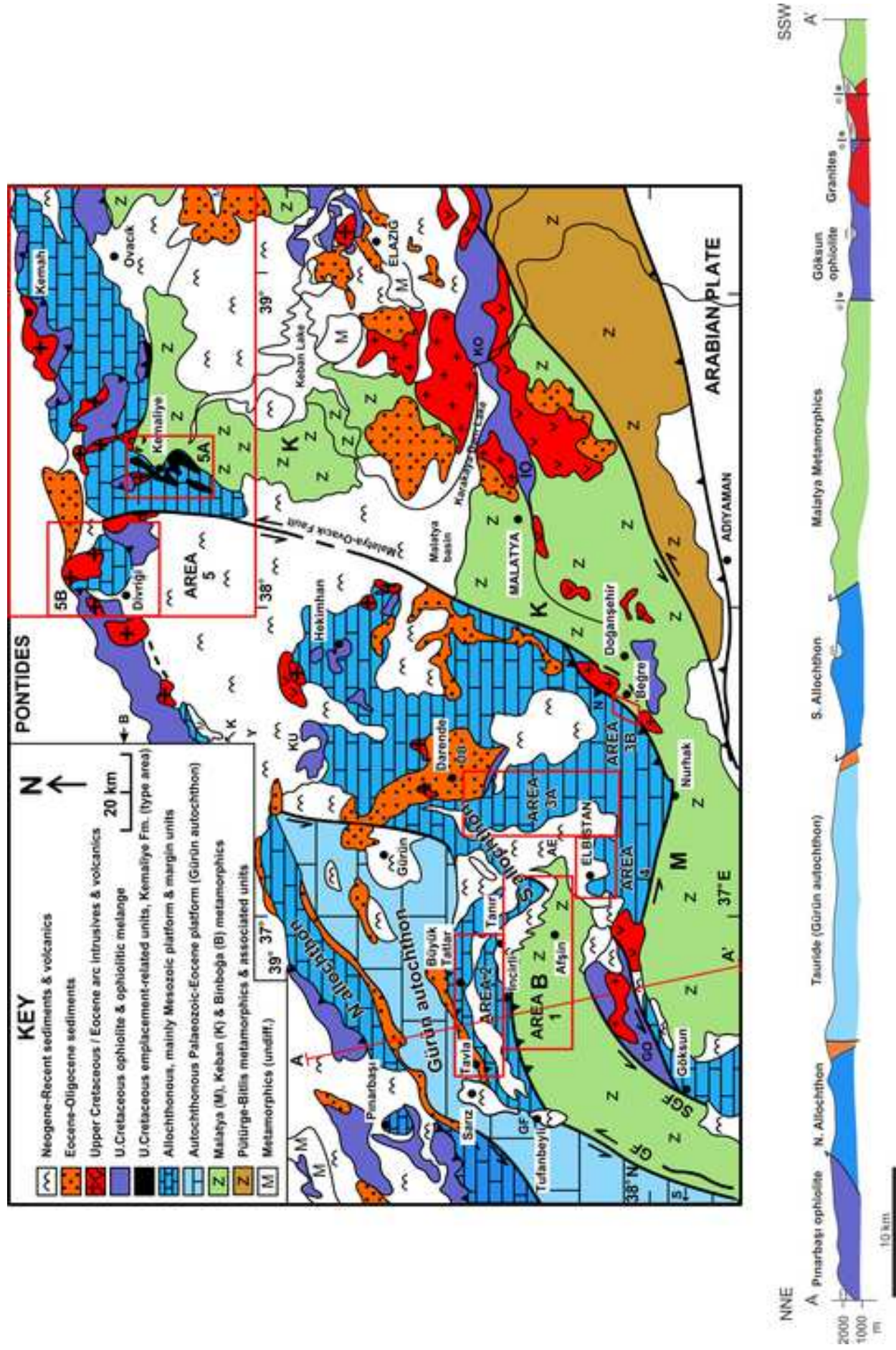


Figure 1





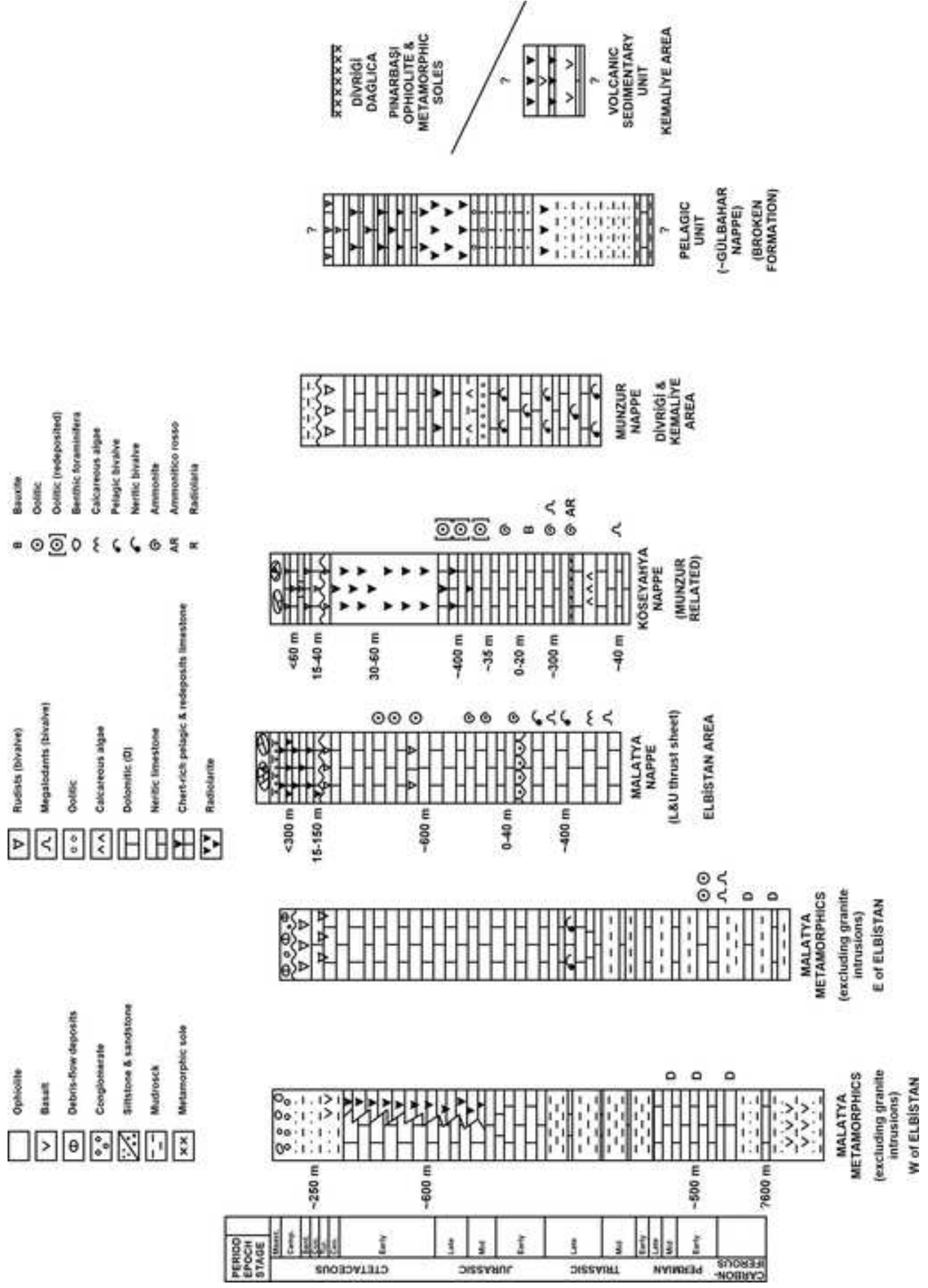
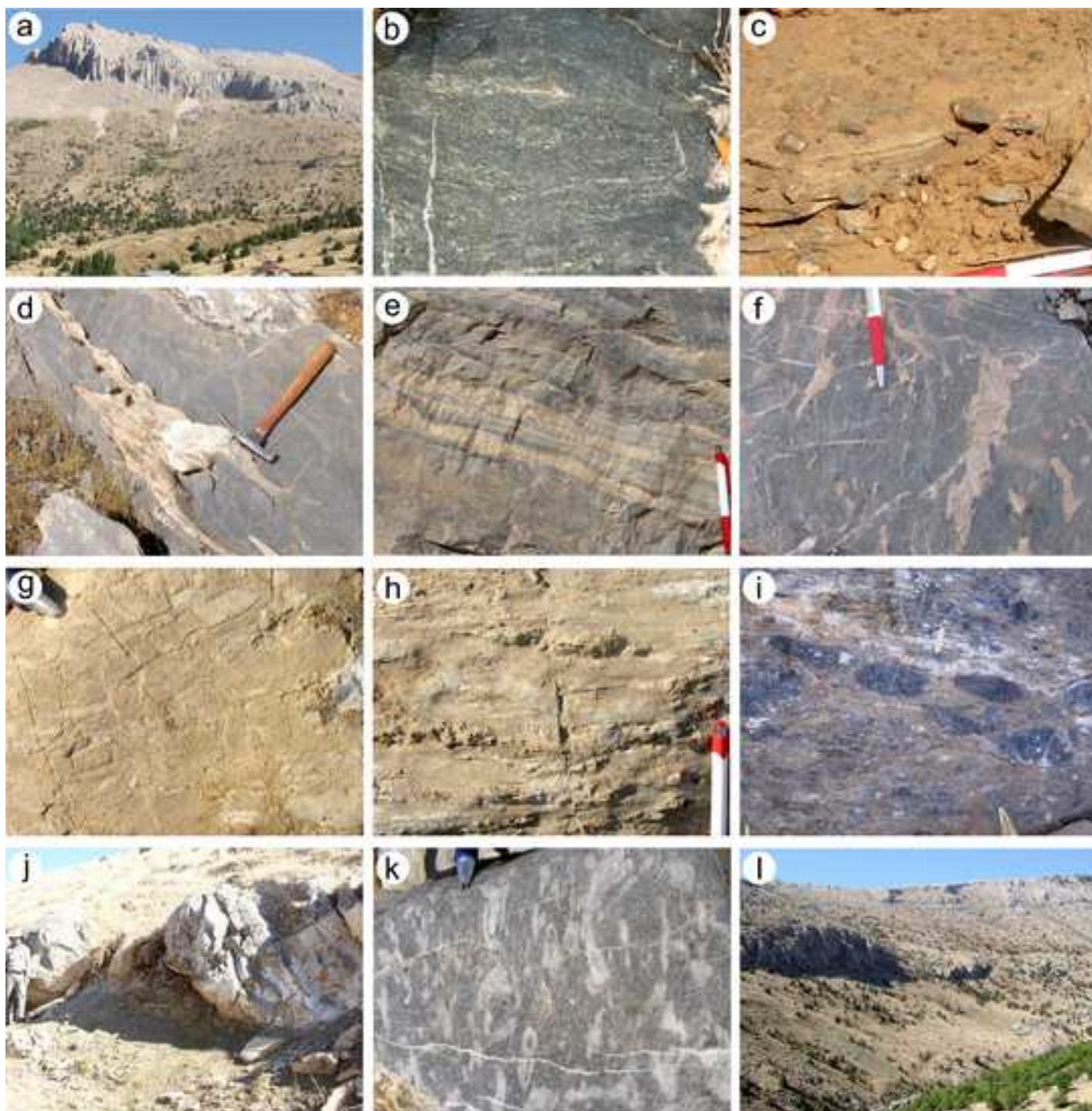


Figure 4

[Click here to access/download;Figure;Fig4.jpg](#)



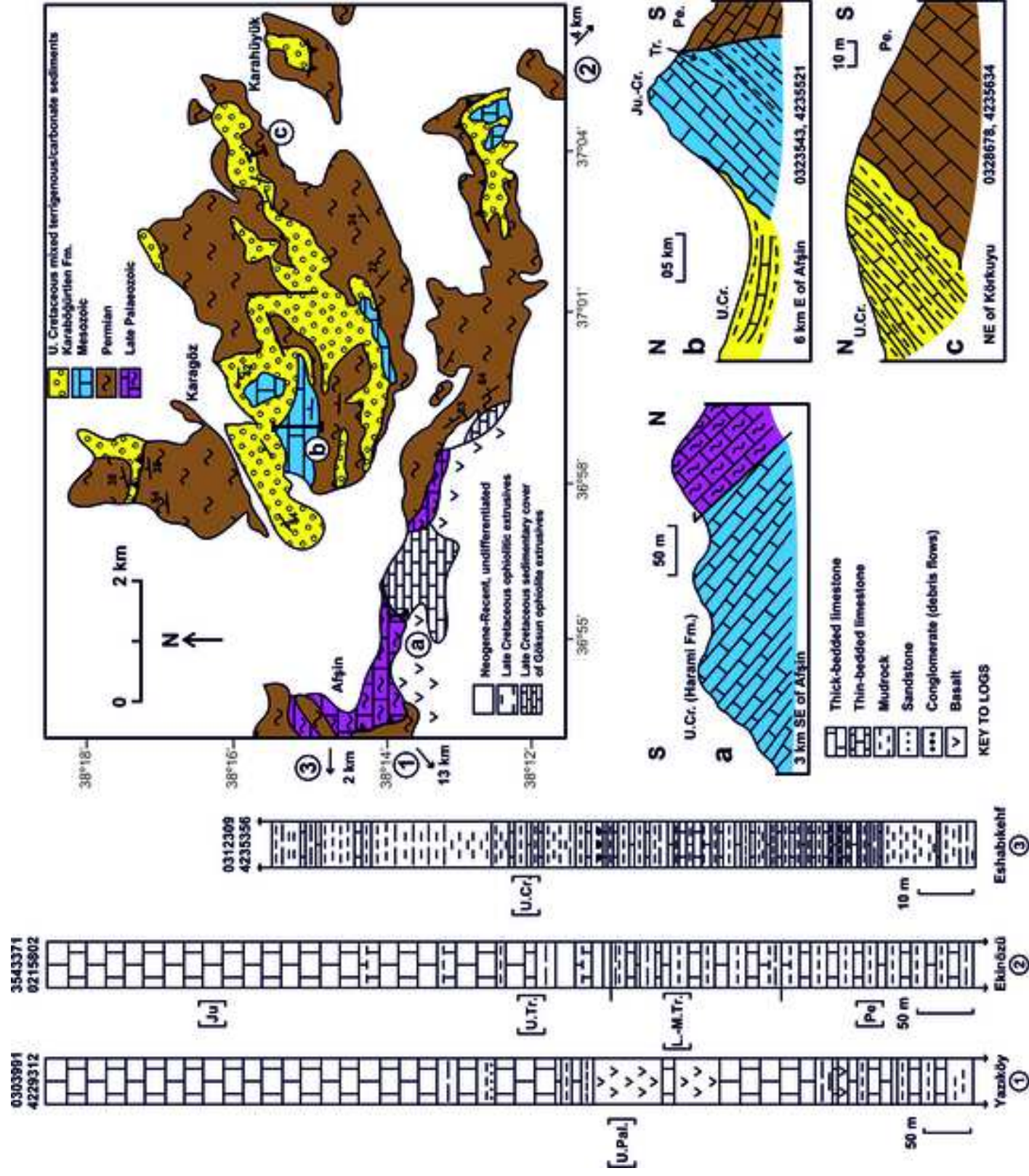
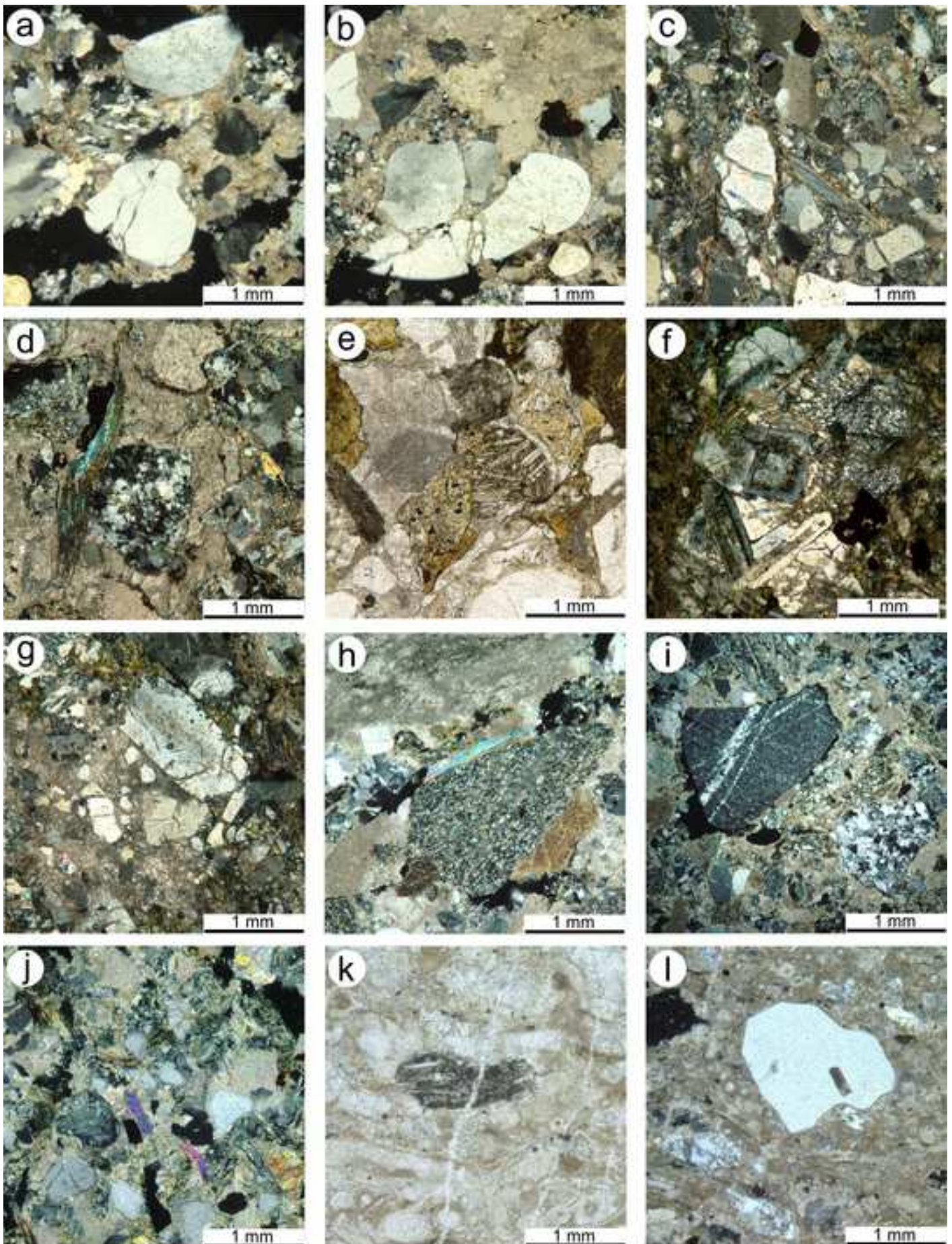
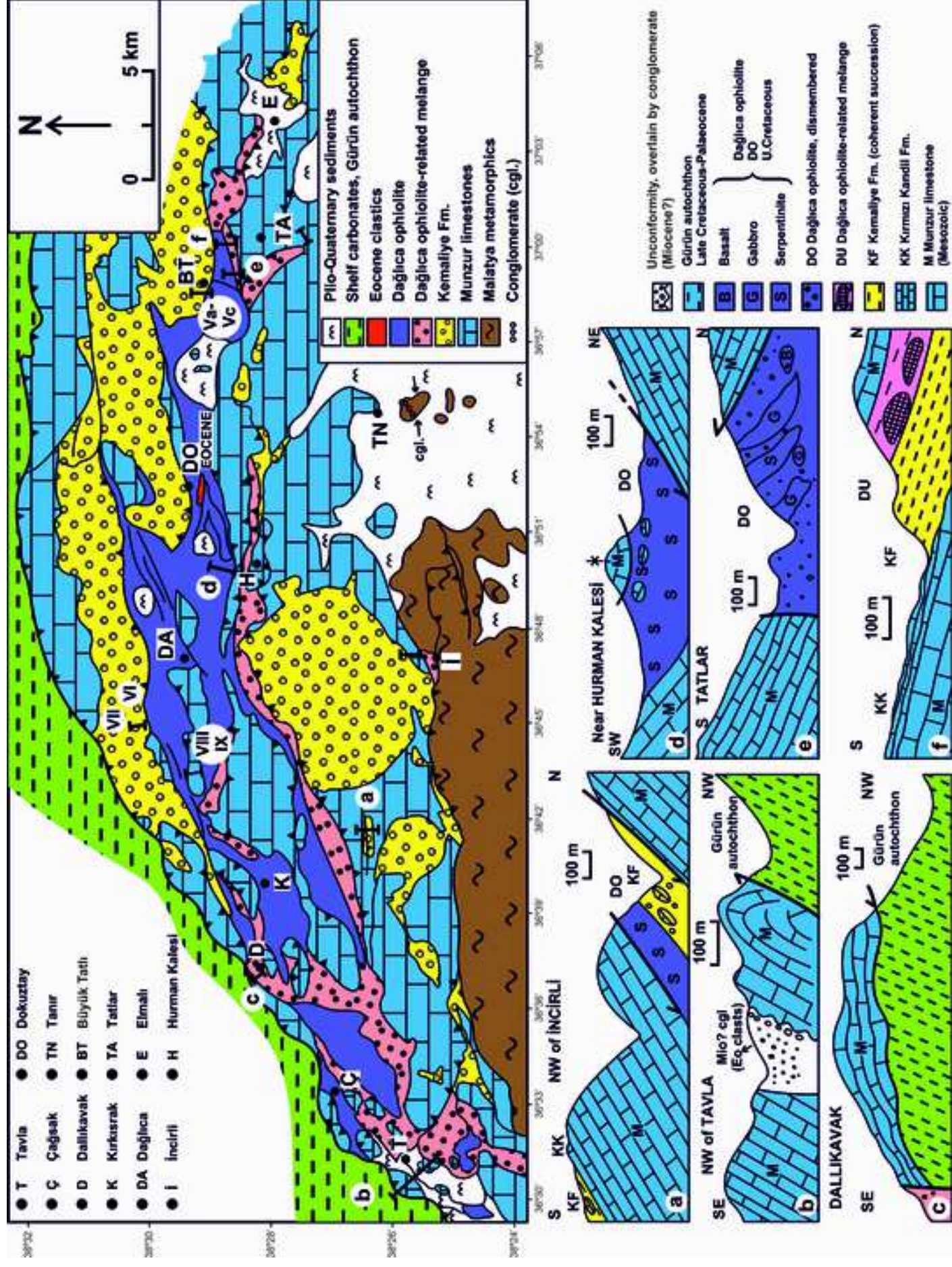


Figure 5





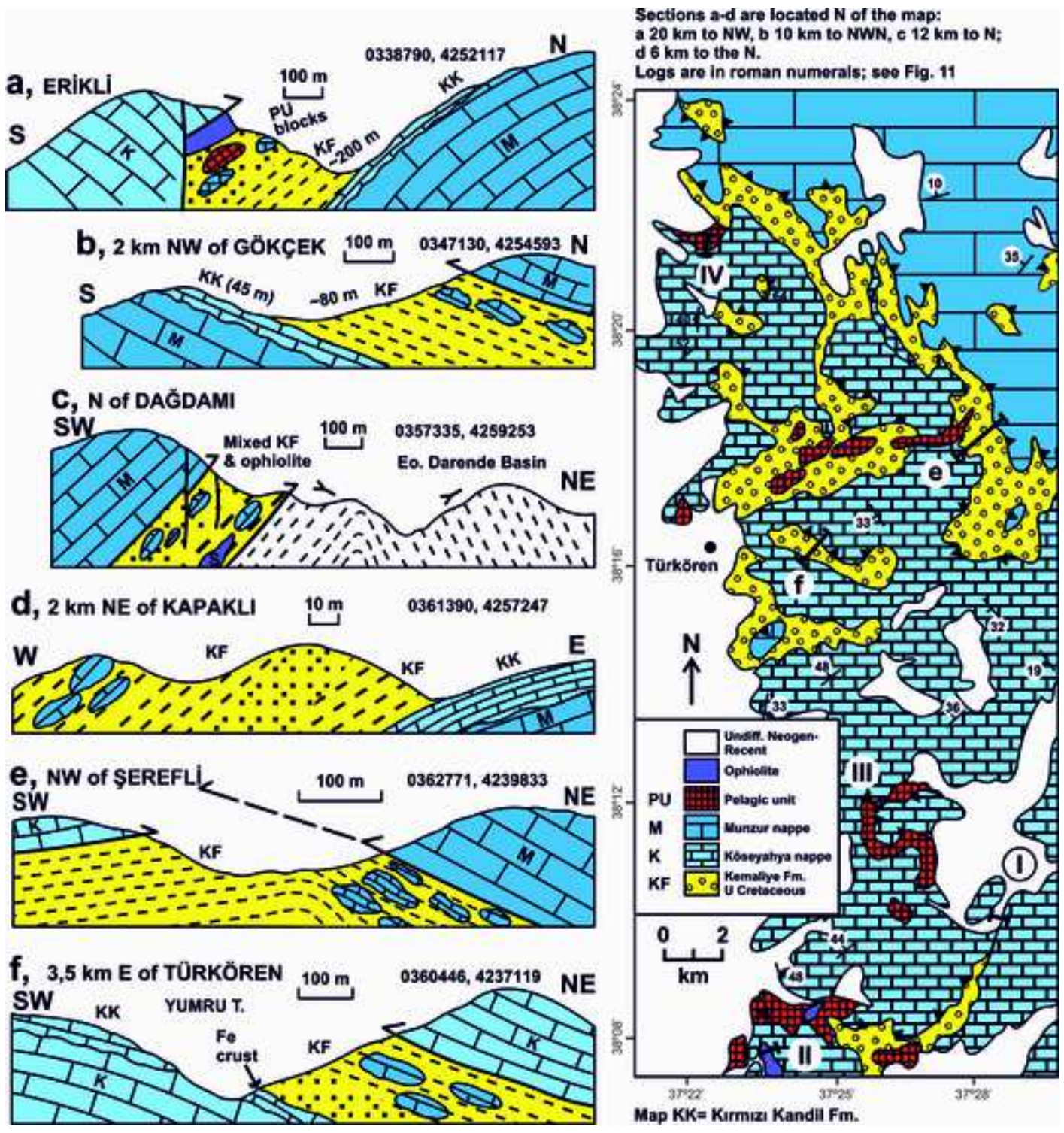
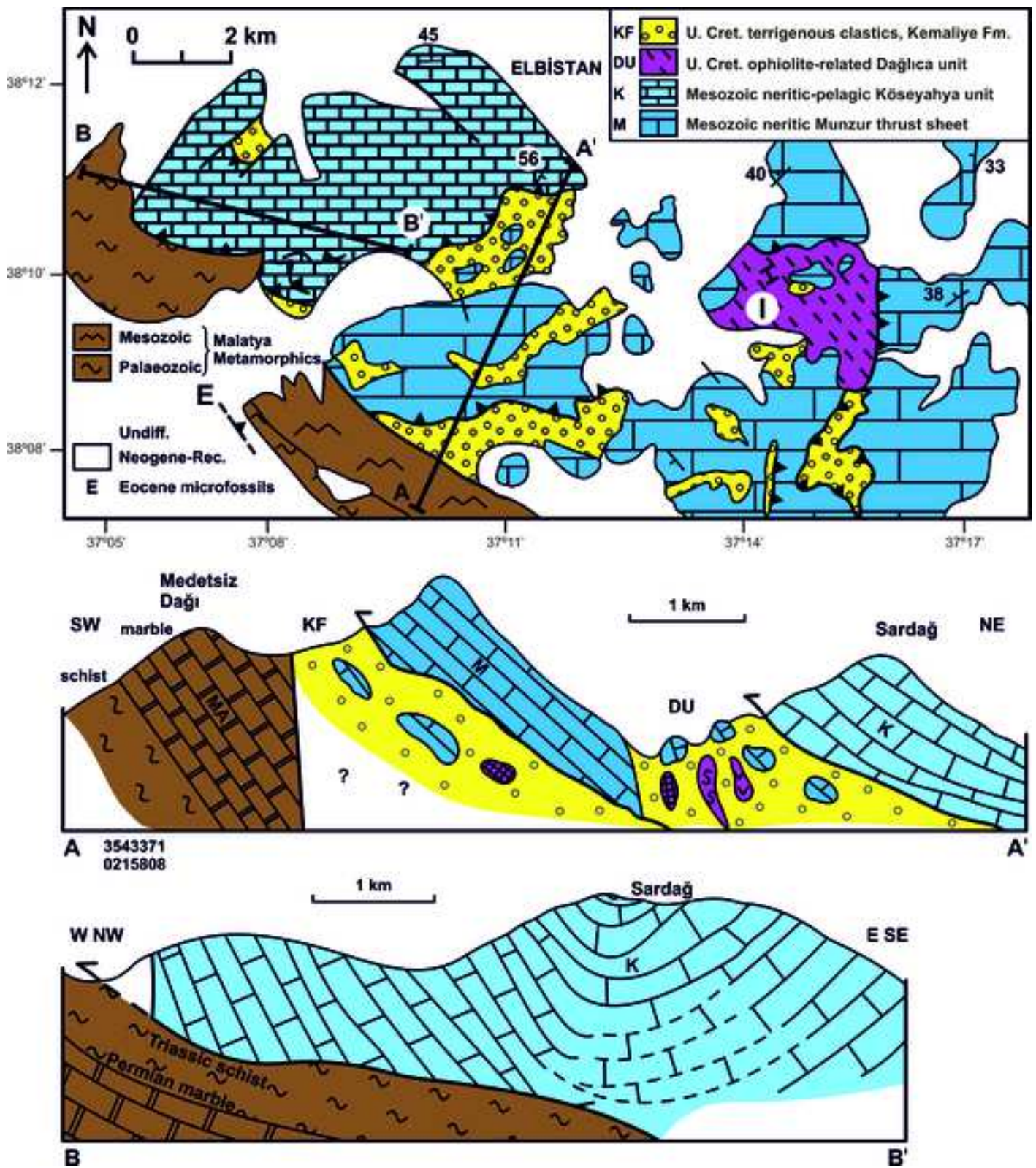


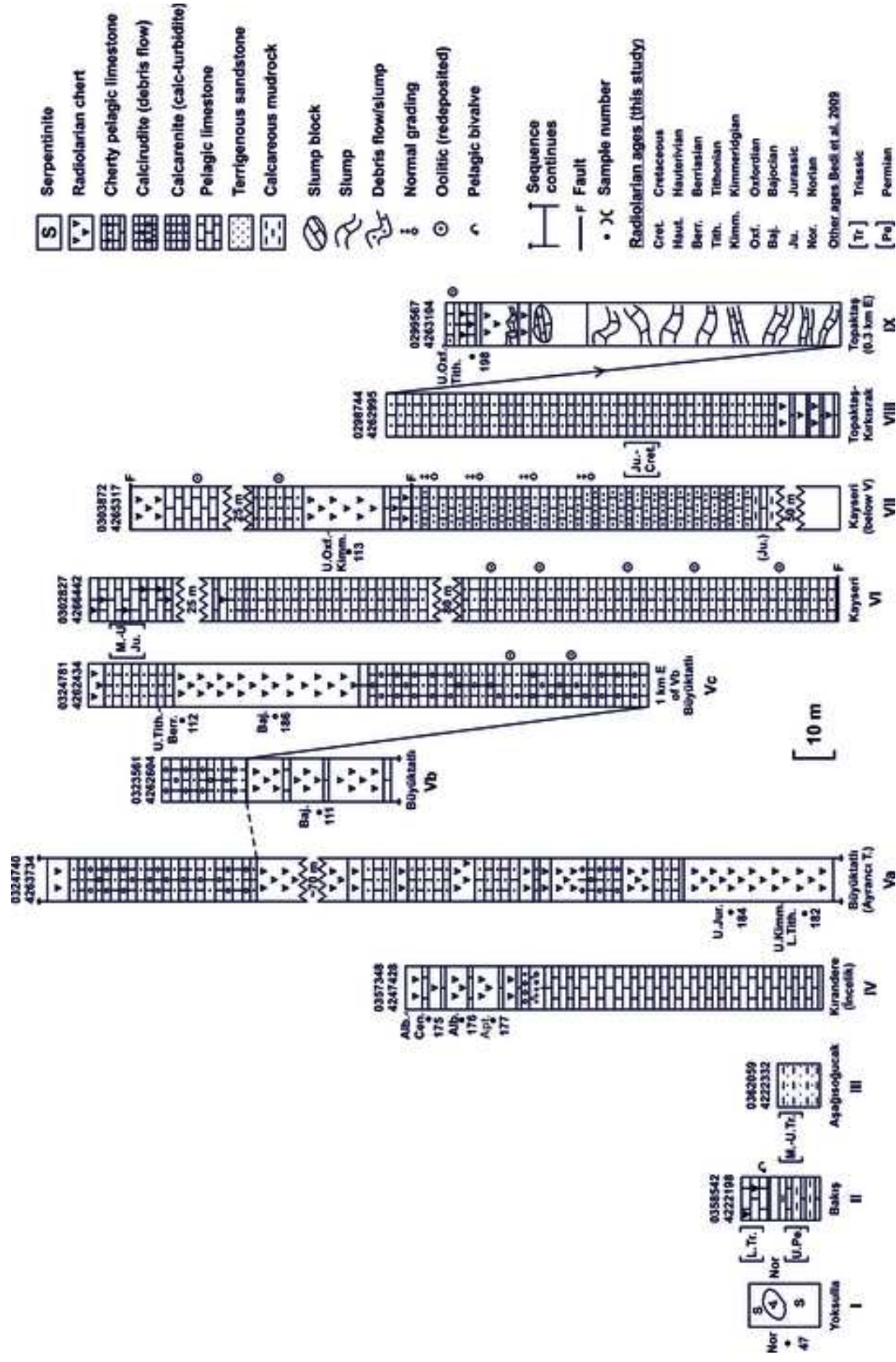
Figure 9

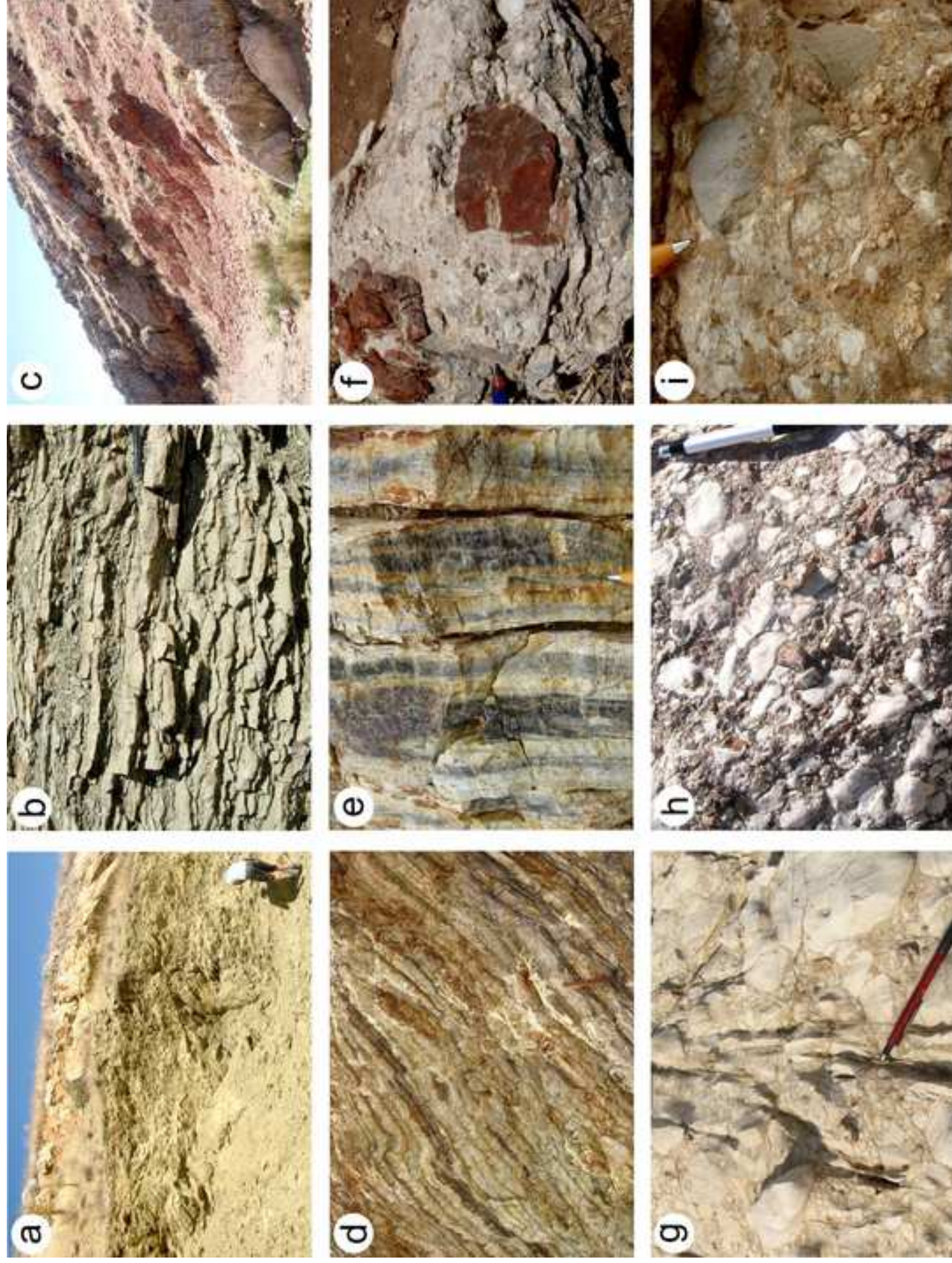
[Click here to access/download;Figure;Fig\\_9REVAR14,4,21\\_MOD](#)











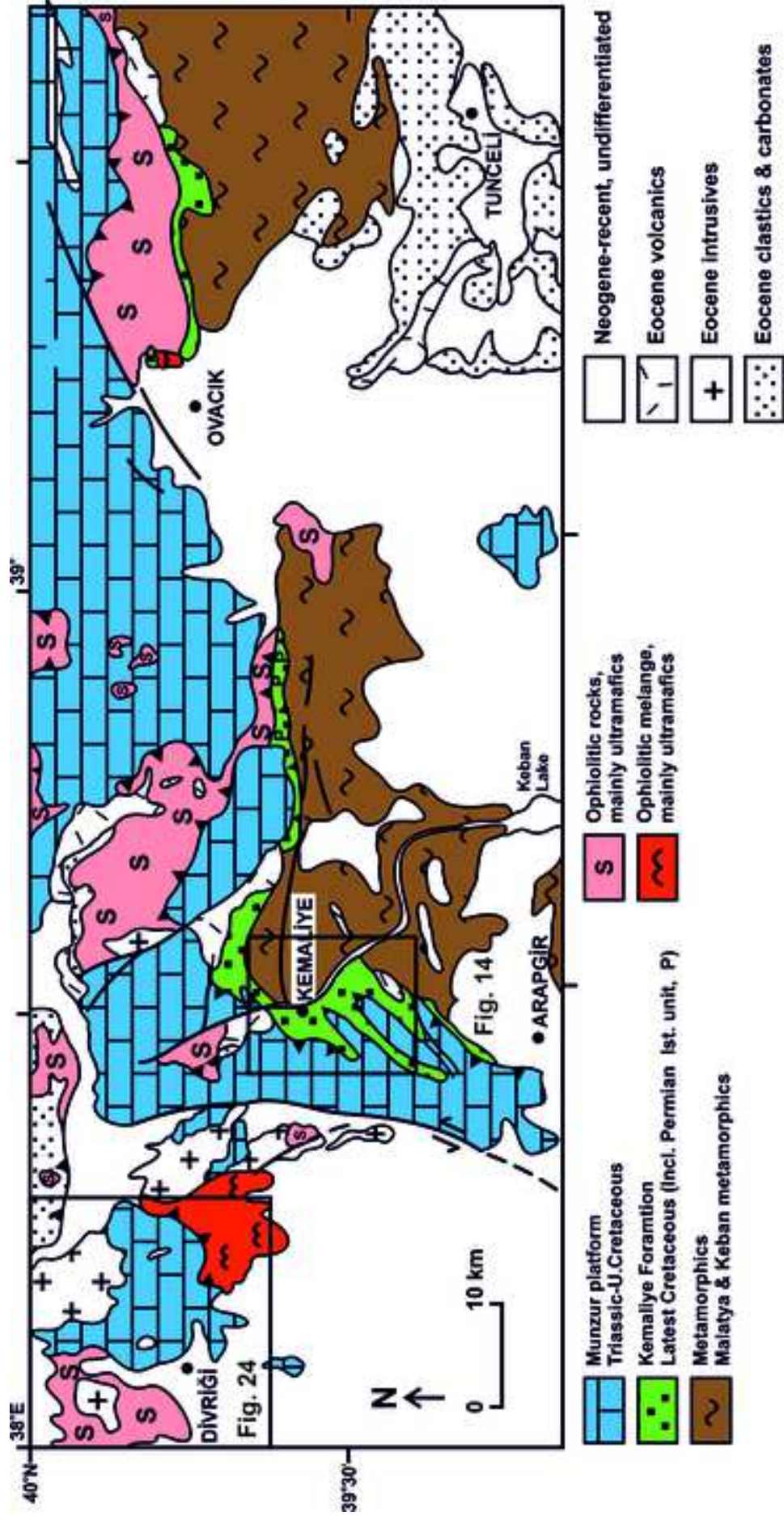


Figure 14

[Click here to access/download;Figure;Fig. 14.ARREV12.1 MOD.jpg](#)

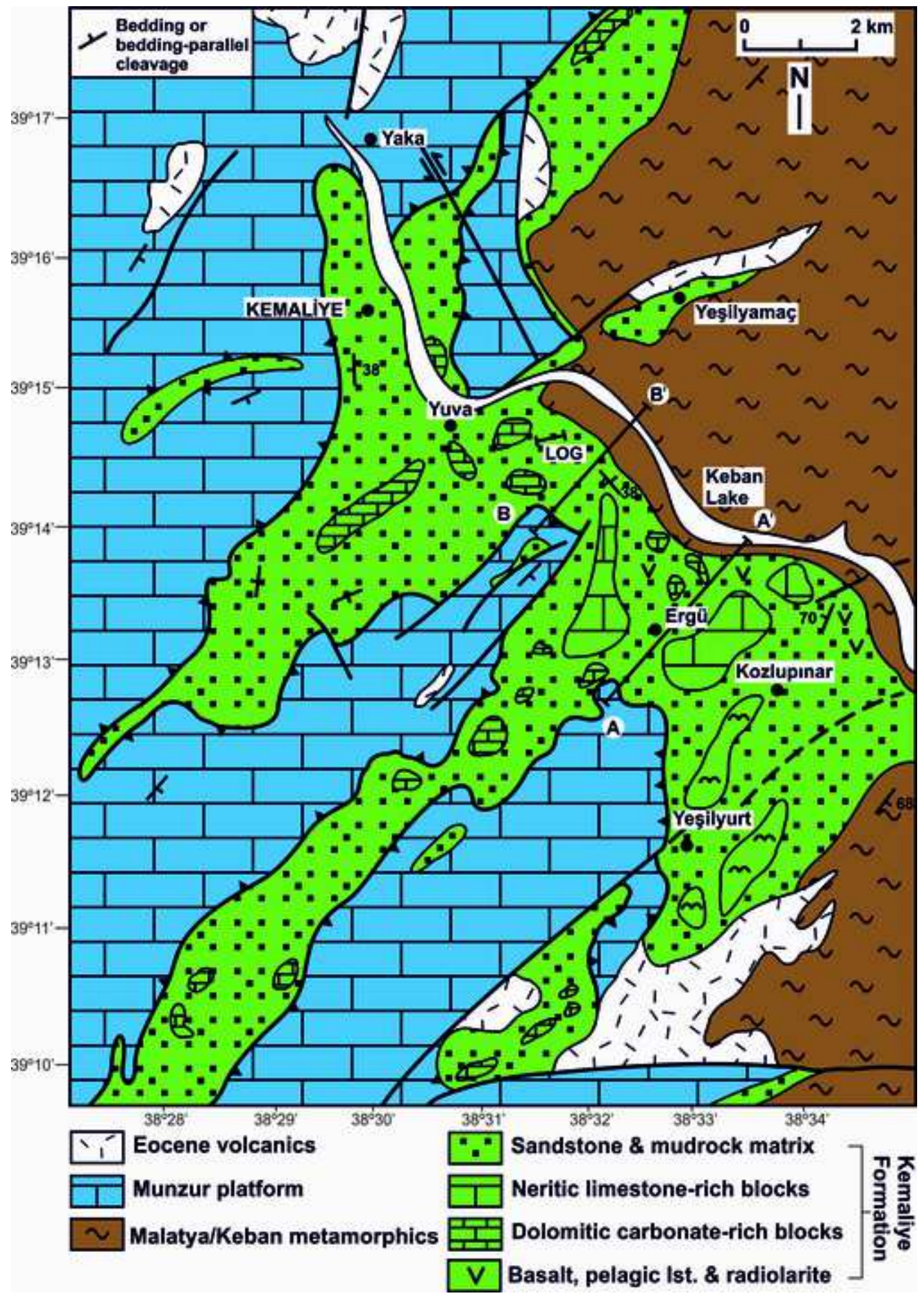
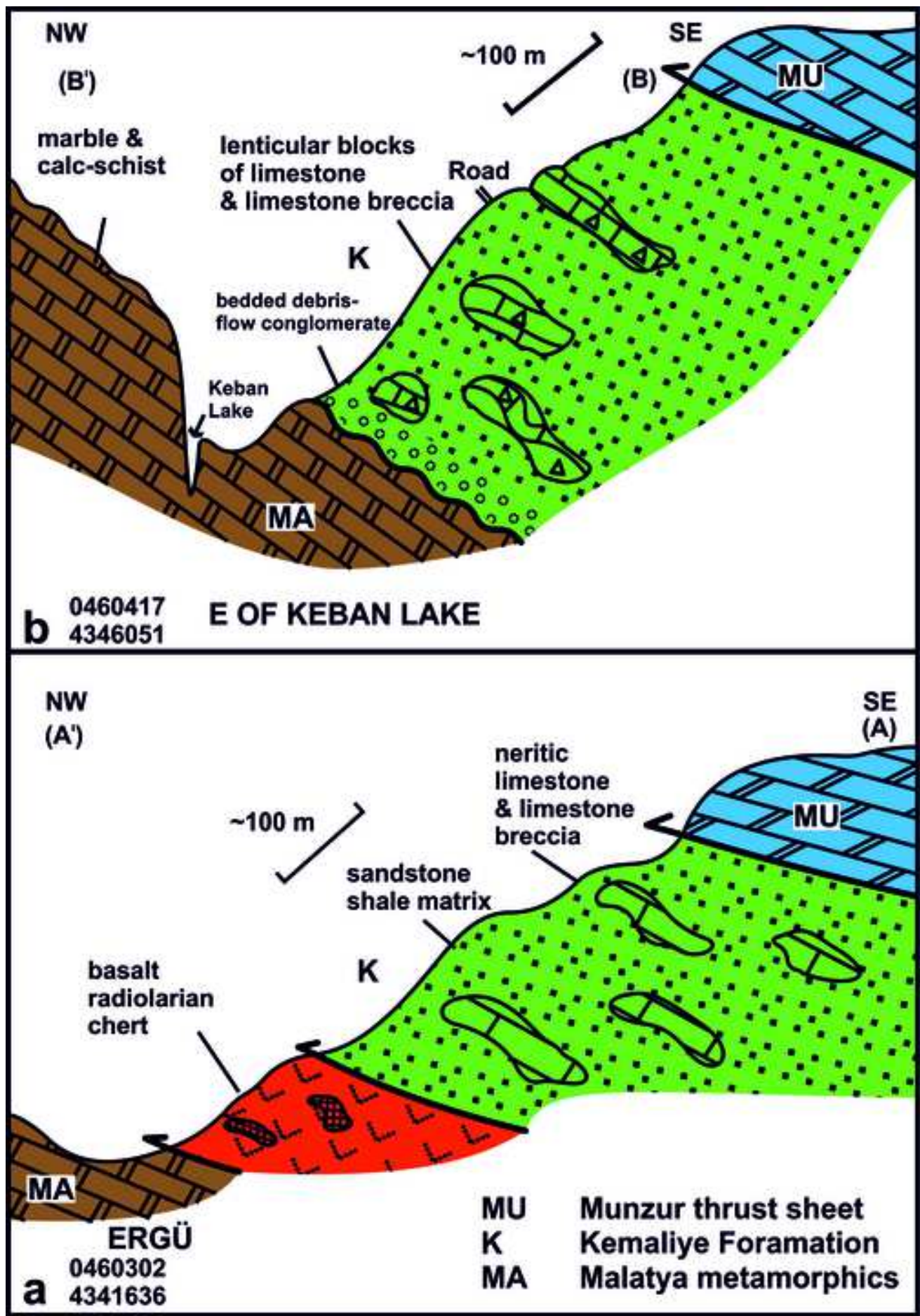


Figure 15



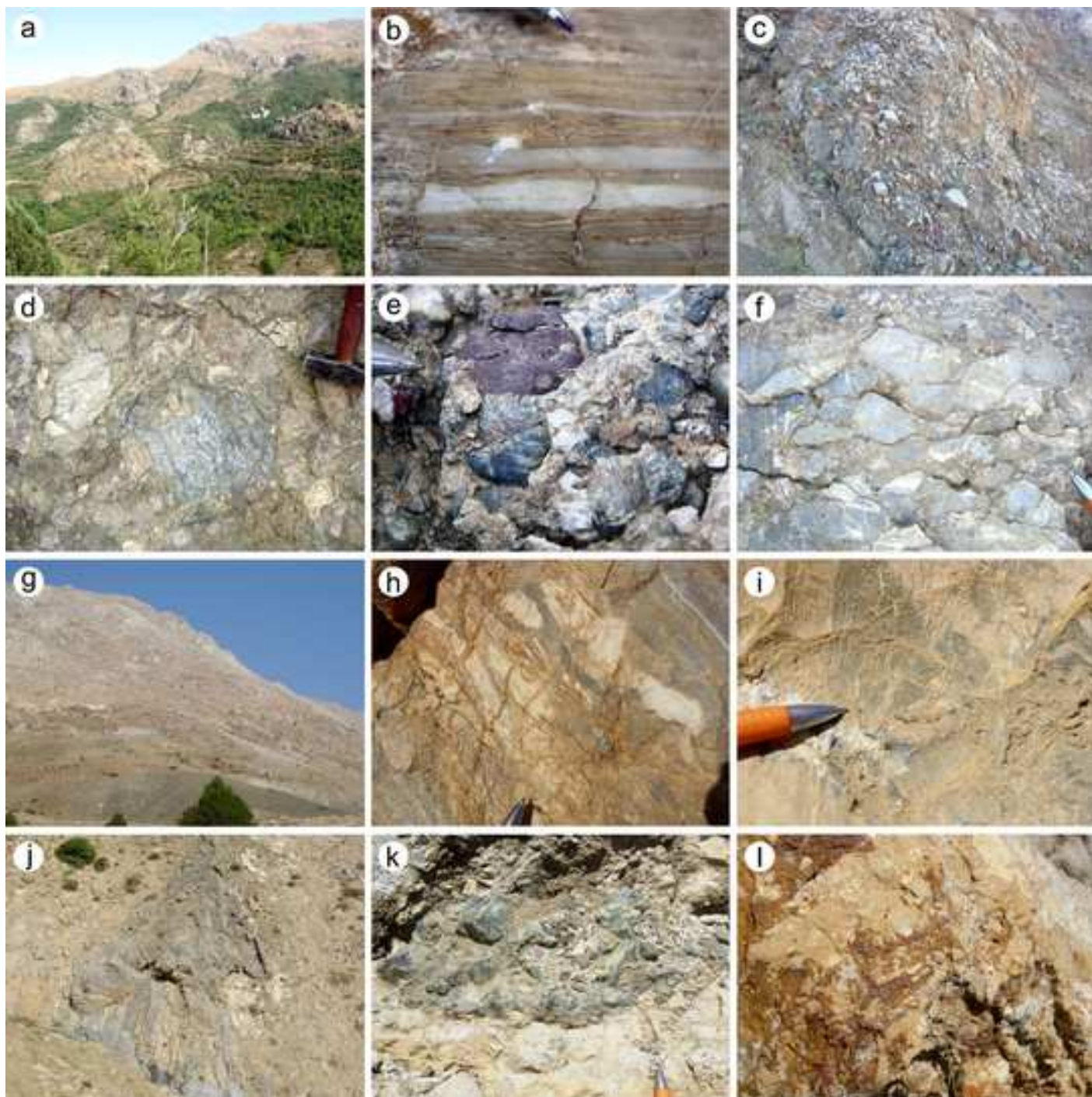
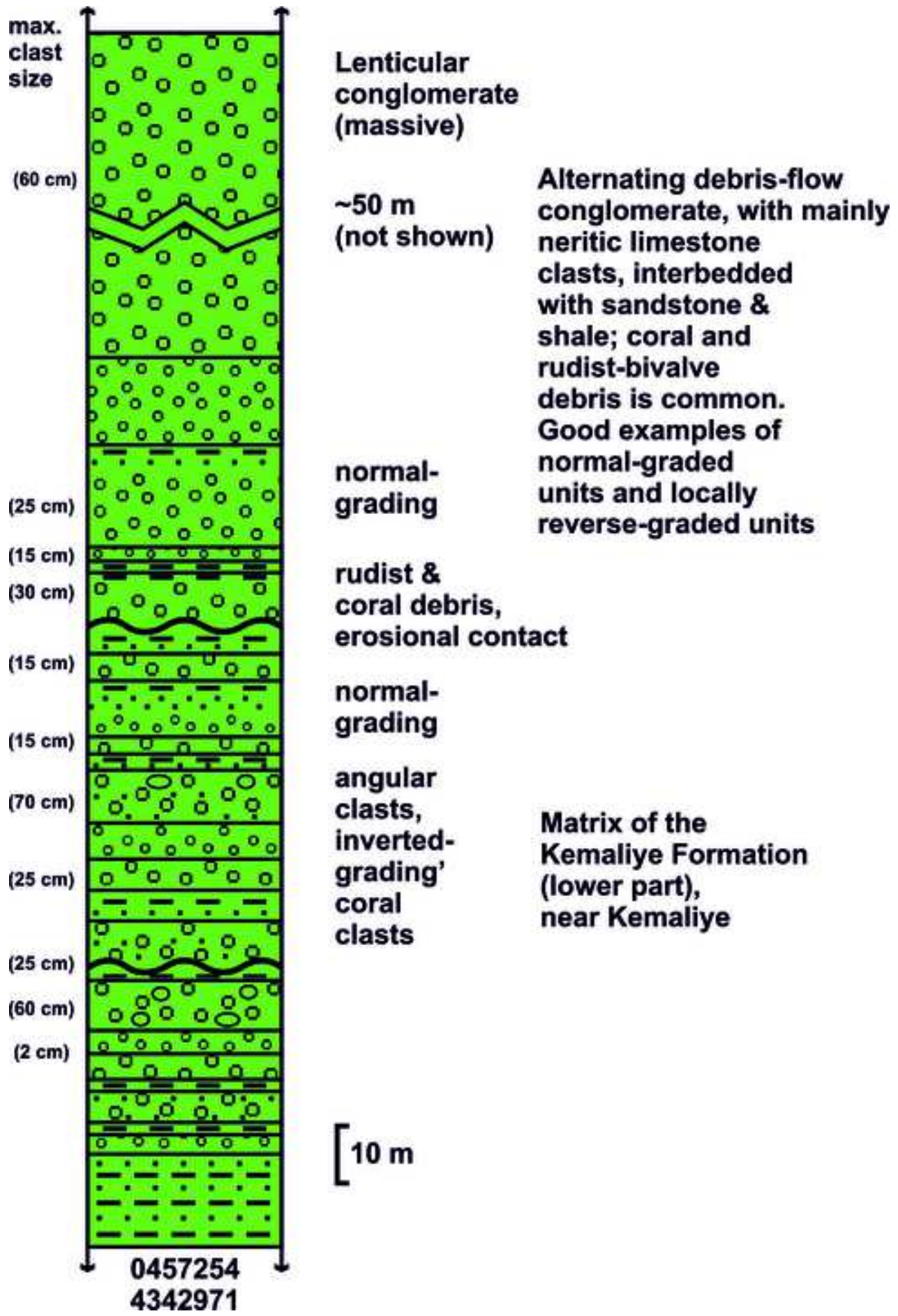
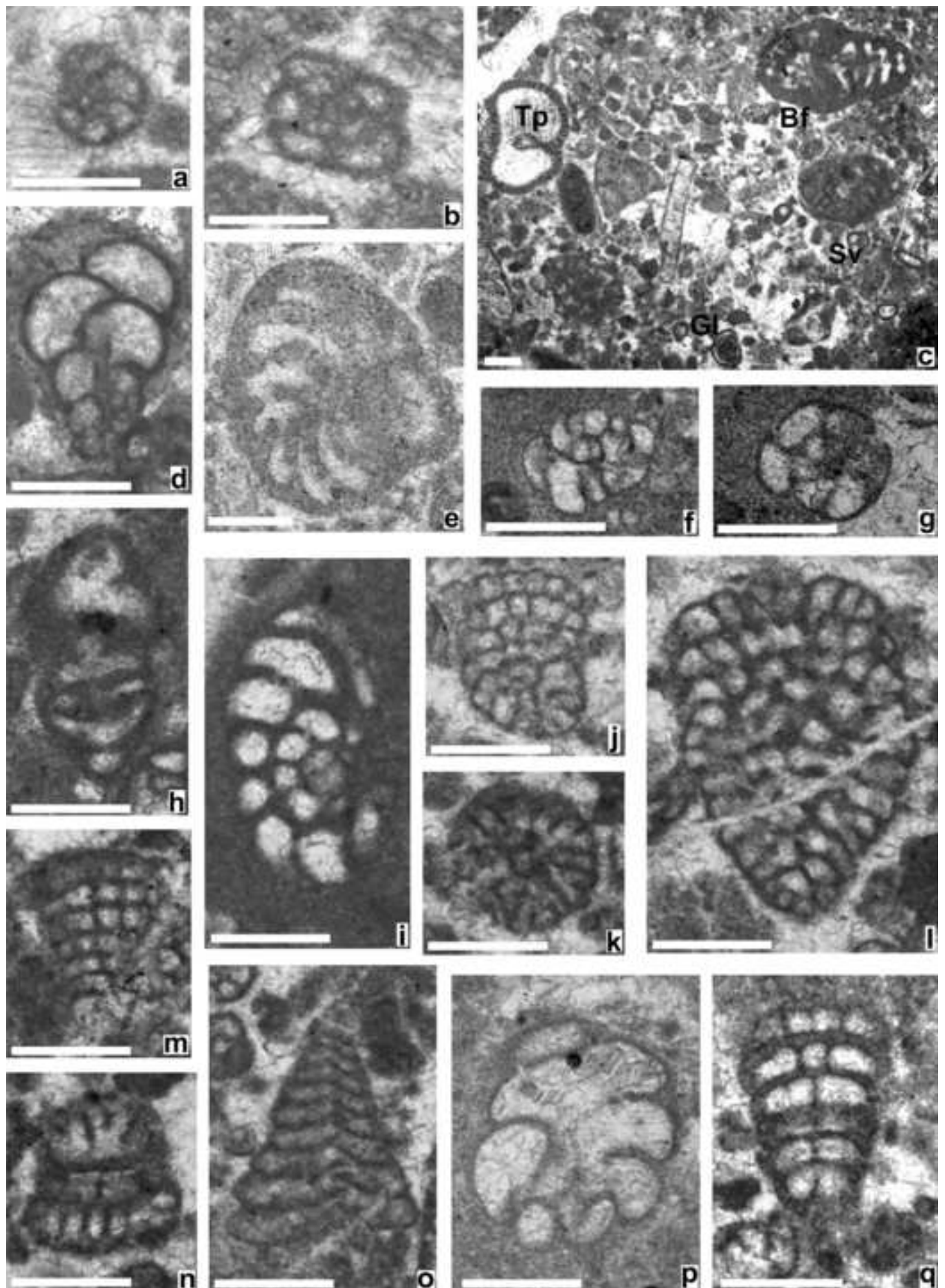
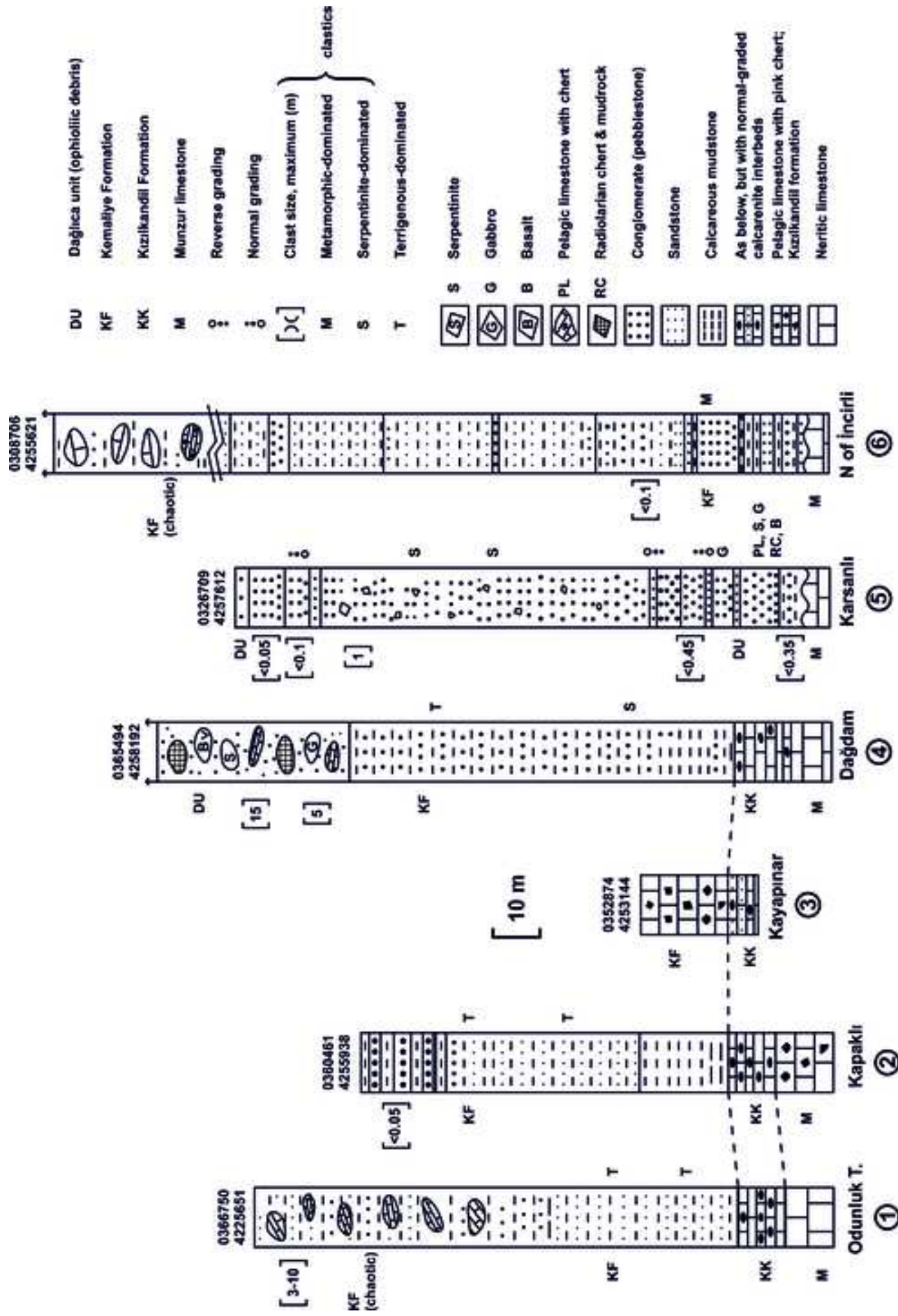


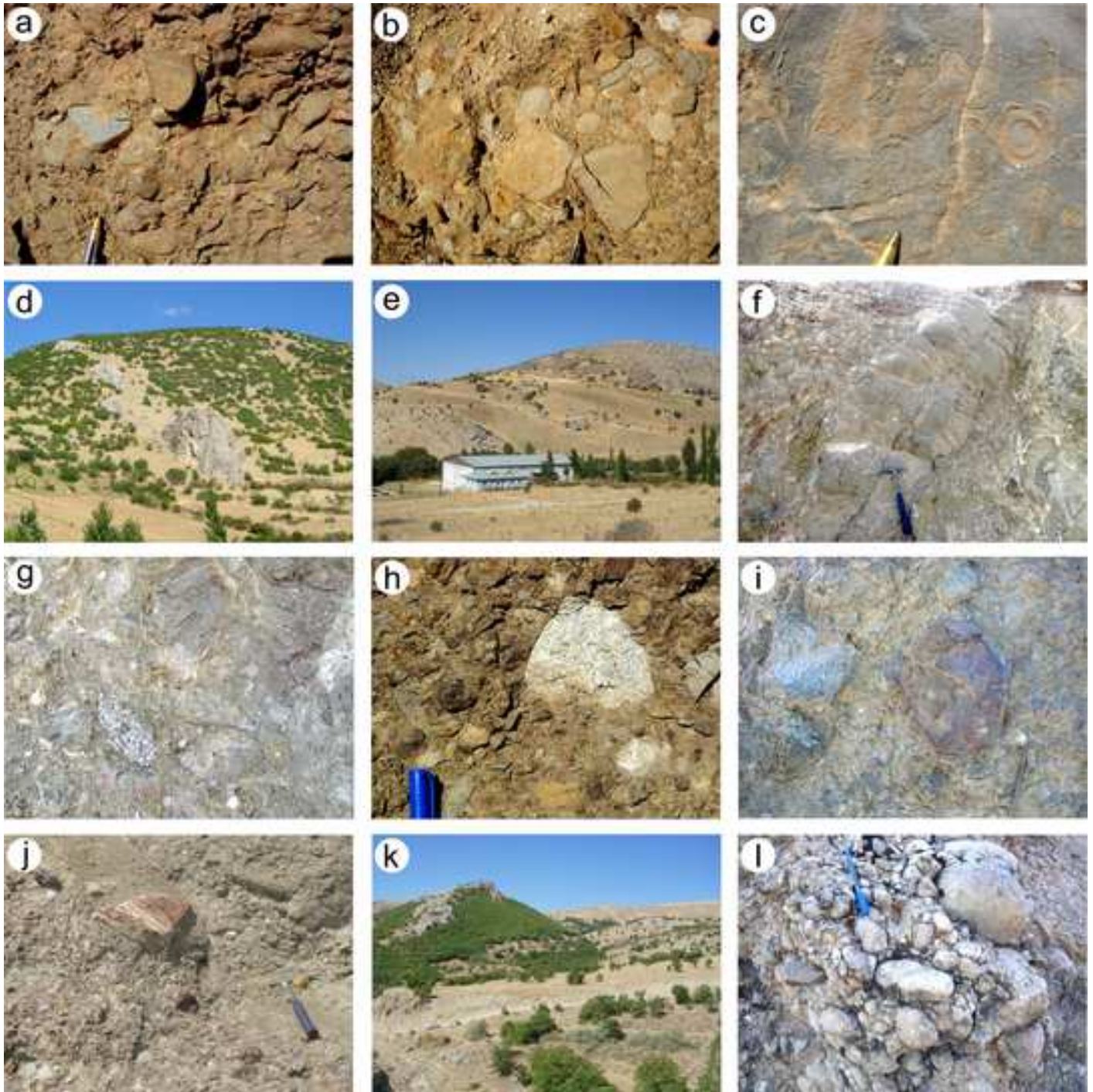
Figure 17

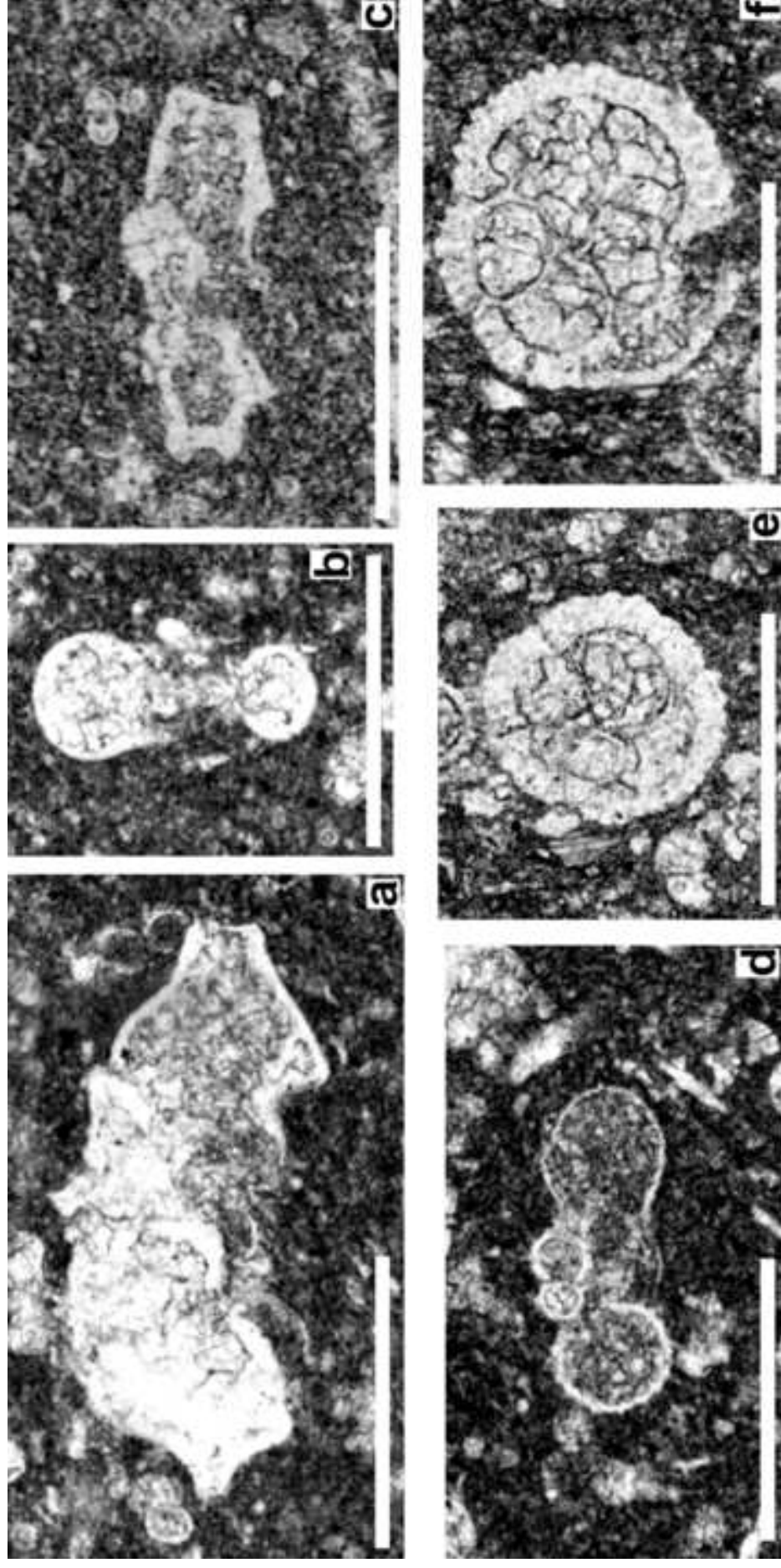


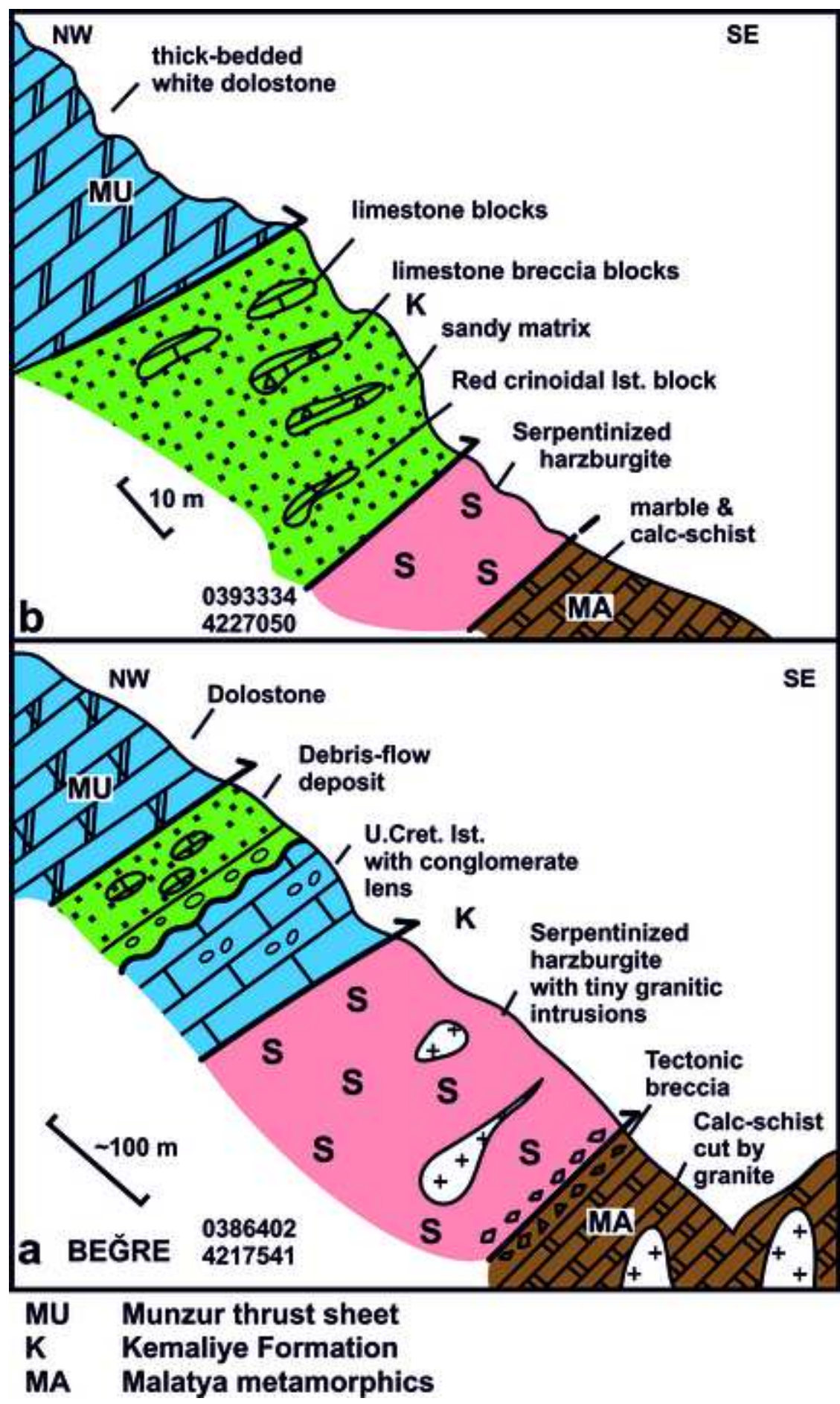


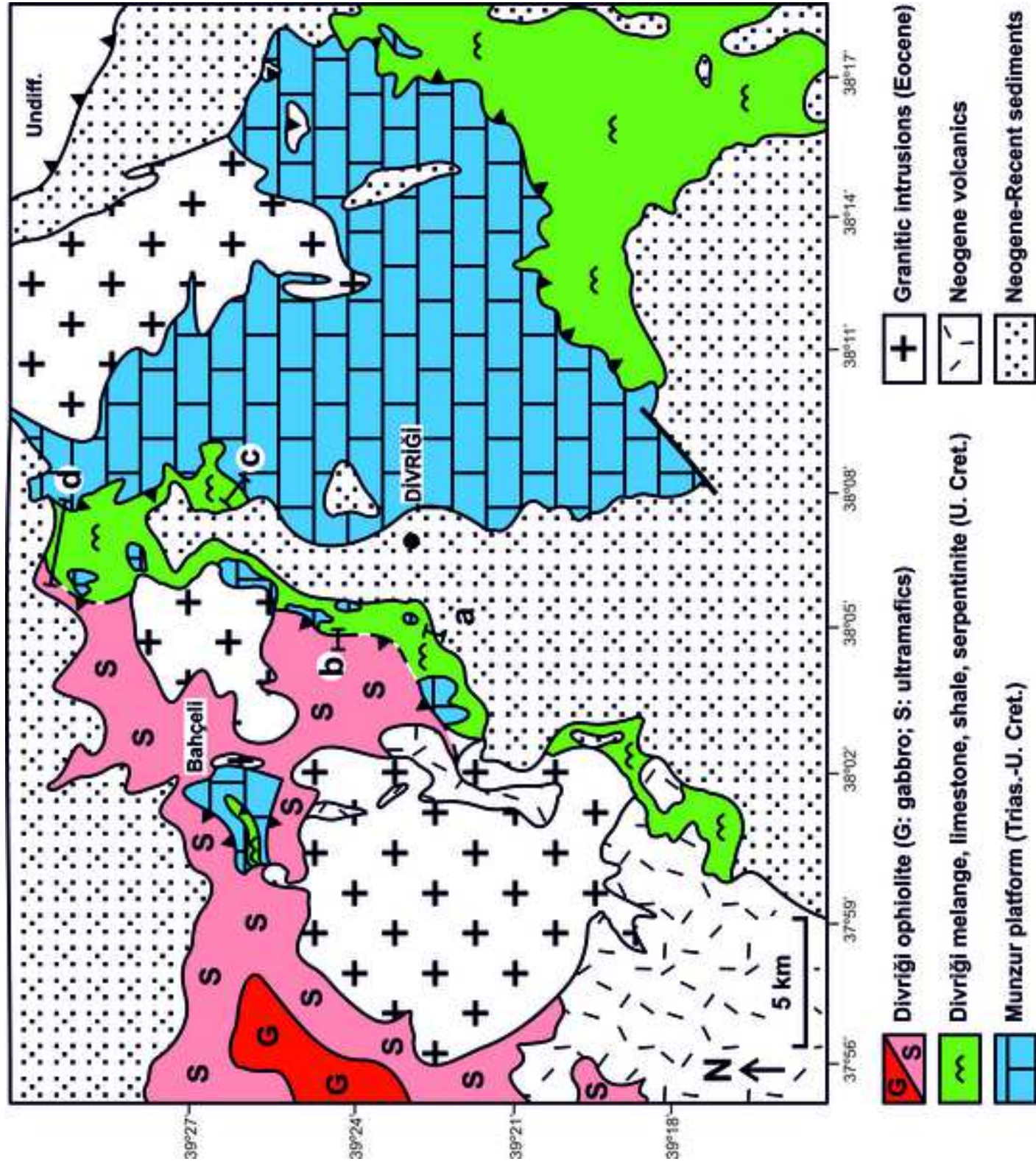


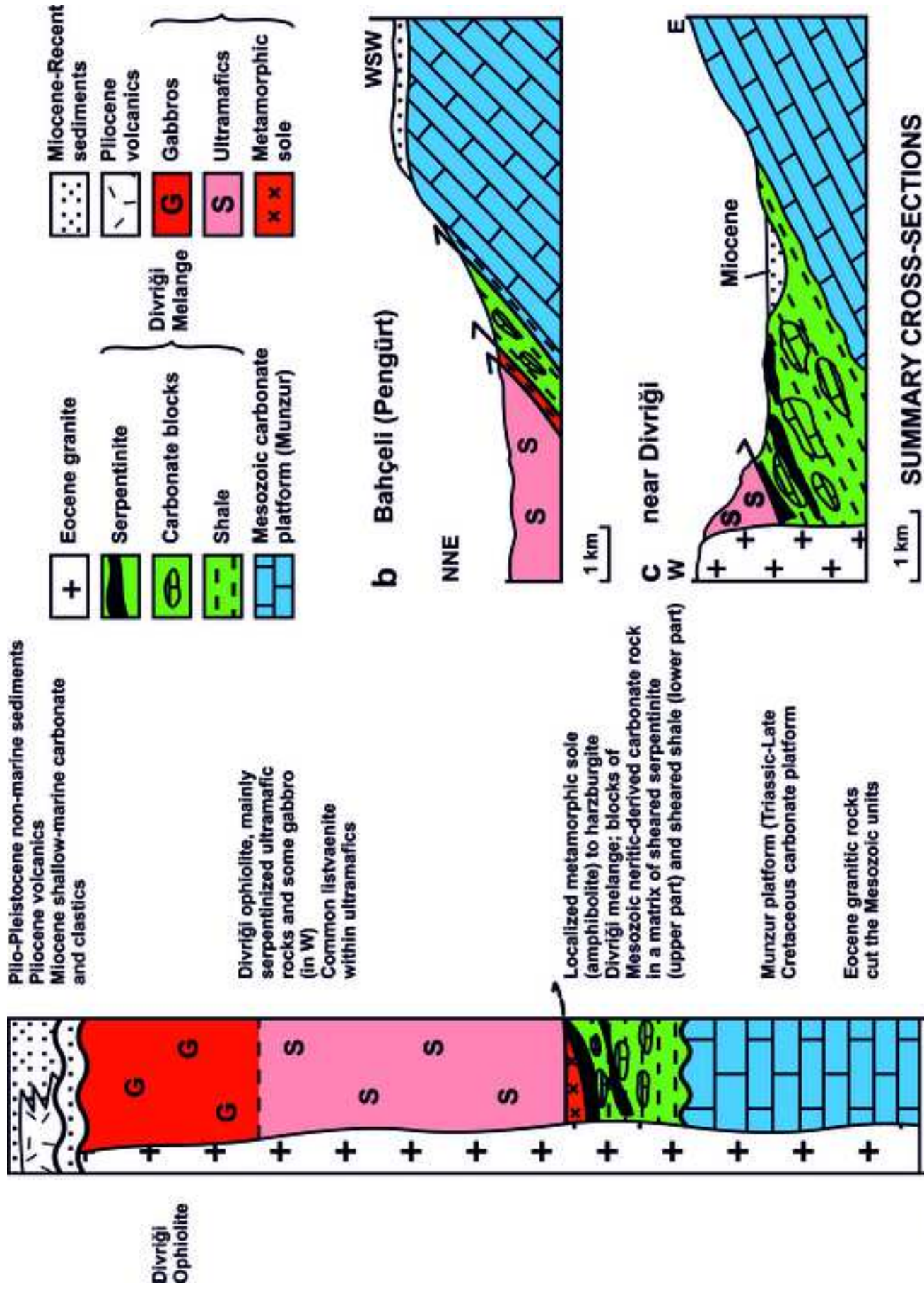


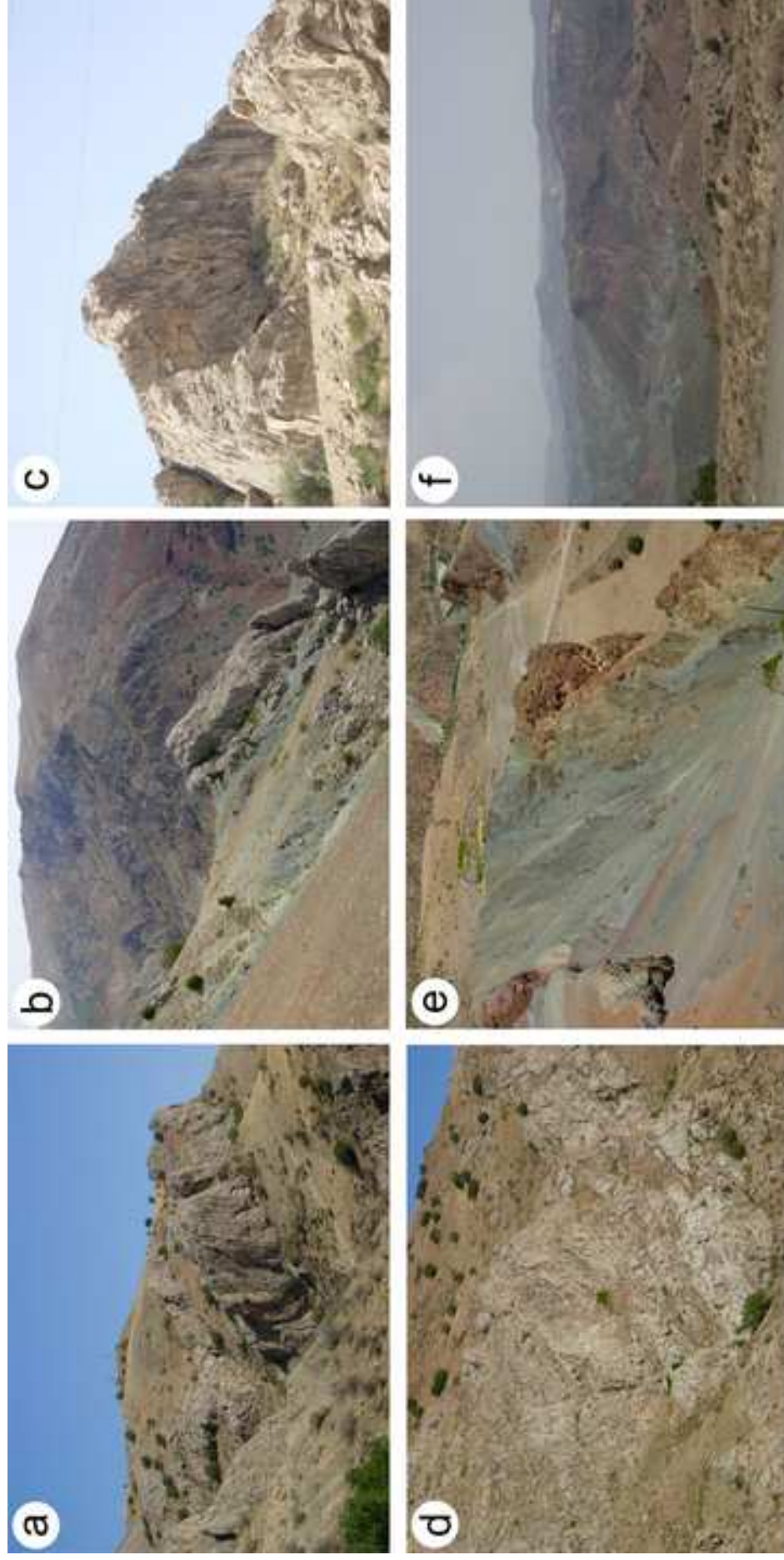














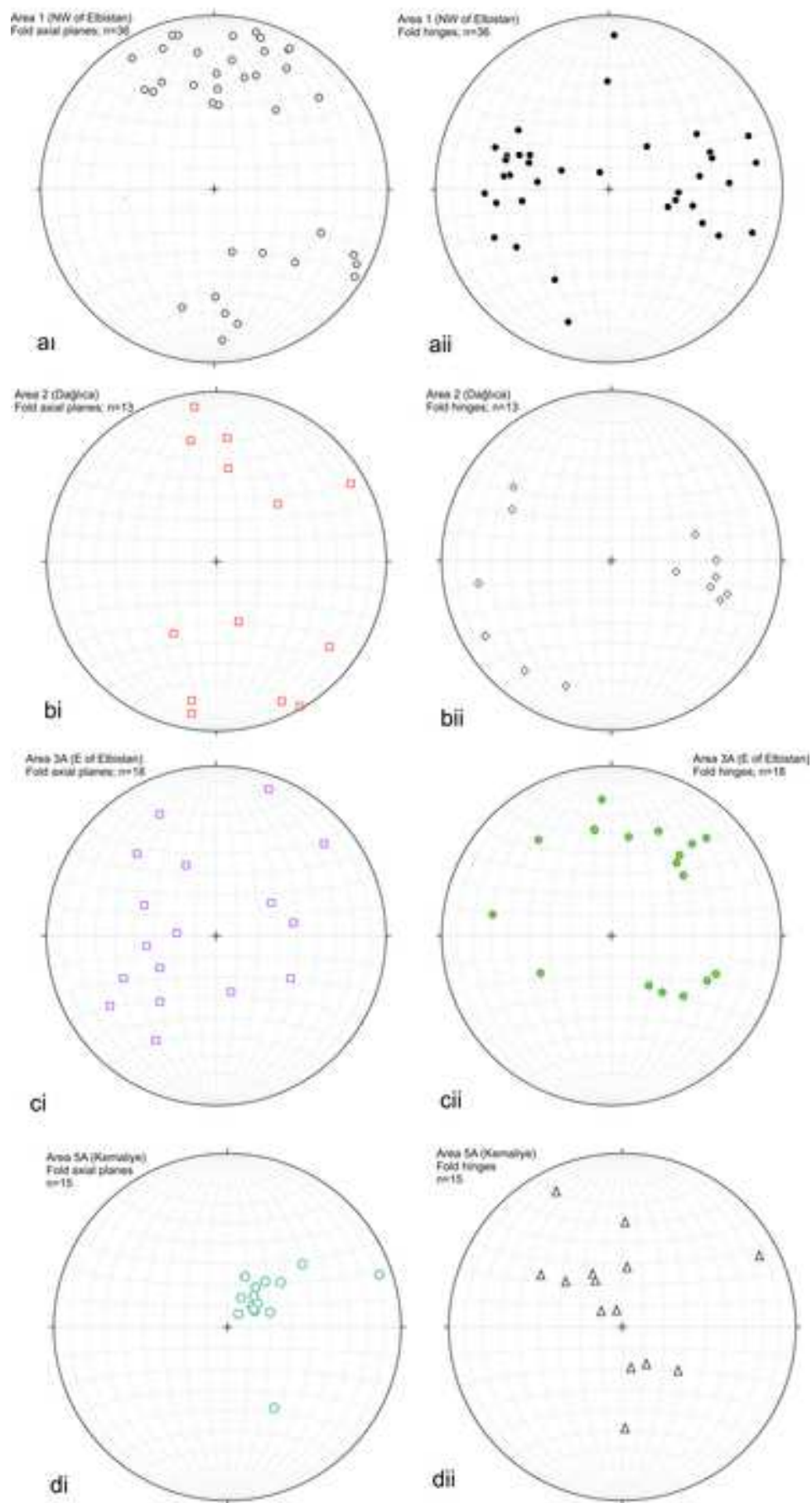
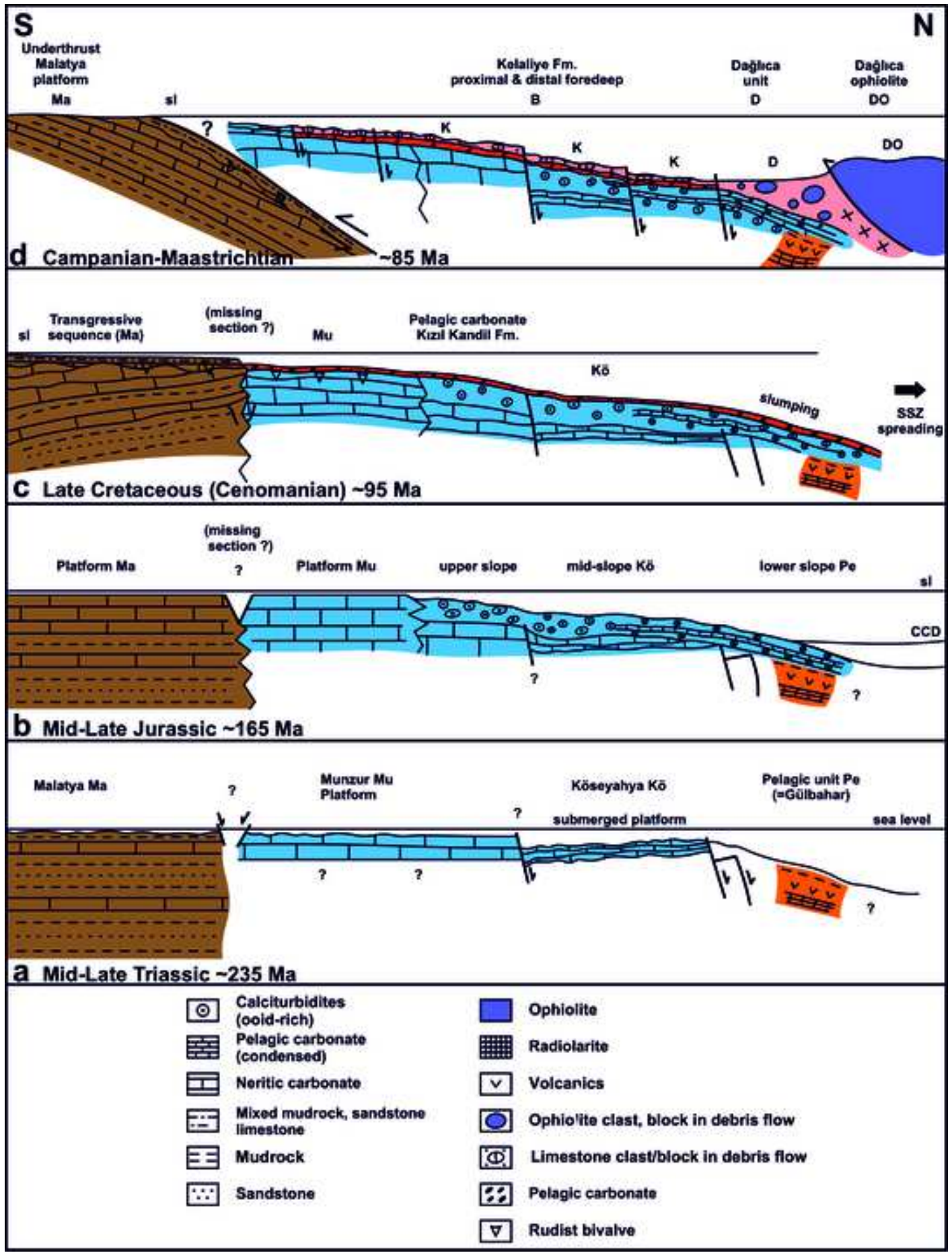
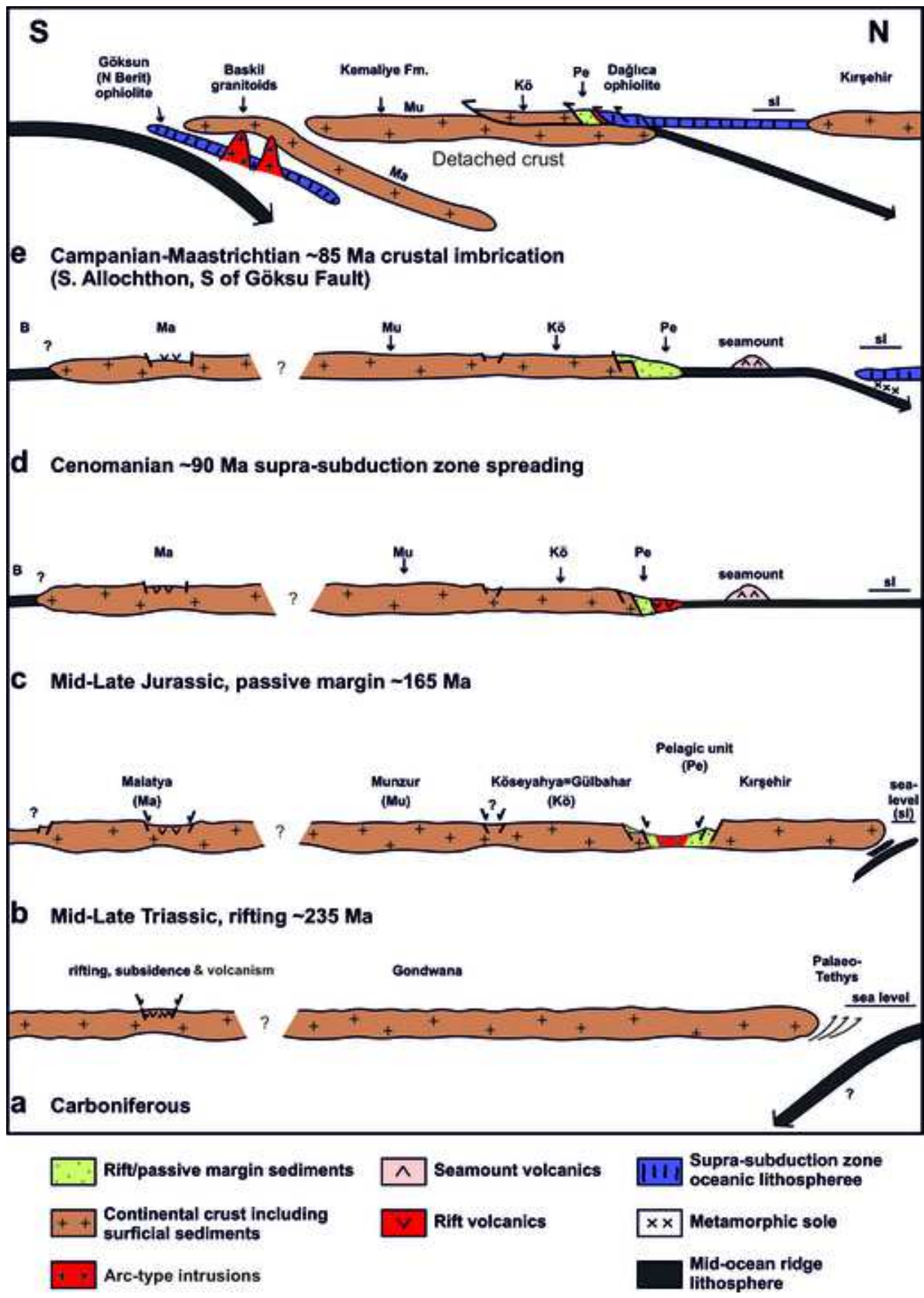
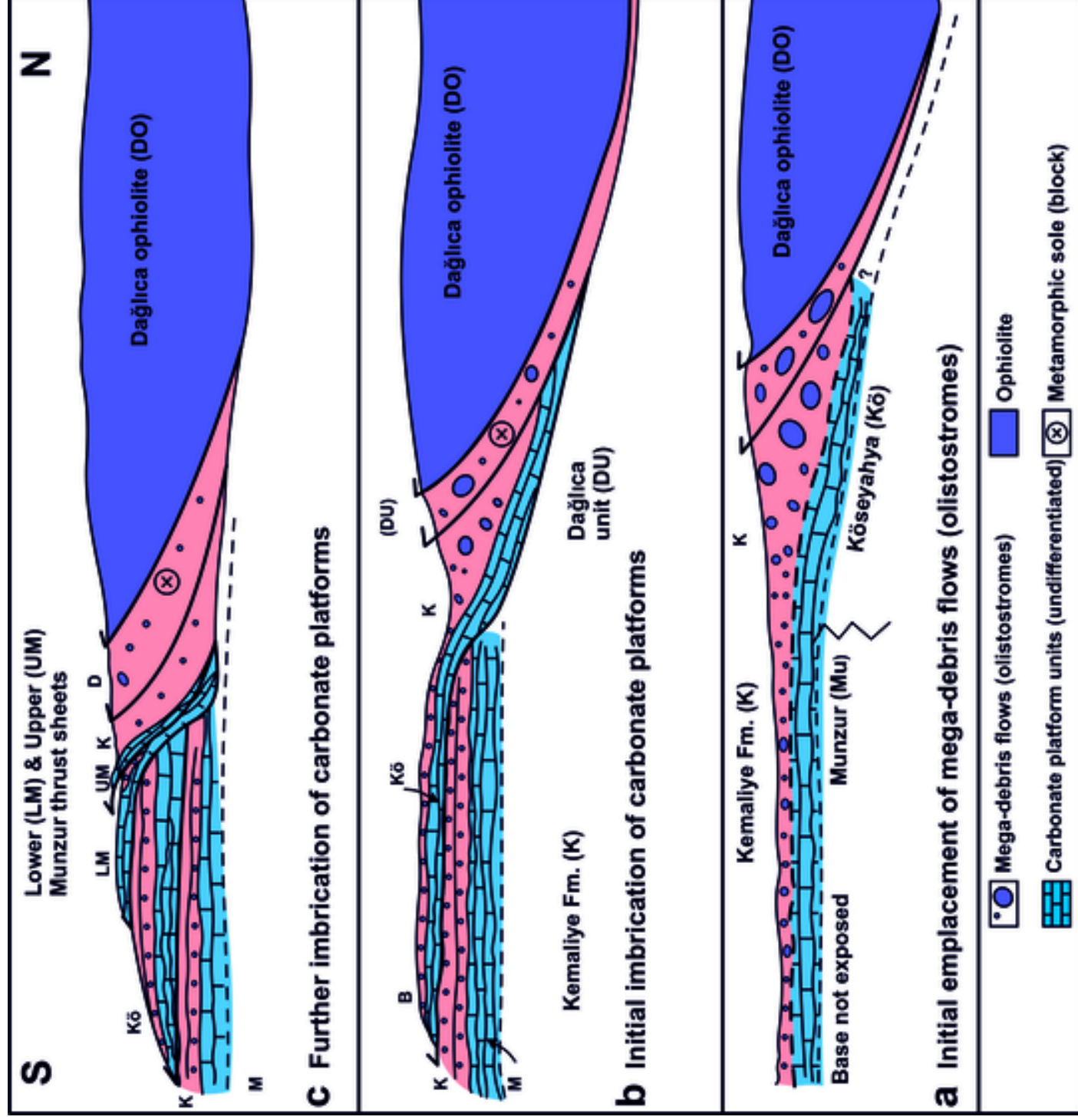


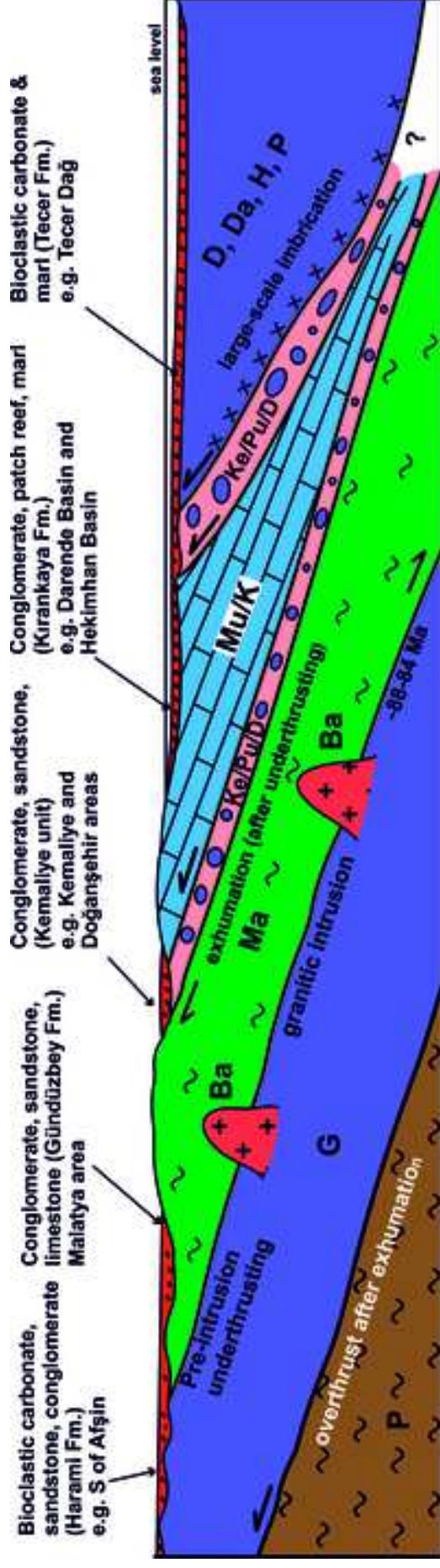
Figure 27

[Click here to access/download;Figure;18.5 Fig\\_27 REVAR12.1.21 2.jpg](#)









**S**

Transgressive sediments (above unconformity)

Ophiolite

Metamorphic sole

Accretionary foredeep debris-flows & melange

Carbonate platforms  
Munzur & Köseyahya (undifferentiated)

Granitoid intrusions

Metamorphics

**D, Da, H, P**

Divriği, Dağlıca, Hekimhan & Pınarbaşı ophiolites

**Mu/K**

Munzur & Köseyahya thrust sheets (undifferentiated)

**Du**

Dağlıca unit (ophiolitic debris mainly)

**Ba**

Baskil Granitoids (arc magmatism)

**G**

Göksun (N Berit) ophiolite

**P**

Pütürge (continental crust)

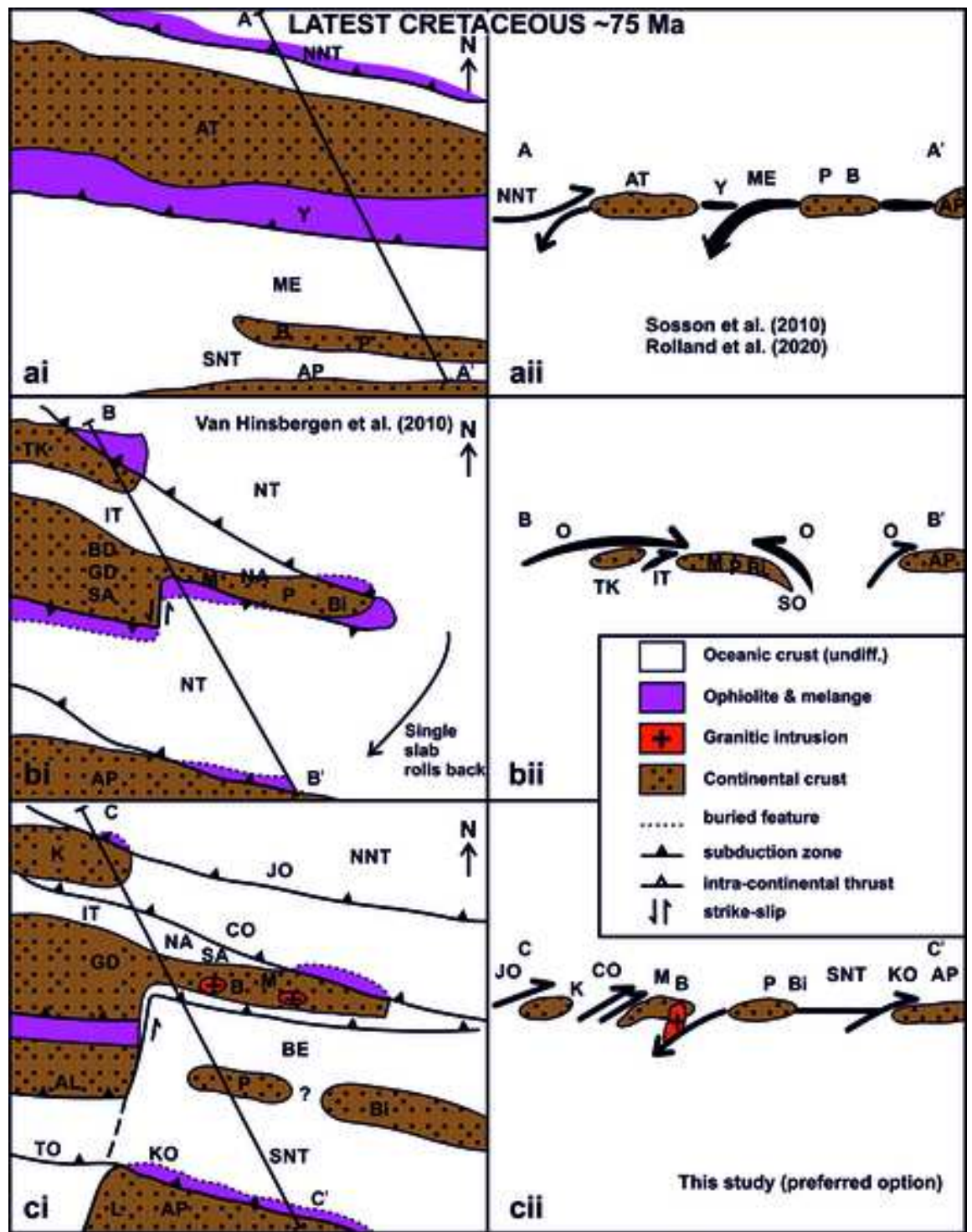
**Ke, Pu, Da**

Kemaliye Fm., Pelagic unit (Gülbahar nappe) & ophiolitic debris

**N**

Figure 31

[Click here to access/download;Figure;Fig. 31 rev 30.jpg](#)



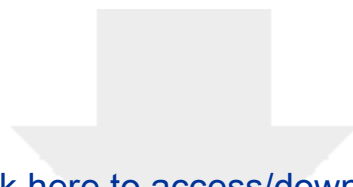
<b>AL</b> Alanya massif	<b>KO</b> Kızıldağ ophiolite	<b>P</b> Pütürge massif
<b>AP</b> Arabian platform	<b>JO</b> Jurassic ophiolite	<b>SA</b> Southern allochthon
<b>AT</b> Anatolide-Tauride block	<b>K</b> Kırşehir block	<b>SNT</b> South Neotethys
<b>B</b> Baskil arc granitoids	<b>L</b> Levant margin	<b>NNT</b> North Neotethys
<b>BI</b> Bitlis massif	<b>M</b> Malatya metamorphics	<b>TK</b> Tavşanlı-Kırşehir block
<b>BE</b> Berit ocean	<b>ME</b> Mesogea	<b>TO</b> Troodos ophiolite
<b>BD</b> Bolkar Dağ	<b>NA</b> Northern allochthon (Munzur)	<b>Y</b> Yüksekova back-arc ocean
<b>CO</b> Cretaceous ocean	<b>NT</b> Neotethys	
<b>GD</b> Geyik Dağ	<b>O</b> Ophiolite (undiff.)	
<b>IT</b> Inner Tauride ocean		

Lithology and location	Radiolarians determined (with comments)	Age
<b>M13-175A</b> Kirandere, near İncelik köy, Area 2. GPS: 0357348 4247428	Radiolarians represented especially by big spherical skeletons probably belonging to <i>Holocryptocanium barbui</i> Dumitrica	<b>Late Albian-Cenomanian</b>
<b>M13-176A</b> Kirandere, near İncelik köy, Area 2. GPS: 0357348 4247428	Sparse, poorly preserved. <i>Acaeniotyle diaphorogona</i> Foreman <i>Acaeniotyle umbilicata</i> (Rüst) <i>Dicerosaturnalis amissus</i> (Squinabol) (up to end-Aptian <i>Dictyomitra communis</i> (Squinabol), Aptian and earlier <i>Praeconocaryomma</i> sp. <i>Xitus spicularius</i> (Aliev) sensu O'Dogherty (1994)	<b>Aptian</b> (based on <i>Dicerosaturnalis amissus</i> (Squinabol) and <i>Dictyomitra communis</i> (according to O'Dogherty, 1994))
<b>M13-177A</b> Kirandere, near İncelik köy, Area 2 GPS: 0357348 4247428	Sparse, poorly preserved. <i>Acaeniotyle diaphorogona</i> Foreman <i>Acaeniotyle umbilicata</i> (Rüst) <i>Dicerosaturnalis amissus</i> (Squinabol), up to the end of Aptian <i>Dictyomitra communis</i> (Squinabol), Aptian and earlier <i>Praeconocaryomma</i> sp. <i>Xitus spicularius</i> (Aliev) sensu O'Dogherty (1994)	<b>Early Albian</b> (based on the first two species and the absence of <i>Dicerosaturnalis</i> (see O'Dogherty, 1994)).
<b>M13-17A</b> <b>Clast in debris flow;</b> Kabaktepe area; Area 3A, E of Elbistan GPS: 0363392 4240699	Rare, quite well preserved; low-diversity. <i>Cecrops septemporatus</i> (Parona) <i>Pantanellium</i> sp. <i>Williriedellum</i> cf. <i>carpathicum</i> Dumitrica (Rare sponge spicules include reniform sclerites)	<b>Late Valanginian – Hauterivian</b>
<b>M13-112A</b> 1 km E of Büyük Tatlı; Area 2; 300m from sample 111A GPS: 0325679 4262229	Abundant, diverse, well preserved (mostly silica-filled). <i>Archaeodictyomitra apiarium</i> (Rüst) <i>Archaeodictyomitra excellens</i> Tan <i>Archaeodictyomitra minoensis</i> (Mizutani) <i>Dicerosaturnalis trizonalis</i> (Rüst) (primitive forms) <i>Ditrabs sansalvadorensis</i> (Pessagno) <i>Emiluvia chica</i> Foreman <i>Emiluvia hopsoni</i> Pessagno <i>Hsuum arabicum</i> Dumitrica <i>Mirifusus diana</i> (Karrer)	<b>Late Tithonian-Berriasian</b>

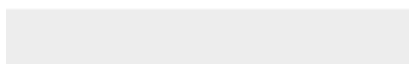
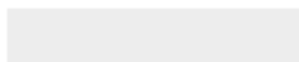
	<p>1. <i>Tethysetta boesii</i> (Parona)  <i>Mirifusus odoghertyi</i> Jud  <i>Pantanellium tredecimporatum</i> (Rüst)  <i>Triactoma tithonianum</i> Rüst</p>	
<p><b>M13-182B</b> Büyük Tatlı;  Area 2  GPS: 37 0324740  4263734</p>	<p>Common; some very well preserved.  <i>Acaeniotyle umbilicata</i> (Rüst)  <i>Archaeodictyomitra excellens</i> (Tan)  <i>Archaeospongoprunum patricki</i> Jud  <i>Dicerosaturnalis trizonalis</i> (Rüst)  <i>Emiluvia chica</i> Foreman  <i>Emiluvia pentaporata</i> Steiger &amp; Steiger  <i>Mirifusus diana</i>e (Karrer)  <i>Pantanellium huazalingoense</i> Pessagno &amp; McLeod  <i>Praeconosphaera sphaeroconus</i> (Rüst)  <i>Pyramispongia barmsteinensis</i> Steiger  <i>Saitoum kapewinteri</i> Dumitrica &amp; Zügel</p>	<p><b>Late Kimmeridgian-early Tithonian</b></p>
<p><b>M13-184A</b>  Büyük Tatlı;;  Area 2  GPS: 37S 0324740  4263734</p>	<p>Radiolarians rather frequent but poorly preserved, represented especially by archaeodictyomitris and pseudodictyomitrids, most of them as inner casts; very rare Emiluvia and others.</p>	<p>Probably <b>late Jurassic</b></p>
<p><b>M13-49A</b>  Near Yuksullu mezra; Area 4 (S of Elbistan);  GPS: 37S 0347339  4225062</p>	<p>Abundant but very poorly preserved, with indistinct superficial ornamentation. (Spumellarians very rare).  <i>Cinguloturris</i> cf. <i>carpatica</i> Dumitrica  <i>Dicerosaturnalis dicranacanthos</i> (Squinabol)  <i>Praeconosphaera sphaeroconus</i> (Rüst)  <i>Pseudodictyomitra primitiva</i> Matsuoka &amp; Yao  <i>Transsuum brevicostatum</i> (Ozoldova)</p>	<p><b>Kimmeridgian – early Tithonian</b></p>
<p><b>M13-198A</b>  Near <b>Topaktaş</b> Tepe; Area 2  GPS: 37S 0299567  4263104</p>	<p>Very rare and very poorly preserved.  <i>Podocapsa amphitreptera</i> Foreman  <i>Triactoma</i> sp.  <i>Xitus</i> sp.</p>	<p><b>Late Oxfordian-Tithonian</b></p>
<p><b>M13-193B</b>  Kayseri, near Hurman Kalesi;  Area 2  GPS: (GPS: 37S 0369890 4333783)  0303387 4265316</p>	<p>Radiolarians common but very poorly preserved.  <i>Emiluvia orea</i> Baumgartner  <i>Mirifusus diana</i>e (Karrer)</p>	<p><b>Late Oxfordian – Kimmeridgian</b></p>
<p><b>M13-49B</b>  Near Yoksullu mezra; Area 4 (S of Elbistan);</p>	<p>Common; generally poorly or moderately preserved.  <i>Emiluvia ordinaria</i> Ozoldova  <i>Emiluvia orea</i> Baumgartner  <i>Parvicingula washitaensis</i> (Mizutani)</p>	<p><b>Late Oxfordian</b></p>




GPS: 0347339 4225062	<i>Podocapsa amphitreptera</i> (Rüst) <i>Zhamoidellum ovum</i> Dumitrica	
<b>M13-186A</b> Büyük Tatlı; area; Area 2 GPS: 37S 0323561 4262607	Common, but poorly or very poorly preserved; some very well preserved including <i>Praewilliriedellum</i> sp. and some <i>Archaeodictyomitra</i> sp. or <i>Hsuum</i> sp. <i>Eucyrtidiellum unumaense</i> (Yao) <i>Cyrtocapsa mastoidea</i> Yao <i>Praewilliriedellum cephalospinosum</i> Kozur <i>Hexasaturnalis suboblongus</i> (Yao) <i>Hexasaturnalis tetraspinus</i> (Yao)	<b>Bajocian</b>
<b>M13-111A</b> 1 km E of Büyük Tatlı; Area 2; GPS 37S 0325679 4262229	Common, relatively well preserved to very poorly preserved; sparse assemblage. <i>Hexasaturnalis hexagonus</i> (Yao) <i>Hexasaturnalis suboblongus</i> (Yao)	<b>Bajocian</b>
<b>M13-48A</b> Near Yoksullu mezra; Area 4 (S of Elbistan); GPS: 37S 0347339 4225062	Abundant but very poorly preserved. <i>Acaeniotylopsis variatus triacanthus</i> Kito & De Wever <i>Hexasaturnalis suboblongus</i> (Yao) <i>Hexasaturnalis tetraspinus</i> (Yao) <i>Pantanellium sincerum</i> Pessagno & Blome	<b>Bajocian</b>
<b>M13-47B</b> Block in serpentinite; N of Yuksullu mezra; Area 4 (S of Elbistan); GPS: 37S 0346001 4225266	Very rare, poorly preserved, especially fragments of spines and saturnalids. <i>Betraccium</i> cf. <i>deweveri</i> Pessagno & Blome, late Norian <i>Deflandrecyrtium</i> cf. <i>nobense</i> Carter <i>Praemesosaturnalis</i> sp. A of Sugiyama (1997)	<b>Late Norian, Betraccium deweveri Zone</b>
<b>ET-12-61</b> Yeşildere Melange, Hekimhan area. (GPS: 37S 0369890 4333783)	Radiolarians common but very poorly preserved, corroded. <i>Dorypyle ? anisa</i> (Squinabol) <i>Pseudodictyomitra pseudomacrocephala</i> (Squinabol) <i>Thanarla veneta</i> (Squinabol) <i>Xitus mclaughlini</i> Pessagno	<b>Late Albian – early Cenomanian</b>



Click here to access/download  
**Supplementary Material**  
Sup Pub Fig. 1 Gurun curl .png



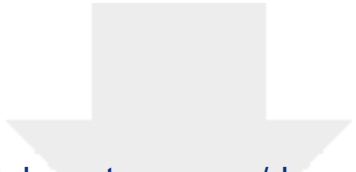


[Click here to access/download](#)

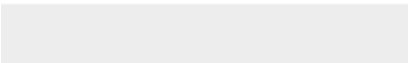
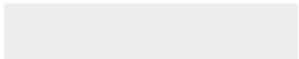
**Supplementary Material**

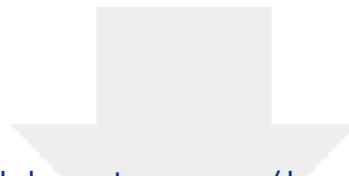
18.5.21 sup fig 2 Tanir\_map\_sections1 copy.jpg



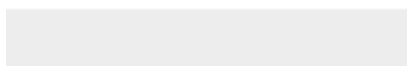
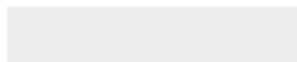


Click here to access/download  
**Supplementary Material**  
Sup Fig. 3 Rev 5.4.jpg





Click here to access/download  
**Supplementary Material**  
Sup. Pub Fig. 4REV 5.4.jpg



6XSSOHPHQWDU\ )LJ

!!

&OLFN KHUH WR DFFHVV GRZQORDG  
6XSSOHPHQWDU\ 0DWHULDO  
6XSB)LJ MSJ



6XSSOHPHQWDU\ )LJ

!!

&OLFN KHUH WR DFFHVV GRZQORDG  
6XSSOHPHQWDU\ 0DWHULDO  
6XSSB)LJ MSJ



6XSSOHPHQWDU\ )LJ

!!



&OLFN KHUH WR DFFHVV GRZQORDG  
**6XSSOHPHQWDU\ 0DWHULDO**  
 6XS 3XE \$75(9 MSJ





6XSSOHPHQWDU\ )LJ

!!



&OLFN KHUH WR DFFHVV GRZQORDG  
**6XSSOHPHQWDU\ 0DWHULDO**  
 6XS 3XE 5(9\$5 MSJ



6XSSOHPHQWDU\ )LJ

!!



&OLFN KHUH WR DFFHVV GRZQORDG  
**6XSSOHPHQWDU\ 0DWHULDO**  
 6XS 3XE 5(9\$5 MSJ

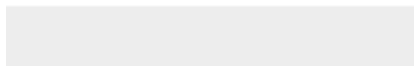


6XSSOHPHQWDU\ )LJ

!!



&OLFN KHUH WR DFFHVV GRZQORDG  
**6XSSOHPHQWDU\ 0DWHULDO**  
6XS 3XE )LJ 5HY\$5 MSJ



6XSSOHPHQWDU\ 7DEOH

!!

&OLFN KHUH WR DFFHVV GRZQORDG  
6XSSOHPHQWDU\ 0DWHULDO  
6XS WDEOH UHYLVHG GR



!"#\$%&%()'\*(+),+ -\*"&#'

+

/ )\*" +,+'0"+%1'0)&.+0%2"+%\*3+#)\*,\$(#'+),+(\*"&".'+(\*+.145('(\*6+'0(.+7%#7"&+0"&"8

!"#\$%&'()\*+&#-'&

/\*#0%#1\$2+"3'2(,4(""%#\$'+)&'567689':+;#"&,+9'<6'="1(3'(\$/6'>,&(?"#6'/\*#'

š Œ u]v š]}v• }( o Œ }μ• (}••]o• Á Œ Œ Œ] }μ Œ Ç < d •  
:(\$%+1("%('2##'4(""%#\$'+)&';@'=6'A)-%&"%4(6'514+)&'&#&\$&+'&\*'0%.(1'-(.),4"%B&6